

# BULLETIN

OF THE POLISH HYDROGEN AND FUEL CELL ASSOCIATION

6<sup>TH</sup> POLISH FORUM

No. 11 (2017)

## SMART ENERGY CONVERSION & STORAGE

3-6.09.2017 Bukowina Tatrzańska

Chairman: prof. Janina Molenda

### Scope:

- hydrogen production & storage
- fuel cells
- Li-ion & Na-ion batteries
- supercapacitors
- solar conversion
- thermoelectrics



Ministry of Science  
and Higher Education  
Republic of Poland

<http://forum.hydrogen.edu.pl>





## Ladies and Gentlemen,

It is my great pleasure to welcome you in the eleventh issue of Bulletin of Polish Hydrogen and Fuel Cell Association, that is completely dedicated to the *6<sup>th</sup> Polish Forum Smart Energy Conversion and Storage* in Bukovina Tatrzańska from September 3<sup>rd</sup> to 6<sup>th</sup>, 2017. The conference is co-organized by Polish Hydrogen and Fuel Cells Association ([hydrogen.edu.pl](http://hydrogen.edu.pl)) and AGH University of Science and Technology. The history of the Forums began in 2005, with the first conference covering a relatively narrow issues of fuel cells and hydrogen technologies. After 12 years of collecting experience and constantly expanding the formula of the Forums, this year's scope includes: hydrogen production and storage, fuel cells, Li-ion and Na-ion batteries, supercapacitors, solar conversion and thermoelectrics. All these topics are highly important for modern energy conversion and storage. Albeit different, they are based on similar mass and charge transport mechanisms, related to ionic and electronic defect structure. This brought the idea of gathering of high-level specialists, including theoreticians, in this field.

Further progress in the field of modern energy conversion and storage technologies depends on a development of the scientific basis of manufacturing of functional materials, which relies on comprehensive studies of their structural, transport, catalytic, thermal and mechanical properties, aiming to describe the relationship between crystal structure, chemical composition, electronic properties, and the catalytic efficiency of the electrochemical processes occurring in electrochemical devices.

An analysis of current technological solutions shows that there is still a gap between current capabilities of fuel cells and practical needs of the hydrogen energy technology. Problems with wide commercialization of fuel cells is associated with strenuous implementation of technology, which is based on technologically immature materials.

Among many aspects of the hydrogen-based economy, the key to its success is solution of the fundamental issues of the used materials. There is a particular place for technology of nanomaterials and studies of the catalytic processes. Understanding on the atomic-level the fundamental processes involved in the catalysis, shall trigger correlated progress in all fields of modern energy technologies.

The grain size dependent defect formation energy and space charge effects are significantly influencing the transport properties. Elucidation of the grain boundaries impact on defects and transport properties will enable designing of materials with tailored properties. An extra difficulty, slowing down the progress in science and technology of the nanomaterials, is related to the stability of nanomaterials and reproducibility of their properties, because, as it was observed in thin films, unique microstructure may provide unique properties.

I hope that this year's conference will be an excellent place for discussion in the field of materials and technologies for modern energy, and also a good school for students and young scientists, beginning their careers. I would like to thank you, the participants, who contribute to make this meeting successful, wishing you an exciting and enjoyable time.

Prof. Janina Molenda  
Chairman of 6<sup>th</sup> Polish Forum  
Smart Energy Conversion and Storage  
President of Polish Hydrogen  
and Fuel Cell Association

## Contents:

### INVITED LECTURES:

<b>Plenary lecture: Joachim Maier</b> (Max Planck Institute for Solid State Research, Germany) <i>The role of defects and size for electrochemical energy storage</i>	10
<b>Janusz Tobola</b> (AGH University of Science and Technology, Poland) <i>Electronic structure calculations in materials converting energy</i>	11
<b>Janina Molenda</b> (AGH University of Science and Technology, Poland) <i>Electronic structure “engineering” as a new approach to materials design for Li-ion and Na-ion batteries</i>	12
<b>Yoshitaka Tateyama</b> (National Institute of Materials Science, Japan) <i>DFT sampling calculation studies on electrode/electrolyte interfaces in batteries</i>	13
<b>René Hausbrand</b> (Technische Universität Darmstadt, Germany) <i>Fundamental insights on battery materials and interfaces by surface science investigations</i>	14
<b>Andrzej Czerwiński</b> (University of Warsaw, Poland) <i>Pd-AB<sub>5</sub> – new hybrid anode in Ni-MH battery</i>	15
<b>Ilan Riess</b> (Technion - Israel Institute of Technology) <i>Identifying the elementary steps of electro-catalytic reactions</i>	16
<b>Constantinos Vayenas</b> (University of Patras, Greece) <i>Triode fuel cells</i>	17
<b>Truls Norby</b> (University of Oslo, Norway) <i>High temperature electrolysis using proton conducting ceramic electrolytes</i>	18
<b>Mogens Mogensen</b> (Technical University of Denmark) <i>Degradation mechanisms of solid oxide cells</i>	19
<b>Philippe Knauth</b> (Aix Marseille University, France) <i>Ion conduction in polymer membranes: application for electrochemical energy technologies</i>	20
<b>Władysław Wieczorek</b> (Warsaw University of Technology, Poland) <i>New strategies in designing electrolytes for ambient temperature batteries</i>	21
<b>Paweł Kulesza</b> (University of Warsaw, Poland) <i>Reduced-graphene-oxide as active support for platinum and non-noble metal catalysts during oxygen electroreduction</i>	22
<b>Anita Trenczek-Zajac</b> (AGH University of Science and Technology) <i>Shape-controlled titanium dioxide for photoelectrolysis</i>	23
<b>Krzysztof Fic</b> (Poznan University of Technology, Poland) <i>Operando studies of electrode/electrolyte interface in electrochemical capacitor</i>	24
<b>Tomasz Story</b> (Institute of Physics of the Polish Academy of Sciences) <i>IV-VI semiconductors as topological materials</i>	25
<b>Nhu-Tarnawska Hoa Kim-Ngan</b> (Pedagogical University of Kraków, Poland) <i>Hydrogen absorption in U-based alloys with bcc structure</i>	26
<b>Piotr Jasiński</b> (Gdańsk University of Technology) <i>Distribution of relaxation times as a tool to separate overlapped electrochemical processes in impedance spectra</i>	27
<b>Konrad Świerczek</b> (AGH University of Science and Technology) <i>MIEC-type ceramic membranes with enhanced transport properties</i>	28

## YOUNG SCIENTISTS FORUM:

<b>Michał Świętosławski</b> (Jagiellonian University) <i>Modified LMO cathode materials. From the idea to the product</i>	30
<b>Łukasz Kondracki</b> (AGH University of Science and Technology) <i>In operando XRD studies as a tool for determination of lithium ions kinetics in electrode materials</i>	31
<b>Sebastian Wachowski</b> (Gdańsk University of Technology) <i>Structural properties and ionic conduction mechanisms in doped ABO<sub>4</sub> oxides</i>	32
<b>Przemysław P. Michalski</b> (Warsaw University of Technology) <i>Structural and electrical properties of LiFe<sub>1-x</sub>Mn<sub>x</sub>BO<sub>3</sub> glasses</i>	33
<b>Grzegorz Brus</b> (AGH University of Science and Technology) <i>Locally resolved microstructure investigation of an anode-supported solid oxide fuel cell stack</i>	34
<b>Paweł Jeżowski</b> (Poznań University of Technology) <i>Energy storage systems using internal hybridization</i>	35
<b>Tomasz Pietrzak</b> (Warsaw University of Technology) <i>Stabilization of superionic δ-Bi<sub>2</sub>O<sub>3</sub> phase at room temperature by thermal nanocrystallization of bismuth oxide glasses</i>	36
<b>G. Ważny, S. Bednarczyk, K. Cichy, M. Majewski, J. Leszczyński, J. Molenda</b> (AGH University of Science and Technology) <i>E-MOTO AGH – power supply for an electric motorcycle</i> <b>+ PRESENTATION OF THE MOTORCYCLE</b>	37

## POSTERS:

<b>A. Lacz</b> (AGH University of Science and Technology) <i>Reactivity of perovskite structure materials towards melted V<sub>2</sub>O<sub>5</sub></i>	P-00
<b>E.N. Naumovich</b> (Institute of Power Engineering) <i>Oxygen nonstoichiometry of mixed-conducting Ba<sub>0.5</sub>Sr<sub>0.5</sub>Co<sub>0.8</sub>Fe<sub>0.2</sub>O<sub>3-δ</sub></i>	P-01
<b>B. Bochentyn</b> (Gdańsk University of Technology) <i>Structural and catalytic properties of transition element-doped ceria layers in SOFCs fueled by biogas</i>	P-02
<b>E. Drożdż</b> (AGH University of Science and Technology) <i>Structural and electrical properties of Cr-doped SrTiO<sub>3</sub> porous materials</i>	P-03
<b>G. Brus</b> (AGH University of Science and Technology) <i>Microstructure oriented model of direct internal reforming SOFC</i>	P-04
<b>K. Motyliński</b> (Institute of Power Engineering) <i>Degradation of the Ni-YSZ anodes of solid oxide fuel cells fed with CH<sub>4</sub>-H<sub>2</sub>O mixtures with low steam-to-carbon ratio</i>	P-05
<b>Ł. Łańcucki</b> (AGH University of Science and Technology) <i>Impact of calcium addition on properties of lanthanum strontium iron oxide</i>	P-06
<b>M. Chalusiak</b> (AGH University of Science and Technology) <i>Development of solid oxide fuel cell manufacturing methodology using robocasting technology</i>	P-07
<b>M. Chalusiak</b> (AGH University of Science and Technology) <i>Dynamic characteristics of a direct internal reforming Solid Oxide Fuel Cell to address fuel starvation</i>	P-08
<b>M. Dudz</b> (Warsaw University of Technology) <i>Microstructure and electric properties of BIYWO:LSM composite cathode for SOFC</i>	P-09
<b>M. Jasiński</b> (Pedagogical University of Cracow) <i>Infrared thermography – powerful instrument for testing SOFC</i>	P-10

<b>M. Krauz</b> (Institute of Power Engineering Ceramic Department Cerel) <i>Metal supported solid oxide fuel cells with electrolyte deposited by pulsed laser deposition</i>	P-11
<b>K. Zheng</b> (AGH University of Science and Technology) <i>Oxygen diffusion in <math>BaGd_{1-x}Yb_xMn_2O_{5+\delta}</math> layered structured perovskites for oxygen storage technology</i>	P-12
<b>K. Cichy</b> (AGH University of Science and Technology) <i>New proton conducting materials for high temperature fuel cells</i>	P-13
<b>W. Skubida</b> (AGH University of Science and Technology) <i>Symmetrical proton ceramic fuel cells – construction and performance</i>	P-14
<b>Z. Du</b> (University of Science and Technology Beijing) <i>First principles calculations of ionic transport in <math>La_2NiO_4</math> candidate material for MIEC-type membranes</i>	P-15
<b>Z. Zhang</b> (University of Science and Technology Beijing) <i><math>La_{2-x}Cu_{1-y}M_yO_{4-\delta}</math> (<math>M = In, Sc, Ga</math>) with mixed ionic-electronic conductivity as oxygen-transport membranes</i>	P-16
<b>J. Milewski</b> (Warsaw University of Technology) <i>Preparation of double layer yttria stabilized zirconia matrix impregnated by lithium/potassium electrolyte for Molten Carbonate Fuel Cells</i>	P-17
<b>K. Hubkowska</b> (University of Warsaw) <i>Electrochemical behavior of a Pd and Pd-noble metal alloys thin film electrodes in concentrated alkaline media</i>	P-18
<b>M. Pająk</b> (University of Warsaw) <i>Hydrogen absorption in a palladium limited volume electrodes from protic ionic liquids</i>	P-19
<b>A. Żywczak</b> (Academic Centre for Materials and Nanotechnology) <i>Physical properties of TiZrNi ribbons and their hydrides</i>	P-20
<b>M. Nowak</b> (AGH University of Science and Technology) <i>Hydrogenation of <math>Ti_{45}Zr_{38}Ni_{17}</math> quasicrystals prepared by rapid quenching method</i>	P-21
<b>R. Tarkowski</b> (Mineral and Energy Economy Research Institute) <i>Underground hydrogen storage in salt caverns: hydrogen reactivity issues</i>	P-22
<b>M. Wojcik</b> (Warsaw University of Technology) <i>Influence of synthesis methods on electrical conductivity and dielectric relaxation in <math>(Ce_{0.9}Gd_{0.1})_{0.85}Pr_{0.15}O_{2-\delta}</math> studied by impedance spectroscopy</i>	P-23
<b>M. Leszczynska</b> (Warsaw University of Technology) <i>Crystal structure and conductivity in praseodymium doped ceria</i>	P-24
<b>K. Dzierzgowski</b> (Gdańsk University of Technology) <i>Synthesis and properties of <math>(Ce, La)NbO_4</math> compounds</i>	P-25
<b>A. Mielewczyk-Gryń</b> (Gdańsk University of Technology) <i>Hydration energetics of the ion-conducting doped lanthanum orthoniobates</i>	P-26
<b>P. Ławniczak</b> (Institute of Molecular Physics Polish Academy of Sciences) <i>The influence of hydrostatic pressure on AC conductivity characteristics in <math>(NH_4)_3H(SeO_4)_2</math> single crystal</i>	P-27
<b>P. Winiarz</b> (Gdańsk University of Technology) <i>Electrical and structural studies on titanium doped <math>Y_3NbO_7</math></i>	P-28
<b>A. Niemczyk</b> (AGH University of Science and Technology) <i>Synthesis and physicochemical properties of layered oxides from <math>La_{2-x}(Sr,Ba)_xMo_{4\pm\delta}</math> (<math>M: Cu, Ni</math>) group</i>	P-29
<b>A. Olszewska</b> (AGH University of Science and Technology) <i>Influence of oxygen content on transport properties of <math>LnBaCo_2O_{5+\delta}</math> and <math>LnBaCo_{1.5}Mn_{0.5}O_{5+\delta}</math> oxides</i>	P-30

<b>I. Lewandowska</b> (Gdańsk University of Technology) <i>The synthesis and properties of <math>\text{LaBaCo}_2\text{O}_{6-\delta}</math> ceramics</i>	P-31
<b>J. Niewiedzial</b> (AGH University of Science and Technology) <i><math>\text{Li}_4\text{Ti}_5\text{O}_{12}</math> doped with nickel, tungsten and chlorine – anode material for li-ion batteries</i>	P-32
<b>D. Olszewska</b> (AGH University of Science and Technology) <i><math>\text{Li}_4\text{Ti}_5\text{O}_{12}</math> doped with nickel, copper and carbon - anode for li-ion batteries</i>	P-33
<b>A. Milewska</b> (AGH University of Science and Technology) <i>Structural evolution of the <math>\text{Na}_x\text{Fe}_{0.33}\text{Ni}_{0.33}\text{Ti}_{0.33}\text{O}_2</math> cathodes</i>	P-34
<b>A. Milewska</b> (AGH University of Science and Technology) <i>Structural, electrical and electrochemical properties of the <math>\text{LiNi}_{0.9-y}\text{Co}_y\text{Mn}_{0.1}\text{O}_2</math> cathodes for Li-ion batteries – electronic structure studies</i>	P-35
<b>A. Milewska</b> (AGH University of Science and Technology) <i>High-voltage <math>\text{Na}_{0.67}\text{Ni}_{0.33}\text{Mn}_{0.67-y}\text{Ti}_y\text{O}_{2-\delta}</math> (<math>0 \leq y \leq 0.33</math>) cathodes for Na-ion batteries</i>	P-36
<b>A. Kulka</b> (AGH University of Science and Technology) <i>High-temperature synthesis and electrochemical properties of <math>\text{MoS}_2</math> – anode material for Na-ion batteries</i>	P-37
<b>K. Walczak</b> (AGH University of Science and Technology) <i>Electrochemical properties of NASICON-<math>\text{Na}_3\text{V}_2(\text{PO}_4)_3</math> and alluaudite-<math>\text{Na}_2\text{Fe}_3(\text{PO}_4)_3</math></i>	P-38
<b>K. Redel</b> (AGH University of Science and Technology) <i>Cathode material based on <math>\text{Na}_x\text{Fe}_{1-y}\text{Mn}_y\text{O}_2</math> for Na-ion batteries</i>	P-39
<b>K. Redel</b> (AGH University of Science and Technology) <i><math>\text{Li}_2\text{MnO}_3</math>-Stabilized <math>\text{LiMO}_2</math> (<math>M = \text{Mn}, \text{Co}, \text{Ni}</math>) composites as positive electrode materials for lithium-ion batteries</i>	P-40
<b>D. Baster</b> (AGH University of Science and Technology) <i><math>\text{Na}_x(\text{Li}_y\text{Ti}_{1-y})\text{O}_2</math> layered oxides as negative electrode for Na-ion batteries</i>	P-41
<b>A. Plewa</b> (AGH University of Science and Technology) <i>An alluaudite <math>\text{Na}_2\text{Fe}_2(\text{SO}_4)_3</math> as earth abundant cathode material for Na-ion batteries</i>	P-42
<b>H. Drulis</b> (Institute of Low Temperatures and Structural Research PAS) <i>Preparation and properties of Ni-MH hydride cells based on <math>\text{La}_2\text{Ni}_9\text{Co}</math> hydrogen storage alloys doped with Al or Sn</i>	P-43
<b>P.P. Michalski</b> (Warsaw University of Technology) <i>Characterization of <math>\text{LiVBO}_3\text{F}</math> glass and nanomaterials</i>	P-44
<b>J. Kotwiński</b> (Warsaw University of Technology) <i>Thermal and electrical properties of mixed sodium-lithium salts containing <math>\text{N}(\text{CF}_3\text{SO}_2)_2^-</math> anion</i>	P-45
<b>J. Świder</b> (Jagiellonian University) <i>Studies of structural and electrochemical properties of electrode nanocomposites with self-assembled conductive carbon layers</i>	P-46
<b>K. Chudzik</b> (Jagiellonian University) <i>Electrochemical stability of modified spinel materials in wide potential range</i>	P-47
<b>K. Kwatek</b> (Warsaw University of Technology) <i><math>\text{Li}^+</math> conducting solid composite electrolytes formed in the <math>\text{LiTi}_2(\text{PO}_4)_3</math>–<math>\text{LiF}</math> system</i>	P-48
<b>K. Kwatek</b> (Warsaw University of Technology) <i>Lithium-ion conducting ceramic composites based on <math>\text{LiTi}_2(\text{PO}_4)_3</math> and <math>\text{Li}_{2.9}\text{B}_{0.9}\text{S}_{0.1}\text{O}_{3.1}</math> glass</i>	P-49
<b>W. Ślubowska</b> (Warsaw University of Technology) <i>Electrochemical performance of <math>\text{LiVPO}_4\text{F}</math> prepared by microwave radiation heating</i>	P-50
<b>M. Bakierska</b> (Jagiellonian University) <i>Bio-derived and hierarchically arranged carbons for high-performance lithium-ion batteries and supercapacitors</i>	P-51

<b>M. Bakierska</b> (Jagiellonian University) <i>Performance of li-ion batteries based on modified <math>\text{LiMn}_2\text{O}_4</math> spinel cathode materials and commercial carbon anodes</i>	P-52
<b>M. Lis</b> (Jagiellonian University) <i>Studies of structural changes induced by lithium extraction from <math>\text{LiMn}_2\text{O}_{3.99}\text{S}_{0.01}</math></i>	P-53
<b>R. Knura</b> (Jagiellonian University) <i>Studies of temperature effect on electrochemical performance of <math>\text{CCL/LiFePO}_4</math> nanocomposites with commercial anode</i>	P-54
<b>B. Hamankiewicz</b> (University of Warsaw) <i>Determination of physicochemical and electrochemical parameters of silicon-based electrode as an anode in lithium-ion battery</i>	P-55
<b>M. Krajewski</b> (University of Warsaw) <i>Structural, morphological and electrochemical properties of <math>\text{Li}_2\text{MnSiO}_4</math> composites</i>	P-56
<b>M. Przybylczak</b> (Institute of Non-Ferrous Metals) <i><math>\text{Na}_{0.4}\text{MnO}_2/\text{C}</math> composites as cathode materials for na-ion batteries</i>	P-57
<b>M. Rybski</b> (AGH University of Science and Technology) <i>Influence of vacancy defects and alloying on electronic properties of <math>\text{Li}_x\text{Co}_{1-y-z}\text{Ni}_y\text{Mn}_z\text{O}_2</math> from band structure calculations</i>	P-58
<b>M. Wilamowska-Zawłocka</b> (Gdansk University of Technology) <i>Composites based on silicon oxycarbide and carbon nanoparticles as anode materials for lithium-ion cells</i>	P-59
<b>P. Pólrolniczak</b> (Institute of Non-Ferrous Metals) <i>Novel silane-based electrolyte for high energy lithium-sulfur batteries</i>	P-60
<b>W. Zając</b> (AGH University of Science and Technology) <i>A-site composition as a factor tailoring disorder in <math>\text{La}_{2/3-x}\text{Li}_{3x}\text{TiO}_3</math> solid electrolyte</i>	P-61
<b>T. Polczyk</b> (AGH University of Science and Technology) <i>Surface engineered <math>\text{La}_{2/3-x}\text{Li}_{3x}\text{TiO}_3</math> perovskite for lithium solid-state batteries</i>	P-62
<b>ML. Di Vona</b> (University of Rome Tor Vergata) <i>Composite anion conducting polymers for electrochemical energy technologies</i>	P-63
<b>M. Szkoda</b> (Gdansk University of Technology) <i>Effect of the geometry of the titania nanotubes on the photoactivity of organic-inorganic junction</i>	P-64
<b>P. Kielczykowska</b> (AGH University of Science and Technology) <i>Integrated energy storage systems from solar panels for households</i>	P-65
<b>Tomasz K. Pietrzak</b> (Warsaw University of Technology) <i>Evidence of the metal-insulator transition in <math>\text{M}_x\text{V}_2\text{O}_5\text{--P}_2\text{O}_5</math> glasses and nanomaterials (<math>\text{M} = \text{Li}, \text{Na}, \text{Mg}</math>)</i>	P-66
<b>Tomasz K. Pietrzak</b> (Warsaw University of Technology) <i>Synthesis and characterization of nanocrystallized <math>\text{Li}(\text{Fe}_{1-x}\text{Mn}_x)_{0.88}\text{V}_{0.08}\text{PO}_4</math> cathode materials (<math>x = 0.25, 0.5, 0.75</math>)</i>	P-67
<b>Ł. Łańcucki</b> (AGH University of Science and Technology) <i>Structural and electrical properties of Cr and Y doped <math>\text{SrTiO}_3</math> porous materials</i>	P-68

## INVITED LECTURES



## PLENARY LECTURE:

### The role of defects and size for electrochemical energy storage

*Joachim Maier*

Max Planck Institute for Solid State Research  
Heisenbergstr. 1, 70569 Stuttgart, Germany  
e-mail: s.weiglein@fkf.mpg.de

Keywords: energy conversion, storage, batteries, defects, size effects

A mechanistic understanding of Li or Na storage in modern electrodes has to rely on defect chemistry (charge carrier chemistry). In contrast to the usual high temperature treatment, additional complications such as frozen-in defects, extensive defect interactions and anomalies in nanocrystalline have to be considered [1].

Of special interest are storage phenomena that involve interfaces, which demands understanding of charge carrier chemistry in space charge zones and mesoscopic systems [2]. Three examples are considered in greater detail: Job-sharing storage in  $\text{LiO}_2$ -Ru-composites [3], ultrafast synergistic mass storage and removal in composites of superionic conductors and graphite [4] and finally ultrafast storage kinetics in graphene [5].

#### REFERENCES

1. J. Maier, *Angewandte Chemie International Edition* **52** (2013) 4998
2. L. J. Fu, C. C. Chen, D. Samuelis, J. Maier, *Physical Review Letters* **112** (2014) 208301
3. J. Maier, *Nature Materials* **4** (2005) 805
4. C.-C. Chen, L.-J. Fu, J. Maier, *Nature* **536** (2016) 159
5. M. Kühne, F. Paolucci, J. Popovic, P. M. Ostrovsky, J. Maier, J. H. Smet, *Nature Nanotechnology*, in press, 2017

# Electronic structure calculations in materials converting energy

J. Tobola, B. Wiendlocha, J. Molenda\*, M. Rybski, S. Kaprzyk

Faculty of Physics and Applied Computer Science

\*Faculty of Energy and Fuels

AGH University of Science and Technology, Al. Mickiewicza 30, 30-059 Krakow, Poland

e-mail: tobola@ftj.agh.edu.p

Keywords: electronic band structure, thermoelectricity, Li-ion batteries, KKR-CPA

## INTRODUCTION

It is widely known that some bulk materials exhibiting specific physical properties may convert various forms of energy, i.e. due to thermoelectric, electrochemical or magnetocaloric phenomena. The conversion efficiency of such materials is strongly related to their electronic properties, namely electronic structure details that are responsible for transport, magnetic or electrochemical behaviours. In order to theoretically optimize their performance, more profound and reliable description of quantum mechanisms responsible for observed effects is required, which in turn demands first principles electronic structure calculations to allow for modeling of selected physical properties.

## RESULTS AND DISCUSSION

The Korringa–Kohn–Rostoker (KKR) [1-2] method based on Green function multiple scattering theory was used to calculate electronic band structure and relevant kinetic parameters of electrons on the Fermi surface. Moreover, the coherent potential approximation (CPA) was employed to account for chemical disorder effects (alloying, vacancy defects) on electronic structure [1]. In the first part of this work, recent results of electronic structure calculations as well as modeling of electron transport properties in selected thermoelectric (TE) bulk materials are discussed [3-5]. We focus mostly on effect of unusual electronic structure features (e.g. band convergence or interplay between nonparabolic dispersion relations and remarkable anisotropy of electron transport properties), intentional doping as well as the spin-orbit interactions on TE performance, which can be optimized by proper adjustment of carrier concentration for a given temperature range. Electron transport behaviors are directly related to electronic states near the Fermi energy and searching for accurate information on k-space electron features appears to be the key factor for reliable modeling, or even predicting, of TE behaviors. Fortunately, *ab initio* electronic band structure calculations combined with the Boltzmann transport theory were established to be a quite convenient way to study electron transport in materials. In practice, it is performed via highly accurate calculation of ground state properties of electrons near Fermi surface. Finite temperature effects, especially interesting in investigations of thermopower or electrical conductivity, are not explicitly taken into account in such calculations, but modifications of ground state electronic properties with temperature can be incorporated through the Fermi–Dirac function.

In the second part of this work, comprehensive experimental and theoretical studies on impact of electronic structure features on discharge curves in  $A_xMO_2$  ( $A = \text{Li, Na}$ ;  $M = \text{V, Co}$ ) battery systems are presented. Novel approach to explain apparently different characters of the discharge/charge curve in  $\text{Li}_x\text{CoO}_2$  (monotonous curve) and  $\text{Na}_x\text{CoO}_{2-y}$  systems (step-like curve) has been proposed as based on electronic structure calculations. In the case of  $\text{Na}_x\text{CoO}_{2-y}$  it was evidenced that the origin of the observed step-like character of the discharge/charge curve of  $\text{Na}_x\text{CoO}_{2-y}$  is due to the specific features of the electronic structure, arisen from the presence of the oxygen vacancies and sodium ordering. Unlikely, the semiconductor-metal crossover observed in  $\text{Li}_x\text{CoO}_2$ , when decreasing Li content, can be coherently explained by the Fermi level shift into the valence states, without apparent effect of defects on electronic states. The two aforementioned cases are compared to the  $\text{Li}_x\text{VO}_2$  system, where standard LDA calculations have failed, i.e. leading to metallic state unlike semiconducting one observed from electron transport measurements. The inclusion of extra electronic correlations (via  $U$  parameter) leads to the energy gap opening at the Fermi level, indicating that strong electronic correlations are presumably responsible for metal-semiconductor-metal crossovers.

## ACKNOWLEDGMENT

This work was partly supported by the Polish National Center of Science (NCN) under the grants DEC-2011/02/A/ST3/00124 and UMO-2015/19/B/ST8/00856

## REFERENCES

- [1] A. Bansil, S. Kaprzyk, P. E. Mijnarends, J. Tobola, *Phys. Rev. B* **60** (1999) 13396
- [2] T. Stopa, S. Kaprzyk, J. Tobola, *J. Phys. C: Cond. Matt. Phys.* **16** (2004) 4921
- [3] K. Kutorasiński, B. Wiendlocha, S. Kaprzyk, J. Tobola, *Phys. Rev. B* **8** (2014) 115205
- [4] K. Kutorasiński, B. Wiendlocha, S. Kaprzyk, J. Tobola, *Phys. Rev. B*, **91** (2015) 205201
- [5] B. Wiendlocha, K. Kutorasiński, S. Kaprzyk, J. Tobola, *Scripta Mater.* **111** (2016) 33
- [6] J. Molenda, D. Baster, M. Molenda, K. Świerczek, J. Tobola, *Phys. Chem. Chem. Phys.* **16**(2014)1484
- [7] A. Milewska K. Świerczek, J. Tobola, F. Boudoire, Y. Hu, D. K. Bora, B. S. Mun, A. Braun, J. Molenda, *Sol. St. Ionics* **263** (2014) 110
- [8] B. Gędziorowski, J. Tobola, A. Braun, J. Molenda, *Func. Mater. Lett.* **9** (2016) 1641006.

# Electronic structure “engineering” as a new approach to materials design for Li-ion and Na-ion batteries

Janina Molenda

AGH University of Science and Technology,  
Faculty of Energy and Fuels, Department of Hydrogen Energy,  
al. Mickiewicza 30, 30-059 Krakow, Poland  
e-mail: molenda@agh.edu.pl

Keywords: electronic model of intercalation process, layered transition metal oxides, transport properties

The author of this work basing on her own investigations of  $A_xMO_2$  cathode materials ( $A=Li, Na$ ;  $M=3d$ ) has demonstrated that the electronic structure of these materials plays an important role in the electrochemical intercalation process. Electronic model of intercalation process (EMI) is presented. The obtained globally unprecedented results of research on the electronic aspect of lithium and sodium intercalation into transition-metal compounds [1-3], indicating a direct relation between the electronic structure of cathode materials and the parameters of Li-ion and Na-ion batteries (character of discharge curve, energy density, current density), present the final step with regard to the determination of this extremely important relation and establish a new tool that can be used to design functional materials for Li-ion and Na-ion batteries.

During years of development, the methodology involving the measurement of structural and transport characteristics (electrical conductivity and thermoelectric power), electronic specific heat and oxygen K-edge NEXAFS studies as a function of the content of alkaline component at characteristic points of the discharge curve, supported by electronic structure calculations performed using KKR-CPA method with accounting for chemical disorder proved to be very efficient in complex cathodes systems such as  $Li_xCoO_2$ ,  $Li_xNi_{1-y-z}Co_yMn_zO_2$ ,  $Na_xCoO_{2-y}$  and  $Na_xCo_{1-y}Mn_yO_2$ .

In  $Li_xCoO_2$  system we showed strong correlation between electronic structure, character of the charge curve and transport properties evolution related to insulator-metal transition of Anderson type. Contrary to  $Li_xCoO_2$ , in  $Li_xNi_{1-y-z}Co_yMn_zO_2$  electrical conductivity decreases with lithium deintercalation degree. Results of KKR – CPA calculations exhibit quite unusual behaviour, related to the presence of the vacancy defects on oxygen sublattice. The formation of extra broad peaks inside the energy gap leads to its strong reduction and in general finite DOS values at  $E_F$  are seen for all Li contents. The observed irregular behaviours of temperature dependence of thermoelectric power and the change in its sign with Li content in  $Li_xNi_{0.55}Co_{0.35}Mn_{0.1}O_2$  and  $Li_xNi_{0.65}Co_{0.25}Mn_{0.1}O_2$  can be tentatively interpreted by variable DOS character due to the presence of extra peaks of O vacancy defects. The observed variations of the electromotive force of the  $Li/Li^+/Li_xNi_{0.9-y}Co_yMn_{0.1}O_2$  cells are in good

agreement with calculated variations of chemical potential of electrons (i.e. the Fermi level variations) of the cathode material.

We show that the observed step-like character of OCV discharge curve of  $Na/Na^+/Na_xCoO_{2-y}$  cell reflects the step-like character of  $E_F$  variation in peaked density of states of  $Na_xCoO_{2-y}$  related to oxygen nonstoichiometry (Fig. 1).

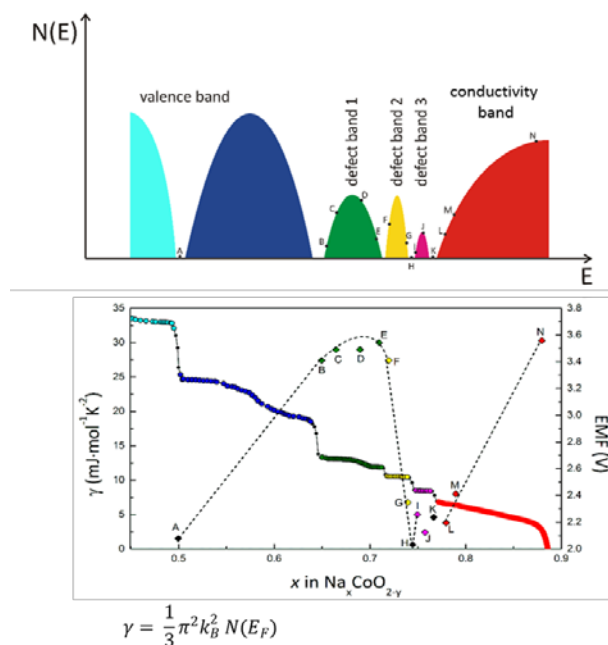


Fig. 1. DOS of  $Na_xCoO_{2-y}$  from electronic specific heat and step-like character of the discharge curve of  $Na/Na^+/Na_xCoO_{2-y}$  cell.

## ACKNOWLEDGMENTS

This work was funded by the National Science Centre Poland (NCN) under the “OPUS 10” programme on the basis of the decision number UMO-2015/19/B/ST8/00856 and “OPUS 12” programme on the basis of the decision number UMO-2016/23/B/ST8/00199.

## REFERENCES

- [1] J. Molenda, D. Baster, M. Molenda, K. Świerczek, J. Tobola, Phys. Chem. Phys. Chem. 16 (2014) 14845
- [2] J. Molenda, D. Baster, M. U. Gutowska, A. Szewczyk, R. Puźniak, J. Tobola, Funct. Mater. Lett. 7 (2014) 144000
- [3] J. Molenda, D. Baster, A. Milewska, K. Świerczek, D.B. Bora, A. Braun, J. Tobola, Solid State Ionics (2014)



# DFT sampling calculation studies on electrode/electrolyte interfaces in batteries

Yoshitaka Tateyama

Center for Green Research on Energy and Environmental Materials (GREEN) and Research and Services Division of Materials Data and Integrated System (MaDIS), National Institute of Materials Science (NIMS), 1-1 Namiki, Tsukuba, Ibaraki 305-0044, Japan  
Elements Strategy Initiative for Catalysts and Batteries (ESICB), Kyoto University, Kyoto University, Goryo-Ohara, Nishikyo-ku, Kyoto 615-8245, Japan  
e-mail: TATEYAMA.Yoshitaka@nims.go.jp

Keywords: solid-liquid & solid-solid interfaces, solid electrolyte interphase, electric double layer, space-charge layer

## INTRODUCTION

There remain many long-standing issues on interfacial phenomena in batteries. Representative is structure and characteristics of solid electrolyte interphase (SEI) formed in the anode / electrolyte interface. Recently, role of the cathode electrolyte interphase (CEI) in the cathode side has attracted much attention as well. In the field of all-solid-state battery (ASSB), the origin and the remedy of interfacial resistance, a most serious bottleneck, has been debated. Those interfacial phenomena are crucial for improving the performance and the reliability of the secondary batteries, whereas they have not been fully understood yet because of the difficulty in the in-situ measurements as well as accurate calculations.

To elucidate these issues from the theoretical/computational side, we have developed highly-efficient DFT-based sampling (free energy calculation) code, stat-CPMD, for supercomputers such as the K computer, a flagship supercomputer in Japan, as well as interface sampling techniques. Then, we have addressed (1) the formation mechanisms and the structural characters of SEI films at Li-intercalated graphite anode / EC-based organic electrolyte [1-3], and (2) investigated effects of the space-charge layer as well as the reaction layer on the interface states between the cathode and the sulfide solid electrolyte in ASSBs [4,5].

## RESULTS AND DISCUSSION

For the former, we found a novel mechanism of the VC additive effect on the EC solvent that VC passivates EC anion-radical generated by the reductive decomposition, in contrast to the conventional mechanism with sacrificial reduction of VC. Examining the aggregation and the adhesion of the decomposed organic components, we have proposed a “near-shore aggregation mechanism” in which the decomposed products aggregate in the near-shore region in the electrolyte and coalesce with the anode surface. Though not confirmed yet, this mechanism can give explanations consistent with the experimental observations. In addition to the organic SEI component, we have recently examined the characters of inorganic components such as LiF and Li<sub>2</sub>CO<sub>3</sub>.

As an ASSB model system, LiCoO<sub>2</sub> (LCO),  $\beta$ -Li<sub>3</sub>PS<sub>4</sub> (LPS), and LiNbO<sub>3</sub> (LNO) were selected for cathode, sulfide electrolyte, and buffer layer, respectively. We carried out first-principles calculation sampling of the several possible interface configurations, and obtained the stable structures and the electronic states. Besides, we calculated the site-dependent Li chemical potentials with respect to Li metal. The results indicate that the Li

depletion can proceed at the beginning of the charge process, which may correspond to the space-charge layer scenario, and the interposition of buffer layer can suppress the depletion. Furthermore, we evaluated the interfacial ion diffusion by examining possible exchange of cations between the cathode and the electrolyte. The results show that the Co and P mixing is preferred at the LCO/LPS interface, and the LNO interposition can suppress these mixings. Interestingly, the Li-depletion tendency still exists under these circumstances. Therefore, the Li-depletion is likely to be a major factor of the interfacial resistance.

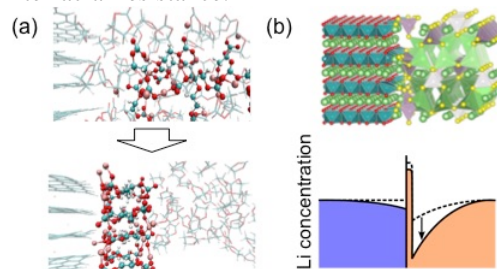


**Figure:** (a) Schematic mechanism of SEI formation, (b) Li depletion scheme for interfacial resistance in ASSBs.

## ACKNOWLEDGMENTS

These works were done in collaboration with Dr. K. Sodeyama and Dr. J. Haruyama (NIMS), Dr. Y. Okuno and K. Ushirogata (FUJIFILM Corporation), as well as Dr. Y. Kawamura and Dr. T. Baba (Toyota Motor Corporation). The author also appreciates Dr. K. Takada for helpful discussion.

## REFERENCES

- 1) K. Ushirogata, K. Sodeyama, Y. Okuno, Y. Tateyama, *J. Am. Chem. Soc.* **135**, 11967-11974 (2013).
- 2) K. Ushirogata, K. Sodeyama, Y. Tateyama, Y. Okuno, *J. Electrochem. Soc.* **162**, A2670-2678 (2015).
- 3) Y. Okuno, K. Ushirogata, K. Sodeyama, Y. Tateyama, *Phys. Chem. Chem. Phys.* **18**, 8643-8653 (2016).
- 4) J. Haruyama, K. Sodeyama, L. Han, K. Takada, Y. Tateyama, *Chem. Mater.*, **26**, 4248-4255 (2014).
- 5) J. Haruyama, K. Sodeyama, Y. Tateyama, *ACS Appl. Mater. Interfaces*, **9**, 286-292 (2017).

# Fundamental insights on battery materials and interfaces by surface science investigations

Rene Hausbrand

Surface Science Division, Institute of Material Science  
Darmstadt University of Technology, Jovanka-Bontschits-Str. 2  
D-64287 Darmstadt, Germany  
e-mail: hausbrand@surface.tu-darmstadt.de

Keywords: Li-ion batteries, photoelectron spectroscopy, electronic structure, electrode-electrolyte interface

## INTRODUCTION

Lithium-Ion batteries are important devices for present and future energy storage, offering high energy density and durability. Positive electrode (cathode) materials are predominantly transition metal oxides containing lithium, such as oxides with a layered structure. Electrolytes are either liquid in the case of conventional cells, or solid in the case of thin film cells or bulk solid electrolyte cells. The electronic (and ionic) structure of cathode materials is a key for their properties, such as electrode potential, degradation and reactivity.

This contribution gives an overview of surface science investigations on battery materials, addressing both electronic structure of layered-oxide cathode materials and cathode-electrolyte interface formation. Presently, space charge and reaction layer formation at cathode-electrolyte interfaces is of special interest due to its relevance for the application of high voltage cathode materials and the manufacture of solid state batteries.

## EXPERIMENTAL

Well-defined surfaces/interfaces are prepared and analyzed with surface sensitive analytical methods, predominantly with photoelectron spectroscopy (XPS, UPS). Such a surface science approach offers the possibility to analyze the electronic and chemical structure of surfaces and interfaces, allowing conclusions on the electronic structure of the bulk, on reactivity with other phases, and on electrochemical interface formation [1]. Specifically, we prepare layered-oxide thin films by sputter deposition and analyze their electronic structure in the pristine state and after electrochemical delithiation. Moreover, we evaluate interface formation with liquid or solid electrolyte by stepwise condensation of solvent or stepwise deposition of glassy solid electrolyte, respectively, and probe interface formation with other ionic compounds and interface evolution upon annealing.

## RESULTS AND DISCUSSION

Both experimental results on thin films and theoretical calculations demonstrate that the band structure of common  $\text{Li}(\text{Co},\text{Ni},\text{Mn})\text{O}_2$  layered cathode materials changes upon de-intercalation, i.e. that it is not rigid, showing increased TM3d-O2p hybridization at low lithiation states [2]. This behavior promotes O-anion oxidation and irreversible oxygen loss at high electrode potentials.

Low temperature solvent adsorption onto  $\text{LiCoO}_2$  thin films results in the formation of interface layers

and space charge layers, which can be related to catalytic surface activity and lithium (ion) transfer, respectively [3]. Nevertheless, we find high VB – HOMO offsets for all of these interfaces, which is usually identified with electrochemical stability. The results demonstrate that phenomena such as interface dipoles and surface states need to be considered to correctly describe electron transfer and reactivity.

In the case of  $\text{LiCoO}_2$ -LiPON interfaces we observe growth effects and space charge layer formation [4]. Annealing results in reaction, demonstrating that (also) this interface is not chemically stable, in agreement with recent calculations [5].

Additional work on  $\text{LiCoO}_2$  interfaces with other ionic compounds, such as LiF,  $\text{Li}_2\text{O}$  and LiPO, indicates that both interface dipole potentials as well as site energy of Li-ions control the double layer formation for the investigated interfaces. The observed interface phenomena can be understood in the framework of defect formation across the interface(s) and energy level diagrams of the (single) materials.

## CONCLUSIONS

The chemical instability of cathode materials in contact with electrolyte phases results for the investigated cathode materials in lithium and oxygen loss as well as surface layer formation. Investigations of electronic and ionic structure of cathode materials and their interfaces give fundamental insights into interface phenomena and their impact on surface layer formation as well as on Li-ion transfer, supporting the design of interfaces with improved properties.

## ACKNOWLEDGMENT

This work was supported by the German Science Foundation (DFG) and the Federal Ministry of Education and Research (BMBF). The contributions of Wolfram Jaegermann and Gennady Cherkashinin are gratefully acknowledged.

## REFERENCES

1. R. Hausbrand et al., *Progress in Solid State Chemistry* **42** (2014) 175
2. G. Cherkashinin et al., *Chemistry of Materials* **27** (2015) 2875
3. T. Späth et al., *Journal of Physical Chemistry C* **120** (2016) 20142
4. R. Hausbrand et al., *Material Science and Engineering B* **192** (2015) 3
5. Zhu, Y.Z. et al., *Acs Applied Materials & Interfaces* **7** (2015) 23685

# Pd-AB<sub>5</sub> – new hybrid anode in Ni-MH battery

A. Czerwiński<sup>1,2,\*</sup>, M. Łukaszewski<sup>1</sup>, K. Hubkowska<sup>1</sup>, M. Symonowicz<sup>1</sup> and M. Soszko<sup>2</sup>

<sup>1</sup>Warsaw University, Faculty of Chemistry, Pasteura 1, 02-093 Warsaw, Poland

<sup>2</sup>Industrial Chemistry Research Institute, Rydygiera 8, 01-793 Warsaw, Poland

\*e-mail: aczerw@chem.uw.edu.pl

Keywords: hydrogen sorption, hybrid hydride AB<sub>5</sub>+Pd anode

## INTRODUCTION

Palladium and its alloys with Rh, Ru and Pt represent a large group of materials absorbing hydrogen. Similar systems with less expensive metals can be used in batteries, fuel cells or for hydrogen storage. A new type of a hydride cell has been constructed and studied, in which the negative electrode (serving as the anode during discharging) will consist of a hybrid system of metal hydride-alloy components and an electrochemical capacitor [1], connected in parallel. The proposed system is innovative and neither articles nor patents have appeared on that subject so far [2]. This solution is based on limited volume electrodes (LVE) AB<sub>5</sub>-type [3] and Pd alloy electrodes [4].

## EXPERIMENTAL

All experiments were carried out in 6M KOH solution with the use of Autolab 30 in three-electrode system with a Pd+AB<sub>5</sub> working electrode, an Hg/HgO/6M KOH as reference electrode and a Au plate as auxiliary electrode. Before electrochemical measurements the solution was purged with Ar for 20 min., while during the measurements Ar stream floated above the solution. The temperature was controlled by a thermostat Lauda Eco Re 630. Cyclic voltammetry (CV), chronoamperometry (CA) and chronopotentiometry (CP) were used as the main experimental techniques.

## RESULTS AND DISCUSSION

The AB<sub>5</sub>-Pd system is optimized for obtaining maximum power from absorbed hydrogen oxidation processes during discharging, while during charging hydrogen would be inserted into anodic electrode system, mainly to the capacitor electrode, from where the charge is continuously transferred to AB<sub>5</sub> alloy electrode with higher capacity. The elaboration of this system would be a significant contribution to the development of future hydrogen power engineering, where it was an intermediate element in energy receiving from hydrogen between direct hydrogen combustion and fuel cells. Numerous fundamental studies on that system has been done and many physical and chemical parameters, including thermodynamic ones, were determined. In order to verify the idea of establishing a new type of a hybrid cell, the following preliminary experiment has been carried out. The cell was constructed, where the anode consisted of a thin layer electrodes made from AB<sub>5</sub> alloy and gold grid plated with thin Pd layer (ca. 1 μm), connected in parallel. 6 M KOH was used as the electrolyte. The analysis of currents obtained during

absorbed hydrogen oxidation reveals that in first 100 s the contribution of charge originating from hydrogen absorbed in Pd is ca. 42% of the total values originating both from AB<sub>5</sub> alloy and Pd. It results from the comparison of discharging currents obtained during the very first seconds that in the system containing H/Pd the current intensity and the cell power has raised by ca. 50%, although the total mass contribution of Pd in the hybrid cell Pd + H/AB<sub>5</sub> was only 0.36%.

## CONCLUSIONS

The preliminary results obtained for AB<sub>5</sub>+Pd hybrid system confirmed that:

1. the oxidation of absorbed hydrogen in H/Pd and H/AB<sub>5</sub> systems proceeds in the same potential range;
2. the process of hydrogen oxidation from Pd occurs much more faster than from AB<sub>5</sub> alloy, which is connected with the difference in overpotentials of that process and the rates in hydrogen diffusion in different metals.
3. the use of a hybrid system consisted of different types of hydrides leads to a significant increase in the power (discharging currents) of the hydride cell.

## ACKNOWLEDGMENT

This work is financially supported by the National Center of Science (NCN) grant No.2015/17/B/ST8/03377 (ID 289956) and University of Warsaw, Department of Chemistry.

## REFERENCES

1. M. Łukaszewski, A. Żurowski, A. Czerwiński, *J. Power Sources* **185** (2008) 1598
2. A. Czerwiński, M. Karwowska, K. Hubkowska, Patent Pending, PL P.414861, 2015 (Poland)
3. M. Karwowska, T. Jaroń, K. Fijalkowski; P. Leszczynski, Z. Rogulski, A. Czerwiński, *Journal of Power Sources* **263** (2014) 304
4. M. Łukaszewski, A. Czerwiński, *Journal of Solid State Electrochemistry* **15** (2011) 2489



# Identifying the elementary steps of electro-catalytic reactions

Ilan Riess

Physics Department, Technion-IIT,  
Haifa 3200003, Israel  
e-mail: riess@tx.technion.ac.il

The determination of the precise elementary steps in a catalytic or electro-catalytic process is, in many cases, not possible. This, for instance, is the case in identifying the steps of electrocatalysis at SOFC cathodes. The overall reaction at the cathode is clear, namely an  $O_2$  molecule is reduced and dissociated, oxygen ions  $O^{2-}$  are incorporated into a mixed conducting (MIEC) cathode or directly into a solid electrolyte (SE). However, the series of elementary steps are not well established. Among others the role of the oxygen vacancy is not really known. Is the oxygen vacancy required in the initial step of chemical adsorption to enable dissociation of the molecule or is it involved only in the final step of the reaction when a single oxygen ion, obtained from a molecule beforehand dissociated, enters a the vacancy?

We discuss a novel experimental method, suggested recently [1,2], for identifying, in a surface reaction, series of elementary steps which include dissociation of adsorbed molecules and end in a slow step. The method is demonstrated by applying it to cathodic reactions on oxides. It relies on  $^{18}O$  isotope exchange. The series of elementary steps is determined from the dependence of the concentration of  $^{16}O^{18}O$  molecule evaporated, on the oxygen partial pressure,  $P(O_2)$ , and dopant concentration in the oxide  $[A]$ , in any as in  $Y_2O_3$  doped  $ZrO_2$ . The dependence has the form  $r \propto P(O_2)^{m_1}[A]^{m_2}$ . In many cases the rate of  $^{18}O_2$  dissociation has a similar dependence  $J_0 \propto P(O_2)^{m_3}[A]^{m_4}$ . The four powers ( $m_1, \dots, m_4$ ) are shown to be specific for each series of elementary steps in a set of ten electro-catalytic processes examined. The method allows, among others, to determine in which step an oxygen vacancy is involved.

The method is of fundamental significance. The  $r(^{16}O^{18}O)$  and  $J_0$  vs.  $P(O_2)$  and  $[A]$  relations are first shown to hold for two consecutive reactions.<sup>1,2</sup> The latter allows to identify a whole series of elementary steps which include dissociation of the oxygen molecule and which ends by a slow step. The fast elementary steps are combined into a first fast reaction which is followed by a slow step as the second reaction. The method can be applied to other materials. In the case of exposure of an hydride to  $D_2$  and evaporation of HD, slight changes are introduced into the method in order to account for the isotope mass dependence of the chemical reaction constants. ter of the discharge curve of  $Na/Na^+/Na_xCoO_{2-y}$  cell.

## REFERENCES

1. I. Riess, Solid State Ionics, **280**, 51 (2015).
2. I. Riess, Solid State Ionics, (in press).

# Triode fuel cells

**Constantinos G. Vayenas<sup>1,2</sup>**

<sup>1</sup>Department of Chemical Engineering, University of Patras, Caratheodory 1 St,  
GR-26504 Patras, Greece

<sup>2</sup>Academy of Athens, Panepistimiou 28 Ave., GR-10679 Athens, Greece  
e-mail: cg.vayenas@upatras.gr

Triode operation of fuel cells is an alternative approach for enhancing fuel cell power output under severe poisoning conditions which lead to high overpotentials. This innovation was developed in 2004, applied firstly on SOFCs and later on PEMFCs [1-5]. In a triode fuel cell, in addition to the anode and the cathode, there is a third auxiliary electrode in contact with the solid electrolyte (e.g. polymer electrolyte membrane in the case of PEMFCs). This electrode forms together with the cathode, a second (auxiliary) electric circuit operating in parallel with the conventional main circuit of the fuel cell (Figure 1). The auxiliary circuit runs in the electrolytic mode, pumping ions (i.e. protons in the case of a PEMFC) from the cathode to the auxiliary electrode. In this way, imposition of a potential difference between the auxiliary electrode and the cathode permits the primary circuit of the fuel cell to operate under previously inaccessible, i.e. larger than 1.23 V, anode – cathode potentials. This ability introduces a new controllable variable in fuel cell operation and can lead to significant increase in the power output of a fuel cell, and can also decrease overpotential losses at the anode and cathode electrodes, leading to an enhancement of the overall thermodynamic efficiency. Two parameters are used to quantify the performance of a triode cell, i.e. power enhancement ratio,  $\rho$  ( $= P_{fc}/P_{fc}^0$ ) and the power gain ratio  $\Lambda$  ( $= \Delta P_{fc}/P_{aux}$ ), where  $P_{fc}, P_{fc}^0$  is the power in triode and conventional mode respectively,  $P_{aux}$  is the power sacrificed in the auxiliary circuit and  $\Delta P_{fc}$  the increase in the fuel cell power output.

A simple mathematical model based on Kirchhoff's laws is presented, describing conventional fuel cell operation which enables one to extract the ohmic resistance values between the three electrodes which are all in electrolytic contact. Subsequently, a similar model, also based on Kirchhoff's laws, can describe the triode operation, using the resistance values extracted from conventional operation and allowing for the computation of the power enhancement ratio,  $\rho$ , and the gain ratio  $\Lambda$ , as a function of the pre-calculated resistances, the geometry and operating conditions of the fuel cell. This model also provides the boundary conditions for solving, via finite differences, the Nernst-Planck equation inside the electrolyte during triode operation. The model solution has demonstrated the crucial role of the ionic resistance between anode and auxiliary electrode and was used in the development of a novel, more efficient triode assembly which was studied under humidified hydrogen (3%

H<sub>2</sub>O) as well as under CO poisoning mixtures of hydrogen (3% H<sub>2</sub>O – CO) in a PEMFC unit.

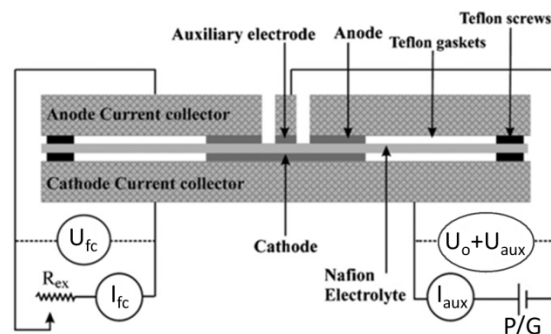


Figure 1: Schematic of the triode fuel cell concept, showing the geometry of the triode PEM fuel cell and the electrical circuits. The fuel cell cathode acts simultaneously as an electrode of the auxiliary circuit. P/G: potentiostat–galvanostat.

## REFERENCES

- [1] S.P. Balomenou, C.G. Vayenas. Journal of The Electrochemical Society, 151, 11 (2004), A1874.
- [2] S.P. Balomenou, F. Sapountzi, D. Presvytes, M. Tsampas, C.G. Vayenas. Solid State Ionics, 177 (2006), 2023-2027.
- [3] C. R Cloutier & D. P. Wilkinson, Triode Operation of a Proton Exchange Membrane (PEM) Methanol Electrolyser. ECS Trans. 25, 47–57 (2010).
- [4] F.M. Sapountzi, S.C. Divane, M.N. Tsampas, C.G. Vayenas, Electrochimica Acta, 56 (2011), 6966-6975.
- [5] F.M. Sapountzi, M.N. Tsampas, C. Zhao, A. Boreave, L. Retailleau, D. Montinaro, P. Vernoux. Solid State Ionics, 277 (2015), 65-71.

# High temperature electrolysis using proton conducting ceramic electrolytes

Truls Norby

Department of Chemistry, University of Oslo,  
SMN, FERMIØ, Gaustadalleen 21, NO-0349 Oslo, Norway  
E-mail: truls.norby@kjemi.uio.no

Renewable energy needs to be converted to, stored, transported, and used as hydrogen and other fuels and chemicals. Conversely, production of hydrogen, fuels, and fertilizers and other chemicals, needs to be based on future renewable rather than today's fossil energy. This will make electrolysis of water of increasing importance. In the presence of renewable or waste heat or steam – like from industrial plants or geothermal or solar-thermal sources – high temperature electrolysis of superheated steam can in principle be done at much higher electrical efficiency than at near-ambient temperatures. A solid oxide electrolyser (SOE) extracts oxide ions from steam, making pure dry oxygen on one side and hydrogen mixed with steam on the other. In comparison, a proton ceramic electrolyser (PCE) extracts protons from steam, making pure dry hydrogen on one side and a mixture of steam and oxygen on the other. This enables the PCE to be operated more safely (no undiluted compressed oxygen), produce pure dry hydrogen directly and at the highest available (total) pressure of the electrolyser, and avoid the risk of oxidation of the Ni hydrogen-side electrode in the case of too low current (and hence hydrogen to steam ratio). Moreover, the PCE can in principle operate at somewhat lower temperature than the SOE due to a lower activation energy for proton mobility compared to that of oxygen vacancies.

However, materials, components, and system developments have reached a far less mature stage for PCEs than for competing types of electrolyses. Challenges addressed today comprise in particular aspects of the electrolyte (normally Y-doped BaZrO<sub>3</sub>-based; synthesis and sintering reproducibility, stability, mechanical properties, grain boundary resistance, proton-acceptor-trapping, p-type electronic conductivity at the oxygen side) and the oxygen side electrode (typically doped or double transition-metal perovskites; hydration and partial proton conduction, stability in steam, compatibility with electrolyte). In addition come challenges related to sealing, interconnects, and scale-up.

We will look at current advances in the above-mentioned topics, as well as developments of segmented-in-series tubular electrolyser cells and how they can be assembled in multi-tubular units and modules for serving hydrogen supply needs at different scales. We will also look at developments towards metal-supported planar PCEs. Finally, we will look briefly at principles for using PCEs in co-electrolysis of steam and CO<sub>2</sub> to syngas and at extraction of hydrogen from natural gas using renewable electricity at unprecedented efficiency and –

in the right market situation – lowest cost of hydrogen with CO<sub>2</sub> sequestration built in where desired.



## Degradation mechanisms of Solid Oxide Cells (SOC)

**Mogens B. Mogensen**

Technical University of Denmark,  
Frederiksborgvej 399, Building 780,  
4000 Roskilde  
E-mail: momo@dtu.dk

Recently, our understanding of the degradation of solid oxide fuel cells (SOFCs) and solid oxide electrolysis cells (SOECs) have improved significantly. The lecture will be about the common solid oxide cell type consisting of nickel - yttria stabilized zirconia (Ni-YSZ) support and Ni-YSZ fuel electrode, YSZ electrolyte,  $\text{Gd}_2\text{O}_3$  substituted ceria (CGO) reaction barrier layer, and perovskite structured oxygen electrode of either lanthanum strontium cobalt ferrite (LSCF) or lanthanum strontium cobaltite (LSC). The most important degradation mechanisms of this cell type will be briefly explained. This SOC is fully reversible in the sense that it works almost equally well in both electrolysis and fuel cell mode, and actually, the degradation mechanisms are associated with the mode of operation to an extent that the degradation mechanisms also are kind of reversible, i.e. the degradation mechanisms may be totally suppressed by alternating the operation mode between fuel cell and electrolysis cell with a few hours interval. A brief description of measures against degradation in each operation mode by correct cell design and in particular correct operation will also be given.

# **Ion conduction in polymer membranes: application for electrochemical energy technologies**

**Philippe Knauth**

Aix Marseille University (AMU), CNRS, UMR 7246 Madirel, Marseille, France  
and International Associated Laboratory "Ionomer Materials for Energy"  
(AMU, Univ. Rome Tor Vergata, CNRS)  
E-mail: philippe.knauth@univ-amu.fr

Ionomer membranes are nanostructured materials, where the hydrophobic polymer backbone domains are separated by hydrated nanochannels containing the ionic groups (at the interfaces) and hydrated ions that can migrate in an electric field.

Such membranes can be used as electron-blocking and ion conducting separator in various electrochemical energy technologies, such as polymer fuel cells and electrolyzers, lithium-ion and redox flow batteries.

In my talk, I will present some of our recent results, including the synthesis and properties of cation-conducting [1,2], anion-conducting [3-7] and amphoteric polymers [8,9] and the electrochemical deposition of ionomer separators [10-12].

1. P. Knauth et al. Chemomechanics of acidic ionomers: Hydration isotherms and physical model, *J. Power Sources*, 267, 692 (2014).
2. R. Narducci et al. Cation-conducting ionomers made by ion exchange of sulfonated polyetheretherketone. *Membr. Sci.*, 465, 185 (2014).
3. M.L. Di Vona et al. Anion-conducting ionomers: Study of type of functionalizing amine and macromolecular cross-linking, *Int. J. Hydrogen Energy*, 39, 14039 (2014).
4. L. Pasquini et al. Anion-conducting sulfaminated aromatic polymers by acid functionalization, *RSC Advances*, 5, 56636 (2015).
5. L. Pasquini et al. Ionic Conductivity and Fluoride Ion Diffusion Coefficient in Quaternized Polysulfones, *ChemPhysChem*, 16, 3631 (2015).
6. R. Narducci et al., Mechanical properties of anion exchange membranes by combination of tensile stress-strain tests and dynamic mechanical analysis, *J. Polymer Sci. B: Polymer Physics*, 54, 1180 (2016).
7. L. Pasquini et al. Effects of anion substitution on hydration, ionic conductivity and mechanical properties of anion-exchange membranes, *New Journal of Chemistry*, 40, 3671-3676 (2016).
8. R. Narducci et al., Low Permeability PEEK-based Ampholytic Membranes, *ChemPlusChem*, 81, 550 (2016).
9. P. Knauth, L. Pasquini, M. L. Di Vona, Comparative study of the cation permeability of protonic, anionic and ampholytic membranes, *Solid State Ionics*, 300, 97-105 (2017).
10. V. Morizur et al. New aromatic polymer electrolytes for application in lithium metal batteries, *New Journal of Chemistry*, 40, 7840 (2016).

11. M. Braglia et al. Anodic Electropolymerization of Sulfonated Poly(phenyl ether): Study of Precursor Isomers and Polymer Growth, *ChemistrySelect* 1, 3114 (2016).

12. I. V. Ferrari et al. Electrochemically engineered single Li-ion conducting solid polymer electrolyte on titania nanotubes for microbatteries, *J. Power Sources*, in press (2017).

# New strategies in designing electrolytes for ambient temperature batteries

W. Wiczorek, M. Dranka, P. Jankowski, T. Trzeciak and J. Zachara

Faculty of Chemistry

Warsaw University of Technology, Noakowskiego 3, 00-664 Warszawa, Poland

e-mail: wladek@ch.pw.edu.pl

Keywords: electrolytes, water, ionic liquids, oligoethers, batteries

## INTRODUCTION

The objective of the present work is to explore water-based electrolytes and apply such novel, green electrolyte in different types of modern batteries including lithium-ion, lithium-air, lithium-sulphur and sodium-ion batteries. Application of aqueous electrolytes solves very important troubles affecting present battery technologies, with organic carbonates based electrolyte: danger of ignition, toxicity, environmental hazards and difficult recycling.

Hereby we propose new generation of batteries that contains concentrated water based electrolytes. In the present work by changing composition and structure of these electrolytes we strongly believe that we can enhance electrochemical stability in comparison with standard aqueous electrolytes. Key point in this concept is incorporation of TDI salts family. The proposed mechanism of electrolyte stability enhancement has been proved by Warsaw University of Technology in polyglycol system, since polyglycols and water molecules have similar coordination properties. Despite narrow electrochemical stability window of water (1.23 V), our preliminary studies evidenced that water molecules trapped in LiTDI complexes are less sensitive to electrochemical decomposition.

Contrary to commercial batteries, this new battery type will exhibit high safety level and will be environmental friendly: widespread, non-toxic and non-inflammable. Moreover, the replacement of organic based electrolyte by aqueous one will lead to a drastic reduction of the cost. Water has high dielectric constant and donor number, which influences high dissociation degree resulting in high conductivity of such solution. Unfortunately, the electrochemical stability of water is usually poor, whereby it has not been considered to application in high-voltage batteries for a very long time. Recent studies show that it is possible to extend stability window of water-based electrolytes by proper adjustment of electrolyte composition. A proof of concept has been tested and confirmed by K. Xu in US Army Laboratory using well-known commercially available lithium salt – lithium bis (trifluoromethylsulfo) imide LiTFSI.

Our initial calculations show that highly aggregated LiTDI-water systems exhibit extraordinary electrochemical stability enabling them to operate in high-voltage modern batteries. Even higher electrochemical stability can be obtained by replacing some amount of water with ionic liquid or monodentate solvent molecules (e.g. EC, PC etc.).

This concept has been recently proved for glyme based system.

In the present work this idea is significantly broaden to the ability of specific interactions between new types of anions and water molecules. It is a complete change of thinking leading to safer battery since water is usually considered as a natural “enemy” in *ex definitio* non aqueous systems. The observed phenomena might be valid not only for Li-ion but also for similar systems like Na-ion batteries but possibly also for Li-S and Li-air systems.

# Reduced-graphene-oxide as active support for platinum and non-noble metal catalysts during oxygen electroreduction

*Paweł J. Kulesza<sup>a</sup>, Beata Dembinska, Sylwia Zoladek<sup>a</sup>, Iwona A. Rutkowska<sup>a</sup>, Krzysztof Miecznikowski<sup>a</sup>, Enrico Negro<sup>b</sup>, Vito Di Noto<sup>b</sup>*

<sup>a</sup>Faculty of Chemistry, University of Warsaw, Pasteura 1, PL-02-093 Warsaw

<sup>b</sup>Department of Industrial Engineering, Università degli Studi di Padova in Department of Chemical Sciences, Via Marzolo 1, 35131 Padova, Italy

Keywords: electrocatalysis, oxygen reduction, fuel cell research

The present study refers to a novel and unique approach of fabrication and deposition of gold nanoparticles on the surfaces of reduced graphene oxide and multi-walled carbon nanotubes. Among important issues is application of inorganic (rather than organic) capping ligand, heteropolymolybdate, to modify and stabilize (as well as probably also to link with the oxygen or hydroxyl groups on graphene surfaces) gold nanoparticles. During operation in alkaline medium or neutral media, polyoxometallates disappear but catalytically highly active gold remains and it exhibits excellent stability. The resulting material has occurred to show highly potent electrocatalytic properties toward electroreductions of oxygen in alkaline solution. What is even more important is that both carbon nanotubes and graphene have occurred to act effectively as carriers for gold nanostructures. Mutual activating interactions are feasible. The fact, that the optimum graphene-based catalytic system produced the oxygen reduction peak current comparable to that observed at the model platinum containing catalyst, would imply the efficient four-electron-type reduction mechanism.

The reduced graphene-oxide-supported gold nanoparticles and traces of iridium have also been considered here together with loadings of platinum as catalytic materials for reduction of oxygen in alkaline and acid media, respectively. Comparison is made to the analogous systems based on conventional Vulcan carbon carriers. Gold nanoparticles are prepared by the chemical reduction method, in which the NaBH<sub>4</sub>-prereduced Keggin-type phosphomolybdate heteropolyblue acts as the reducing agent for the precursor (HAuCl<sub>4</sub>). It is reasonable to expect that the polyoxometallate-assisted nucleation of gold has occurred in the proximity of oxygenated defects existing on carbon substrates; and the Au nanoparticles (Au loading, 30 μg cm<sup>-2</sup>) remain well-dispersed on the carbon as evident from transmission electron microscopy. High electrocatalytic activity of the reduced-graphene oxide-supported Au nanoparticles toward reduction of oxygen in alkaline medium is demonstrated using cyclic and rotating ring-disk electrode (RDE) voltammetric experiments. Among important issues are possible activating interactions between gold and the support, as well as presence of structural defects existing on poorly organized graphitic structure of reduced graphene oxide (as

evident from Raman spectroscopy). When using the silica or titania functionalized reduced graphene oxide as carriers for Au (or Ir) and Pt nanoparticles, the resulting systems have exhibited typically higher (certainly not lower) O<sub>2</sub>-reduction currents (relative to those recorded at conventional Vulcan-supported Pt at the same loading) in acid medium (0.5 M H<sub>2</sub>SO<sub>4</sub>). The RDE data are consistent with even lower formation of hydrogen peroxide. Furthermore, the durability of this family of catalysts was outstanding. Finally, by doping the reduced graphene oxide supported Pt with traces of Ir (<1 μg cm<sup>-2</sup>), decreases amounts of produced H<sub>2</sub>O<sub>2</sub> (<1%) at potentials 0.6 V (vs RHE) or lower. In conclusion, the proposed system can function as active support for dispersed Pt nanoparticles leading to their high activity (even at loadings as low as 30 μg cm<sup>-2</sup> during electroreduction of oxygen both in alkaline and acid media).

Graphene-type carbon nanostructures have also been explored as supports (carriers) for dispersed metallic silver nanocenters which exhibit electrocatalytic activity toward reduction of oxygen in alkaline media. To facilitate fabrication, immobilization and distribution of Ag(0) nanoparticles, various types of graphene (e.g. reduced graphene oxide, CF<sub>x</sub> graphene with carbon black) have been modified with the silver analogue of polynuclear Prussian Blue, namely with ultra-thin silver(I) hexacyanoferrate(II,III) layers. Following the heat-treatment step at temperatures as high as 400-600°C, some thermal decomposition of the cyanometallate network occurs and, consequently, metallic silver sites are generated. Their formation and distribution are facilitated by the voltammetric potential cycling in KOH electrolyte. The most promising electrocatalytic results with respect to the reduction of oxygen (the highest currents and the most positive electroreduction potentials) have been obtained when graphene nanostructures are combined with Vulcan XC-72R nanoparticles.

## ACKNOWLEDGEMENT

This work supported within Graphene Flagship Horizon 2020 Project of European Union. Partial support from *Maestro* Project of NCN, Poland is also appreciated.



# Shape-controlled titanium dioxide for photoelectrolysis

A. Trenczek-Zajac

AGH University of Science and Technology, Faculty of Materials Science and Ceramics,  
al. A. Mickiewicza 30, 30-059 Krakow, Poland  
e-mail: anita.trenczek-zajac@agh.edu.pl

Keywords: TiO<sub>2</sub>, narrow band-gap semiconductors, water splitting

## INTRODUCTION

There are several requirements that semiconductors used for photoelectrolysis have to fulfil to achieve high efficiency. The most important criteria are: the efficient absorption of visible light, an effective charge transfer, the limited recombination losses, and correctly adjusted the conduction and valence band in relation to the redox potentials of the water decomposition reaction. TiO<sub>2</sub> fulfils nearly all of these requirements, but its main drawback in terms of its application as a photoanode is its overly wide band gap  $E_g=3.0$  eV, resulting in an absorption edge that corresponds to UV. This means that the fundamental optical excitation requires wavelengths shorter than  $\sim 400$  nm, i.e. UV radiation which does not exceed 4% of the total solar spectrum. Among large number of different modifications of TiO<sub>2</sub> that have been proposed in order to achieve a better match between the absorption edge of TiO<sub>2</sub> with the solar spectrum functionalized structures based on shape-controlled metal oxides seem to be particularly interesting; especially heterostructures composed of TiO<sub>2</sub> and narrow band-gap semiconductor (NBG).

Different structure-architecture classes were proposed by Miller et al. [1]:

- *simple mixture of two compounds (e.g. TiO<sub>2</sub>-SnO<sub>2</sub>) – randomly distributed throughout oxides* – the electronic interactions between the components of the metal oxide semiconductor composite play an important role in conductivity and the photoelectrochemical properties of these systems. By varying the electronic structure of the composite, the characteristics of the heterogeneous photocatalysts can be changed.

- *well-defined interface in between two layers of compounds (e.g. Cu<sub>2</sub>O/TiO<sub>2</sub>), as in a bi-layer, where the Cu<sub>2</sub>O is the top layer deposited onto the TiO<sub>2</sub> layer* - this type of heterostructures allows easier modification of well-defined interfaces, including diffusion across the junction, or the possibility of creating new mixed phases. However, due to a smaller surface area and the fact that only one of components is available for interaction (e.g. with gas), there are certain limitations with regard to its application.

- *structures decorated with second-phase particles (e.g. TiO<sub>2</sub>@CdS) – the TiO<sub>2</sub> host material is covered by particles of a second material (CdS)* – this class of heterostructures has been applied with great success in catalysis/photocatalysis, photovoltaics, gas sensing, and next-generation li-ion batteries.

The objective of this work was to develop a new strategy in relation to functionalized structures based on shape-controlled metal compounds. Heterostructures of TiO<sub>2</sub> and narrow band-gap semiconductors were the

main subject of this study. For a better understanding of this issue, the photoelectrochemical behavior of morphology-controlled TiO<sub>2</sub> were compared to that of functionalized TiO<sub>2</sub>/NBG structures. The synthesis and behavior of different types of structures that include particles dispersed onto titanium dioxide with different shape was analyzed taking into account their electronic and photoelectrochemical properties.

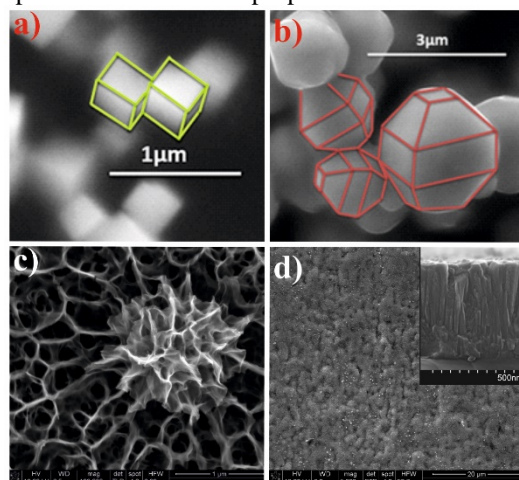


Figure 1. SEM images for TiO<sub>2</sub> NCs (a), flower-like nanostructures (b), and thin film (c).

## EXPERIMENTAL

The structural characterization was performed by means of X-ray Diffraction (XRD). Scanning Electron Microscopy (SEM) was applied in order to observe the differences in surface structure and morphology. The optical reflectance spectra were recorded with a Jasco V-670 double beam spectrophotometer equipped with a 150 mm integrating sphere over a wide wavelength range from 220 to 2200 nm. The activity towards water photoelectrolysis was tested in the photoelectrochemical cell (PEC).

## RESULTS AND DISCUSSION

Particles of narrow band-gap semiconductors were deposited using soft-chemistry methods on the surface of TiO<sub>2</sub> characterised by different dimensionality and morphology. It was found that deposition parameters and the TiO<sub>2</sub> substrate architecture influence on the photoelectrochemical behaviour of the modified materials.

## ACKNOWLEDGMENT

This work is supported by the National Science Centre (NCN) under grant 2016/21/B/ST8/00457.

## REFERENCES

1. D.R. Miller, S.A. Akbar, P.A. Morris, *Sensors and Actuators B* **204**(2014)250

# Operando studies of electrode/electrolyte interface in electrochemical capacitor

**K. Fic, E. Frackowiak,**

Institute of Chemistry and Technical Electrochemistry  
Poznan University of Technology, Sq. M. Skłodowskiej-Curie 5  
60-965 Poznan, Poland  
e-mail: elzbieta.frackowiak@put.poznan.pl

Keywords: supercapacitor, activated carbon, *operando* studies, electrode/electrolyte interface

## INTRODUCTION

The electrochemical capacitor (EC) with aqueous electrolyte presents many benefits in comparison to capacitor operating with organic electrolyte even if the cell operating voltage is limited by the thermodynamic stability of water, i.e. 1.23V. The aqueous medium allows getting a better charge propagation and conductivity, capacitor construction out of glove box and its low cost. However, water based capacitors suffer from limited energy because of their lower operating voltage. The capacitance and voltage are the two main components of the formula of energy. New attitudes to enhance the EC voltage range, as well as capacitance values, will be shown. Introducing redox active species in the electrolyte and/or at the electrode/electrolyte interface is a good strategy to involve faradaic reactions as an additional source of pseudocapacitance. The electrosorption of hydrogen into microporous carbon plays a dual role: an increase of capacitance values and a shift of operating potential to more negative values. Such redox species as halides (iodides  $I^-/I_2$ , bromides  $Br^-/Br_2$ ), pseudohalides (thiocyanates  $SCN^-$ ) are extremely beneficial for the positive electrode [1-5]. The effect of carbon porosity on charge accumulation, reversible energy storage, and power delivery is crucial; the pore size should match with the ion dimensions especially if they are bulky. Carbons with a suitable micro/meso ratio allow the redox active species to be efficiently used at the electrode/electrolyte interface.

## EXPERIMENTAL

Activated carbons in the form of powder/tissue were used as electrode materials. Carbon tissue served as self-standing electrodes without using a binder. All carbons were carefully characterized physico-chemically by nitrogen sorption, surface chemistry measurements. Most of the experiments were performed in Swagelok system where electrodes have a mass of 8-10 mg. The detailed testing of such capacitors (by galvanostatic charge/discharge, cyclic voltammetry, electrochemical impedance spectroscopy, floating, etc.) was performed to evaluate capacitance values, charge dynamics, self-discharge as well as energy and power values. Long-term stability of the capacitor system operating in various redox active electrolytes was investigated. Apart from detailed electrochemical characterization, *in-situ* Raman spectroscopy was used (DXR Thermo Fischer, USA). The evolution of gases was also monitored during polarization by mass spectrometry.

## RESULTS AND DISCUSSION

Most of the electrochemical experiments were performed in such electrolytic solutions as sulphates, nitrates, iodides of alkali metals. Extension of operating voltage was possible in the case of neutral medium, and a drastic increase of energy has been proved (Fig. 1).

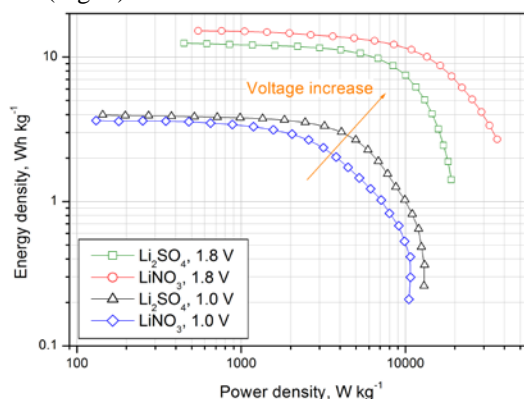


Fig. 1 Ragone plot for capacitor operating in two electrolytes and various voltage ranges

Different mechanisms of degradation take place at the operating voltage limit (1.8V). *Operando* techniques, e.g. *in-situ* Raman spectroscopy have been used in various electrolytes to evaluate the stability of the carbon electrode against oxidation in the presence of neutral and redox species. It has been shown that strong anodic polarization causes CO and CO<sub>2</sub> evolution and oxygen evolving was not observed. The limit of optimal potential for both electrodes and reversibility of redox reactions were precisely evaluated.

## ACKNOWLEDGMENT

Financial support by Swiss Contribution within the Polish Swiss Research Programme, Project PSPB 107/2010 INGE, and 03/31/DSPB/0334 is greatly acknowledged.

## REFERENCES

1. F. Béguin, V. Presser, A. Balducci, E. Frackowiak, *Adv. Mater.* 26 (2014) 2219–2251
2. M. He, K. Fic, E. Frackowiak, P. Novák, E.J. Berg, *Energy Storage Materials* 5 (2016) 111–115
3. M. He, K. Fic, E. Frackowiak, P. Novák, E.J. Berg, *Energy Environ. Sci.* 9 (2016) 623–633
4. K. Fic, M. He, E.J. Berg, P. Novák, E. Frackowiak *Carbon* (2017) accepted
5. B. Górka, P. Bujewska, K. Fic, *Phys. Chem. Chem. Phys.* 19 (2017) 7923–7935

# IV-VI semiconductors as topological materials

**T. Story, K. Dybko, P. Dziawa, W. Knoff, L. Kowalczyk, B.J. Kowalski, A. Łusakowski, A. Szczerbakow, M. Szot, B. Taliashvili, W. Wołkanowicz, M. Zięba**

Institute of Physics, Polish Academy of Sciences,  
al. Lotników 32/46, 02-668 Warsaw, Poland  
e-mail: story@ifpan.edu.pl

Keywords: topological insulators, IV-VI semiconductors, thermoelectricity

## INTRODUCTION

IV-VI compounds (PbTe, PbSe, PbS, SnTe, GeTe) and their alloys are narrow-gap semiconductors crystallizing in the rock-salt structure and known for very good thermoelectric and infrared optoelectronic properties [1,2]. Recently, these materials have been recognized as a new class of topological materials - topological crystalline insulators (TCI) [3,4]. In  $\text{Pb}_{1-x}\text{Sn}_x\text{Te}$  and  $\text{Pb}_{1-x}\text{Sn}_x\text{Se}$  substitutional alloys the chemical composition, temperature, and hydrostatic pressure induced band inversion takes place between conduction and valence bands. The terminal compounds SnTe and SnSe (in the rock-salt crystal structure) exhibit the inverted band ordering whereas in PbTe and PbSe the band ordering is topologically trivial. The TCI states were discovered by surface sensitive techniques such as angle-resolved photoemission spectroscopy (ARPES) and scanning tunneling spectroscopy [4-7]. In this work, we use the ARPES technique and the thermoelectric Nernst-Ettingshausen effect [8] to experimentally determine the temperature and chemical composition dependence of the band inversion and the topological transition in quaternary TCI materials  $\text{Pb}_{1-x-y}\text{Sn}_x\text{Mn}_y\text{Se}$  and  $\text{Pb}_{1-x-y}\text{Sn}_x\text{Mn}_y\text{Te}$ .

## EXPERIMENTAL

The rock-salt IV-VI topological (TCI) materials were grown as bulk monocrystals possessing (001) oriented crystal facets. We employed either the self-selecting vapor growth SSVG method ( $\text{Pb}_{1-x}\text{Sn}_x\text{Te}$  and  $\text{Pb}_{1-x}\text{Sn}_x\text{Se}$ ) or the Bridgman method ( $\text{Pb}_{1-x-y}\text{Sn}_x\text{Mn}_y\text{Te}$  and  $\text{Pb}_{1-x-y}\text{Sn}_x\text{Mn}_y\text{Se}$ ). Epitaxial layers of  $\text{Sn}_{1-y}\text{Mn}_y\text{Te}$  were also grown by molecular beam epitaxy (MBE) technique on  $\text{BaF}_2$  (111) substrate. The structural, electric, and optical properties of these TCI materials were experimentally examined by X-ray diffraction, electrical conductivity, Hall effect, and photoluminescence techniques. We experimentally studied the temperature ( $T=9\text{-}300\text{ K}$ ) and chemical composition dependence of the ARPES photoemission spectra for freshly in-vacuum cleaved (001) surface of bulk crystals. The effect of Mn was established by a direct comparison of the ARPES spectra for crystals with Mn content varying from 0 (a reference system) up to 3 at. %. To independently experimentally determine the band inversion temperature the Nernst-Ettingshausen effect was studied as a function of temperature.

## RESULTS AND DISCUSSION

The ARPES spectra revealed, below the topological transition temperature, the Dirac-like, metallic in-gap

surface states. The topological transition temperature can be controlled by either Sn or Mn content. The effect is particularly strong for Mn ions with just 3 at.% of Mn decreasing the transition temperature from 250 K to almost 0 (for crystals with  $x=0.35$ ). For the selenide system we studied the entire rock-salt composition range ( $x=0\text{-}0.4$ ) and constructed the composition - temperature phase diagram. We also showed that the maximum observed on the temperature dependence of the Nernst-Ettingshausen coefficient is a convenient indicator of the transition temperature. The composition dependence of the topological properties of IV-VI materials originates from the band structure changes. It is theoretically confirmed by our density functional theoretical (DFT) calculations of the effect of band inversion in substitutional IV-VI alloys. Upon increasing Mn content one observes a rapid increase of the band gap for the trivial band ordering but a decrease for the inverted one.

## CONCLUSIONS

The composition - temperature topological phase diagrams of  $\text{Pb}_{1-x}\text{Sn}_x\text{Se}$  and  $\text{Pb}_{1-x}\text{Sn}_x\text{Te}$  with Mn magnetic ions were experimentally determined based on the ARPES studies revealing a rapid decrease of the topological transition temperature to the TCI state upon increasing Mn content. This experimental finding is explained by considering the effect of Mn ions on the band gap of IV-VI crystals as theoretically shown in band structure calculations of  $\text{Pb}_{1-x}\text{Sn}_x\text{Mn}_y\text{Te}$  and  $\text{Pb}_{1-x-y}\text{Sn}_x\text{Mn}_y\text{Se}$  substitutional solid solutions.

## ACKNOWLEDGMENT

This work was supported by National Science Centre (NCN) project 2014/15/B/ST3/03833.

## REFERENCES

1. K. Dybko, M. Szot, A. Mycielski et al, *Applied Phys. Lett.* **108** (2016) 133902.
2. G. Karczewski, M. Szot, S. Kret et al., *Nanotechnology* **26** (2015) 135601.
3. Y. Ando, *J. Phys. Soc. Jpn.*, **82** (2013) 102001.
4. P. Dziawa, B.J. Kowalski, K. Dybko et al, *Nat. Mat.* **11** (2012) 1023.
5. B.M. Wojek, P. Dziawa, B.J. Kowalski et al, *Phys. Rev. B* **90** (2014) 161202.
6. B.M. Wojek M.H. Berntsen, V. Jonsson et al, *Nat. Commun.* **6** (2015) 8463.
7. P. Sessi, D. Di Sante, A. Szczerbakow et al, *Science* **354** (2016) 1269.
8. K. Dybko, P. Pfeffer, M. Szot et al, *New J. Phys.* **18** (2016) 013047.

# Hydrogen absorption in U-based alloys with *bcc* structure

*N.-T.H. Kim-Ngan<sup>1</sup>, L. Havela<sup>2</sup>, S. Sowa<sup>1,2</sup>, V. Buturlim<sup>2</sup>, M. Krupska<sup>2</sup> and M. Paukov<sup>2</sup>*

<sup>1</sup>Institute of Physics, Pedagogical University, Podchorążych 2, 30084 Krakow, Poland

<sup>2</sup>Charles University, Faculty of Mathematics and Physics, Ke Karlovu 5, 12116 Prague, Czech Republic

e-mail: tarnawsk@up.krakow.pl

Keywords: hydrogen, storage

## INTRODUCTION

Metallic uranium consisting of the orthorhombic  $\alpha$ -U phase (at and below the ambient temperature) strongly reacts to hydrogen at very low pressures (mbar), forming uranium-trihydride ( $\text{UH}_3$ ) which is the only binary uranium hydride.  $\text{UH}_3$  has two crystal structures: the metastable  $\alpha$ - $\text{UH}_3$  phase formed at low temperatures which slowly converts to the stable  $\beta$ - $\text{UH}_3$  phase at high-temperatures. Both phases are cubic with similar crystal densities.  $\text{UH}_3$  is a nasty pyrophoric powder which self-ignites in air and thus it is considered as a hazard during the storage of uranium metal. The high-temperature body-centered cubic  $\gamma$ -U phase can be retained down to room temperature by alloying with transition metals. The U-based alloys crystallizing in the cubic  $\gamma$ -U phase have a higher corrosion resistance and better accommodate radiation damage (than those with  $\alpha$ -U phase) and thus they are considered as better materials for nuclear fuels.

We have succeeded in a stabilization of the cubic  $\gamma$ -U phase down to room temperature by alloying with Mo, Zr, Pt, Nb, Ru, Ti. Especially, by using the splat-cooling technique with ultrafast cooling rate of  $10^6\text{K/s}$  we could reduce the necessary alloying amount in retaining such a phase [1]. We have performed the hydrogenation experiments and underlined the hydrogen absorption ability in these splat-cooled alloys as well as hydrogen influence on the electromagnetic properties.

## EXPERIMENTAL, RESULTS AND DISCUSSION

Splat cooled  $\text{U}_{1-x}\text{T}_x$  alloys ( $\text{T} = \text{Mo, Zr, Pt, Nb, Ru, Ti}$ ) were prepared by splat-cooling technique. For Mo, Pt, Nd, Ru alloying, the  $\gamma$ -U phase has developed fully at  $x = 11\text{-}15\text{ at.}\%$ , while for Zr and Ti it is stabilized at a higher amount of  $x = 30\text{ at.}\%$ . All splat-cooled alloys consisted of pure  $\gamma$ -U phase are very stable in the air and ambient hydrogen atmosphere. For the hydrogenation, the samples were placed in an alumina crucible into a reactor, which could be pressurized to 150 bar of  $\text{H}_2$  gas. The U-Mo and U-Zr alloys can absorb hydrogen but only upon applying pressures higher than 2.5 bars. [2,3]. The hydrogenation of U-Ti alloys requires much high pressures ( $> 50\text{ bar}$ ) and a longer time exposure to  $\text{H}_2$  gas. Hydrogenation of  $\text{U}_{1-x}\text{T}_x$  alloys consisted of  $\gamma$ -U phase leads to 3 different structures in the formed hydrides. Using Zr alloying we succeed to synthesize the (crystalline)  $\alpha$ - $\text{UH}_3$  phase as a pure phase without a transformation to  $\beta$ - $\text{UH}_3$ . Using Mo alloying leads to a formation of the  $\beta$ - $\text{UH}_3$  phase in a new form - the nanocrystalline one. Using Ti alloying, we obtain a mixture of crystalline  $\alpha$ - $\text{UH}_3$  and  $\beta$ - $\text{UH}_3$  in the

hydrides with 10-15 at.% Ti, while those with higher Ti concentrations reveal the nanocrystalline  $\beta$ - $\text{UH}_3$  structure. For determination of the total hydrogen concentration, we have performed the desorption in a closed evacuated volume at 500-600°C. The total amount of  $\text{H}_2$  released corresponds to 2.7 H atoms per 1 U atom in all investigated hydrides. Thus the general formula is  $(\text{UH}_3)_{1-x}\text{T}_x$ .

All  $\gamma$ -U alloys are weak Pauli paramagnets revealing superconductivity below 2.2 K [4]. The related hydrides  $(\text{UH}_3)_{1-x}\text{T}_x$  are ferromagnets with much enhanced Curie temperatures  $T_C$  reaching even if 200 K ( $T_C$  of  $\alpha$ - $\text{UH}_3$  and  $\beta$ - $\text{UH}_3$  is in the range of 170-180 K). The uranium magnetic moment is of about  $\mu_U = 0.9\mu_B/\text{U}$ . It is induced by hydrogen absorption as a result of a reduction of the  $5f$  bandwidth and an increase of the density of state at the Fermi level due to a reduction in the overlap of the  $5f$  wave functions between nearest U neighbors caused by a crystal structure expansion.

## CONCLUSIONS

Despite of a large flexibility of the crystal structure, the physical properties of hydrides formed from  $\gamma$ -U alloys are only weakly affected by alloying atoms. It indicates that the U-H interaction instead of U-U separation and related band effects plays a dominant role. A large hydrogen storage was found in these  $\gamma$ -U-based hydrides: the stoichiometry always corresponds to about 3 H atoms per 1 U atom. Besides, hydrogen can be easily released by heating up the materials in 500°-600°C in vacuum. It is crucial that such hydrides are not pyrophoric and their handling and use are safe. It opens a possibility to use them for hydrogen storage applications. Actually, it is a very practical technique to produce the  $\gamma$ -U alloys in a powder form by a combination of hydrogenation, followed by crushing of the brittle hydrides into powders and then by hydrogen desorption (of the powders) in a vacuum.

## ACKNOWLEDGMENT

This work was supported by the Czech Science Foundation (Grant 15-01100S). Experiments were partly performed at MLTL (<http://mltl.eu/>) supported within the program of Czech Research Infrastructures (project No. LM2011025).

## REFERENCES

1. N.-T.H. Kim-Ngan et. al., *J. Alloys Compd.* **580** (2013) 223-231.
2. I. Tkach et al., *Phys. Rev. B* **88** (2013) 060407R.
3. I. Tkach et al., *Phys. Rev. B* **91** (2015) 115116.
4. N.-T.H. Kim-Ngan et al., *J. Nucl. Mater.* **479** (2016) 287-294.

# Distribution of relaxation times as a tool to separate overlapped electrochemical processes in impedance spectra

*M.Stachowiak<sup>a</sup>, J.Bartoszek<sup>a</sup>, J.Karczewski<sup>b</sup>, S.F.Wang<sup>c</sup> Yi-Xin Liu<sup>c</sup> and P.Jasiński<sup>a</sup>*

<sup>a</sup> Faculty of Electronics, Telecommunications and Informatics, Gdansk University of Technology, 80-233 Gdansk, ul. Narutowicza 11/12, Poland

<sup>b</sup> Faculty of Applied Physics and Mathematics, Gdansk University of Technology, 80-233 Gdansk, ul. Narutowicza 11/12, Poland

<sup>c</sup> Institute of Materials Science and Engineering, National Taipei University of Technology, 1, Sec. 3, Zhongxiao E. Rd., Taipei 10608 Taiwan, R.O.C.  
e-mail: pijas@eti.pg.gda.pl

Keywords: distribution of relaxation times, impedance spectra, solid oxide cells

## INTRODUCTION

Impedance spectroscopy is a standard tool for investigation of electroceramic devices like fuels cells or electrolyzers. It allows investigating ohmic and polarization resistances and potentially link the polarization resistance with the limiting electrochemical process. However, frequently the electrochemical processes have very similar characteristic frequency and pointing the exact process is very challenging. Therefore, recently a distribution of relation times (DRT) is used to analyze the impedance spectra and better separate the processes [1,2]. This analysis is especially useful for the analysis of solid oxide electrolyzer cells (SOECs), for which more than 6 electrochemical processes can be foreseen. Although, the analysis is rather complicated, analysis tools start to be available on-line [3].

## EXPERIMENTAL

The analysis will be performed on both, simulated impedance spectra as well as measured on solid oxide cells. The measured spectra were collected using the Solartron 1260 impedance analyser coupled with the Solartron 1287 potentiostat/galvanostat.

## RESULTS AND DISCUSSION

In this work usefulness of DRT analysis will be discussed. Especially, the limitation of DRT analysis will be pointed and issues related to data discretization and selection of DRT parameters will be analyzed. The examples of DTR analysis will be provided and connected with exact DRT solutions of standard electrochemical processes. The data will be linked with results obtained on solid oxide cells. Issues related to polarization resistance analysis based on DRT plot will be discussed.

## ACKNOWLEDGEMENTS

This work was supported by the 2nd Polish-Taiwanese/Taiwanese-Polish Joint Research Project DZP/PL-TW2/6/2015 - Innovative Solid Oxide Electrolyzers for Storage of Renewable Energy granted by the National Centre for Research and Development of Poland and Ministry of Science and Technology of Taiwan.

## REFERENCES

- [1] B.A. Boukamp, Fourier transform distribution function of relaxation times; application and limitations, *Electrochim. Acta.* 154 (2015) 35–46. doi:10.1016/j.electacta.2014.12.059.
- [2] B.A. Boukamp, A. Rolle, Analysis and Application of Distribution of Relaxation Times in Solid State Ionics, *Solid State Ionics.* (2016). doi:10.1016/j.ssi.2016.10.009.
- [3] F. Ciucci, C. Chen, Analysis of Electrochemical Impedance Spectroscopy Data Using the Distribution of Relaxation Times: A Bayesian and Hierarchical Bayesian Approach, *Electrochim. Acta.* 167 (2015) 439–454. doi:10.1016/j.electacta.2015.03.123.



# MIEC-type ceramic membranes with enhanced transport properties

***Konrad Świerczek<sup>1\*</sup>, Hailei Zhao<sup>2,3#</sup>, Zhihong Du<sup>1,2</sup>, Zijia Zhang<sup>1,2</sup>, Yao Lu<sup>1,2</sup>***

<sup>1</sup>AGH University of Science and Technology, Faculty of Energy and Fuels, Mickiewicza 30, 30-059 Krakow, Poland <sup>2</sup>University of Science and Technology Beijing, School of Materials Science and Engineering, Beijing 100083, China

<sup>3</sup>The Beijing Municipal Key Laboratory of New Energy Materials and Technologies, Beijing 100083, China  
e-mail: \*xi@agh.edu.pl, #hlzhao@ustb.edu.cn

Keywords: oxygen transport membranes, MIEC oxides

## INTRODUCTION

Membrane technology, which was commercialized in many industrial applications, including treatment of chemicals, food, gas, water, wastewater, etc., emerged recently as having a great potential also in clean and renewable power applications [1]. Usage of dense ceramic membranes having mixed ionic-electronic conductivity (MIEC) is considered as very promising for production of a high purity hydrogen and oxygen via gas separation route, production and processing of syngas, e.g. by a partial oxidation of methane. For example, if the oxidation of methane is proceeded over oxygen-permeable MIEC-type membrane, separation and catalytic processes can be achieved in a single step with proper carbon monoxide to hydrogen ratio in the product ( $\text{CO}:\text{H}_2 = 1:2$ ), making such reforming effective (the reaction is exothermic) and relatively low cost. One may also consider steam reforming of methane proceeded over a hydrogen-permeable MIEC-type membrane. Another important application of ceramic membranes is in gas separation technology [2]. By using such the membrane, oxygen can be preferentially transferred from a gas mixture, allowing to obtain a high-purity  $\text{O}_2$  for further usage (e.g. in oxy-combustion processes), but also other gases can be separated from their mixtures, such as hydrogen, using hydrogen-permeable membrane. The most important issues, which are determining applicability of ceramic membranes, are related to their structural and transport properties, as well as chemical stability in a wide range of oxygen partial pressures at elevated temperatures, and limited reactivity in  $\text{CO}_2$ -containing atmospheres, with structural transformations, precipitation of secondary phases and oxygen vacancy ordering strongly hindering the oxygen flux through the oxide material.

In this review-type paper various approaches are discussed and summarized concerning development of functional MIEC-type membranes. The presented strategies cover chemical doping to stabilize highly oxygen-conducting cubic perovskite phase, formation of solid solutions and substitution with higher valence metals to increase amount of interstitial oxygens in Ruddlesden-Popper-type oxides, as well as creating functional layers and preparation of composite-type membranes.

## EXPERIMENTAL

Characterization of physicochemical properties of candidate MIEC-type membrane materials is of crucial importance. Precise determination of structural properties (high-temperature X-ray diffraction studies), thermogravimetric studies in various atmospheres, as well as measurements of transport properties (AC impedance spectroscopy, DC conductivity evaluation, calculation of

chemical diffusion coefficient  $D$  and surface exchange reaction coefficient  $K$ ), and oxygen flux through membrane are required to fully characterize considered compounds.

## RESULTS AND DISCUSSION

Majority of oxides exhibiting high mixed ionic-electronic transport possess either perovskite-type or perovskite-related (e.g. Ruddlesden-Popper-type) crystal structure. In such materials electronic component of the electrical conductivity is governed by a double exchange mechanism, while ionic component in  $\text{ABO}_{3-\delta}$  oxides proceeds by the oxygen vacancy mechanism. However, in some  $\text{A}_2\text{BO}_{4\pm\delta}$ -type materials (e.g. nickelates), apart from conduction of  $\text{V}_{\text{O}}^{\bullet\bullet}$ , interstitial oxygen are also mobile at elevated temperatures. Despite low activation energy of such interstitial transport, due to 2D-type conduction, the observed macroscopic conductivity of polycrystalline sinters is rather low. This might be improved by a functional layer having 3D conductivity. Also, a B-site doping allows for a modification of the oxygen content in the samples, which may prove useful in order to develop a highly-conducting, barium-free Cu-containing  $\text{A}_{2-x}\text{Cu}_{1-y}\text{M}_y\text{O}_{4\pm\delta}$  and  $\text{A}_{2-x}\text{Cu}_{1-y}\text{Ni}_y\text{M}_z\text{O}_{4\pm\delta}$ . In another approach, literature reports show that Ba- and Fe-containing oxides can be stabilized in the cubic perovskite phase by the appropriate chemical doping, yielding materials showing excellent oxygen permeation properties. Concept of a dual phase membranes is also evaluated in this paper, showing possible gains, but also arising drawback of such the approach.

## CONCLUSIONS

Different materials engineering methods are shown to be effective in the improvement of physicochemical properties of candidate oxides for MIEC membranes.

## ACKNOWLEDGMENTS

The project was funded by the National Science Centre, Poland on the basis of the decision number UMO-2015/19/B/ST8/00871.

## REFERENCES

1. A. Gugliuzza, A. Basile (Editors), *Membranes For Clean And Renewable Power Applications*, Woodhead Publishing Limited, 2014.
2. K. Li, *Ceramic Membranes For Separation And Reaction*, John Wiley & Sons Ltd, 2007.

# YOUNG SCIENTISTS FORUM

# Modified LMO cathode materials. From the idea to the product

M. Świątosławski<sup>\*1</sup>, M. Bakierska<sup>1</sup>, M. Lis<sup>1</sup>, K. Chudzik<sup>1</sup>, K. Mech<sup>2</sup>, M. Molenda<sup>1</sup>

<sup>1</sup>Jagiellonian University, Faculty of Chemistry, Ingardena 3, 30-060 Krakow, Poland

<sup>2</sup>AGH University of Science and Technology, Academic Centre for Materials and Nanotechnology, Mickiewicza 30, 30-059 Krakow, Poland

\*e-mail: m.swietoslowski@uj.edu.pl

Keywords: Li-ion battery, cathode material, LiMn<sub>2</sub>O<sub>4</sub>, commercialization, process scaling

## INTRODUCTION

This presentation will bring the overall work of scientists from Technology of Materials and Nanomaterials Research Group (Jagiellonian University) on the topic of modified spinel materials for Li-ion batteries. The main goal of this presentation is to show the audience the route from the idea of the material through its optimization, scaling the synthesis, up to preparation of the product ready for commercialization. I'd like to share our experience and point out mistakes which were made upon this over the decade of work. The presentation will focus on the lithium-manganese spinel materials modified by doping with various elements. The main enhancements and deterioration of material's parameters, the general influence of the dopants on the structure and properties of the material will be shown. The most important optimization factors like synthesis conditions, materials' morphology and composition will be illustrated and described in details.

## EXPERIMENTAL

All of the materials presented in this work were obtained using sol-gel synthesis. This type of preparation methods allowed good control of materials' morphology and chemical composition which were crucial in terms of achieving outstanding properties and electrochemical stability of presented LMO-based cathodes. The presentation will gather information of laboratory scale synthesis as well as the scaling process and details of construction of pilot scale production line of selected LMO-based cathode materials.

## RESULTS AND DISCUSSION

The complex evaluation of nanometric LMO-based cathode materials using wide range of research methods will be shown in the presentation. The comprehensive studies of physicochemical and electrochemical properties of the materials from the first synthesis attempts up to series of materials with various chemical composition will be presented.

## CONCLUSIONS

The family of modified LMO-based cathode materials which were designed and prepared by the Technology of Materials and Nanomaterials Research Group exhibit extraordinary working parameters and the developed synthesis procedure gives materials with

repetitive properties. Basing on this the developed technology is being prepared for commercialization.

## ACKNOWLEDGMENT

This work is financially supported by National Centre for Research and Development – Poland, under research grant no. LIDER/463/L-6/14/NCBR/2015.

## REFERENCES

1. M. Bakierska, M. Świątosławski, M. Gajewska, A. Kowalczyk, Z. Piwowska, L. Chmielarz, R. Dziembaj, M. Molenda, *Materials*, 9 (2016) 5, 366
2. M. Bakierska, M. Świątosławski, M. Molenda, R. Dziembaj, *Materials*, 9 (2016) 8, 696
3. M. Bakierska, M. Świątosławski, A. Chojnacka, D. Majda, R. Dziembaj, M. Molenda, *Materials Technology* 31 (2016) 11, 614-622
4. M. Molenda, M. Bakierska, D. Majda, M. Świątosławski, R. Dziembaj, *Solid State Ionics* 272 (2015) 127
5. M. Molenda, R. Dziembaj, Z. Piwowska, M. Drozdek, *Solid State Ionics* 179 (2008) 88-92
6. M. Molenda, R. Dziembaj, E. Podstawka, L.M. Proniewicz, Z. Piwowska, *Journal of Power Sources* 174 (2007) 613-618
7. R. Dziembaj, M. Molenda, *Journal of Thermal Analysis and Calorimetry*, 88 (2007) 1, 189-192
8. M. Molenda, R. Dziembaj, E. Podstawka, W. Łasocha, L.M. Proniewicz, *Journal of Physics and Chemistry of Solids* 67 (2006) 1347-1350
9. M. Molenda, R. Dziembaj, A. Kotwica, W. Łasocha, *Materials Science-Poland* Vol. 24, No. I. (2006)
10. M. Molenda, R. Dziembaj, D. Majda, M. Dudek, *Solid State Ionics* 176 (2005) 1705 – 1709
11. M. Molenda, R. Dziembaj, E. Podstawka, L.M. Proniewicz, *Journal of Physics and Chemistry of Solids* 66 (2005) 1761-1768
12. R. Dziembaj, M. Molenda, *Journal of Power Sources* 119-121 (2003) 121-124
13. R. Dziembaj, M. Molenda, D. Majda, S. Walas, *Solid State Ionics* 157 (2003) 81- 87L.

# In operando XRD studies as a tool for determination of lithium ions kinetics in electrode materials

Lukasz Kondracki<sup>1</sup>, Andrzej Kulka<sup>1</sup>, Konrad Świerczek<sup>1,2</sup>, Magdalena Ziąbka<sup>3</sup>, Janina Molenda<sup>1#</sup>

<sup>1</sup>AGH University of Science and Technology, Faculty of Energy and Fuels,  
Department of Hydrogen Energy, al. A. Mickiewicza 30, 30-059 Krakow, Poland

<sup>2</sup>AGH Centre of Energy, AGH University of Science and Technology,  
ul. Czarnowiejska 36, 30-054 Krakow, Poland

<sup>3</sup>AGH University of Science and Technology, Faculty of Materials Science and Ceramics,  
al. A. Mickiewicza 30, 30-059 Krakow, Poland

# e-mail: molenda@agh.edu.pl

Keywords relaxation methods; diffusion coefficient  $D$ ; surface exchange coefficient  $k$ ; *in operando* XRD

## INTRODUCTION

Various tools have been successfully developed in order to quantify transport coefficients of mobile species in solid state materials. In particular, electrical conductivity or mass relaxation measurements have been successfully utilized to determine values of self or chemical diffusion coefficient  $D$  and surface exchange coefficient  $k$  for various systems, including mixed ionic-electronic conductors. In this work a detailed *in operando* XRD investigations of structural properties of  $\text{Li}_x\text{Mn}_2\text{O}_4$  manganese spinel are shown to be a complementary, successful method of determination of  $D$  and  $k$  in the working electrode. Kinetics of lithium ions transport are estimated on the basis of rate of structural changes of the cathode material during a relaxation stage after a high current charge, i.e. during structural relaxation of the material.

## EXPERIMENTAL

For *in operando* XRD measurements, a custom-made gas-tight cell made from Teflon and stainless steel containers, joint by screws and sealed by gaskets was used. A beryllium window served as an X-ray transparent medium and a current collector at the same time. Duration of a single scan was set as 60 s, and the gathered data range covered (311) and (222) reflection peaks of the  $\text{LiMn}_2\text{O}_4$ . The electrochemical tests during *in operando* XRD measurements were performed using an Autolab PGSTAT302N potentiostat/galvanostat. Collection time of a single measurement (60 s) in comparison to the time of the GITT stages (180 s for charge and over 1000 s for relaxation) enabled us to capture the dynamic evolution of the unit cell parameters, which further served for determination of transport parameters of mobile lithium ions in  $\text{Li}_x\text{Mn}_2\text{O}_4$ -based electrode. The obtained XRD data were refined by Rietveld method with GSAS/EXPGUI set of software [1], comparison of *ex situ* XRD data with *in operando* XRD measurements was used in order to estimate the electrode placement in the  $z$ -axis, which was used as a constant in all subsequent Rietveld fittings. The obtained relaxation of the lattice cell parameter  $a$  of the spinel structure was fitted with ECRTOOLS [2].

## RESULTS AND DISCUSSION

Normalized changes of the lattice cell parameter  $a$  during relaxation process, along with relaxation-type

fitting curve for the same composition of  $x = 0.9$  are shown in Fig. 1.

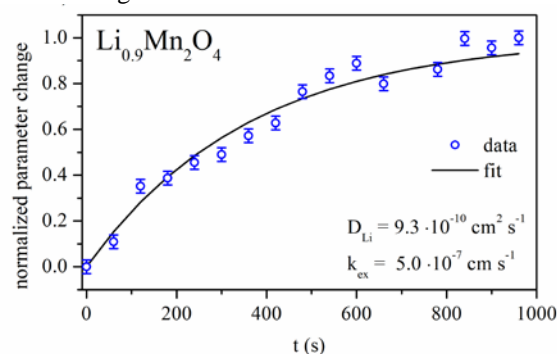


Fig. 1. Results of fitting of relaxation of the normalized lattice cell parameter  $a$  for lithium content  $x = 0.9$ .

The obtained results of lithium diffusion coefficient  $D$  are consistent with data found in literature derived from different techniques: GITT, PITT, and EIS.

## CONCLUSIONS

We have developed a novel, *in operando* XRD-based method of determination of transport coefficients of mobile lithium ions in working electrode. The developed approach is shown to be easily applicable, and can be successfully used for virtually all intercalation-type electrode materials displaying single-phase mechanism of deintercalation and linear dependence of structural features on mobile ion content. With comparison to data from different techniques (e.g. GITT, PITT or EIS), the effective diffusion length can be evaluated, and the obtained  $D$  and  $k$  coefficients are meaningful in terms of the absolute values and dependence on lithium content in the active material.

## ACKNOWLEDGMENT

The project was funded by the National Science Centre Poland on the basis of the decision number DEC-2012/05/E/ST5/03772 and UMO-2015/19/B/ST8/00856.

## REFERENCES

1. A.C. Larson, R.B. Von Dreele, Los Alamos Natl. Lab. Rep. LAUR (2000) 86–748
2. F. Ciucci, Solid State Ionics 239 (2013) 28–40

# Structural properties and ionic conduction mechanisms in doped ABO<sub>4</sub> oxides

*S. Wachowski, P. Winiarz, A. Mielewczyk-Gryn, K. Zagórski, P. Jasiński\*, M. Gazda*

Gdańsk University of Technology – Faculty of Applied Physics and Mathematics, Department of Solid State Physics, Narutowicza 11/12, 80-233 Gdańsk, Poland

\*Gdańsk University of Technology – Faculty of Electronics, Telecommunications and Informatics, Department of Biomedical Engineering, Narutowicza 11/12, 80-233 Gdańsk, Poland  
e-mail: swachowski@mif.pg.gda.pl

Keywords: lanthanum niobate, lanthanum arsenate, protonic conductors, solid state electrolytes

## INTRODUCTION

Acceptor doped lanthanum orthoniobate is a solid state proton conductor combining considerable proton conductivity, reaching  $10^{-3}$  S/cm at 900 °C under wet conditions, and chemical stability [1,2]. It is therefore considered as a potential candidate for a solid electrolyte in electrochemical devices, such as fuel cells, gas sensors, and electrolyzers.

Lanthanum orthoniobate undergoes a second order phase transition from tetragonal to monoclinic structure at about 500 °C, which is accompanied by an increase in the activation energy of the conductivity [3,4] and a nearly twofold change of the thermal expansion coefficient (TEC) [5,6]. This is disadvantageous from an applicational point of view. For instance, a significant change in TEC may yield thermal incompatibility between the electrolyte and electrodes which could lead to strain, cracking and, in the end, failure of the electrochemical device. This challenge can be tackled by substituting Nb by different isovalent elements, such as As, Sb, Ta, and V to alter the phase transition temperature [5]. Models have been proposed which relate the structural changes with fundamental properties of the substituents, e.g. different electronegativity [5], ionic radii [7] or coordination number [8], however, none of them gives the full description of these phenomena.

This work summarizes the studies on the influence of isovalent substitution on structural properties of lanthanum niobates and effects on the ionic conductivity of the materials.

## EXPERIMENTAL

Lanthanum niobate doped with antimony or arsenic has been synthesized with methods described elsewhere [5,9]. The structure of the samples has been determined by X-ray Diffraction method supported by Rietveld analysis. The microstructure was analysed with the use of Scanning Electron Microscopy with Energy Dispersive X-ray Spectroscopy.

The electrical conductivity has been measured by Electrochemical Impedance Spectroscopy. Brick Layer Model has been utilized to determine grain and grain boundary contributions to total conductivity. Conductivity has been measured as a function of temperature, oxygen and water vapour partial pressure for the separation of the influence of different charge species on the total conductivity.

The diffusion coefficient of oxygen ions has been determined by the isotope exchange method combined with Secondary Ion Mass Spectroscopy.

## RESULTS AND DISCUSSION

Measurements of the conductivity have shown a difference of total conductivity for approximately one order of magnitude higher in wet than in dry air. H-D isotope exchange experiment has shown that ratio of total conductivity in H<sub>2</sub>O and D<sub>2</sub>O humidified air is close to the value of  $1/\sqrt{2}$  within the temperature range between 400 and 800 °C. Moreover, conductivity as a function of  $p_{O_2}$  has shown that material is a predominantly ionic conductor. Diffusion coefficient measurement has revealed that fast diffusion path for oxygen ion is present along the grain boundaries, whereas inside the grains oxygen transport is slow.

## CONCLUSIONS

It has been shown that in wet oxidizing atmospheres, in the temperature range of 400 – 800 °C, protons are the dominating charge carriers in LaNb<sub>1-x</sub>Sb<sub>x</sub>O<sub>4</sub>. Therefore, LaNb<sub>1-x</sub>Sb<sub>x</sub>O<sub>4</sub> is a high-temperature proton conductor in this temperature range. Furthermore, the total conductivity depends on the Sb concentration in the compound mostly due to the impact of the substitution on the grain boundary conductivity levels. The highest measured conductivity value was about  $10^{-4}$  S/cm at 900 °C in wet air.

## ACKNOWLEDGMENT

This work was financially supported by the National Science Center, Poland Grant No. 2015/17/N/ST5/02813.

The authors would like to thank prof. R. Haugsrud and prof. S. Skinner for their support and contribution to this research.

## REFERENCES

- [1] R. Haugsrud, T. Norby, J. Am. Ceram. Soc. 90 (2007) 1116.
- [2] R. Haugsrud, T. Norby, Nat. Mater. 5 (2006) 193.
- [3] H. Fjeld, K. Toyoura, R. Haugsrud, T. Norby, Phys. Chem. Chem. Phys. 12 (2010) 10313.
- [4] T. Mokkelbost, I. Kaus, R. Haugsrud, T. Norby, T. Grande, M.-A. Einarsrud, J. Am. Ceram. Soc. 91 (2008) 879.
- [5] S. Wachowski, A. Mielewczyk-Gryn, M. Gazda, J. Solid State Chem. 219 (2014) 201.
- [6] T. Mokkelbost, H.L. Lein, P.E. Vullum, R. Holmestad, T. Grande, M.-A. Einarsrud, Ceram. Int. 35 (2009) 2877.
- [7] A.D. Brandão, J. Gracio, G.C. Mather, V.V. Kharton, D.P. Fagg, J. Solid State Chem. 184 (2011) 863.
- [8] F. Vullum, F. Nitsche, S.M. Selbach, T. Grande, J. Solid State Chem. 181 (2008) 2580.
- [9] T.S. Bjørheim, T. Norby, R. Haugsrud, J. Mater. Chem. 22 (2012) 1652.



# Structural and electrical properties of $\text{LiFe}_{1-x}\text{Mn}_x\text{BO}_3$ glasses

Agata Gołębiewska, Jakub S. Otrębski, Przemysław P. Michalski, Jan L. Nowiński, Jerzy E. Garbarczyk

Faculty of Physics

Warsaw University of Technology, ul. Koszykowa 75

00-662 Warszawa, Poland

e-mail: michalski@if.pw.edu.pl

Keywords: lithium borate glass, nanocrystallization, cathode materials for Li-ion batteries

## INTRODUCTION

Lithium borates containing transition metal ions with nominal composition  $\text{LiMBO}_3$  (where  $M = \text{Fe, Mn, Co, Ni} \dots$ ) are potential candidates for cathodes in Li-ion batteries. Due to the possibility of  $\text{Li}^+$  reversible intercalation/deintercalation, 2.7 V potential vs.  $\text{Li/Li}^+$  and gravimetric capacity reaching 220 mAh/g [1], these materials may find a usage in mobile devices like smartphones and notebooks. One of their disadvantages is low electronic conductivity – e.g. in case of  $\text{LiFeBO}_3$  only  $4 \cdot 10^{-7} \text{ S/cm}$ .

$\text{LiMBO}_3$  materials are currently not very well recognized in the literature – up to the moment there is no more than 100 publications devoted to this topic. The researchers are mostly concerned on electrochemical properties of polycrystalline materials; there are almost no works on structural and electrical properties of nanomaterials. Taking into account the as-mentioned advantages of borates, we strongly believe that they require closer attention, mostly on improving the conductivity values.

## EXPERIMENTAL

In this work, we would like to shed some light on structural and electrical properties of glass-ceramics composites obtained using a novel method of thermal nanocrystallization of precursor amorphous materials. This method is suitable for borate materials due to their good glass-forming properties [2]. Glasses of nominal composition  $\text{LiFe}_{1-x}\text{Mn}_x\text{BO}_3$  ( $x = 0, 0.25, 0.5, 0.75, 1$ ) were obtained using conventional melt-quenching method: stoichiometric amounts of precursors:  $\text{Li}_2\text{CO}_3$ ,  $\text{FeC}_2\text{O}_4 \cdot 2\text{H}_2\text{O}$ ,  $\text{Mn}(\text{CH}_3\text{COO})_2 \cdot 4\text{H}_2\text{O}$  and  $\text{H}_3\text{BO}_3$  were mixed in a mortar, melted at 1200 °C in non-oxidizing atmosphere for 15 minutes and rapidly quenched. The amorphousness of the as-prepared samples was confirmed with X-ray diffractometry (XRD Phillips X'Pert Pro) and thermal events occurring in the samples were observed with differential thermal analysis (DTA, TA Q600). Temperature-dependent X-ray measurements were performed in nitrogen atmosphere. Electrical conductivity was measured upon heating and subsequent cooling with impedance spectroscopy (IS, Solatron 1260) within wide frequency range 10 mHz – 10 MHz. The amplitude of oscillating voltage was equal to 0.1 V. The transference numbers of glassy and nanocrystalline materials were measured using Hebb-Wagner method.

## RESULTS AND DISCUSSION

The results for  $x = 0$  ( $\text{LiFeBO}_3$ ) are very encouraging. After proper thermal treatment, a material containing  $\text{FeBO}_3/\text{LiFeBO}_3$  nanograins embedded in glass with conductivity value equal to  $1.4 \cdot 10^{-5} \text{ S/cm}$  was obtained – almost two orders of magnitude higher than in case of polycrystalline one (Fig. 1) [3]. with Secondary Ion Mass Spectroscopy.

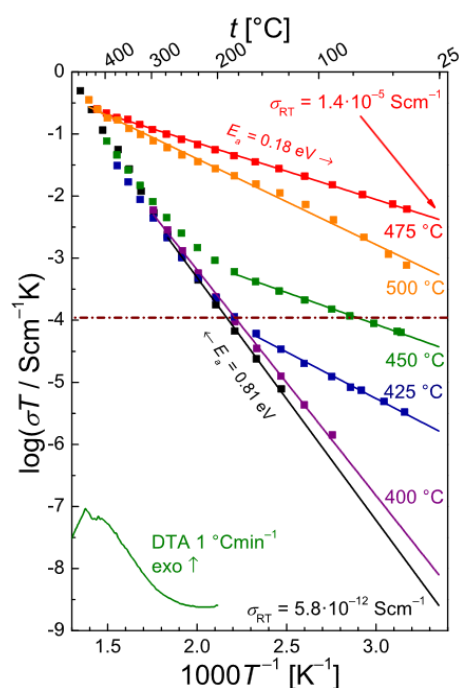


Fig. 1. Electrical conductivity of  $\text{LiFeBO}_3$  glass upon heating to various temperatures and cooling down to RT. DTA for 1°C/min and conductivity of polycrystalline  $\text{LiFeBO}_3$  (dotted line) are showed for comparison.

## CONCLUSIONS

This research have shown that thermal nanocrystallization of glassy analogs of  $\text{LiFe}_{1-x}\text{Mn}_x\text{BO}_3$  resulted in highly conducting material that may be used as a cathode in Li-ion battery.

## REFERENCES

1. A. Yamada, N. Iwane, S. Nishimura *et al.*, *J. Mater. Chem.* **21** (2011) 10690–10696.
2. J.E. Shelby, Introduction to glass science and technology, The Royal Society of Chemistry, 2005.
3. P.P. Michalski, T.K. Pietrzak, J.L. Nowiński *et al.*, *Solid State Ionics* **302** (2017) 40–44.

# Locally resolved microstructure investigation of an anode-supported solid oxide fuel cell stack

*G. Brus, H. Iwai\*, H. Yoshida\* and J.S. Szymd*

AGH University of Science and Technology, 30 Mickiewicza Ave., 30-059 Krakow, Poland

\* Kyoto University, Nishikyo-ku, 615-8245 Kyoto, Japan

e-mail: brus@agh.edu.pl

Keywords: SOFC, reforming kinetics, methane/steam reforming, direct reforming, microstructure, FIB-SEM

## INTRODUCTION

In this research a 100 W solid oxide fuel cells stack was tested. After 3700 hours of continuous operation a subsequent post-test analysis of the anodes' microstructure was conducted using a combination of focused ion beam and scanning electron microscopy. The obtained data was reconstructed into three-dimensional images, based on which the microstructure parameters were obtained. The microstructure parameters were quantified at different locations. Additionally, microstructure of a supplementary sample called the reference cell was investigated. The reference cell did not participate in the aging test and macrostructure analysis was conducted at an as-received cell. The analysis covers the critical spots including upstream, center, downstream and the vicinity of sealing.

## EXPERIMENTAL

The stack-aging test was conducted using a SOFC Modular Stack Test Bench (MSTB, hereafter). The MSTB system presented in this study was designed and produced by SOLIDPOWER. In this study a six cells stack with standard power output 100 W was tested. Each cell has an anode-supported structure, adopting Ni-YSZ cermet for the anode, dense YSZ for the electrolyte and three layers for the composite cathode. The active surface area available for the electrochemical reaction was 48 cm<sup>2</sup>.

## RESULTS AND DISCUSSION

After the aging test the electric furnace was cooled down and opened. The investigated stack was disassembled and selected cells were analyzed using FIB-SEM electron tomography coupled with 3D reconstruction and microstructure parameters quantification. The obtained results indicate strong non-homogeneous microstructure morphology changes after long-term operation. The most vivid change is the drop of triple phase boundary length. In the open literature a cell power generation is generally proportional to triple-phase boundary. Therefore, it could be expected that when TPB drops significantly during long-term operation, the cell performance should also drop. However, the presented research unravels an opposite trend. The stack performance increased slightly during first few hundreds hours of the operation. A careful microstructure analysis unravel that multiple changes in microstructure morphology could cause overlapping degradation and optimization.

## ACKNOWLEDGMENT

This work was partially supported by the Polish National Science Centre (Grant no. 2015/19/D/ST8/00839) and partially by the PAN-JSPS Joint Research Project, by the New Energy and Industrial Technology Organization (NEDO, Japan) under the Development of System and Elemental Technology on SOFC.

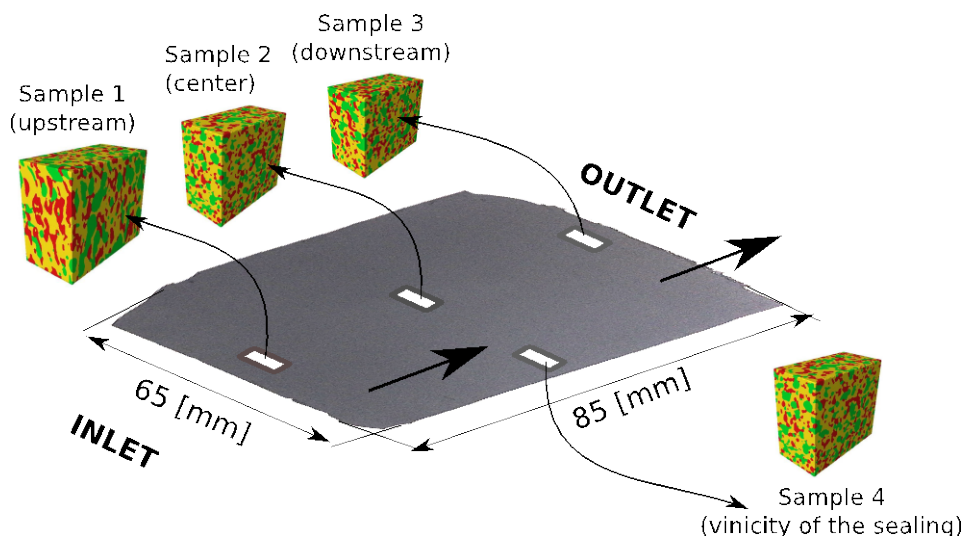


Figure 1 3D reconstructions of anode microstructure at different locations

# Energy storage systems using internal hybridization

*P. Jezowski\* and F. Béguin*

Poznan University of Technology, Institute of Chemistry and Technical Electrochemistry, ul. Berdychowo 4  
60-965 Poznan, Poland

e-mail: pawel.jezowski@put.poznan.pl

Keywords: hybridization, sodium-ion capacitors, lithium-ion capacitors, cathode, anode, energy storage

## INTRODUCTION

Lithium-ion batteries (LIB) and electrochemical capacitors (EC) are the most widely used power sources, for energy and power applications, respectively. LIBs store energy in the form of redox reactions which are limited by the kinetics of lithium ions diffusion, while in the case of ECs energy is stored by electrosorption of ions at the surface of carbon electrodes [1]. Recently, a third device incorporating the two mechanisms, and named lithium-ion capacitor (LIC), emerged. This system is constituted of an electrical double-layer (EDL) electrode made of activated carbon, and a negative one made of graphite intercalation compound (GIC), and the electrolyte is a lithium salt, generally  $\text{LiPF}_6$  in EC:DMC. The activated carbon electrode works in a wide potential range up to ca. 4.0 V vs.  $\text{Li/Li}^+$  while the GIC operates in a narrow potential range ca. 0.1 V vs.  $\text{Li/Li}^+$  [2]. The high voltage of the LIC together with its nearly doubled capacitance as compared to traditional EDLCs enables the system to display much higher energy density than the later, while keeping their power performance.

However, the necessity of intercalating lithium into graphite before operating the LIC complicates the system construction and/or may reduce its performance. The methods proposed for lithium intercalation are based on the use of i) an auxiliary lithium electrode [3], ii) a highly concentrated solution of lithium [4] or iii) a sacrificial cathode material added to activated carbon in the positive electrode [5,6]. Among the three strategies, the implementation of sacrificial materials enables to simplify the device construction and to eliminate issues related with metallic lithium (method i) or fluctuations of electrolyte concentration (method ii).

Taking into account the foregoing, our presentation will introduce a number of sacrificial materials of high irreversible capacity to build LIC and the performance of these systems will be shown. However, as the amount of easily accessible lithium in the Earth's crust is strictly limited, we will also present novel sodium-ion capacitors (NIC) based on the use of sacrificial materials for the sodation of negative carbon electrode.

## EXPERIMENTAL

Various cathodic and anodic materials were synthesized and used for the preparation of self-standing or coated electrodes including C65 conducting soot and a binder. The electrodes were tested under electrical polarization vs metallic lithium or sodium to establish their electrochemical performance and their usefulness for the construction of LIC or NIC, respectively. Cathodic materials with

high amount of irreversibly extracted lithium or sodium were used for the electrochemical pre-lithiation or sodiation of the negative electrode at C/20 (C corresponds to the theoretical capacity of the negative electrode). After pre-lithiation, the cells were cycled at higher currents up to 2C.

## RESULTS AND DISCUSSION

The Ragone plot (Fig. 1) compares the specific energy and power attainable with the LIC (green triangles) and EDLCs operating in organic electrolytes (red crosses and violet circles). The energy density of the LIC is around four times higher than for the EDLCs.

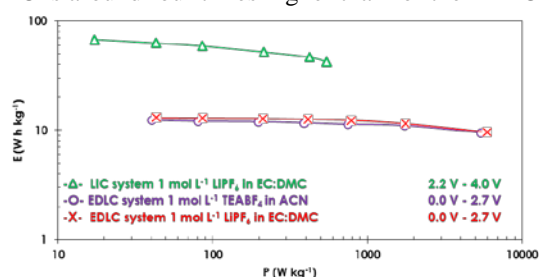


**Fig. 1** Ragone plot comparing the electrochemical performance of LIC and EDLC systems.

## CONCLUSIONS

Energy storage systems utilizing internal hybridization of two energy storage mechanisms are very promising and novel devices supplying high energy and power for various applications. The presented approach can be considered as a step towards smart energy management using innovative electrode materials and cell design.

## ACKNOWLEDGMENT

This research was financially supported by the Ministry of Science and Higher Education: project 03/31/DSPB/0334. The authors wish also to thank the French *Ministère des Affaires Etrangères* and the Polish *Ministerstwo Nauki i Szkolnictwa Wyższego* (Polonium project # 31438NH).

## REFERENCES

1. R. Kötz, M. Carlen, *Electrochimica Acta* **45** (2000) 2483
2. D. Cericola, R. Kötz, *Electrochimica Acta* **72** (2012) 1
3. T. Aida, K. Yamada, and M. Morita, *Electrochem. Solid State Lett.* **9** (2006) A534
4. V. Khomenko, E. Raymundo-Piñero, F. Béguin, *J. Power Sources* **177** (2008) 643
5. M.-S. Park, Y.-G. Lim, J.-H. Kim, Y.-J. Kim, J. Cho, J.-S. Kim, *Adv. Energy Mater.* **1** (2011) 1002
6. P. Jezowski, K. Fic, O. Crosnier, T. Brousse, F. Béguin, *J. Mater. Chem. A* **4** (2016) 1260.

# Stabilization of superionic $\delta$ - $\text{Bi}_2\text{O}_3$ phase at room temperature by thermal nanocrystallization of bismuth oxide glasses

Tomasz K. Pietrzak, Marek WasiucioneK, Jerzy E. Garbarczyk

Faculty of Physics

Warsaw University of Technology, ul. Koszykowa 75

00-662 Warszawa, Poland

e-mail: topie@if.pw.edu.pl

Keywords:  $\delta$ - $\text{Bi}_2\text{O}_3$ , oxygen conductors, nanomaterials

## INTRODUCTION

Crystalline  $\delta$ - $\text{Bi}_2\text{O}_3$  is the best  $\text{O}^{2-}$  ion conductor, but it is stable in a relatively narrow temperature range 729–825 °C only. Its very high ionic conductivity (1 S/cm at 750 °C) has motivated many researchers to look for a method to stabilize this fluorite-type structure to lower temperature. So far the successful strategies to achieve the stabilization of the delta phase have included doping (e.g. by rare-earth elements [1]) or synthesis in form of thin films [2].

Our approach to reach the same goal is significantly different from those two strategies. It consists of two steps: i) preparation of the  $\text{Bi}_2\text{O}_3$  glass (pure or only slightly doped) and ii) thermal nanocrystallization of the glass prepared in stage i). The advantages of such an approach are as follows: a) the final material is pure or nearly pure  $\text{Bi}_2\text{O}_3$  and b) it can be prepared in bulk and is not limited to thin layers only. Our earlier experience with nanocrystallization of glassy analogs of some cathode materials for Li-ion batteries has shown that by the appropriate heat-treatment one can achieve a dramatic (even by a factor of  $10^9$ ) and irreversible enhancement of their electrical conductivity [3,4]. This effect is closely related to changes in the microstructure – namely to formation of nanoscale crystalline grains, with dimensions going down even to a few nanometers, confined in the glassy matrix.

## EXPERIMENTAL

In this research, we firstly obtained a pure  $\text{Bi}_2\text{O}_3$  glass and then subjected it to an appropriate thermal treatment. Bismuth (III) oxide was melted at 1100 °C in a furnace and rapidly quenched. As a result, transparent orange glass with ca. 1 mm in thickness was obtained. Thermal events were observed by DTA measurements and the amorphousness of as-quenched material was confirmed by XRD. Crystallization and phase transitions taking place during heating and cooling were observed *in-situ* by temperature dependent XRD measurements. The microstructure of heat-treated samples was investigated by electron microscopy (both SEM and HRTEM). The total electrical conductivity of nanocrystallized samples as a function of temperature has been determined in preliminary measurements by impedance spectroscopy.

## RESULTS AND DISCUSSION

It was observed by SEM that nanograins (20–40 nm) of  $\delta$ - $\text{Bi}_2\text{O}_3$  phase were formed in glassy matrix

(Fig. 1) upon heating to temperature within the 530–630 °C range, as confirmed by XRD. The phase remained stable after cooling down to room temperature even after ca 1 year of ageing. Heating to higher temperature led to formation of  $\beta$ - $\text{Bi}_2\text{O}_3$  phase, which remained stable down to room temperature.

Preliminary electrical measurements showed an increase in the total conductivity at room temperature from  $10^{-19}$  S/cm (for the initial glass) to  $10^{-12}$  S/cm (for nanocrystalline samples). Analyses of Nyquist plots revealed the presence of a small arc at high frequencies that may be attributed to the conductivity of the interiors of nanocrystallites with  $\delta$ - $\text{Bi}_2\text{O}_3$  phase.

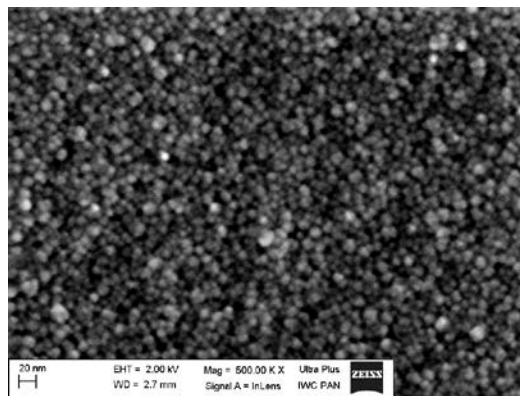


Fig. 1. Nanocrystallites of  $\delta$ - $\text{Bi}_2\text{O}_3$  phase embedded in a glassy matrix.

## CONCLUSIONS

Synthesis of  $\delta$ - $\text{Bi}_2\text{O}_3$  phase stable at room temperature in form of nanocrystallites embedded in glassy matrix in bulk samples is an important result, from viewpoints of basic knowledge as well as applications. Further studies will be focused on syntheses of nanocrystallized samples with the highest possible ionic conductivity.

## REFERENCES

1. M. Leszczynska, X. Liu, W. Wrobel, M. Malys, J.R. Dygas, S.T. Norberg, S. Hull, F. Krok, I. Abrahams, *Journal of Materials Chemistry A* **2** (2014) 18624–18634.
2. H.T. Fan, S.S. Pan, X.M. Teng, C. Ye, G.H. Li, L.D. Zhang, *Thin Solid Films* **513** (2006) 142–147.
3. J.E. Garbarczyk, T.K. Pietrzak, M. WasiucioneK, A. Kaleta, A. Dorau, J.L. Nowiński, *Solid State Ionics* **272** (2015) 53–59.
4. T.K. Pietrzak, M. WasiucioneK, P.P. Michalski, A. Kaleta, J.E. Garbarczyk, *Materials Science and Engineering: B* **213** (2016) 140–147.

# E-MOTO AGH – power supply for an electric motorcycle

***G. Ważny<sup>(1)</sup>, S. Bednarczyk<sup>(1)</sup>, K. Cichy<sup>(1)</sup>, M. Majewski<sup>(2)</sup>, J. Leszczyński<sup>(1)</sup> and J. Molenda<sup>(1)</sup>***

<sup>(1)</sup> AGH University of Science and Technology, Faculty of Energy and Fuels,  
al. A. Mickiewicza 30, 30-059 Krakow, Poland

<sup>(2)</sup> AGH University of Science and Technology, Faculty of Mechanical Engineering and Robotics,  
al. A. Mickiewicza 30, 30-059 Krakow, Poland  
e-mail: gabriela.k.wazny@gmail.com

Keywords: electric motorcycle, electromobility, Li-ion batteries

## INTRODUCTION

In view of decreasing oil resources and unstable economical and political situation on petroleum market, other energy sources for vehicles are needed. The world nowadays meets another problem at the same time: air pollution, especially in big cities. These are the main reasons for electromobility to be considered as the future of world's transportation.

In order to develop markets of electric vehicles, such events as Barcelona SmartMoto Challenge are organized. This year's edition was focused on electric light enduro motorcycles. The contest was divided into two parts: static (product design analysis, business plan), and dynamic (acceleration, enduro track, cones, endurance races) events.

The main goal of E-Moto AGH Team was taking part in this event. Over 20 students from 3 students' scientific circles were involved in the project: Mechanics' SSC – construction, propulsion and business plan, SSC Telephoners – wireless communication, and SSC Hydrogenium – battery package and charging system. This work focuses on the part of project related with power supply for the motorcycle.

## EXPERIMENTAL

Firstly, it was decided that cylindrical lithium-ion cells will be used. In order to choose the most suitable commercially available battery, a few types of them were examined. Batteries were cycled under various current values, in wide range of temperatures. These tests allowed to choose SONY US18650VTC6 as the most suitable model for required application, mainly because of its high current and high capacity. 288 batteries (16 in series and 18 in parallel) were spot welded with a nickel tape using a handmade welder. The most beneficial for battery's lifespan is CC/CV charging protocol, which means that the first step of charging occurs with constant current, which in the end decreases, while the voltage stays constant. This is why the certain type of charger was needed. What is more, while the nominal voltage of a single Li-ion battery is 3,6 V, it cannot be discharged below 2,5 V (minimal discharge voltage) and charged over 4,2 V (maximum charging voltage). Aside from the charger, BMS (Battery Management System) was essential in order to use the battery in a safe way. One of the main functions of BMS is balancing cells' voltage in series, so that they can reach the maximum state of charge.

Safety was one of the main issues considered while working on the project. As the Li-ion batteries heat up

during discharging and – even more – during charging, it was necessary to simulate the heat transfer and design appropriate cooling system. The battery package was closed in a leaktight steel casing and poured with transformer oil. The engine is situated in the back wheel, which is innovative solution, and is powered with an alternating current from the controller, which is supplied by the battery. Custom-made voltage regulator allows to power other components (eg. lights, computer) with 12 V and 5 V.

## RESULTS AND DISCUSSION

Nominal voltage of the battery package is 57,6 V, while its capacity is 54 000 mAh. It allows the motorcycle with 8 kW engine to drive over an hour on a off-road track. The 540 W charger allows to charge the battery during 8 h, with the constant current phase lasting almost 7 h. BMS controls battery voltage during charging and discharging. The computer inside the motorcycle is connected with BMS and collects data about the temperature, velocity and voltage from the battery, calculates remaining distance and used power and displays them on the screen in front of the driver.

## CONCLUSIONS

E-Moto AGH won in Barcelona SmartMoto Challenge 2017 in July three awards: "Static Events second place", "The best body and brakes design" and "The best newbie team". What is more, E-Moto was the fastest motorcycle during track race and cones. Overall, the Team took 4<sup>th</sup> place in the general results.



## ACKNOWLEDGMENT

This work is supported by AGH University of Science and Technology in Cracow under Rector's Grant for Students' Scientific Circles 2017; Faculty of Energy and Fuels; Polish Hydrogen And Fuel Cell Association; Magneto, LLC.



# POSTERS

# Reactivity of perovskite structure materials. Towards melted $V_2O_5$

*A. Lacz, E. Drozd and R. Lach*

Faculty of Materials Science and Ceramics  
AGH University of Science and Technology, Al. Mickiewicza 30  
30-059 Krakow, Poland  
e-mail: alacz@agh.edu.pl

Keywords: perovskite, chemical reactivity, barium cerate, strontium titanate, vanadium oxide

## INTRODUCTION

Materials with perovskite structure are considered as perspective for Solid Oxide Fuel Cells in their standard three layer system anode/electrolyte/cathode and the innovative construction: symmetrical or single cell. Application of ceramic proton conductive electrolyte (Y-doped  $BaCeO_3$ ) instead of typical for SOFC oxide ion conductive (e.g. yttria-stabilized zirconia, doped ceria) allows to decrease fuel cells working temperature and prevent fuel dilution by reaction products. On the other hand, Y-doped  $SrTiO_3$  is considered as an alternative for nickel cermet anode for SOFC technology. Thus, perovskite structure  $ABO_3$ -based materials, seem to be the interesting group toward solid oxide fuel cells applications. Two perovskite structure materials differ with microstructure, chemical stability and electrical properties  $BaCe_{0.9}Y_{0.1}O_3$  and  $Sr_{0.96}Y_{0.04}TiO_3$  were the subject of interest. Their reactivity with melted  $V_2O_5$  is the crucial factor concerning formation the composite in the  $ABO_3 - V_2O_5$  system. Thus, in this work the possibility of formation of composites with perovskite  $ABO_3$  as the major phase and  $V_2O_5$  as the minor one was analysed and discussed.

## EXPERIMENTAL

Solid-state reaction method was applied to synthesise Y-doped  $BaCeO_3$  ( $BaCe_{0.9}Y_{0.1}O_3$ ) and sol-gel method was used for Y-doped  $SrTiO_3$  ( $Sr_{0.96}Y_{0.04}TiO_3$ ) preparation. The high temperature impregnation was applied to analyse the reactivity in the solid  $ABO_3 -$  melted  $V_2O_5$  system and to synthesise the  $ABO_3 - V_2O_5$  materials. Sintered samples of  $ABO_3$  were placed in the  $Al_2O_3$  crucible covered on the top with the  $V_2O_5$  powder and heated to allow vanadium(V) oxide melting.

Crystal structure and phase composition of samples after impregnation were determined by the X-ray diffraction method (Philips X'Pert with  $CuK\alpha$  radiation). Microstructure and chemical composition were defined by Scanning Electron Microscopy SEM (Nova Nano SEM200, FEI & Oxford Instruments) coupled with Electron Dispersive Spectrometry (EDS) (FEI & Oxford Instruments). To explore the reactivity in the  $ABO_3 - V_2O_5$  system XRD, SEM and EDS analysis were performed on the samples surface and further SEM and EDS analysis were also carried out on the samples polished cross-section. The Electrochemical Impedance Spectroscopy (EIS) measurements performed at dry air and 5%  $H_2$  in Ar atmospheres for temperature range 300 – 700°C

allowed to determine the electrical conductivity of synthesized materials. Moreover, chemical resistance of materials toward  $CO_2$  and water vapour was estimated based on the  $CO_2/H_2O$  exposure test in which samples were exposed to  $CO_2$  and  $H_2O$  rich atmosphere at 25°C for 700 hours.

## RESULTS AND DISCUSSION

The reactivity of  $BaCe_{0.9}Y_{0.1}O_3$  and  $Sr_{0.96}Y_{0.04}TiO_3$  with  $V_2O_5$  was analysed consider different temperature and time of the reaction. As the starting temperature 700°C was chosen, since vanadium(V) oxide melts at 690°C. It was found that even at relatively low temperature (700°C) and relatively short time (1 hour) the  $BaCe_{0.9}Y_{0.1}O_3$  decomposition and formation of intermediate products like  $CeVO_3$  and  $CeVO_4$  process.

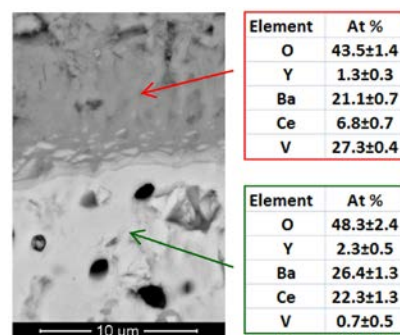


Fig.1.  $BaCe_{0.9}Y_{0.1}O_3 - V_2O_5$  system after 1 hour reaction at 700°C

Similar behaviour, decomposition of perovskite and intermediate products creation, was observed for  $Sr_{0.96}Y_{0.04}TiO_3 - V_2O_5$  system.

## CONCLUSIONS

Both perovskites are chemically unstable in contact with melted  $V_2O_5$ . Moreover, incorporation of vanadium into doped  $ABO_3$  perovskite structure (Y-doped  $BaCeO_3$  and Y-doped  $SrTiO_3$ ) process. Thus, due to high reactivity the perovskite structure materials towards melted  $V_2O_5$  it is rather unlikely to synthesise the composite in the analyse  $ABO_3 - V_2O_5$  system by simple impregnation.

## ACKNOWLEDGMENT

This work is supported by the National Science Centre of the Republic of Poland under Grant No 2014/14/E/ST5/00763.

# Oxygen nonstoichiometry of mixed-conducting $\text{Ba}_{0.5}\text{Sr}_{0.5}\text{Co}_{0.8}\text{Fe}_{0.2}\text{O}_{3-\delta}$

*E.N. Naumovich, M.V. Patrakeev\* and A.A. Yaremchenko\*\**

Thermal Processes Dep., Institute of Power Engineering, Augustówka 36, 02-981 Warsaw, Poland  
e-mail: Yevgeniy.Naumovich@ien.com.pl

\* Institute of Solid State Chemistry, UB RAS, 91 Pervomayskaya Str., 620990 Yekaterinburg, Russia

\*\* CICECO – Aveiro Institute of Materials, DEMAC, University of Aveiro, 3810-193 Aveiro, Portugal

Keywords: mixed conductor, coulometric titration, oxygen nonstoichiometry, SOFC cathode, ceramic membrane

## INTRODUCTION

$\text{Ba}_{0.5}\text{Sr}_{0.5}\text{Co}_{0.8}\text{Fe}_{0.2}\text{O}_{3-\delta}$  (BSCF) exhibits outstanding mobility of oxygen ions in cubic perovskite lattice and, therefore, attracts significant attention as a promising material for electrochemical applications – solid oxide fuel cell cathodes, dense mixed-conducting membranes for oxygen separation, and electrocatalysts for oxygen evolution reaction. Complicated phase relationships in this solid solution under oxidizing conditions impede however its practical utilization. The key feature of BSCF as mixed ionic-electronic conductor is its high oxygen deficiency which results, however, in instability of perovskite lattice and phase separation occurring in air at temperatures  $\leq 900^\circ\text{C}$  and accompanied with deterioration of relevant properties. Still, BSCF remains a good model mixed conductor. The present work was focused on the detailed study and analysis of  $p(\text{O}_2)$ - $T$ - $\delta$  diagram of BSCF in the entire range where the perovskite phase is stable.

## EXPERIMENTAL

BSCF samples were synthesized by glycine-nitrate combustion technique and sintered in air at  $1100^\circ\text{C}$ . Oxygen nonstoichiometry was studied by coulometric titration technique using YSZ solid electrolyte cells. Absolute oxygen content in reference point was determined thermogravimetrically via reduction in a flow of dry  $10\%\text{H}_2\text{-N}_2$  mixture. Atomistic lattice simulations were performed in GULP [1] software.

## RESULTS AND DISCUSSION

According to coulometric titration results (Fig.1), oxygen content ( $3-\delta$ ) in cubic perovskite phase of BSCF cannot exceed  $\sim 2.52$ . Further oxidation leads to phase separation and segregation of hexagonal phase. Redox cycling between single-phase perovskite and multiphase mixture is accompanied by hysteresis in  $3-\delta - \log p(\text{O}_2)$  curves. For values  $\delta > 0.6$ , one can observe a change in mechanism of the equilibration with a gas phase, however the absence of hysteresis and smooth bending of the isotherms suggest that this should be a transition in point defects interaction rather than structural changes. For oxidizing region ( $\delta > 0.48$  and  $p(\text{O}_2) > 10^{-4}$  atm), point defects interactions may be successfully described using the approaches for high-defected lattices developed earlier [2]. In the case of BSCF, the key assumptions include an existence of the  $\text{B}^{4+}$  cations in the octahedral environment and attraction between  $\text{B}^{2+}$  cations and oxygen vacancies. These approaches were confirmed by atomistic Monte-Carlo simulations. For the reduced state ( $\delta > 0.6$ ), the

existence of  $\text{B}^{4+}$  cations is considered to be unlikely, and self-ionization should be omitted.

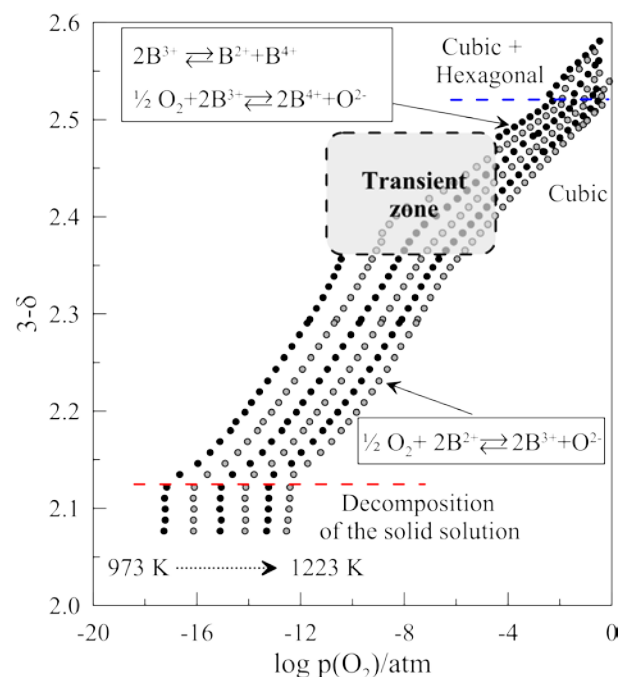


Fig.1. Oxygen nonstoichiometry of BSCF vs.  $p(\text{O}_2)$  at  $700\text{-}950^\circ\text{C}$ .

## CONCLUSIONS

Coulometric titration studies of  $p(\text{O}_2)$ - $T$ - $\delta$  diagram of BSCF demonstrated that a single phase with average cubic perovskite structure exists in the range  $\delta = 0.48\ldots 0.87$ . The mechanism of equilibration with a gas phase was found to change at  $\delta \approx 0.6$ . This transition can be explained as result of depletion of 6-coordinated B-site species -  $\text{Fe}^{4+}$  and  $\text{Co}^{4+}$ . These results may play key role in development of the MIEC membranes and novel SOFC cathodes.

## ACKNOWLEDGMENT

Authors would like to acknowledge financial support by the FCT, Portugal (IF/01072/2013/CP1162/CT0001 and CICECO-Aveiro Institute of Materials POCI-01-0145-FEDER-007679 (FCT ref. UID/CTM/50011/2013)) and from NCBR, Poland (project POIR.01.02.00-00-0013/16 NewSOFC, co-founded from the European Regional Development Fund under the Operational Programme Smart Growth).

## REFERENCES

1. J.D.Gale, A.L.Rohl, *Mol. Simul.* 29 (2003), 291-341.
2. E.N. Naumovich *et al.*, *Solid State Ionics* 177 (2006) 457-470.

# Structural and catalytic properties of transition element-doped ceria layers in SOFCs fueled by biogas

***B.Bochentyn<sup>a</sup>, B.Holówko<sup>a</sup>, D.Szymczewska<sup>b</sup>, M.Gazda<sup>a</sup> and P.Jasiński<sup>b</sup>***

<sup>a</sup> Faculty of Electronics, Telecommunications and Informatics, Gdansk University of Technology, 80-233 Gdansk, ul. Narutowicza 11/12, Poland

<sup>b</sup> Faculty of Applied Physics and Mathematics, Gdansk University of Technology, 80-233 Gdansk, ul. Narutowicza 11/12, Poland  
e-mail: bbochentyn@mif.pg.gda.pl

Keywords: solid oxide fuel cells, biogas, catalysts

## INTRODUCTION

Cerium oxide is a catalyst of reactions of steam conversion and oxidation of carbohydrates [1-2]. It may increase the efficiency of SOFC anode operation throughout acceleration of the process of charge exchange in the triple phase boundary (TPB) [3]. It is widely used in sulfur removal processes and increases coking resistance in catalytic processes [4]. The addition of copper (Cu) also resists coking formation and sulfur adsorption better than Ni [5]. Kurokawa et al. have reported that a power density of a fuel cell with CeO<sub>2</sub>-infiltrated Ni-YSZ anode in H<sub>2</sub> fuel containing 40 ppm of H<sub>2</sub>S was 3 orders of magnitude higher than that for the unmodified reference fuel cell [6]. Moreover, the infiltrated fuel cell was able to operate for 500 h, whereas the reference one degraded within 13 minutes [6]. Although, Cu-doped ceria in principle performs well at intermediate temperatures, the copper anode can present several limitations related to its poor thermal stability as a consequence of the low melting point of copper [7]. Another solution for direct methane oxidation can be ceria doping with iron which presents higher thermal stability and chemical reactivity with respect to copper.

## EXPERIMENTAL

In this work five nanocrystalline compounds of transition-metal doped ceria Ce<sub>0.8</sub>M<sub>0.2</sub>O<sub>2-δ</sub> (M=Mn,Fe,Co,Ni,Cu) were fabricated by a reverse microemulsion method. Resulting powders will be deposited in a form of layers on the surface of SOFC anode in order to act as electrochemically active materials for biogas reforming process. The aim of modification is to increase a lifetime and efficiency of commercially available solid oxide fuel cell operating with biogas without the need of an external reformer.

The XRD, SEM, AFM, EDX and XPS methods will be used to investigate structural properties and composition of fabricated materials. Furthermore, the electrical properties of SOFCs with catalytic layers deposited on the Ni-YSZ anode site will be examined by current density-time and current density-voltage dependence measurements in hydrogen (24h) and biogas (168h). The obtained results will be compared with a performance of a reference (unmodified) cell, which degrades gradually with time mainly due to a deposited carbon. The usage of additional catalytic layer should enhance the SOFC resistance for degradation in biogas atmosphere.

## RESULTS AND DISCUSSION

As a result of a reverse microemulsion synthesis method the desirable single-phase powdered materials were obtained. A mean size of crystallites in these compounds did not exceed 10 nm. These materials will be applied as potential catalytic layers for Solid Oxide Fuel Cells. On the basis of our previous investigations we suppose that fuel cells with ceria-based layers should be stable in time in both hydrogen and biogas atmospheres, whereas the fuel cell without a catalytic layer deteriorates gradually in time.

## REFERENCES

1. Q. Fu, H. Saltsburg, M. Flytzani-Stephanopoulos, *Science* **301** (2003) 935–938
2. Z.L. Zhan, S.A. Barnett, *Science* **308** (2005) 844–847.
3. K. Ahn, H.P. He, J.M. Vohs, R.J. Gorte, *Electrochem. Solid-State Letters* **8** (2005) A414–A417.
4. M.Gonga, X.Liu, J.Tremblay, Ch.Johnson, *Journal of Power Sources* **168** (2007) 289–298
5. M. Boder, R. Dittmeyer, *Journal of Power Sources* **155** (1) (2006) 13–22
6. H. Kurokawa, T. Sholklafter, C. Jacobson, L. De Jonghe, S. Visco, *Electrochem. Solid-State Lett.* **10** (2007) B135-B138
7. Hornéa, G. Munuera, A. Fuerte, M.J. Escudero, L. Daza, A. Martínez-Arias, *Journal of Power Sources* **196** (2011) 4218–4225

# Structural and electrical properties of Cr-doped SrTiO<sub>3</sub> porous materials

*E. Drożdż, A. Łącz, Ł. Łańcucki*

AGH University of Science and Technology, Faculty of Materials Science and Ceramics,  
al. A. Mickiewicza 30, 30-059 Kraków, Poland  
e-mail: edrozd@agh.edu.pl

Keywords: Cr-doped SrTiO<sub>3</sub>, anode materials for SOFC

## INTRODUCTION

SrTiO<sub>3</sub> is one of the best known and widely used perovskite materials which is also considered as a potential material for application in electrochemical devices for energy conversion. The modification of properties of SrTiO<sub>3</sub> can be achieved by its doping in one (or simultaneously both) cationic sublattices with various admixtures. A lot of papers have been devoted to study on defects and electrical properties of donor doped SrTiO<sub>3</sub> materials, in contrary acceptor doping is not widely discussed. Acceptor admixture can not only improve the electrical properties of the material, but also positively affect its catalytic properties in oxidation-reduction reactions. In addition, most of the research concerns dense materials, but the potential applications of SrTiO<sub>3</sub> are rather related to the use of porous materials. One of the less-studied acceptor doping systems is Cr-doped SrTiO<sub>3</sub>. Thus, the idea of synthesis of porous chromium-doped strontium titanate materials with different chromium amount and study their structural and electrical properties.

## EXPERIMENTAL

Porous undoped and Cr-doped SrTiO<sub>3</sub> materials were obtained by wet synthesis (sol-gel method). Ti(O-iPr)<sub>4</sub>—titanium(IV) isopropoxide, chromium nitrate and strontium nitrate were applied as precursors of chromium-doped strontium titanate. These reagents were dissolved in ethanol and next cations were complexed by addition of citric acid. The obtained sol was heated on magnetic stirrer at around 200 °C (for densification) and next the powders were calcinated at 900°C in air atmosphere. Then, the pallets were formed (under pressure 5·10<sup>5</sup> Pa) and next sintered at 1200°C for 3 hours.

Thus, a series of samples of the general formula SrTi<sub>1-x</sub>Cr<sub>x</sub>O<sub>3</sub> where x=0, 1, 2, 4, 6 mol.% were obtained.

Phase composition and unit cell parameters were determined based on XRD measurements carried out on Philips X'Pert Pro diffractometer with monochromatized Cu-K<sub>α</sub> radiation. The observation of pallets fracture morphology was performed using scanning electron microscopy (SEM) (Nova NanoSEM 200 FEI and Oxford Instruments) coupled with X-ray energy dispersive spectroscopy (EDAX company apparatus). The electrical properties of obtained samples were examined by means of impedance spectroscopy (Solartron, FRA 1260 with dielectric interface 1294) and supplemented by the results of DC measurements.

## RESULTS AND DISCUSSION

The XRD analysis indicated that in the case of undoped and Cr-doped materials the only present phase was perovskite structure named tausunite. Moreover, this analysis shown decrease of cell parameter with increasing amount of chromium dopant what explains the incorporation of Cr into Ti position as the ionic radii of Ti(IV) and Cr(III) are 74.5pm and 69pm, respectively.

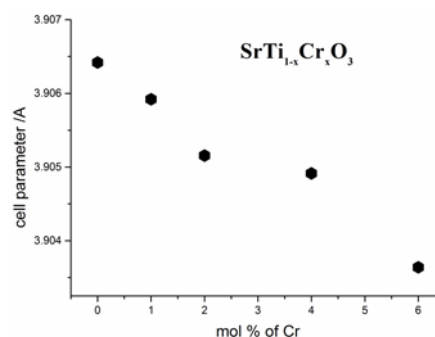


Fig. 1. The values of cell parameter for undoped and Cr-doped SrTiO<sub>3</sub> samples.

Average particle size estimated by means of Scherrer formula was around 120 ± 15 nm without any influence of dopant amount. The total porosity of pallets sintered at 1200°C was around 48 vol.%.

The analysis of electrical properties was carried out in air and of H<sub>2</sub>/Ar atmospheres. Based on the EIS and DC studies, it was found that in air atmosphere the conductivity of doped samples increases with the amount of introduced chromium. In contrary, in reduction atmosphere (H<sub>2</sub>/Ar mixture), the conductivity of doped samples is lower than that of pure SrTiO<sub>3</sub>.

## CONCLUSIONS

A series of single-phase porous strontium titanate materials doped by different amounts of chromium were obtained by the sol-gel method. The results of XRD research indicate the incorporation of chromium into the titanium sublattice.

The results of the electrical tests show the opposite effect of the introduced dopant on the conductivity of the samples in the oxidizing and reducing atmosphere.

## ACKNOWLEDGMENT

This work is supported by the National Science Centre of the Republic of Poland under Grant No 2014/14/E/ST5/00763



# Microstructure oriented model of direct internal reforming SOFC

*G. Brus, H. Iwai\*, H. Yoshida\* and J.S. Szmyd*

AGH University of Science and Technology, 30 Mickiewicza Ave., 30-059 Krakow, Poland

\* Kyoto University, Nishikyo-ku, 615-8245 Kyoto, Japan

e-mail: brus@agh.edu.pl

Keywords: SOFC, reforming kinetics, methane/steam reforming, direct reforming, microstructure, FIB-SEM

## INTRODUCTION

This paper presents experimental and numerical studies on the methane reforming process conducted directly on a Ni/YSZ anode. Direct reforming has not been practically applied so far. Feeding methane directly into the anode results in either carbon deposition and thermal stress at high temperatures or poor performance at low operating temperatures. To optimize the anode and assure safe operation condition, detailed knowledge about the entire reforming process is required. In the present paper, measurements including different thermal boundary conditions, the fuel flow rate and the steam-to-methane ratios were performed. After the experiment anode microstructure was directly observed using combination of focused ion beam and scanning electron microscope coupled with 3D reconstruction techniques. This approach allows associating the rate equation with Ni-pore contact surface and anode's microstructure. The reforming rate equation derived from experimental data was used in the microstructure-oriented numerical model to predict gas composition, potential distribution, and electrochemical performance of a cell under direct reforming conditions.

## EXPERIMENTAL

The anode-supported button type solid oxide fuel cell sample used in the presented study is a commercial product manufactured by SOLID Power. The geometry of the sample is presented in Figure 1(a). The sample was located between two ceramic tubes in the electric furnace as it is presented in Figure 2 (b). The ceramic tubes have a double co-axial structure with an inter-tube for incoming gases and an outer-tube for the exhaust gases. The anode and the cathode were connected to the measuring devices with platinum wires. Platinum meshes were welded with platinum wires and connected

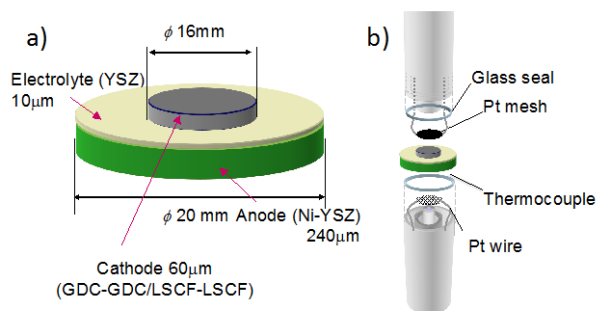


Figure 1 Investigate cell a) geometry of the cell b) location in testing system

## RESULTS AND DISCUSSION

The microstructure parameters obtained from FIB-SEM electron tomography were employed in numerical model. The computations were preformed for the same condition as the experiment due to verification process of the numerical results. The OCV was adopted from the experiment and cell's polarization was calculated. The results of the experiment versus numerical simulation are presented in Fig. 2. Two parameters to be investigated are temperature and the fuel composition. As can be seen from Fig.2 temperature has very significant effect on the cell performance. Much smaller effect can be observed for steam-to-methane ratio. The results for different SC are almost identical for both numerical prediction and the experimental results. Generally the results of computation are in good agreement with experimentally obtained data. Most of the measurement points are located in the vicinity of the numerical prediction.

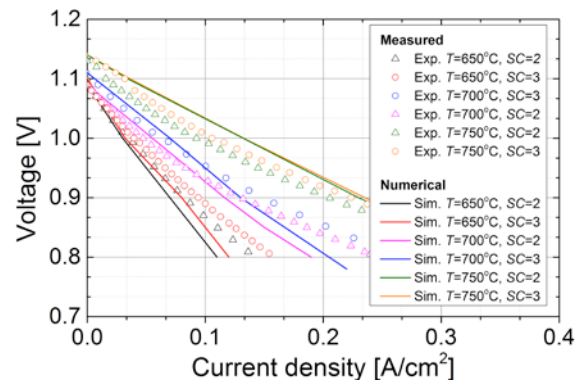


Figure 2 Current-voltage characteristic, experiment versus simulation

## CONCLUSIONS

In the presented research microstructure parameters obtained from FIB-SEM electron tomography and 3D reconstruction technique were implemented into numerical model to simulate direct reforming process. It was shown that applying such combined approach leads to the successful prediction of a cell current-voltage characteristic for different modelling conditions.

## ACKNOWLEDGMENT

This research was supported by the Foundation for Polish Science, Grant No. First TEAM/2016-1/3. The experiment was supported by the New Energy and Industrial Technology Organization (NEDO, Japan), and partially by Japan Society for the Promotion of Science (JSPS KAKENHI Grant Number JP15H03930).

# Degradation of the Ni-YSZ anodes of solid oxide fuel cells fed with CH<sub>4</sub>-H<sub>2</sub>O mixtures with low steam-to-carbon ratio

Konrad Motyliński, Yevgeniy Naumovich, Marek Skrzypkiewicz and Jakub Kupecki

Thermal Processes Department  
Institute of Power Engineering, ul. Augustówka 36  
02-981 Warsaw, Poland  
e-mail: konrad.motyliniski@ien.com.pl

Keywords: solid oxide fuel cells, anode degradation, methane steam reforming

## INTRODUCTION

Solid oxide fuel cells are high temperature electrochemical energy conversion devices which operate at elevated temperature, typically in range from 600°C to 900°C. The elevated temperature allows to use internal reforming process of hydrocarbonaceous fuels, thus SOFCs can be directly fueled with gases containing hydrocarbons and their mixtures with different H/C ratio. SOFCs can operate in regimes where the amount of steam in the mixture is insufficient for suppression of the carbon formation and deposition. This can be due to the thermal cracking of hydrocarbons or the Boudouard decomposition of carbon monoxide. In the case of internal reforming, two chemical reactions are occurring on the anode, the deep-endothermic steam conversion and the exothermic electrochemical oxidation. Such conditions potentially result in the accelerated degradation of the SOFC anode or in growing of local cracks in the fuel cell body. In this study an intermediate-term test (1000 h) of AS-SOFC based on Ni-YSZ fueled with wet CH<sub>4</sub> was performed, where the steam-to-carbon ratio (S/C) was gradually decreased. The structural damage and the degradation of the performance of the cell were observed and described.

## EXPERIMENTAL METHODOLOGY

The test was performed on a single, planar 5 cm x 5 cm anode supported solid oxide fuel cell (AS-SOFC) based on Ni-YSZ anode with the effective area of the cathode of approximately 16 cm<sup>2</sup>. The cell was sealed inside a ceramic housing, placed between two current collectors. Gold was adopted as the current collector for cathode side while Crofer 22APU<sup>®</sup> for anode side [1]. The operating temperature for the whole test was kept at 750±1°C. In course of the study 50 Nml/min of CH<sub>4</sub> was used as the main component of the fuel mixture. Before entering the SOFC, methane was passed through the humidifier (Cellcraft P-10) hence the S/C ratio was adjusted to the desired values, starting from 2.0. Throughout the 1000 h test, SOFC was under constant current load of 2 A which was applied by the galvanostat (Zahner PP240). The only varied parameter was S/C, which was gradually decreased down to the value of 0.15. The electrochemical impedance spectroscopy technique (EIS) was used to monitor the cell degradation. The *post mortem* analysis of the cell was realized using SEM-EDS (JEOL JSM-6010PLUS/LA).

## RESULTS AND DISCUSSION

Throughout the entire duration of the test the step change of steam-to-carbon ratio was approximately 0.1, starting from value of 2.0 down to 0.15. For each S/C several EIS measurements were performed. The collected data showed that with the decreased S/C the fuel cell resistance increased, but without the qualitative changes in impedance pattern, which can be described as two RQ arcs with RL chain in high frequencies (similar to observed in [2]). This might imply the fuel cell degradation without potential carbon deposition on the electrochemically-active surface. The *post mortem* analysis showed that during the test small cracks occurred near the fuel inlet (Fig. 1).

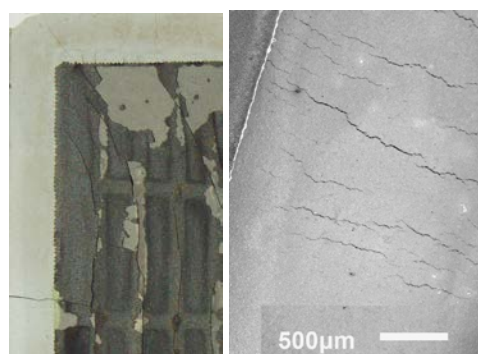


Fig. 1 Cracks near the fuel inlet:  
left - cathode, right - SEM of the anode

## CONCLUSIONS

The results of the 1000 h test showed that fuelling SOFC with the CH<sub>4</sub>-H<sub>2</sub>O mixture might result in faster degradation of the cell compared to usage of reformat gas as the fuel. The *post mortem* analysis showed also that both the endothermic and the exothermic reactions might cause the thermal cracks, resulting in leakage of gases. To confirm the proposed conclusion and investigate the mechanisms in depth additional tests are needed.

## ACKNOWLEDGMENT

This work was financially supported by the National Science Centre, Poland, Grant No. 2015/19/N/ST8/01876.

## REFERENCES

1. Y. Liu, *Journal of Power Sources* **179** (2008) 286-291
2. S. Bebelis, S. Neophytides, *Solid State Ionics* **152-153** (2002) 447-453

# Impact of calcium addition on properties of lanthanum strontium iron oxide

***L. Łańcucki, K. Wojciechowski, A. Łącz, P. Pasierb***

Faculty of Materials Science and Ceramics  
AGH University of Science and Technology, Al. Mickiewicza 30  
30-059 Krakow, Poland  
e-mail: lancucki@agh.edu.pl

Keywords: perovskite, lanthanum strontium iron, chemical reactivity, oxide, calcium doping, chemical stability

## INTRODUCTION

Perovskite type oxides  $ABO_3$ , particularly orthoferrites, are an interesting class of materials. They are used for a variety of applications, such as electrode materials for high temperature solid oxide fuel cells, and as dense catalysts for the partial oxidation of hydrocarbons. Among the orthoferrites,  $La_{0.5}Sr_{0.5}FeO_3$  is of great significance for its various technological applications. Since the success of many promising technologies is strongly dependent on the dense membrane synthesis procedure, considerable effort has been focused on the preparation of lanthanum strontium ferrites and optimization of the experimental conditions. The challenge for these methods is to decrease the synthesis temperature by doping with alkali earth ions, to produce ultrafine  $La_{0.5}Sr_{0.5-x}Ca_xFeO_3$  dense membranes, with improved mechanical and catalytic properties.

## EXPERIMENTAL

Citrate method was applied to synthesise  $La_{0.5}Sr_{0.5-x}Ca_xFeO_3$  (where x was 0; 0.025; 0.05; 0.075 and 0.1). The proper amounts of  $La_2O_3$ ,  $Sr(NO_3)_2$ ,  $Fe(NO_3)_3$  and CaO were dissolved in the solution of citric acid. The final concentration of all ions (La, Sr, Fe, Ca) to citric acid was 1:2 solutions were then dried at 100 °C for 24h and obtained powders were further dried at 200 °C for 3h. Crystal structure and phase composition of samples after doping were determined by the X-ray diffraction method (Philips X'Pert with  $CuK\alpha$  radiation). Microstructure and chemical composition were defined by Scanning Electron Microscopy SEM (Nova Nano SEM200, FEI & Oxford Instruments) coupled with Electron Dispersive Spectrometry (EDS) (FEI & Oxford Instruments). Additionally, chemical resistance of obtained samples, toward  $CO_2$  and water vapour was estimated based on the  $CO_2/H_2O$  aging test in which membranes were exposed to pure  $CO_2$  and  $H_2O$  (100% RH) atmosphere at ambient temperature for 700 hours.

## RESULTS AND DISCUSSION

It was noticed that addition of calcium had no impact on  $La_{0.5}Sr_{0.5-x}Ca_xFeO_3$  phase composition, as all samples exhibited hexagonal ( $P6_3cm$ ) cell type. Additionally implementation of Ca into  $La_{0.5}Sr_{0.5}FeO_3$  structure had only slight effect on crystallite size as it decreased from ~58 nm for  $La_{0.5}Sr_{0.5}FeO_3$  to 53 nm for  $La_{0.5}Sr_{0.4}Ca_{0.1}FeO_3$ . It should be noticed that addition of calcium had impact on sintering properties of obtained systems. The sintering shrinkage of doped samples increased with the amount of Ca. Furthermore

it also improved density and decreased porosity of obtained samples. As presented in table below.

**Table 1.** Sintering shrinkage and density calculated for  $La_{0.5}Sr_{0.5-x}Ca_xFeO_3$  samples.

Sample	Shrinkage [%]	Density [g/cm <sup>3</sup> ]
$La_{0.5}Sr_{0.5}FeO_3$	8.30	5.107
$La_{0.5}Sr_{0.475}Ca_{0.025}FeO_3$	11.07	5.405
$La_{0.5}Sr_{0.450}Ca_{0.050}FeO_3$	11.69	5.570
$La_{0.5}Sr_{0.425}Ca_{0.075}FeO_3$	12.30	5.654
$La_{0.5}Sr_{0.400}Ca_{0.100}FeO_3$	12.61	5.693

Furthermore it was noticed that for samples with the largest amount of calcium no open porosity was observed. Additionally Ca addition had impact on grain size of obtained samples as presented in Figure 1.

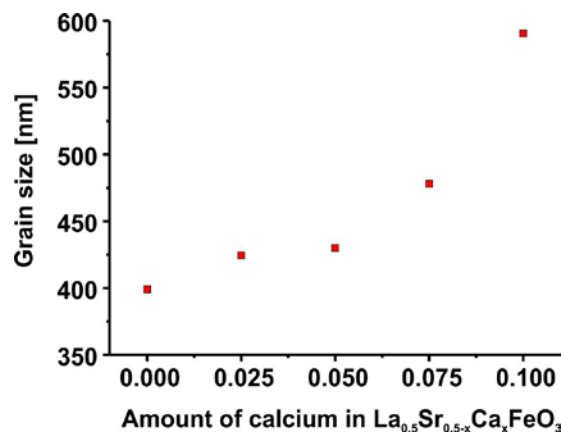


**Figure 1.** Grain size calculated for  $La_{0.5}Sr_{0.5-x}Ca_xFeO_3$  samples

It should be noticed that calcium addition had no impact on chemical stability of obtained samples as all of those did not exhibit any degradation symptoms after 700 h test in  $CO_2/H_2O$  atmosphere.

## ACKNOWLEDGMENT

Authors are grateful for financial support of the Statutory Project Science (Ministry of Science and Higher Education no. 11.11.160.438) at the Faculty of Materials Science and Ceramics.

# Development of solid oxide fuel cell manufacturing methodology using robocasting technology

*M. Chalusiak, G. Brus, K. Berent\*, M. Możdziej and J.S. Szmyd*

Faculty of Energy and Fuels, AGH University of Science and Technology

\*Academic Centre for Materials and Nanotechnology, AGH UST

30-059 Krakow, Poland

e-mail: chalusiak@agh.edu.pl

Keywords: solid oxide fuel cell, robocasting, additive manufacturing, microstructure

## INTRODUCTION

Additive Manufacturing (AM) techniques offer the potential to fabricate the high-precision SOFCs components with good reproducibility. Nowadays, they become methods of a great importance in modern industry [1,2]. Robocasting, also referred as direct-write assembly, is unique among these techniques, because it allows one to build ceramic parts via computer controlled deposition of a thick slurry and form three-dimensional structures layer-wise at a room temperature [3,4].

A technological domain, in which these features are highly desirable, is the solid oxide fuel cell technology. This is especially relevant for the planar SOFC design, where the multi-material layers used in the components are well-interconnected and have different microstructural properties [2]. Although several methods for SOFC manufacturing are present in the industry, there is still a shortage of accurate, moldless techniques and Robocasting has a great potential to fill this void.

In this work, button-like solid oxide fuel cell is manufactured with Robocasting AM technology. Commercial LSM and Ni/YSZ are used for cathode and anode, respectively. LSM material is in the form of ready-made paste, while Ni/YSZ is a ceramic dense slurry with tailored composition and viscoelastic properties. Electrode materials are deposited on dense YSZ electrolyte cermet with state-of-the-art robotic deposition device. The cell microstructure parameters are developed using FIB-SEM tomography and its performance is evaluated in electrochemical tests.

## EXPERIMENTAL

The process of SOFC manufacturing consists of three stages: slurry preparation, extrusion and sintering. Ni/YSZ slurry is used for extrusion. Poly(vinyl butyral) (Butvar B98, Sigma Aldrich, USA) is used as binder with additions of poly(ethylene glycol) (Mw=400, PEG, Sigma Aldrich, USA) as plasticizer. A stable suspension of Ni/YSZ is made by addition of toluene/ethanol (60/40 vol.%) and mixing in planetary ball mixer (Retsch PM200, Germany) with zirconia balls. Suspension is then dried in elevated temperatures to partially evaporate the solvent. PVB and PEG are fully dissolved in toluene/ethanol solution and added to Ni/YSZ blend. To make a uniform slurry and dispose air bubbles, the suspension is additionally mixed in high-speed mixer (SpeedMixer, FlackTek Inc.). A so prepared ceramic ink is housed in a syringe and deposited through

cylindrical nozzles on thin electrolyte and sintered. The deposition and sintering procedure is repeated with ready-made cathode paste on the other side of electrolyte. Next, a ready button-cell undergoes electrochemical tests and FIB-SEM tomography.

## RESULTS AND DISCUSSION

During rheological tests SOFC viscosity is evaluated for different shear rate applied to the examined fluid. The SOFC anode microstructure is examined using FIB-SEM tomography device, available in Academic Centre of Materials and Nanotechnology. Exemplary results of conducted tests are presented in Fig.2.

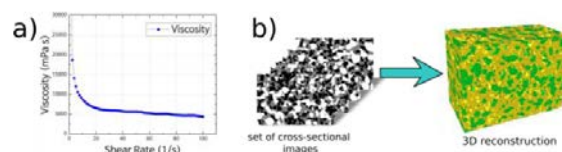


Fig. 2. Exemplary results of: a) rheological tests b) FIB-SEM tomography.

## CONCLUSIONS

A set of tests, conducted in this work, gives a significant insight into SOFC materials properties and its' impact on the cell performance, as it is capable of monitoring macroscopic changes via I-V curves and find a cause of these changes in microscopic properties of utilized materials.

## ACKNOWLEDGMENT

This work is carried out within the FIRST TEAM programme of the Foundation for Polish Science co-financed by the European Union under the European Regional Development Fund.

## REFERENCES

1. N.M. Farnandos, L. Kleiminger, T. Li, A. Hankin, G.H. Kelsall, *Electrochimica Acta* **213** (2016), 324-331
2. V. Esposito, C. Gadea, J. Hjelm, D. Marani, Q. Hu, K. Agersted, S. Ramousse, S.H. Jensen, *Journal of Power Sources* **273** (2015), 89-95
3. P. Miranda, E. Saiz, K. Gryń, A.P. Tomsia, *Acta Biomaterialia* **2** (2006), 457-466
4. P. Miranda, E. Saiz, S. Deville, K. Gryń, G. Liu, R.K. Nalla, A.P. Tomsia, *Journal of Biomedical Materials Research* (2007)



# Dynamic characteristics of a direct internal reforming Solid Oxide Fuel Cell to address fuel starvation

*M. Chalusiak, G. Brus, M. Możdziej, K. Berent\* and S. Kimijima\*\**

Faculty of Energy and Fuels, AGH University of Science and Technology

\*Academic Centre for Materials and Nanotechnology, AGH UST, 30-059 Kraków, Poland

\*\*Shibaura Institute of Technology, Saitama, Japan

e-mail: chalusiak@agh.edu.pl

Keywords: solid oxide fuel cell, dynamic model, reforming, fuel starvation, reaction rate

## INTRODUCTION

Solid Oxide Fuel Cells owe their growing interest and rapid development to highly efficient, environmentally friendly performance, attracting a lot of attention as a perspective clean power generation technology [1]. Ability of SOFCs to utilize both hydrogen and carbon monoxide leads to a solution for a deficiency of naturally occurring hydrogen, pointing direct internal reforming process as a hydrogen supply for SOFCs. The ability to internally reform a range of hydrocarbon fuels within SOFC represent the significant advantage of SOFCs. However, it engages numerous phenomena in one place, making the whole process difficult to predict, especially in terms of thermal management and fuel starvation [2]. Brus et al. [3] confirmed a SOFC anode degradation due to microstructure changes and stated hydrogen starvation as a responsible factor. In this work, authors develop a two-dimensional transient model of a single planar Direct Internal Reforming Solid Oxide Fuel Cell anode channel. The aim of this work is to investigate the fuel starvation phenomenon occurring under specific conditions, by solving mass and energy transport equations using the in-house code in MATLAB environment.

## EXPERIMENTAL

A methane steam reforming reaction provides the fuel cell with hydrogen by converting methane and water vapour in endothermic process. Reaction rates of above reactions, essential to elaborate an accurate model of DIR-SOFC, were derived in experiment (Fig.1) conducted in Shibaura Institute of Technology in Japan. During the experiment, high purity methane, together with steam were supplied into a tubular reformer via flow controller and evaporator. The reformer was filled with known amount of Ni/YSZ powder. The gas composition after the reforming process was analysed by gas chromatography. The catalyst material was industrial catalyst provided by AGC Seimi Chemical Co. Ltd. ink is housed in a syringe and deposited through cylindrical nozzles on thin electrolyte and sintered. The deposition and sintering procedure is repeated with ready-made cathode paste on the other side of electrolyte. Next, a ready button-cell undergoes electrochemical tests and FIB-SEM tomography. To derive correct kinetics data, the reaction has to occur in a whole volume of catalyst. This can be accomplished by keeping the reforming conversion rate low. To achieve a low level of methane conversion, the fuel was additionally mixed with nitrogen. During calculations, Arrhenius type of

dependency and Langmuir - Hinselwood equilibrium approach were used to calculate reforming process kinetics [2,4].

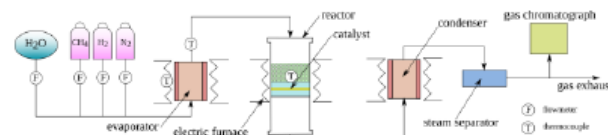


Fig. 1. Experimental set-up.

## RESULTS AND DISCUSSION

A parametric study were carried out for a group of parameters, which determine the heat and mass transfer in DIR-SOFC. Ni/YSZ anode microstructure parameters were used to evaluate reforming reaction rate. A state of hydrogen starvation was presented in Fig.2.

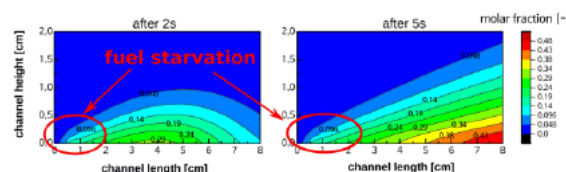


Fig. 2. Fuel starvation phenomenon in DIR-SOFC anode channel.

## CONCLUSIONS

A hydrogen starvation was reported under specific conditions in the inlet section of anode channel. Reforming reaction rate has an impact on species and temperature distribution, as well as on fuel starvation in anode channel.

## ACKNOWLEDGMENT

This work is carried out within the FIRST TEAM programme of the Foundation for Polish Science co-financed by the European Union under the European Regional Development Fund.

## REFERENCES

1. G. Brus, Int. J. Hydrogen Energy **37**, 22 (2012), 17225–17234
2. M. Możdziej, G. Brus, A. Sciazko, Y. Komatsu, S. Kimijima, and J.S. Szmyd, Flow, Turbul. Combust. **97**, 1 (2016), 171–189
3. G. Brus, K. Miyoshi, H. Iwai, M. Saito, H. Yoshida, Int. J. Hydrogen Energy **40**, 21 (2015), 6927–6934
4. V. N. Nguyen, R. Deja, R. Peters, L. Blum, Chem. Eng. J. **292**, 3 (2016), 113–122

# Microstructure and electric properties of BiYWO:LSM composite cathode for SOFC

Dudz M.<sup>\*(a)</sup>, Wrobel W.<sup>(a)</sup>, Malys M.<sup>(a)</sup>, Borowska-Centkowska A.<sup>(a)</sup>, Abrahams I.<sup>(b)</sup>, Fung K-Z.<sup>(c)</sup>, Krok F.<sup>(a)</sup>

(a) Faculty of Physics, Warsaw University of Technology, Koszykowa 75, 00-662 Warszawa, Poland

(b) Centre for Materials Research, School of Biological and Chemical Sciences, Queen Mary University of London

(c) Material Science and Engineering, National Cheng Kung University, 1# University Road, Tainan, Taiwan

e-mail: dudz@if.pw.edu.pl

Keywords: SOFC, cathode, composite, grain size

## INTRODUCTION

Novel electrode materials for IT-SOFC are widely investigated. Oxygen reduction process at the cathode is limited to three-phase interface (gas / electrode / solid electrolyte - so called Triple Phase Boundary – TPB). Therefore, to obtain good cathode, with the long TBP, highly conducting ionic and electronic conductors, either MIEC (mixed ionic electronic conductors) or composite materials, are required. Additionally, for the highly porous cathode oxygen exchange process can occur over the whole surface of electrode. In this work composite cathode (CC), build of LSM and bismuth based oxide, (BiYWO), was studied. Selected oxide ion conductor ( $\text{Bi}_3\text{Y}_{0.9}\text{W}_{0.1}\text{O}_{6.15}$  - BiYWO) was shown to provide one of the highest oxide ion conductivity at high and intermediate temperatures, but also good long-term stability [1]. The LSM ( $\text{La}_{0.8}\text{Sr}_{0.2}\text{MnO}_3$ ) component is a good electronic conductor commonly used for SOFC cathodes, but shows also high interfacial polarization effects [2]. Both components of composite cathode, LSM and BiYWO, exhibit similar thermal expansion coefficients. The influence of the BiYWO grain size on the electrical properties as well as the influence of composite cathode composition and microstructure on the ASR values will be discussed.

## EXPERIMENTAL

LSM component of the composite was prepared using cellulose-modified glycine-nitrate method. BiYWO compound was prepared using solid state reaction method as well as self-combustion method to obtain micron (micro composite) and nano (nano composite) grains, respectively. Composite cathodes (CC) were obtained by mixing BiYWO and LSM components in various volume ratios,  $f$ , from  $f = 1$  (BiYWO compound) to  $f = 0$  (LSM compound). Symmetrical cells CC/YSZ/CC were prepared using screen printing method. Impedance spectroscopy and transference numbers measurements were applied to determine ionic and electronic components as well as the total conductivity of prepared composites. Microstructure of the samples was determined with SEM imaging.

## RESULTS AND DISCUSSION

In the Fig.1. total conductivity of composite  $f = 0.6$  prepared with two methods is compared. In the case of BiYWO component prepared by solid state reaction (micro composite) total conductivity of composite is significantly higher than the total conductivity of a composite with nano grain BiYWO phase (prepared by wet chemistry method). Also nano grain composite

show curvature characteristic for ionic component (BiYWO phase) of composite, whereas in the case if micro composite activation energy is typical for LSM compound.

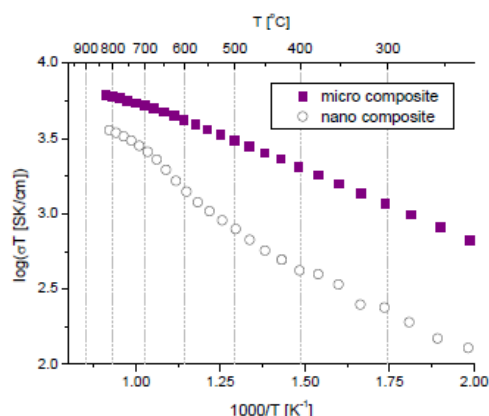


Fig.1. Arrhenius plot of total conductivity for  $f = 0.6$  composites with micro (filled symbols) and nano grain (open symbols) BiYWO compound

In the Fig. 2 area specific resistance (ASR) for prepared composite cathode,  $f=0.75$ , and reference LSM cathode is presented.

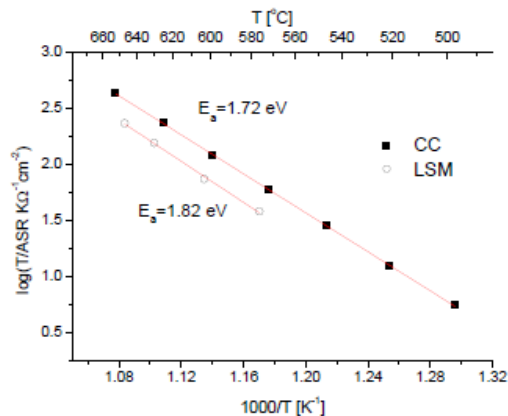


Fig.2. Temperature dependence of ASR for the  $f=0.75$  composite and LSM compound

## ACKNOWLEDGMENT

This work was supported by the National Centre for Research and Development Poland under grant number DKO/PL-TW1/6/2013.

## REFERENCES

1. A. Borowska-Centkowska, M. Leszczynska-Redek, W. Wrobel, M. Malys, M. Krynski, S. Hull, F. Krok, I. Abrahams, *Structure and conductivity in tungsten doped d-Bi3YO6*, Solid State Ionics, submitted.
2. C. Sun, R. Hui, J. Roller, J Solid State Electrochem (2010) 14:1125–1144



# Infrared thermography – powerful instrument for testing SOFC

*M. Jasiński*

Pedagogical University of Cracow, Podchorążych 2 street  
30-084 Cracow, Poland  
e-mail: mjasinski@up.krakow.pl

Keywords: solid oxide fuel cells, SOFC, thermography

## INTRODUCTION

Solid oxide fuel cells (SOFC) are promising devices for the co-generation of electricity and heat (CHP), both, in portable and stationary applications [1, 2]. One of the major problems in case of fuel cells is the use of materials for their construction retaining chemical, structural, electrical and thermo-mechanical properties for a long time under extreme conditions of high temperature and pressure. In order to meet these requirements, fuel combustion processes in different operating conditions as well as the chemical and structural changes leading to a reduction in the efficiency of the SOFC cell type should be examined and analyzed.

Midwave-infrared (MWIR) thermography is a method allowing observation of the cell electrode surface and examination of its temperature providing much more detailed information on the processes occurring on the surface of cells than spot temperature by thermocouple measurement.

Recent studies of SOFC cells support the potential of the method for testing thermal imaging of the small (a few millimeters in diameter) fuel cells [3, 4]. Brett et al. independently [5] indicated a need for use of large full-scale fuel cells, due to the lack of the fuel cell polarization in case of small size cells.

## EXPERIMENTAL

An innovative presented in this work relies on showing the applicability of the midwave infrared thermography to study full-size, solid oxide fuel cells (diameter approximately 100 mm). Infrared observations were made via quartz plate. Measurements has been performed using thermal imaging camera equipped with cooled to 85 K InSb detector. The test stand for thermal and electrical measurements of fuel cell has been constructed using a resistance tube furnace.

## RESULTS AND DISCUSSION

Infra-red thermography has been applied to the study of the operational IT-SOFC's to determine the temperature changes and spatial distribution associated with different current densities for anodes of full-size SOFC cells. Recorded images of full-scale commercial fuel cells showed a very good resolution. There is much more detailed information about the reactions at the surface, than from small button-type fuel cells.

## CONCLUSIONS

The small surface temperature variations detected by mid-infrared camera provide real-time analysis of the

early stages of SOFC failure, demonstrating the promise of this convenient imaging technique for system diagnostics.

## ACKNOWLEDGMENT

This work is supported by National Science Center under grant UMO-2013/11/N/ST8/00834.

## REFERENCES

1. K. Alanne, A. Saari, V.I. Ugursal, J. Good, J. Power Sources 158 (2006) 403-416.
2. A. Atkinson, S. Burnett, R.J. Gorte, J.T.S. Irvine, A.J. McEvoy, M. Mogensen, S.C. Singhal, J. Vohs, Nat. Mater. 3 (2004) 17-27.
3. M.B. Pomfret, D.A. Steinhurst, D.A. Kidwell, J.C. Owrutsky, J. Power Sources 195 (2010) 257-262.
4. M.B. Pomfret, D.A. Steinhurst, J.C. Owrutsky, J. Power Sources 233 (2013) 331-340.
5. J. Gang, K. Reifsnider, H. Xinyu, J. Fuel Cell Sci. Technol. 5 (2008), 031006-031001-031006.

# Metal supported Solid Oxide Fuel Cells with electrolyte deposited by Pulsed Laser Deposition

**Mariusz Krauz<sup>a</sup>, Ryszard Kluczowski<sup>a</sup>, Michał Kawalec<sup>a</sup>, Bogusław Budner<sup>b</sup>, Michael L. Korwin-Pawłowski<sup>c</sup>, Waldemar Mróz<sup>b</sup>**

<sup>a</sup> Institute of Power Engineering Ceramic Department Cerel, 1 Techniczna Street, 36-040 Boguchwała

<sup>b</sup> Institute of Optoelectronics, Military University of Technology, 2 Kaliskiego Street, 00-908 Warsaw, Poland

<sup>c</sup> Université du Québec en Outaouais, Département d'informatique et d'ingénierie, Gatineau (Québec), Canada

e-mail: krauz@cerel.pl

Keywords: metal support, fuel cells, PLD

## INTRODUCTION

In every configuration of SOFC one of the layers of the cell takes the function of the element assuring the mechanical stability of the cell during its operation. The layer assuming that function is called the substrate and is fabricated as the thickest element of the fuel cell. The other components of the fuel cell can be thin, which reduces the amount and the cost of expensive materials.

Using as the base of differentiation the type of the substrate, the basic configurations of SOFC are as follows: cells in which the anode forms the substrate (ASC - Anode Supported Cells), or the cathode (CSC - Cathode Supported Cells), cells on electrolyte substrate (ESC - Electrolyte Supported Cells). Cells formed on metallic substrates (MSC - Metal Supported Cells) are representative of the modern third generation of fuel cells. The type of the configuration defines the required working temperature range, the kind and quantity of materials used and also the kind of technology used for the fabrication of the individual layers composing the fuel cell.

## EXPERIMENTAL

In presentation we concentrate on the functional optimization of the electrolyte layer composed of 8YSZ and GDC, deposited by pulsed laser deposited method (PLD).

On Figure 1 is presented a schematic of the MS-SOFC in its planar configuration, which was realized in the course of this work. Indicated are also the initial candidate materials for individual layers of the cell to be used.



Fig. 1. Schematic of the MS-SOFC in its planar configuration and initial candidate materials.

MS – Metal Support (SS 316L, SS 430L, Croffer)

AC – Anode Contact Layer (NiO)

AF – Anode Functional Layer (NiO+8YSZ, NiO+GDC)

E – Electrolyte (8YSZ, GDC)

C – Cathode (LSC, LSCF)

In the course of this work new materials and new construction and fabrication concepts of individual components of metal-supported fuel cells such as high pressure injection moulding, ink-jet printing and laser and magnetron deposition of thin films were tested.

The diagnostic of the physical parameters of the layers were conducted using the methods of materials analysis (SEM-EDS, AFM, XRD and XPS) and then electrical characterization of the complete cells.

In order to evaluate the applicability of the PLD method to depositing thin electrolyte layers we have deposited the 8YSZ and GDC material at different experimental conditions. The electrolyte was deposited using an excimer ArF laser operating at the 193 nm wavelength. The laser pulse duration was  $t \sim 15\text{-}20$  ns, the energy reaching the surface of the target was  $E = 315$  mJ/pulse, the focus area was  $\sim 4.5$  mm<sup>2</sup>; the energy density at the focus was  $\sim 3.5 \cdot 10^8$  W/cm<sup>2</sup>. The electrolyte was deposited on the anode layer formed by screen printing on the metal substrate fabricated by high pressure injection moulding. The SEM images of 8YSZ layer deposited by PLD method are presented on Figure 2.

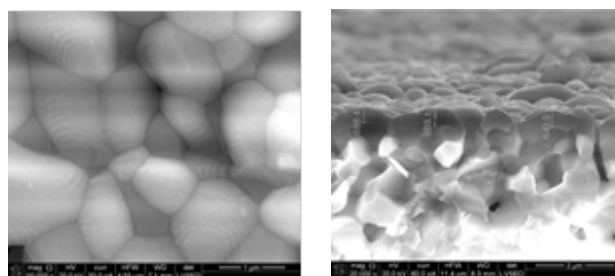


Fig. 2. The SEM images of 8YSZ layer deposited by PLD method

## CONCLUSIONS

The preliminary results of the analysis of the deposited layers of the 8YSZ electrolyte indicate at the possibility of depositing with the PLD method of gas-tight layers of a thickness of about 1÷3 micrometers.

## ACKNOWLEDGMENT

This work was supported by the Ministry of Science and Higher Education under statutory activities no OC/01/STAT/2016.

# Oxygen diffusion in BaGd<sub>1-x</sub>Yb<sub>x</sub>Mn<sub>2</sub>O<sub>5+δ</sub> layered structured perovskites for oxygen storage technology

Kun Zheng\*, Jacek Jagusztyn

AGH University of Science and Technology, Faculty of Energy and Fuels, Department of Hydrogen Energy,  
al. A. Mickiewicza 30, 30-059 Krakow, Poland

AGH University of Science and Technology, AGH Centre of Energy,  
ul. Czarnowiejska 36, 30-054 Krakow, Poland

\*E-mail: zheng@agh.edu.pl

Keywords: Oxygen diffusion, oxygen storage, layer-structured perovskites

## INTRODUCTION

Oxygen is the most omnipresent element which is indispensable in the energy productions, manufacturing industries, and other vital activities. However, a precise control of redox reactions for novel/better oxygen-related functionalities is required in the applications. Due to the increased demands of instant regulation of oxygen partial pressure in the gas phase, oxygen-storage materials with reversibly storing/releasing oxygen under oxidizing/reducing conditions are of great interest. Recently, BaLnMn<sub>2</sub>O<sub>5+δ</sub> – BaLnMn<sub>2</sub>O<sub>6+δ</sub> (Ln and Y) system was found to possess very good oxygen storage-related properties [1-3]. BaLnMn<sub>2</sub>O<sub>5+δ</sub> oxides belong to a group of A-site cation-ordered double perovskites. Ordering originates from the large mismatch between ionic radii of Ba<sup>2+</sup> and Ln<sup>3+</sup> cations. In case of the oxidized BaLnMn<sub>2</sub>O<sub>6</sub>, the structure can be considered as stacking of two primitive perovskite unit cells along c-axis, giving structure with alternating layers of BaO<sub>6</sub> and LnO<sub>6</sub> octahedra. Oxygen anions from Ln-related layer can be extracted relatively easy, and for instance, fully (BaYMn<sub>2</sub>O<sub>5</sub>) and partially (BaYMn<sub>2</sub>O<sub>5.5</sub>) reduced compounds were obtained. The excellent oxygen storage properties of BaYMn<sub>2</sub>O<sub>5+δ</sub> was shown by Motohashi et al. with measured reversible oxygen storage capacity almost equal to the theoretical one (3.85 wt.%), low temperatures of reduction and oxidation processes, and fast kinetics of changes of δ at 500 °C [2]. A-site modification of BaYMn<sub>2</sub>O<sub>5+δ</sub> by substitution of Y<sup>3+</sup> by other Ln<sup>3+</sup> cations will allow to obtain improved oxygen storage properties. The substitution of Y<sup>3+</sup> by smaller cations allows to reduce the unit cell volume changes between oxidized and reducing materials. Until now, the smallest Ln cation substituted in BaLnMn<sub>2</sub>O<sub>5+δ</sub> materials is Er [3]. In this work, even smaller cation Yb was doped in BaGd<sub>1-x</sub>Yb<sub>x</sub>Mn<sub>2</sub>O<sub>5+δ</sub> perovskites, in order to lower the unit cell volume changes between oxidized and reducing materials.

## RESULTS AND DISCUSSION

In this study, up to our knowledge, in the first time BaGd<sub>1-x</sub>Yb<sub>x</sub>Mn<sub>2</sub>O<sub>5+δ</sub> (x = 0, 0.2, 0.4, 0.6, 0.8, 1) double perovskites are synthesized. The crystal structure of investigated materials in oxidizing/reducing atmospheres are systematically studied. The in-situ study of BaGd<sub>1-x</sub>Yb<sub>x</sub>Mn<sub>2</sub>O<sub>5+δ</sub> oxidation in air allows to investigate the oxygen transport in the double perovskites (see Fig. 1), and it shows that the oxygen transport in

BaGd<sub>0.6</sub>Yb<sub>0.4</sub>Mn<sub>2</sub>O<sub>5</sub> is two-dimensional (changes of unit cell parameters *a* and *b*) and occurs only through the Gd<sub>0.6</sub>Yb<sub>0.4</sub>- related layer structure. The transport properties (electrical conductivity in oxidizing/reducing atmospheres, and oxygen diffusion coefficients) are investigated. The oxygen storage measurements of those synthesized oxides show the promising applications in the oxygen storage technology.

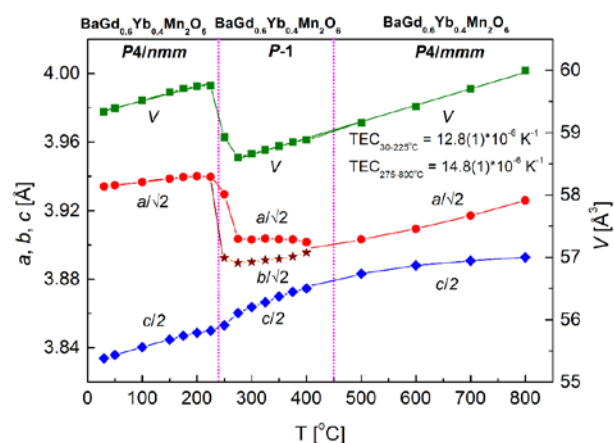


Fig. 1. In-situ study of BaGd<sub>0.6</sub>Yb<sub>0.4</sub>Mn<sub>2</sub>O<sub>5+δ</sub> oxidation in air.

## CONCLUSIONS

The doping effect of Yb at Gd-site in BaGd<sub>1-x</sub>Yb<sub>x</sub>Mn<sub>2</sub>O<sub>5+δ</sub> was systematically investigated and it shows that the increase of Yb significantly increases the oxygen mobility (reduction kinetic), but it also decreases the oxygen storage capacity. BaGd<sub>0.6</sub>Yb<sub>0.4</sub>Mn<sub>2</sub>O<sub>5+δ</sub> has the fastest oxygen diffusion kinetic and the smallest grain size in the series of BaGd<sub>1-x</sub>Yb<sub>x</sub>Mn<sub>2</sub>O<sub>5+δ</sub> oxides. The oxygen transport in BaGd<sub>0.6</sub>Yb<sub>0.4</sub>Mn<sub>2</sub>O<sub>5</sub> is two-dimensional and occurs only through the (*a*, *b*) Gd<sub>0.6</sub>Yb<sub>0.4</sub>- related layer structure.

## ACKNOWLEDGMENT

K. Zheng acknowledges the financial support from the Foundation for Polish Science (FNP).

## REFERENCES

1. Klimkowicz, et al., Mater. Res. Bull. 65 (2015) 116
2. T. Motohashi, et al., Chem. Mater. 22 (2010) 3192
3. K. Świerczek, et al., J. Solid State Chem. 203 (2013) 68

# New proton conducting materials for high temperature fuel cells

*K. Cichy, A. Polednik, W. Skubida, K. Świerczek*

AGH University of Science and Technology, Faculty of Energy and Fuels,  
al. A. Mickiewicza 30, 30-059 Krakow, Poland  
e-mail: cichykac93@gmail.com

Keywords: hydrogen, fuel cells, proton conductivity, perovskites

## INTRODUCTION

Fuel cells (FC) are electrochemical devices which directly convert chemical energy of fuel and oxidizer into electricity. Their high efficiency and relatively low negative influence on environment make such devices a promising alternative to currently applied solutions in power generation sector. One of the main types of FCs are Solid Oxide Fuel Cells (SOFC). Essential aspect that must be taken into consideration in selection of materials and design of SOFC-based stacks is a high operation temperature, reaching 800-1000 °C. While this gives an opportunity to apply SOFCs in combined heat and power generation systems, it brings a lot of challenges, especially in terms of degradation of materials. Conventionally, SOFCs are built using oxygen ion-conducting electrolyte. Relatively new concept of implementation of proton-conducting electrolytes gives some major benefits, such lowering of operation temperature, better fuel utilisation, as well as elimination of some of materials' issues [1].

In this work, a group of indium- and tin-based oxides, as well as Zr-containing perovskite-type oxides has been investigated in terms of possible application for manufacturing electrolyte and composite electrodes for Proton Ceramic Fuel Cells (PCFC).

## EXPERIMENTAL

Materials from the group of  $\text{BaIn}_{1-x}\text{Sn}_x\text{O}_{3-\delta}$  ( $x = 0.1-0.3$ ) and  $\text{Ba}_{0.9}\text{La}_{0.1}\text{Zr}_{0.25}\text{Sn}_{0.25}\text{In}_{0.5}\text{O}_{2.8}$  perovskite-type oxides were obtained by a high temperature solid state reaction. Barium carbonate and respective oxides (purity grade  $\geq 99.9\%$ ) were homogenized using a high-energy rotational-vibratory mill and then heat-treated at 950 °C for 24 h in air. Prepared precursors were uniaxially pressed into pellets and annealed in a temperature range of 1300-1500 °C for 4-6 h. Structural measurements were carried out in 10-110 deg range. High temperature X-Ray diffraction measurements were carried out in a 25-900 °C temperature range. Thermogravimetric (TG) measurements were carried out in three different atmospheres: synthetic air, argon and helium. Each measurement consisted of two heating and cooling cycles with 5 °C min<sup>-1</sup> heating/cooling rate in a range from 25 to 900 °C. Studied powders were also dried in 800 °C for 12 h, cooled down to 400 °C, and then the weight change was recorded during the hydration process in the humidified (3 vol.% H<sub>2</sub>O) synthetic air flow. Transport properties were measured by means of electrochemical impedance spectroscopy. Dense pellets of the considered materials were covered with platinum electrodes, and the measurements were carried out in a 0.1-10<sup>6</sup> Hz frequency range at

temperatures between 300 and 800 °C in a flow of dry and humidified air. Laboratory PCFCs were constructed and tested under various temperature and fuel flow rate conditions. Anodes were prepared as a composite of nickel oxide and  $\text{Ba}_{0.9}\text{La}_{0.1}\text{Zr}_{0.25}\text{Sn}_{0.25}\text{In}_{0.5}\text{O}_{2.8}$  electrolyte (3:2 wt. ratio) and cathodes as a composite of commercial  $\text{La}_{0.8}\text{Sr}_{0.2}\text{Fe}_{0.8}\text{Co}_{0.2}\text{O}_{3-\delta}$  powder and the electrolyte (1:1 wt. ratio). Both electrodes were screen-printed on the dense electrolyte pellet.

## RESULTS AND DISCUSSION

Studied  $\text{BaIn}_{1-x}\text{Sn}_x\text{O}_{3-\delta}$  oxides turned out to be very sensitive to water vapour content and showed interesting structural changes at temperatures below 500 °C, including significant variations of a unit cell parameter and structural transitions. While proton conductivity for e.g.  $\text{BaIn}_{0.8}\text{Sn}_{0.2}\text{O}_{2.6}$  composition reached relatively high value of  $1.7 \cdot 10^{-3} \text{ S cm}^{-1}$  at 550 °C and fast kinetics of the water intake/release, because of a mechanical weakness of the sinters, it was not possible to construct gas-tight PCFCs using studied  $\text{BaIn}_{1-x}\text{Sn}_x\text{O}_{3-\delta}$  oxides. With modification of chemical composition (introduction of Zr cations at the B-site and some amount of La at the A-site) an improvement of mechanical stability of the electrolyte was achieved. However, the synthesized  $\text{Ba}_{0.9}\text{La}_{0.1}\text{Zr}_{0.25}\text{Sn}_{0.25}\text{In}_{0.5}\text{O}_{2.8}$  electrolyte showed lower proton conductivity  $0.8 \cdot 10^{-3} \text{ S cm}^{-1}$  at 550 °C and also a decreased proton transference number. The tested PCFC cell with the mentioned electrolyte and composite electrodes reached power density equal to only 0.8 mW cm<sup>-2</sup> at 550 °C. It was found that NiO at the anode was reduced during cell's operation to Ni, and anode's chemical stability was good, but  $\text{La}_{0.8}\text{Sr}_{0.2}\text{Fe}_{0.8}\text{Co}_{0.2}\text{O}_{3-\delta}$  partially reacted at the cathode's side in humidified air.

## CONCLUSIONS

$\text{BaIn}_{1-x}\text{Sn}_x\text{O}_{3-\delta}$  oxides show interesting structural and proton transport properties, but suffer from mechanical stability issues. Modification of chemical composition to produce  $\text{Ba}_{0.9}\text{La}_{0.1}\text{Zr}_{0.25}\text{Sn}_{0.25}\text{In}_{0.5}\text{O}_{2.8}$  electrolyte allowed to construct and test laboratory-scale PCFC.

## ACKNOWLEDGMENT

The project was funded by the National Science Centre Poland (NCN) on the basis of the decision number DEC-2012/05/E/ST5/ 03772.

## REFERENCES

1. T. Ishihara (Ed.) Perovskite Oxide for Solid Oxide Fuel Cells, Springer, 2009

# Symmetrical proton ceramic fuel cells – construction and performance

Wojciech Skubida, Konrad Świerczek\*

AGH University of Science and Technology, Faculty of Energy and Fuels,  
al. A. Mickiewicza 30, 30-059 Krakow, Poland

\*e-mail: xi@agh.edu.pl

Keywords: hydrogen, fuel cells, proton conductors

## INTRODUCTION

It is known that one of the ways to improve performance of Solid Oxide Fuel Cells, especially considering lowering of the operating temperature, is to replace the oxygen ion-conducting electrolyte with material exhibiting proton conductivity [1]. However, in most of the cases, the reported so far electrochemical performance and long term stability of the cells based on the various oxide proton conductors are still inadequate for practical application. This is mostly due to a lack of proper electrode materials, which are compatible with the electrolytes, as well as because of fundamental issues related to proton, oxygen ion and electron conduction in a particular material at the same time.

In this work we present a new approach towards Proton Ceramic Fuel Cells, based on a concept of usage of the same material on the anode and cathode side. The idea of symmetrical cell (symmetrical Proton Ceramic Fuel Cell – sPCFC) simplifies manufacturing process and may limit unwanted chemical reactivity. Beneficial effects are expected if identical, composite electrodes are used in a construction of sPCFC, in which the protonic component of the conductivity is realized by the same phase as in the solid electrolyte. In the composite the electronic component is ensured by perovskite phase, having apart from suitably high electrical conductivity in reducing and oxidizing conditions, also good chemical stability, as well as exhibiting fast ionic transport. In this work usage of  $\text{Sr}_2\text{Fe}_{2-x}\text{Mo}_x\text{O}_{6-\delta}$  perovskite-type materials for preparation of such electrode composites, as well as construction and testing of sPCFC is shown. The mentioned perovskite materials exhibit high electrical conductivity in both, air and hydrogen environments, excellent redox stability, and already have been shown to deliver promising performance when applied as electrodes in symmetrical SOFCs utilizing oxygen-conducting electrolytes [2, 3].

## sPCFC CONSTRUCTION, RESULTS AND DISCUSSION

Selected  $\text{Sr}_2\text{Fe}_{2-x}\text{Mo}_x\text{O}_{6-\delta}$  oxides were prepared by a typical, high-temperature solid state route, with respective oxides and barium carbonate used as the starting materials. After milling in a high-efficiency mill, the mixtures were pressed into pellets and annealed. The electrode material was fired in synthetic air at 1100 °C for 30 h.  $\text{Ba}_{0.9}\text{La}_{0.1}\text{Zr}_{0.25}\text{Sn}_{0.25}\text{In}_{0.5}\text{O}_{2.8}$  oxide was used as the electrolyte material, and was prepared by two different heating treatments. First, respective oxides and barium carbonate powders were milled and calcined twice at 950 °C. Then, one part of the powder was annealed at 1200 °C, in order to obtain

single phase material suitable for manufacturing composite electrodes, while the other was pelletized and annealed at 1600 °C in order to obtain dense electrolyte sinters. The composite electrode material for sPCFC was prepared as a mixture of  $\text{SrFe}_{0.75}\text{Mo}_{0.25}\text{O}_{2.875}$  oxide and  $\text{Ba}_{0.9}\text{La}_{0.1}\text{Zr}_{0.25}\text{Sn}_{0.25}\text{In}_{0.5}\text{O}_{2.8}$  electrolyte powders (75:25 wt.% ratio), and was milled in a high-efficiency mill for 1 h. The mixture was screen printed on the electrolyte pellet on both sides and annealed at 1200 °C for 2 h. Electrodes were covered with thin layer of platinum paste with platinum wires used as interconnectors and again, annealed at 850 °C.

The manufactured electrodes for sPCFC were found to be mechanically stable and relatively well-adhered. The thickness of the used electrolyte was about 0.4 mm and for the electrodes 0.06 mm each. The measured impedance spectra consisted of three well-separated components, which could be interpreted as ohmic, bulk and grain boundary resistances. While the electrolyte area specific resistance (ASR) was found to be relatively low, ca. 3.7  $\Omega \text{ cm}^2$  at 600 °C, it increased drastically with electrodes being sintered on. The ASR of whole cell was 120  $\Omega \text{ cm}^2$  in humidified air and 235  $\Omega \text{ cm}^2$  in 5 vol.%  $\text{H}_2$  in Ar (symmetrical configuration of gas flow). Consequently, during operation the constructed sPCFC delivered low power density of about 1.3  $\text{mW cm}^{-2}$  at 600 °C. The value increased to 5  $\text{mW cm}^{-2}$  at 800 °C, but at such high temperature the protonic conduction in the electrolyte is negligible.

## CONCLUSIONS

As shown above, symmetrical cell construction in the case of PCFCs with proton-conducting electrolyte seems justified, and research in this field is worth continuation. However, it seems that manufacturing of effectively-working electrodes is difficult, and at the same time, essential in order to improve performance of such cells performance.

## ACKNOWLEDGMENTS

The project was funded by the National Science Centre, Poland on the basis of the decision number UMO-2016/21/N/ST8/00268.

## REFERENCES

1. N. Ito, M. Iijima, K. Kimura, S. Iguchi, J. Power Sources 152 (2005) 200
2. Q. Liu, X. Dong, G. Xiao, F. Zhao, F. Chen, Adv. Mater. 22 (2010) 5478-5482
3. A. B. Muñoz-García, D.E. Bugaris, M. Pavone, J.P. Hodges, A. Huq, F. Chen, H.C. zur Loye, E.A. Carter, J. Am. Chem. Soc., 134 (2012) 6826-6833

# First principles calculations of ionic transport in $\text{La}_2\text{NiO}_4$ candidate material for MIEC-type membranes

**Zhihong Du** <sup>(a,b)</sup>, **Zijia Zhang** <sup>(a,b)</sup>, **Hailei Zhao** <sup>(a,c)</sup>, **Konrad Świerczek** <sup>(b,d)\*</sup>

<sup>(a)</sup> University of Science and Technology Beijing, School of Materials Science and Engineering, Beijing 100083, China

<sup>(b)</sup> AGH University of Science and Technology, Faculty of Energy and Fuels, Mickiewicza 30, 30-059 Krakow, Poland

<sup>(c)</sup> The Beijing Municipal Key Laboratory of New Energy Materials and Technologies, Beijing 100083, China

<sup>(d)</sup> AGH Centre of Energy, AGH University of Science and Technology, ul. Czarnowiejska 36, 30-054 Krakow, Poland

e-mail: xi@agh.edu.pl

Keywords: first principles calculations,  $\text{La}_2\text{NiO}_{4\pm\delta}$ , membrane

## INTRODUCTION

Majority of known oxides, which are exhibiting high mixed ionic-electronic transport properties possess either perovskite-type or perovskite-related (e.g. Ruddlesden-Popper-type) crystal structure. In a series of  $\text{A}_{n+1}\text{B}_n\text{O}_{3n+1}$  compounds, for  $1 < n < \infty$  the structure can be described as comprising  $n$  perovskite-like layers separated by rock salt-like layers. In the whole  $\text{A}_{n+1}\text{B}_n\text{O}_{3n+1}$  series, electronic component of the electrical conductivity is governed by the double exchange mechanism (B-O-B) with an essential contribution from oxygen, which  $p$ -orbitals have to overlap effectively with  $d$ -orbitals of transition metal present at the B-site, for the effective charge transport. In the case of  $\text{A}_2\text{BO}_{4\pm\delta}$  oxides, mechanism of the charge transport is essentially the same, but as the perovskite layers form 2-dimentional network, the transport occurs in layers, with only a small perpendicular contribution. For example, literature data show high electronic component of the electrical conductivity in  $\text{La}_2\text{NiO}_{4+\delta}$ , but in general, depending on chemical composition, temperature and oxygen partial pressure, such  $\text{A}_2\text{BO}_{4\pm\delta}$  materials may exhibit ionic transport through the oxygen vacancies ( $\delta < 0$ ) or interesting, interstitial-type transport ( $\delta > 0$ ). This interstitial oxygen diffusion is unique, due to a low activation energy [1, 2].

## EXPERIMENTAL

In this work we report on first principles calculations (Materials Studio, CASTEP code) of oxygen defects (oxygen vacancy and interstitial oxygen) formation energy and migration energy of the interstitial oxygen in the case of  $\text{La}_2\text{NiO}_{4\pm\delta}$ .

## RESULTS AND DISCUSSION

Based on the performed calculation we have found that the oxygen vacancies are hard to form in  $\text{La}_2\text{NiO}_{4-\delta}$ , as the formation energy was established as high as about 9 eV. However, in the Ni-containing material the interstitial oxygen formation energy is negative and was calculated as equal about -4.8 eV. This result indicate that the interstitial oxygen defects are easily to form in  $\text{La}_2\text{NiO}_{4+\delta}$ , which is consistent with the reported experimental results, as well as performed TG studies. Then, we have calculated the possible migration paths of the interstitial oxygen and found that the migration energy is too high for the diffusion

to proceed directly from one interstitial position to the nearby site. Our results show that the most probable mechanism is the diffusion across a path between the terminal oxygen of  $\text{NiO}_6$  octahedra and the next nearby interstitial oxygen site. The calculated migration energy was found to be only about 0.6 eV. This confirms reported low activation energy of the ionic component of the conductivity in  $\text{A}_2\text{BO}_{4\pm\delta}$ -type nickelates.

The performed studies also show that in order to further improve the ionic conductivity of  $\text{La}_2\text{NiO}_{4+\delta}$ , introduction of more interstitial oxygens is needed, but also modification of the B-O bond strength within the diffusion path seems reasonable, and may be achieved by cations doping, such as Co and Cu.

## CONCLUSIONS

We have shown applicability of ab initio studies in evaluation of oxygen defect formation in  $\text{A}_2\text{BO}_{4\pm\delta}$ -type lanthanum nickelate, confirming experimental data of the oxygen content and activation energy of the ionic conduction. The approach seems easily applicable also for other Ruddlesden-Popper-type oxides.

## ACKNOWLEDGMENTS

The project was funded by the National Science Centre, Poland on the basis of the decision number UMO-2015/19/B/ST8/00871.

## REFERENCES

1. A.C. Tomkiewicz, M. Tamimi, A. Huq, S. McIntosh, *J. Mater. Chem. A* 3(2015)21864
2. T. Ishihara (Editor), *Perovskite Oxide for Solid Oxide Fuel Cells*, Springer, 2009



# La<sub>2-x</sub>Cu<sub>1-y</sub>M<sub>y</sub>O<sub>4-δ</sub> (M – In, Sc, Ga) with mixed ionic-electronic conductivity as oxygen-transport membranes

Zijia Zhang <sup>(a,b)</sup>, Zhihong Du <sup>(a,b)</sup>, Anna Niemczyk <sup>(b)</sup>, Hailei Zhao <sup>(a,c)</sup>, Konrad Świerczek <sup>(b)\*</sup>

<sup>(a)</sup> University of Science and Technology Beijing, School of Materials Science and Engineering, Beijing 100083, China

<sup>(b)</sup> AGH University of Science and Technology, Faculty of Energy and Fuels, Mickiewicza 30, 30-059 Krakow, Poland

<sup>(c)</sup> The Beijing Municipal Key Laboratory of New Energy Materials and Technologies, Beijing 100083, China  
e-mail: xi@agh.edu.pl

Keywords: oxygen transport membranes, A-site deficiency, B-sublattice doping

## INTRODUCTION

Oxygen-transport membranes (OTM), based on mixed ionic-electronic conductors (MIEC) have gained an increasing attention recently, due to a possibility for economical, efficient and environmentally-friendly production of oxygen from air, as well as their potential integration in oxy-fuel technologies with CO<sub>2</sub> capture. E.g. in the oxy-fuel process, a part of the flue gas, which contains CO<sub>2</sub>, is recycled and used as sweep gas, therefore, OTMs should not only exhibit a high oxygen flux, but also show good stability under CO<sub>2</sub>-containing atmospheres [1]. Problems with a limited CO<sub>2</sub> stability of majority of currently considered materials can be avoided by a development of alkaline earth-free membrane compounds. In this regard, A<sub>2</sub>BO<sub>4</sub> oxides with K<sub>2</sub>NiF<sub>4</sub>-related structure are of a particular interest, due to the expected moderate value of their thermal expansion and improved stability. Majority of the reported data show relatively high electronic component of the electrical conductivity in A<sub>2</sub>BO<sub>4±δ</sub> nickelates and cuprates, but while for Ni-containing materials unique, interstitial-type oxygen ionic transport occurs, in Cu-containing compound a deviation from oxygen stoichiometry is much smaller, with a tendency of formation of the oxygen vacancies. Further modification of the oxygen content in such oxides is possible by chemical substitution. In this respect, possibility of A-site nonstoichiometry and B-site M<sup>3+</sup> doping is explored in this work in La<sub>2-x</sub>Cu<sub>1-y</sub>M<sub>y</sub>O<sub>4-δ</sub>.

## EXPERIMENTAL

Powders with La<sub>1.9</sub>CuO<sub>4-δ</sub>, La<sub>1.9</sub>Cu<sub>0.95</sub>M<sub>0.05</sub>O<sub>4-δ</sub> (M – In, Sc, Ga) and La<sub>1.9</sub>Cu<sub>0.9</sub>M<sub>0.1</sub>O<sub>4-δ</sub> were prepared by a combined citric and ethylenediaminetetraacetic acid sol-gel method. The as prepared precursor powders were uniaxially pressed to obtain pellets, which was followed by a sintering conducted in air at 850-950 °C.

## RESULTS AND DISCUSSION

As shown in Fig. 1a for an exemplary La<sub>1.9</sub>CuO<sub>4-δ</sub> composition, a single phase material can be obtained with a moderate deficiency at the A-site of a parent La<sub>2</sub>CuO<sub>4</sub>. It was found that In<sup>3+</sup> has a very low solid solubility limit if doped at the B-site of La<sub>2-x</sub>CuO<sub>4-δ</sub>, which is likely due to its relatively large ionic radius. However, substitution of Cu with smaller cations, like Sc and Ga, was successful (Fig. 1b).

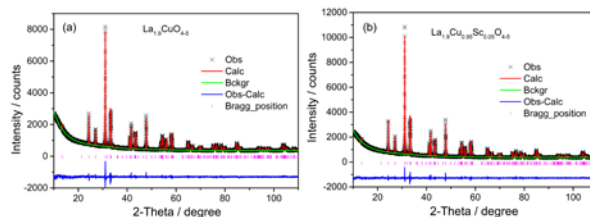


Fig. 1. XRD data with refinement for La<sub>1.9</sub>CuO<sub>4-δ</sub> (a) and La<sub>1.9</sub>Cu<sub>0.95</sub>Sc<sub>0.05</sub>O<sub>4-δ</sub> (b).

The obtained samples were evaluated in terms of their oxygen content and its evolution with temperature (Fig. 2), as well as transport properties. The measured total electrical conductivity was found to be in 10-20 S cm<sup>-1</sup> range at higher temperatures, up to 800 °C. The results indicate that by the appropriate choice of the chemical composition in La<sub>2-x</sub>Cu<sub>1-y</sub>M<sub>y</sub>O<sub>4-δ</sub> series, it is possible to obtain samples having improved mixed ionic and electronic conductivity.

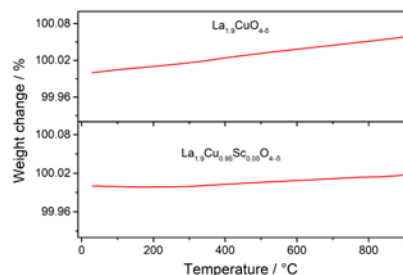


Fig. 2. TG curves of La<sub>1.9</sub>CuO<sub>4-δ</sub>, and La<sub>1.9</sub>Cu<sub>0.95</sub>Sc<sub>0.05</sub>O<sub>4-δ</sub>.

## CONCLUSIONS

Doping of metal ions with higher valence at the B-site may allow to increase the absolute value of the oxygen content in copper-based A<sub>2-x</sub>BO<sub>4</sub>-type oxides. This may play a pivotal role in terms of optimization of the electronic and ionic transport properties of the compounds, especially in terms of application as MIEC-type ceramic gas membranes.

## ACKNOWLEDGMENTS

The project was funded by the National Science Centre, Poland on the basis of the decision number UMO-2015/19/B/ST8/00871.

## REFERENCES

1. R. Kneer, D. Toporov, M. Förster, D. Christ, *Energy Environ. Sci.* 3 (2010)198

# Preparation of double layer Yttria Stabilized Zirconia matrix impregnated by lithium/potassium electrolyte for molten carbonate fuel cells

*J. Milewski<sup>1,\*</sup>, T. Wejrzanowski<sup>2</sup>, K.-Z. Fung<sup>3</sup>, Ł. Szablowski<sup>1</sup>, R. Baron<sup>2</sup>, J.-Y. Tang<sup>3</sup>, A. Szczęśniak<sup>1</sup>, C.-T. Ni<sup>3</sup>*

<sup>1</sup>Warsaw University of Technology, Institute of Heat Engineering, 21/25 Nowowiejska Street  
00-665 Warsaw, Poland

<sup>2</sup>Warsaw University of Technology, Faculty of Material Science Engineering, 141 Wołoska Street  
02-507 Warsaw, Poland

<sup>3</sup>National Cheng Kung University, 1 University Road  
R.O.C. 70101, Taiwan

\*Corresponding author: milewski@itc.pw.edu.pl

Keywords: hydrogen, fuel cells

## INTRODUCTION

Fuel cells operating at elevated temperatures are suitable for medium and large scale applications, thus they have good prospects for commercialization, Molten Carbonate Fuel Cells (MCFCs) appear among the most promising in this respect. MCFC has a number of advantages over other high temperature fuel cells: (i) high energy efficiency and high electromotive force, (ii) nickel instead platinum as a catalyst, (iii) electrolyte thickness of about 1 mm is much more easier to manufacture, (iv) it can be used as a CO<sub>2</sub> separator due to its ability to capture carbon dioxide from the cathode side.

LiAlO<sub>2</sub> is a very effective support for molten carbonates, however, there is a limited number of manufacturers, and so, it makes it very expensive. In a single conducting electrolyte, the cathode inlet needs to contain an adequate ratio of CO<sub>2</sub> to O<sub>2</sub>, (2:1), this results in a low oxygen partial pressure at the cathode inlet (taking into account that oxygen is being delivered in air at an initial molar fraction of 21%). The low pressure of oxygen results in a relatively low Nernst voltage, and finally decreases the MCFC performance. By using a dual conducting electrolyte, it is possible to obtain a more favorable ratio between carbon dioxide and oxygen (CO<sub>2</sub>:O<sub>2</sub><2), achieving higher maximum voltages what translates itself into higher efficiency.

An excellent performance was obtained for the YSZ-carbonate composite and nanocomposite electrolytes prepared using eutectic carbonates with a mixture of Li<sub>2</sub>CO<sub>3</sub>/K<sub>2</sub>CO<sub>3</sub>. High temperature membranes based on dual carbonate and oxide electrolytes have been shown to selectively separate CO<sub>2</sub> above 600°C.

In this paper, the testing results of composite electrolyte layer based on Yttria Stabilized Zirconia and Lithium/Potassium carbonates for its electrochemical performance as a matrix for MCFC are presented. The voltage-current density curves were collected in the range of temperatures: 500–800°C.

The idea is to use a dual conductive composite electrolyte as a matrix for Molten Carbonate Fuel Cells. This results in an improvement in the performance of the MCFC, by, especially, increasing the ionic conductivity by additional O<sup>2-</sup> conduction.

## EXPERIMENTAL

The YSZ matrices were formed by solid state reaction: desired amount of YSZ were ball-milled in ethanol for 12 hours. The powder mixture was calcined at 1,200°C for 6 hours. The calcined powder was subsequently ball milled and dried. Finally, the dried powder was sieved through the 200-mesh screen. To manufacture a YSZ tape, YSZ powder was ball-milled for 24 h with commercial binder solution (B73305, Ferro) based on a volume ratio 1:1. The YSZ slurry was subsequently debubbled and followed by tape-casting using a doctor blade (see Fig. 1).

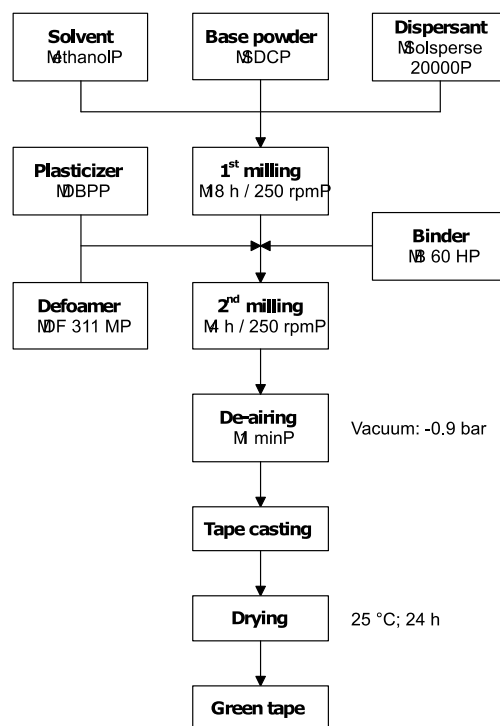


Fig. 1. Matrix preparation procedure

## ACKNOWLEDGMENT

The project is co-financed by Polish National Centre for Research and Development of Polish-Taiwanese/Taiwanese-Polish Joint Research Call granted by decision number DZP/PL-TWIII/16/2016.

# Electrochemical behavior of a Pd and Pd-noble metal alloys thin film electrodes in concentrated alkaline media

*K. Hubkowska<sup>1</sup>, M. Soszko<sup>2</sup>, M. Symonowicz<sup>1</sup>, M. Łukaszewski<sup>1</sup>, A. Czerwiński<sup>1,2,3</sup>*

<sup>1</sup> Warsaw University, Department of Chemistry, Pasteura 1, 02-093 Warsaw, Poland

<sup>2</sup> Industrial Chemistry Research Institute, Rydygiera 8, 01-793 Warsaw, Poland

<sup>3</sup> Faculty of Chemistry, Biological and Chemical Research Centre, University of Warsaw, Żwirki i Wigury 101, 02-089 Warszawa, Poland

\* E-mail: khubkowska@chem.uw.edu.pl

**Keywords:** Pd limited volume electrode, hydrogen sorption,  $\alpha \leftrightarrow \beta$  phase transition potential, hydrogen pretreatment procedure, alkaline solutions

## INTRODUCTION

Pd and Pd-noble metal alloys behavior in concentrated (6 M) basic solutions of KOH, NaOH and the mixture of LiOH and KOH is presented (in comparison with 0.5 M H<sub>2</sub>SO<sub>4</sub> solution). We describe the influence of the process of hydrogen pretreatment procedure on the hydrogen absorption properties of Pd thin films, namely the value of potential of hydrogen oxidation, the amount of absorbed hydrogen and the  $\alpha \rightarrow \beta$  phase transition potentials with respect to our previous works focused on electrochemical behavior of Pd thin film electrodes in acidic electrolytes.

## EXPERIMENTAL

Pd and Pd-noble metal alloys limited volume electrodes (0.5  $\mu\text{m}$  thick) were deposited potentiostatically on a gold wire (0.5 mm diameter). After deposition the electrodes were subjected to hydrogen pretreatment procedure. During the pretreatment procedure the solution was purged with, removing gaseous oxygen and hydrogen. Before other electrochemical measurements were performed the solution was purged with Ar for 20 min., while during the measurements Ar stream floated above the solution. The measurements were carried out in a three-electrode system with a Pd-LVE working electrode, an Hg/HgO/6M KOH (or in case of the acidic electrolyte: Hg/Hg<sub>2</sub>SO<sub>4</sub>/0.5M H<sub>2</sub>SO<sub>4</sub>) reference electrode and a Pt gauze auxiliary electrode. CH Instruments model 760D was utilized in electrochemical measurements. Analytical grade reagents (Avantor, Sigma-Aldrich, Alfa-Aesar) and water purified in Hydrolab and Millipore systems were used to prepare all the solutions. The potentials were recalculated with respect to the reversible hydrogen electrode (RHE) in the working solution with the use of Hydroflex Hydrogen Reference Electrode purchased from Gaskatel GmbH, Germany. All measurements were done in the temperature of 298 K. The parameter of H/M was calculated on the basis of the charge obtained from the integration of the hydrogen oxidation cyclic voltammetry signals and the deposition charge of Pd.

## RESULTS AND DISCUSSION

The changes in the CV response after prolonged hydrogen absorption/desorption in 6 M KOH electrolyte are qualitatively identical to those reported earlier for a Pd electrode pretreatment in acidic

solutions [1]. This behavior indicates that after many cycles of hydrogen absorption/desorption in Pd electrodeposits these processes become electrochemically more reversible. i.e. faster than in a freshly prepared electrode. Typically, a steady-state CV (mirrored in a constant position of hydrogen peaks) in an acid (0.5 M H<sub>2</sub>SO<sub>4</sub>) can be obtained already after several tenths of cycles, while in all basic solutions studied here (6 M KOH, 6 M NaOH and a mixture of 2 M LiOH + 4 M KOH) no less than ca. 300 cycles were required for the CV stabilization. The alpha-beta phase transition is placed at ca. 50 mV vs. RHE in all cases, with only small deviations (within ca. 5 mV) for a given electrolyte. The value of  $E_{\alpha \rightarrow \beta}$  deviation was estimated on the basis of several H/Pd ratio vs E profiles plotted after multiple repeatable measurements. Also, the amounts of hydrogen electrosorbed in Pd-LVEs in the  $\alpha$  and  $\beta$  phases are practically the same for each solution studied. The maximum H/Pd values at the lowest edge of the potential range applied in these studies are ca. 0.73-0.74, regardless of the kind of the electrolyte, i.e. they are the same in both basic and acidic solutions.

## CONCLUSIONS

The hydrogen pretreatment procedure is hindered in basic solutions in comparison with acid, therefore the electrode should be polarized long enough to obtain repeatable course of CV curves in subsequent CV cycles. There is no difference between the course of CV curve (the shape and the position of hydrogen absorption and desorption signals) and H/Pd vs E curves after hydrogen pretreatment procedure in alkaline and acid media. The  $\alpha \rightarrow \beta$  phase transition potential, regardless of the type of solution, equals to approx. 50 mV vs RHE ( $\pm 2.5\text{mV}$ ). The continuous Pd electrode cycling does not affect the hydrogen capacity.

## ACKNOWLEDGMENT

This research was funded from grant no. 2015/17/B/ST8/03377 (ID 289956) of the Polish National Centre.

## REFERENCES

1. K. Hubkowska, M. Łukaszewski, A. Czerwiński, *Electrochim. Acta* 56, 2344 (2011)

# Hydrogen absorption in a palladium limited volume electrodes from protic ionic liquids

*M. Pająk<sup>1,\*</sup>, K. Hubkowska<sup>1</sup>, and A. Czerwiński<sup>1,2</sup>*

<sup>1</sup>University of Warsaw, Faculty of Chemistry, Pasteura 1, 02-093 Warsaw, Poland

<sup>2</sup>Industrial Chemistry Research Institute, Rydygiera 8, 01-793 Warsaw, Poland

\*e-mail: mpajak@chem.uw.edu.pl

Keywords: hydrogen sorption, palladium, protic ionic liquids

## INTRODUCTION

Palladium absorbs hydrogen, even at room temperature and pressure and has an exceptionally high absorption capacity. It forms palladium hydrides,  $\text{PdH}_x$ , with values of  $x$  up to 1. The sorption of hydrogen in Pd-LVE electrode has been studied in aqueous solutions of acids and bases [1, 2] and there are very few reports on the hydrogen sorption in ionic liquids [3, 4]. Therefore we decided to investigate this process in selected protic ionic liquids (PILs) as a class of solvents that have negligible vapour pressure, good thermal and chemical stability and no corrosive properties which make them alternative electrolytes [4]. PILs are combinations of Brønsted acids and bases. Brønsted bases are acceptors of the protons from the Brønsted acids and thereby they acts as proton-carriers in the liquids [5].

## EXPERIMENTAL

All electrochemical experiments were carried out in protic ionic liquid under Ar with the use of three-electrode system with a Pd-LVE working electrode, an Ag wire as a quasi-reference electrode and a Pt gauze as auxiliary electrode. Cyclic voltammetry (CV), chronoamperometry (CA) and chronopotentiometry (CP) were used as the main experimental techniques.

## RESULTS AND DISCUSSION

Pd limited volume electrodes (LVE) were obtained electrochemically from the  $\text{PdCl}_2$  aqueous solution. After many cycles of hydrogen absorption/desorption in Pd-LVE (hydrogen pretreatment procedure [2]), these processes become electrochemically more reversible than in a freshly prepared electrode. The same effect has been observed in case of hydrogen sorption measurement in aqueous solutions of acids and bases. However, even after many CA and CV cycles of hydrogen sorption in ionic liquid medium, the process of hydrogen sorption is much less reversible compared with acids and basis (see Fig. 1). This behavior indicates that the creation of defects (facilitating further hydrogen transport) in Pd lattice is hindered by e.g. the slow proton transfer from PIL.

## CONCLUSIONS

Hydrogen absorption in palladium electrode occurs from the reduction of labile protons of PIL. Cyclic voltammetry measurements show that the reduction reaction takes place with slower kinetics than in aqueous solutions because of the slower proton

transfer from PIL to the electrode connected with low lability of hydrogen and high viscosity of the electrolyte.

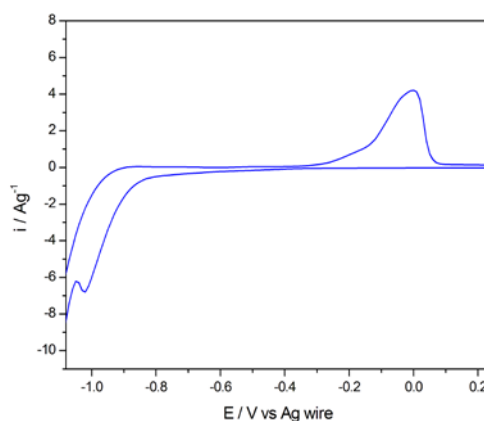


Fig. 1 Cyclic voltammetry curve of Pd-LVE electrode in ammonium protic ionic liquid after hydrogen pretreatment procedure; scan rate:  $1\text{mVs}^{-1}$

## ACKNOWLEDGMENT

This work is financially supported by the National Center of Science (NCN) grant No.2015/17/B/ST8/03377 (ID 289956) and University of Warsaw, Faculty of Chemistry.

## REFERENCES

1. A. Czerwiński, I. Kiersztyn, M. Grdeń, J. Czapla *Journal of Electroanalytical Chemistry* **471** (1999) 190
2. K. Hubkowska, M. Soszko, M. Symonowicz, M. Łukaszewski, A. Czerwiński *Electro-catalysis* (2017) doi:10.1007/s12678-017-0379-5
3. J. Tremblay, N. L. Nguyen, D. Rochefort, *Electrochemistry Communications* **34** (2013) 102
4. Y. Meng, L. Aldous, R. G. Compton, *Green Chemistry* **12** (2010) 1926
5. H. Nakamoto, M. Watanabe, *Chemical Communications* (2007) 2539

# Physical properties of TiZrNi ribbons and their hydrides

A. Żywczak<sup>a</sup>, L. Gondek<sup>b</sup>, T. Kozieł<sup>c</sup>

<sup>a</sup>Academic Centre for Materials and Nanotechnology,

<sup>b</sup>Faculty of Physics and Applied Computer Science,

<sup>c</sup> Faculty of Metals Engineering and Industrial Computer Science,

AGH University of Science and Technology, Kraków, Poland

e-mail: zywczak@agh.edu.pl

Keywords: Hydrogen-storage materials, Nano-materials, quasicrystals

## INTRODUCTION

The TiZrNi compounds also are promising candidates for metal-hydride based batteries, protective coatings and memory shape alloys. The Ti-Zr-Ni compounds can be synthesized in the amorphous, quasicrystalline and crystalline phases. Quasicrystals have unique structures with a new type of translational long-range order. Ti-based quasicrystals belong to the second largest group of the stable quasicrystals. The large hydrogen uptake capacity makes the TiZrNi quasicrystals a good material for hydrogen storage [1]. The quasicrystalline Ti-Zr-Ni alloys (the i-phase) may be obtained by the melt spinning technique, the mechanical alloying and the magnetron sputtering.

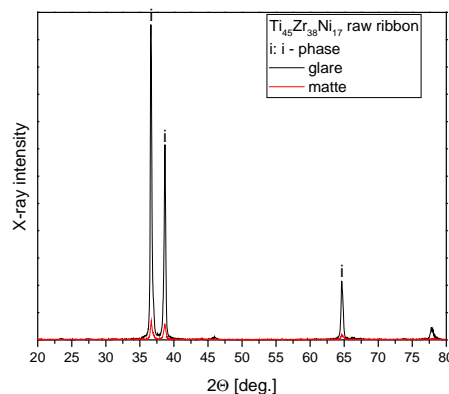
## EXPERIMENTAL

The alloy with a nominal composition of  $\text{Ti}_{45}\text{Zr}_{38}\text{Ni}_{17}$  (at.%) was prepared by arc melting of a mixture of high purity elements with purities of 99.9% or higher in a Ti-gettered argon atmosphere. To ensure homogeneity, the 30 g ingot was remelted five times. Thin ribbons 10 mm in width and 30  $\mu\text{m}$  in thickness) were prepared by single-roller melt spinning under argon atmosphere at a constant over-pressure of 50 kPa and linear wheel speed of 20 m/s. The obtained quasicrystal samples were hydrogenated using the Setaram PCT-PRO Sievert's apparatus. X-ray diffraction (XRD) method was used for a quality assessment of the obtained quasicrystal and their hydrides.

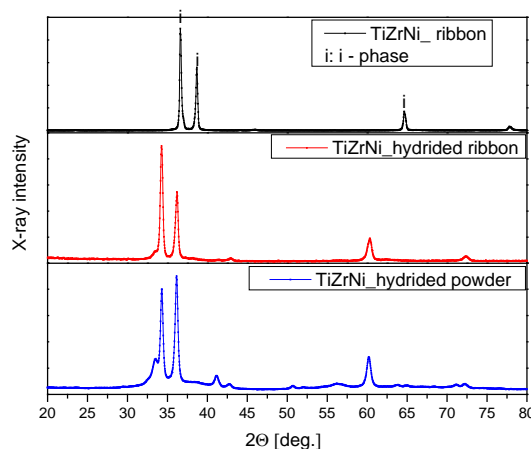
## RESULTS AND DISCUSSION

Fig 1 show the XRD pattern of the i-phase of both side of ribbon directly received from melt spinning. The air-side surface (glare-black line) of ribbon has greater the size of quasi-crystalline grains and better the intensity of the XRD peaks compare to the wheel-side surface (matte-red line) of ribbon.

The raw ribbon was given hydrogenation (Fig 2 b). We checked XRD peaks, and we observed the same peaks were moved into low angles for the both side of ribbon, it is mean than whole ribbon was hydrogenated. The hydrogen concentrations are 1 wt.%. The ribbon was milled to increase surface of absorbing hydrogen (Fig 2c). The hydrogen content are above 2 wt.%. Additionally, a number of small reflections in XRD pattern can be indexed as the some crystal phase.



**Fig 1.** The X-ray diffraction patterns for the  $\text{Ti}_{45}\text{Zr}_{38}\text{Ni}_{17}$  i-phase both side of raw ribbon.



**Fig 2.** The X-ray diffraction patterns for the  $\text{Ti}_{45}\text{Zr}_{38}\text{Ni}_{17}$  i-phase raw ribbon (a), after hydrogenation ribbon (b) and after hydrogenation powder from ribbon (c).

## CONCLUSIONS

We managed to get a quasi-crystalline ribbon and it was hydrogenated. In order to increase the hydrogen content of the material, the ribbon was milled.

## REFERENCES

1. A. Takasaki, K.F. Kelton, J. Alloys Compd. 347 (2002) 295.

# Hydrogenation of $\text{Ti}_{45}\text{Zr}_{38}\text{Ni}_{17}$ quasicrystals prepared by rapid quenching method

*M. Nowak<sup>1,\*</sup>, K. Świerczek<sup>1</sup>, A. Żywczak<sup>2</sup>, A. Takasaki<sup>3</sup>*

<sup>1</sup>AGH University of Science and Technology, Faculty of Energy and Fuels  
Department of Hydrogen Energy, al. A. Mickiewicza 30, 30-059 Krakow, Poland

<sup>2</sup>AGH University of Science and Technology,  
Academic Centre of Materials and Nanotechnology, Al. Mickiewicza 30, 30-059 Kraków, Poland

<sup>3</sup>Shibaura Institute of Technology, Faculty of Engineering, 3-7-5 Toyosu, Koto-ku, 135-8548 Tokyo, Japan  
e-mail: mnowak.agh@gmail.com

Keywords: quasicrystals, hydrogenation, rapid quenching

## INTRODUCTION

Development of a hydrogen storage material having a high and reversible capacity is one of the crucial challenges for future progress of the hydrogen economy. Presently, hydrogen storage materials are mostly based on transition metal-containing alloys, e.g.  $\text{LaNi}_5$ , which can reversibly absorb 1.4 wt.% of hydrogen [1]. Among novel materials, which may exhibit higher capacity, quasicrystalline compounds are now intensively studied. Quasicrystals are a group of materials discovered by Shechtman in 1994 [2]. Despite that they do not possess translational symmetry, their X-ray diffraction patterns show sharp peaks indicating long-range order. For example, local structure of  $\text{Ti}_{45}\text{Zr}_{38}\text{Ni}_{17}$  icosahedral phase is comprised of Bergman two-shell atomic clusters which contain totally 140 tetrahedral interstitials where hydrogen atoms can be introduced. In this work, structural characterization of  $\text{Ti}_{45}\text{Zr}_{38}\text{Ni}_{17}$  quasicrystals prepared by a rapid quenching method is presented. The obtained materials were hydrogenated in a reaction with gas phase, allowing to establish pressure-composition isotherms, showing high hydrogen capacity.

## EXPERIMENTAL

Ti, Zr and Ni metallic powders were melted in an induction furnace under argon atmosphere, and then melt-spun onto a copper wheel rotating at 20, 30, 40 and 50  $\text{m s}^{-1}$ . The obtained ribbons were grounded in mortar and sieved through 75  $\mu\text{m}$  sieve. Structural studies (XRD) were carried out in 20-80 deg range using  $\text{CuK}\alpha$  radiation on Rigaku SmartLab diffractometer. Elemental analysis and chemical characterization were performed using JSM-7100F electron microscope equipped with EDS adapter. Prepared powders were hydrogenated in a high-pressure vessel at 300, 400 and 500 °C. For the studies, the vessel filled with respective powder was evacuated by a rotary pump, and then back-filled with pure (99.99999%) hydrogen gas. In the next step the vessel was heated to a desired constant temperature. Hydrogenation was carried out in a pressure range of 0,0001-2,5 MPa.

## RESULTS AND DISCUSSION

Fig. 1 depicts XRD data recorded for  $\text{Ti}_{45}\text{Zr}_{38}\text{Ni}_{17}$ , which was obtained in a rapid quenching process. Sharp peaks originating from the I-phase (36.5, 38.5 and 64.5 deg) can be detected for all samples produced

with different rotating speeds. Surprisingly, a little difference in the structural features can be seen. In particular, no crystalline phases were detected at the lowest rotation speed, as well as glassy-like phase at the highest speed.

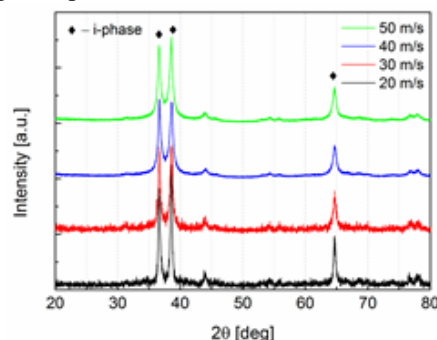


Fig. 1. XRD data for  $\text{Ti}_{45}\text{Zr}_{38}\text{Ni}_{17}$  obtained at different speeds.

Pressure-composition isotherms for the  $\text{Ti}_{45}\text{Zr}_{38}\text{Ni}_{17}$  material obtained at 30  $\text{m s}^{-1}$  speed are shown in Fig. 2. At 300°C, the plateau-like region can be observed, which may indicate formation of a single hydride phase. The recorded maximum capacity at this temperature is 2.187 wt.%. However, desorption process proceeded slowly and did not reach an equilibrium plateau.

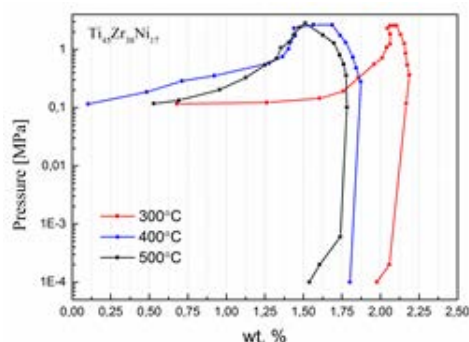


Fig. 2. Pressure-composition isotherms for  $\text{Ti}_{45}\text{Zr}_{38}\text{Ni}_{17}$ .

## CONCLUSIONS

$\text{Ti}_{45}\text{Zr}_{38}\text{Ni}_{17}$  icosahedral phase obtained by a rapid quenching method was tested in terms of possibility of reversible hydrogenation, showing interesting properties.

## REFERENCES

1. G. Liang, J. Huot, R. Schulz, J. Alloys Compd. 320 (2001) 133-139
2. D. Shechtman, I. Blech, D. Gratias, J.W. Cahn, Phys. Rev. Lett. 20 (1984) 1951-1953



# Underground hydrogen storage in salt caverns: hydrogen reactivity issues

*Radosław Tarkowski<sup>1,\*</sup>, Wojciech Skubida<sup>2</sup>, Konrad Świerczek<sup>2</sup>*

<sup>1</sup>Mineral and Energy Economy Research Institute of the Polish Academy of Sciences  
Department of Geoengineering and Environmental Engineering

ul. Wybickiego 7, 31-261 Krakow, Poland

<sup>2</sup>AGH University of Science and Technology, Faculty of Energy and Fuels,  
al. A. Mickiewicza 30, 30-059 Krakow, Poland

\*e-mail: tarkowski@min-pan.krakow.pl

Keywords: underground hydrogen storage, salt caverns, reactivity

## INTRODUCTION

One of the main risks associated with construction and operation of an underground storage of hydrogen in salt deposits is geological uncertainty. This issue can be partially resolved by obtaining a detailed knowledge of each salt deposit being concerned for the storage. Geological structures of salt deposits are varied, from relatively simple ones, in a form of regular layers (bedded deposits, the most suitable for leaching the caverns) to the very complicated ones, like salt domes. Obviously, this is an important aspect, considering choice of location and construction of the underground gas storage for hydrogen, also in Poland [1].

It is expected that underground hydrogen storage caverns may lose their tightness because of a presence within the salt layers of interbedded porous rocks, other than salt, and because of impurities, such as insoluble rocks (mostly anhydrite and clay minerals). As the hydrogen molecule is the smallest known chemical molecule, H<sub>2</sub> gas is characterized by a high permeability, much higher than that of methane. Consequently, storage caverns, which are suitable for keeping of methane, may not be appropriate for a prolonged storage of hydrogen. Because hydrogen is able to diffuse through solids in an ionized form, this aspect has to be taken into account as well.

This paper presents results of studies on processes that may occur in salt caverns during underground storage of hydrogen. The impact of hydrogen gas on rocks (such as salts, anhydrite, clays) is investigated, with the most important parameters that may lead to an irreversible loss of hydrogen during the storage being identified. While salt caverns seem to be one of the most attractive systems for underground hydrogen storage, literature data on the topic contain only a few papers based on experimental data. Up to our knowledge, there is no research based on data from Polish salt deposits.

## EXPERIMENTAL, RESULTS AND DISCUSSION

Investigations presented in this work are focused on reactivity of hydrogen gas with rock salt and interbedded rocks exhibiting higher porosity. The studied samples originate from Kłodawa Salt Mine. Characterization techniques cover X-ray diffraction and scanning electron microscopy measurements of samples before and after hydrogenation, as well as thermogravimetric studies in different atmospheres.

Based on literature references and performed studies it seems that rock salt is a good medium for hydrogen storage, because it does not react with it or dissolve. It also has a favorable geochemical properties. Due to limited reactivity, it can be expected that rock salt cavern will guarantee a long-term stability and tightness of the underground hydrogen reservoir. In addition, fractures that could potentially expand and create escape routes for hydrogen, become sealed by themselves, because of the rheological properties of rock salt.

## CONCLUSIONS

Underground storage of compressed hydrogen in salt caverns seems viable, and this technology may become in a future an important element of power grid, contributing to the improvement of its balance.

## REFERENCES

1. R. Tarkowski, Int. J. Hydrogen Energy 42(1) (2017) 347-355

# Influence of synthesis methods on electrical conductivity and dielectric relaxation in $(\text{Ce}_{0.9}\text{Gd}_{0.1})_{0.85}\text{Pr}_{0.15}\text{O}_{2-\delta}$ studied by impedance spectroscopy

M. Wojcik, M. Malys, M. Holdynski\*, M. Leszczynska-Redek, W. Wrobel and F. Krok

Faculty of Physics, Warsaw University of Technology, Koszykowa 75, 00-662 Warszawa, Poland.

\* Institute of Physical Chemistry, Polish academy of Sciences, ul. Kasprzaka 44/52, 01-224 Warsaw, Poland.  
e-mail: maciej.wojcik.if@gmail.com

Keywords: co-doped ceria, impedance spectroscopy, dielectric relaxation

## INTRODUCTION

Praseodymium doped cerium oxide (PCO) exhibits mixed ionic/electronic conductivity depending on oxygen partial pressure ( $p(\text{O}_2)$ ) and Pr content. On the other hand in gadolinium doped ceria (GDC) high oxide ion transference numbers are observed under normal SOFC oxygen partial pressures. As  $p(\text{O}_2)$  is decreased at elevated temperature, PCO releases oxygen (forming oxygen vacancies) while  $\text{Pr}^{4+}$  and  $\text{Ce}^{4+}$  can be reduced to  $\text{Pr}^{3+}$  and  $\text{Ce}^{3+}$ , increasing electronic conductivity. These properties are interesting in terms of application of these materials in permeation membranes, SOFC electrodes, gas sensors, and oxygen storage materials. Therefore the compounds in the  $\text{CeO}_2\text{-Pr}_2\text{O}_3\text{-Gd}_2\text{O}_3$  system are widely investigated, [eg. 1]

In our studies we examined  $(\text{Ce}_{1-x}\text{Gd}_x)_{0.85}\text{Pr}_{0.15}\text{O}_{2-\delta}$  in range of  $0.0 < x < 0.6$  where the base compound is  $\text{Pr}_{0.15}\text{Ce}_{0.85}\text{O}_{2-\delta}$  and the Ce is partially substituted with Gd to change ionic/electronic conductivity ratio. The results showed that the  $x = 0.1$  composition is interesting due to the highest values of both electronic and ionic conductivities and lowest activation energies.

The aim of the presented studies was the detailed investigation of electrical conductivity and dielectric relaxation properties in  $(\text{Ce}_{1-x}\text{Gd}_x)_{0.85}\text{Pr}_{0.15}\text{O}_{2-\delta}$   $x = 0.1$  composition by impedance spectroscopy measurements in wide frequency range for samples prepared by different synthesis methods.

## EXPERIMENTAL

Polycrystalline samples were prepared by different synthesis methods including: solid state reaction, co-precipitation, self-combustion synthesis. The impedance of the polycrystalline samples was measured in the frequency range from 10 MHz to 0.01 Hz at temperatures between 20°C and 850°C using an automated set-up which allowed measurements of high impedance.

## RESULTS AND DISCUSSION

Impedance spectra were analyzed by non-linear least squares fitting of equivalent circuit (fig. 1), representing grain interiors conductivity with charge carrier relaxation represented by the Cole-Cole function, grain boundaries resistance with parallel non-ideal capacitance, and impedance of platinum electrodes. (The procedure was described in [2]). Full determination of electrical properties of the samples was possible up to about 400°C. At higher temperatures the impedance spectrum was dominated by electrode impedance and only the total conductivity of the sample could be

estimated. Electronic contribution to total conductivity was represented by implementation of additional resistance parallel to ionic resistances of grains and grain boundaries. Values of electronic resistance were estimated from parallel experiment using modified EMF method according to procedure described in ref. [3]. Charge carrier relaxation was modelled and fitted using the Cole-Cole dielectric function and the onset frequency of increase of the intragrain conductivity was assumed as a good estimate of the effective ionic charge carrier hopping rate. Assuming three-dimensional transport of charge carriers, their volume concentration were related to the DC intragrain conductivity and the effective rate of hopping.

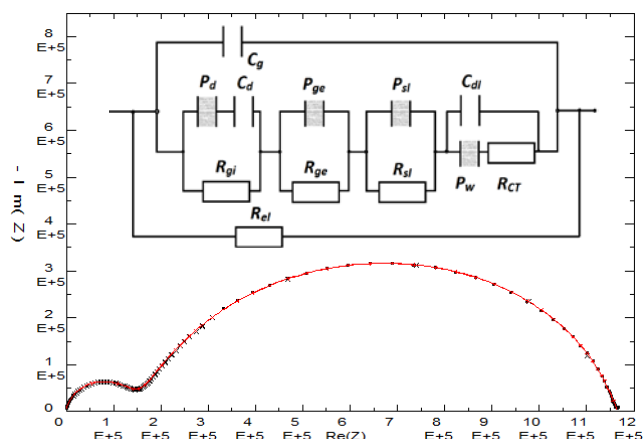


Fig.1 Impedance spectra and equivalent electrical circuit model fitted for  $(\text{Ce}_{0.9}\text{Gd}_{0.1})_{0.85}\text{Pr}_{0.15}\text{O}_{2-\delta}$  measured at 180 °C.

## REFERENCES

- [1] H.L. Tuller, S.R. Bishop, D. Chen, Y. Kuru, J.-J. Kim, T.S. Stefanik, *Solid State Ionics* **225** (2012) 194–197.
- [2] J.R. Dygas, M. Malys, F. Krok, W. Wrobel, A. Kozanecka, I. Abrahams, *Solid State Ionics* **176** (2005) 2085–2093.
- [3] M. Malys, J.R. Dygas, M. Holdynski, A. Borowska-Centkowska, W. Wrobel, M. Marzantowicz, *Solid State Ionics* **225** (2012) 493–497.

# Crystal structure and conductivity in praseodymium doped ceria

*M. Leszczynska, M. Malys, M. Wojcik, W. Wrobel, S. Hull<sup>\*\*</sup>, I. Abrahams<sup>\*</sup> and F. Krok*

Faculty of Physics, Warsaw University of Technology, ul. Koszykowa 75, 00-662 Warszawa, Poland

<sup>\*</sup> Centre for Materials Research, School of Biological and Chemical Sciences, Queen Mary University of London, Mile End Road, London E1 4NS, U.K.

<sup>\*\*</sup>ISIS Facility, STFC Rutherford Appleton Laboratory, Harwell Oxford, Didcot, OX11 0QX, U.K.  
e-mail: leszczynska@if.pw.edu.pl

Keywords: cerium oxide, praseodymium oxide, neutron diffraction, impedance spectroscopy

## INTRODUCTION

Materials based on doped ceria are being adopted as alternatives to traditional oxide ion conducting electrolytes, such as yttria stabilised zirconia (YSZ). Like YSZ, the doped ceria electrolytes exhibit the fluorite structure which is a well-known host structure for fast ionic conduction. There has been growing interest in praseodymium doped cerium oxide, with compositions of general formula  $\text{Ce}_{1-x}\text{Pr}_x\text{O}_{2-\delta}$ . These compounds not only show fast ion conduction, making them suitable as electrolytes, but also, depending on oxygen partial pressure ( $p\text{O}_2$ ) and Pr content, can show significant electronic conductivity [1-3]. Mixed ionic/electronic conductors (MIECs) have a particular advantage for use in solid oxide fuel cells (SOFCs) as they allow for redox reaction over the whole surface of the electrode and not just at the triple phase boundary, (*i.e.*, the boundary between the electrolyte, electrode and gas). This potentially allows for greater efficiency in these devices.

## EXPERIMENTAL

Sample of composition  $\text{Ce}_{0.7}\text{Pr}_{0.3}\text{O}_{2-\delta}$  were prepared by standard solid state reaction. Structural properties of samples were determined using X-ray and neutron diffraction measurements as a function of temperature and annealing time at high temperatures under different gas atmospheres. Total neutron scattering measurements were made in a specially designed gas flow rig on the Polaris diffractometer at the ISIS Facility UK. TGA measurement was performed in air and argon in heating and cooling cycle. Electrical properties as a function of temperature in oxidizing and reducing conditions were obtained by a.c. impedance spectroscopy. Ionic transference numbers were measured using modified EMF method with an external adjustable voltage source in the concentration cell  $\text{O}_2$  ( $p\text{O}_2=1.01\times10^5$  Pa); Pt | oxide | Pt ;  $\text{O}_2$  ( $p\text{O}_2=0.2095\times10^5$  Pa).

## RESULTS AND DISCUSSION

The observed expansion of  $\text{Ce}_{0.7}\text{Pr}_{0.3}\text{O}_{2-\delta}$  lattice with temperature is due to pure thermal expansion of the unit cell and chemical expansion of the unit cell due to oxygen loss from the lattice (data from X-ray diffraction measurement). Neutron diffraction study under different gas atmospheres at elevated temperature allowed for accurate refinement of the oxide ion content in this system and confirmed the initial complete reduction of praseodymium to the +3

oxidation state on heating, with partial reduction of the  $\text{Ce}^{4+}$  on reducing the oxygen partial pressure. The time variation of cubic lattice parameter accurately follows this reduction (Fig. 1). The data obtained in this experiment allowed for accurate refinement of the oxygen content in the system, with values of  $\delta = -0.02(1)$ ,  $0.154(1)$ ,  $0.206(12)$ ,  $0.278(14)$ , for system at room temperature, in  $\text{O}_2$  at  $800^\circ\text{C}$ , in Ar at  $800^\circ\text{C}$  and in Ar/CO at  $800^\circ\text{C}$ , respectively. The ionic transference number measurement using a modified EMF method is *ca.* 0.3 at  $800^\circ\text{C}$  and decrease with decreasing temperature.

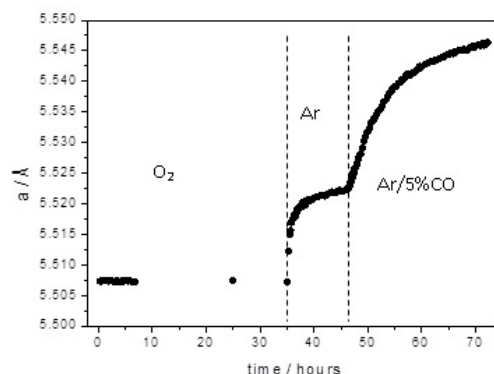


Fig. 1. Lattice parameter variation in  $\text{Ce}_{0.7}\text{Pr}_{0.3}\text{O}_{2-\delta}$  at  $800^\circ\text{C}$  under different flowing gas atmospheres.

## CONCLUSIONS

X-ray and neutron powder diffraction results are consistent with a simple cubic phase (space group  $\text{Fm}\bar{3}\text{m}$ ). The change in the lattice constant is consistent with the observed increase in the nonstoichiometry ( $\delta$ ) over the same partial pressure  $p\text{O}_2$ , and is associated with an increase in the concentration of charge compensating vacancies within the anion sublattice.

## ACKNOWLEDGMENT

This work is supported by National Science Centre, Poland, grant number 2016/23/D/ST5/03293.

## REFERENCES

1. Y. Takasu, T. Sugino, Y. Matsuda, *J. Appl. Electrochem.* **14** (1984) 79
2. P. Shuk, M. Greenblatt, *Solid State Ionics* **116** (1999) 217
3. T.S. Stefanik, H.L. Tuller, *J. Electroceram.* **13** (2004) 799.

# Synthesis and properties of (Ce, La)NbO<sub>4</sub> compounds

*K. Dzierzgowski, A. Mielewczyk-Gryń, S. Wachowski, P. Jasiński\* and M. Gazda*

Faculty of Applied Physics and Mathematics

\*Faculty of Electronics, Telecommunications and Informatics

Gdańsk University of Technology, Gabriela Narutowicza 11/12

80-233 Gdańsk, Poland

e-mail: kdzierzgowski@mif.pg.gda.pl

Keywords: lanthanum niobate, cerium niobate, ionic conductor, solid state electrolytes

## INTRODUCTION

Rare earth ortho-niobates with chemical formula RENbO<sub>4</sub> (where RE is a rare-earth element) are interesting materials due to their ionic conductivity. The main potential applications of these materials are solid oxide fuel cells. RENbO<sub>4</sub> has monoclinic structure at room temperature (Fig. 1). In this work, the structure and conductivity of the (1-x)LaNbO<sub>4</sub>-(x)CeNbO<sub>4</sub> compounds have been examined and compared to the results obtained for lanthanum doped CeNbO<sub>4+δ</sub> (Ce<sub>1-x</sub>La<sub>x</sub>NbO<sub>4+δ</sub>) [1, 2].

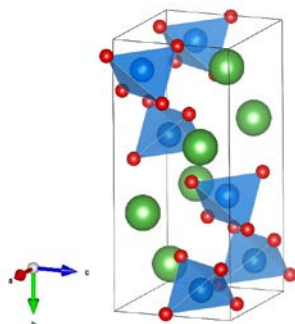


Fig. 1. RENbO<sub>4</sub> unit cell. Blue atoms – niobium, green atoms – rare earth element, red atoms – oxygen [3]

## EXPERIMENTAL

The compounds were synthesized by a solid state reaction route. For LaNbO<sub>4</sub>: La<sub>2</sub>O<sub>3</sub> (Acros Organics, 99.99 %) and Nb<sub>2</sub>O<sub>5</sub> (Alfa Aesar, 99.99 %), for CeNbO<sub>4</sub>: CeO<sub>2</sub> (Buchs SG, 99.99%) and Nb<sub>2</sub>O<sub>5</sub> powders were mixed in an agate mortar and pressed into pellets under pressure of 520 MPa. The pellets were annealed at 1200 °C for 12 h then ground, pressed and heated at 1400 °C for 12 h. In such a way the LaNbO<sub>4</sub> and CeNbO<sub>4</sub> powders were prepared. In the second step, the powders were mixed to obtain (1-x)LaNbO<sub>4</sub>-(x)CeNbO<sub>4</sub> compounds (x = 0.0, 0.25, 0.5, 0.75, 1.0) then they were pressed into pellets and heated at 1400 °C for 12 h.

Structural properties were examined with X-Ray diffraction technique performed on X'Pert PRO MPD Phillips Diffractometer. Electrochemical Impedance Spectroscopy measurements were performed on Solartron 1260 Impedance Analyzer. The impedance was measured in the frequency range from 1Hz to 1MHz at temperatures starting from 750 °C to 350 °C with 50 °C step. Electric properties were measured in both wet and dry atmospheres.

## RESULTS AND DISCUSSION

X-ray diffraction measurements confirmed that obtained samples were composed of two distinct phases: LaNbO<sub>4</sub> and CeNbO<sub>4</sub>. Electrochemical impedance spectroscopy measurements have shown that the activation energy of conductivity in dry air is 0.59 eV and 1.56 eV in CeNbO<sub>4</sub> and LaNbO<sub>4</sub>, respectively. Activation energies of conductivity of the (Ce, La)NbO<sub>4</sub> compounds are similar to this of CeNbO<sub>4</sub> (from 0.52 eV to 0.83 eV). Total conductivities in wet air for obtained materials are presented in Fig. 2.

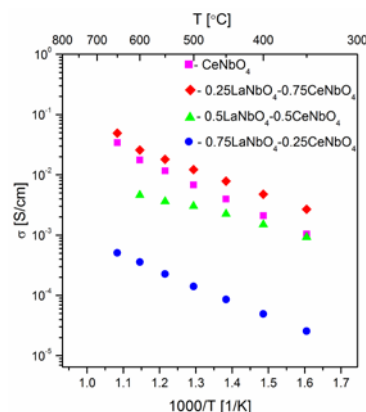


Fig. 2. Total conductivity in wet air for obtained compounds

Total conductivities in wet air at 650 °C for all samples (e.g.  $3.44 \times 10^{-2}$  S/cm for CeNbO<sub>4</sub> and  $4.09 \times 10^{-6}$  S/cm for LaNbO<sub>4</sub>) are consistent with the literature reports [4, 5]. These results show, that the material obtained in this work exhibits similar conductivity to the material obtained by doping a cerium sublattice with lanthanum in Ce<sub>1-x</sub>La<sub>x</sub>NbO<sub>4+δ</sub>.

## REFERENCES

- [1] R. J. Packer, S. J. Skinner, A. A. Yaremchenko, E. V. Tsipis, V. V. Kharton, M. V. Patrakeev, Y. A. Bakhteeva, J. Mater. Chem. 16 (2006) 3503.
- [2] S. J. Skinner, Y. Kang, Solid State Sci. 5 (2003) p. 1475–1479.
- [3] K. Momma, F. Izumi, J. Appl. Crystallogr. 44 (2011), 1272–1276.
- [4] R. J. Packer, S. J. Skinner, A. A. Yaremchenko, E. V. Tsipis, V. V. Kharton, M. V. Patrakeev, Y. A. Bakhteeva, J. Mater. Chem. 16 (2006) p. 3503.
- [5] R. Haugrud, T. Norby, Nat. Mater. 5 (2006) p. 193–196.

# Hydration energetics of the ion-conducting doped lanthanum orthoniobates

**A. Mielewczyk-Gryn, S. Wachowski, K. Dzierzowski, M. Przeźniak-Welenc and M. Gazda**

Gdańsk University of Technology – Faculty of Applied Physics and Mathematics,

Department of Solid State Physics, Narutowicza 11/12, 80-233 Gdańsk, Poland

e-mail: alegryn@pg.gda.pl

Keywords: hydrogen, thermodynamics, thermal analysis

## INTRODUCTION

High temperature proton conductors are materials with a broad spectrum of applications. These compounds can be utilized as electrolytes in devices such as solid oxide fuel cells, gas pumps, and gas separators. Since these applications require constant work performance over extended periods of time at elevated temperatures, knowledge and understanding of the phenomena which occur seems crucial. The majority of the materials used nowadays as electrolytes undergo structural phase transitions. The changes in physical properties caused by such a transition should be known in order to avoid the problems in operating electrochemical devices.

Among many structures showing proton conduction, the most recognized materials exhibiting proton conduction are barium cerate-zirconate system and lanthanum orthoniobates. In the last decade, some studies on these two systems have been undertaken to show how complex the thermochemistry of them is. Starting on the energetics of the formation [1–3], through heat capacities [4], phase transitions thermodynamics [2,5], and what is the most important for the understanding of their electrical performance - hydration energetics [6,7] have been investigated in past decade. For these studies, we chose to examine the series of the doped lanthanum orthoniobates to determine the heats of their hydration in order to reveal underlying phenomena of their ion transport.

## EXPERIMENTAL

The ceramic bulk samples of lanthanum orthoniobates were synthesized by standard solid state synthesis route as described elsewhere [4]. The structure of the powders was confirmed to be single-phase fergusonite by X-ray powder diffraction (Phillips X'Pert Pro). The microstructure was analysed by FEI Quanta Feg 250 Scanning Electron Microscope with Energy Dispersive X-ray Spectroscopy. The chemical state of the dopants has been determined by the means of X-ray photoelectron spectrometry. Thermogravimetric analysis was performed using a Netzsch STA (simultaneous thermal analyzer) Jupiter 449 F1. The sample gas was saturated with water ( $P_{H_2O} = 0.023$  atm), and the weight increase was recorded upon cooling.

## PRELIMINARY RESULTS

Various compositions of doped lanthanum niobates were synthesized. The end member for all samples was  $LaNbO_4$ . The samples doped with antimony and praseodymium were synthesized and their phase

content measured. Figure 1 presents the X-ray diffraction data of the samples co-doped with praseodymium and calcium. All reflections are indexed with I2/c monoclinic space group confirming that the single phase material was synthesized.

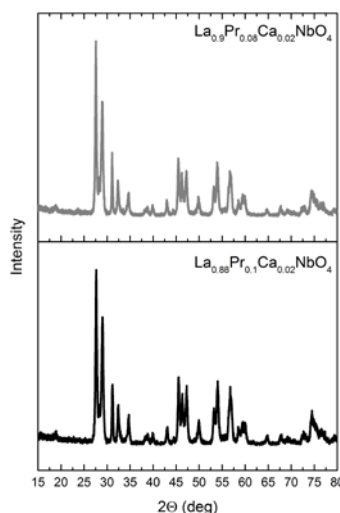


**Figure 1** X-ray diffraction patterns of praseodymium and calcium co-doped lanthanum orthoniobate.

## ACKNOWLEDGMENT

This research has been supported by the Ministry of Science and Higher Education Poland (grant no. 0513/IP2/2016/74).

## REFERENCES

1. A. Mielewczyk-Gryn and A. Navrotsky, *Am. Mineral.* **100**, 1578 (2015).
2. A. Mielewczyk-Gryn, S. Wachowski, K. I. Lilova, X. Guo, M. Gazda, and A. Navrotsky, *Ceram. Int.* **41**, 2128 (2015).
3. M. D. Gonçalves, P. S. Maram, R. Muccillo, and A. Navrotsky, *J. Mater. Chem. A* **2**, 17840 (2014).
4. A. Mielewczyk-Gryn, S. Wachowski, J. Strychalska, K. Zagórski, T. Klimczuk, A. Navrotsky, and M. Gazda, *Ceram. Int.* **42**, 7054 (2016).
5. A. Mielewczyk-Gryn, K. Gdula-Kasica, B. Kusz, and M. Gazda, *Ceram. Int.* **39**, 4239 (2013).
6. Y. Yamazaki, F. Blanc, Y. Okuyama, L. Buannic, J. C. Lucio-Vega, C. P. Grey, and S. M. Haile, *Nat. Mater.* **12**, 647 (2013).
7. Y. Yamazaki, P. Babilo, and S. M. Haile, *Chem. Mater.* **20**, 6352 (2008).



# The influence of hydrostatic pressure on AC conductivity characteristics in $(\text{NH}_4)_3\text{H}(\text{SeO}_4)_2$ single crystal

P. Ławniczak, Ł. Linder M. Zdanowska-Frączek, Cz. Pawlaczyk

Institute of Molecular Physics Polish Academy of Sciences

ul. Mariana Smoluchowskiego 17, 60-179 Poznań, Poland

e-mail: lawniczak@ifmpan.poznan.pl

Keywords: proton conductors , pressure studies, hydrogen bonds

## INTRODUCTION

Universal behavior of frequency dependences of conductivity  $\sigma^*(\omega)$ , [ $\sigma^*(\omega)=\sigma'(\omega)-\sigma''(\omega)$ ] is one of the characteristic features of ionic conductors. Most common disordered ion conductors show a universal frequency response, the so-called first and second universalities [1]. However, up to our publications [2-4], there have not been any reports about observation of such universalities in protonic conductors. We showed that both universal features of conductivity spectra can be also observed in organic proton conductors, i.e. benzimidazolium azelate, with ordered hydrogen structure [2,3]. Recently we have studied universal features of conductivity spectra in solid acid protonic conductors, described by formula  $\text{M}_3\text{H}(\text{XO}_4)_2$  (where  $\text{M} = \text{K}, \text{Cs}, \text{Rb}, \text{NH}_4$ , and  $\text{X} = \text{S}, \text{Se}$ ). Obtained results confirm that even after the phase transitions, that causes radical change of dc conductivity, no changes in mechanism of proton migration occurs [5]. Here we present results of studies of influence of hydrostatic pressure on ac characteristics.

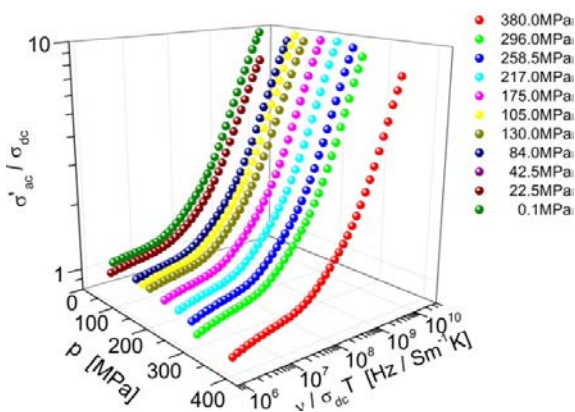
## EXPERIMENTAL

Single crystals of  $(\text{NH}_4)_3\text{H}(\text{SeO}_4)_2$  were obtained by slow evaporation of the saturated solution of  $\text{H}_2\text{O}$ ,  $\text{H}_2\text{SeO}_4$ , and ammonia water at room temperature. The measuring capacitor with a sample was set in a beryl bronze pressure chamber and thereafter the pressure chamber was located in an Oxford flow cryostat. The measurements were made along the trigonal c-axis. The electric conductivity under different isobaric conditions was measured by the admittance method in the frequency range from 100Hz to 1MHz with an impedance analyzer Hewlett-Packard HP 4284A between temperatures 240K and 350K on heating. The high pressures were generated by means of a helium gas compressor. Pressure was measured to an accuracy of 0.2MPa using manganese gauge with a Keithley 2400 Source Meter. The temperature of the sample was set and stabilized with an Oxford Instruments automatic temperature controller ITC4.

## RESULTS AND DISCUSSION

The measurements of electric properties were performed for different values of external pressure, from 0.1MPa (ambient pressure) to 380MPa. High pressure influence electric properties of  $(\text{NH}_4)_3\text{H}(\text{SeO}_4)_2$  i.e. leads to increase in the temperature range of stability of both superionic phases and to a drastic decrease in the temperature width of the ferroelastic phase III [6].

Typical scaled ac conductivity spectra measured for different pressure conditions at  $T=270\text{K}$ , below phase transition, is presented in figure. All curves show exactly the same shape, which means that are independent on pressure.



Master plots for different values of pressure measured at temperature  $T=270\text{K}$ , below the phase transition.

## CONCLUSIONS

The master curves, characteristic indication of first universality, do not change its shape for the measurements under pressure. The same effect was previously observed for the measurements under different values of temperature. Similar universal features of ac conductivity spectra as in common disordered solids are observed.

## ACKNOWLEDGMENT

This work is supported by National Science Centre under grant No. 2014/15/D/ST3/03433.

## REFERENCES

1. K. Funke, R. D. Banhatti, D. M. Laughman, L. G. Badr, M. Mutke, A. Šantič, W. Wróbel, E. M. Fellberg, C. Biermann *Z. Phys. Chem.* **224**(2010)1891
2. P. Ławniczak, M. Zdanowska-Frączek, Z.J. Frączek, K. Pogorzelec-Glaser, Cz. Pawlaczyk *Solid State Ionics* **225**(2012)268
3. M. Zdanowska-Frączek, K. Holderna-Natkaniec, P. Ławniczak, Cz. Pawlaczyk *Solid State Ionics* **227** (2013)40
4. P. Ławniczak, K. Pogorzelec-Glaser, A. Pietraszko, B. Hilczek *Solid State Ionics* DOI: 10.1016/j.ssi.2017.02.013
5. P. Ławniczak, A. Pawłowski, Cz. Pawlaczyk *submitted to publication*
6. Ł. Lindner, M. Zdanowska-Frączek, A. Pawłowski, Z. J. Frączek *Journal Applied Physics* **116**(2014)163513



# Electrical and structural studies on titanium doped $\text{Y}_3\text{NbO}_7$

P. Winiarz<sup>A</sup>, A. Mielewczyk-Gryń<sup>A</sup>, S. Wachowski<sup>A</sup>, P. Jasiński<sup>\*</sup> and M. Gazda<sup>A</sup>

<sup>A</sup>Faculty of Physics and Applied Mathematics

<sup>\*</sup>Faculty of Electronics, Telecommunications and Informatics

Gdańsk University of Technology, ul. Gabriela Narutowicza 11/12

80-233 Gdansk, Poland

e-mail: pwiniarz@mif.pg.gda.pl

Keywords: ionic conductor, protonic conductor, fuel cell, rare earth niobates

## INTRODUCTION

Rare earth niobates have recently been gaining attention as materials with considerably high ionic conductivity [1-3]. The compounds crystallize in defect fluorite structure (Fig.1). Among them, compounds with three various space groups can be distinguished. Yttrium niobate –  $\text{Y}_3\text{NbO}_7$  is an oxygen ion conductor in a wide range of oxygen partial pressures [1]. Acceptor doping of the material, due to an increase of the oxygen vacancies concentration, should rise the total conductivity and effectively improve ionic conductivity. In this work, titanium was chosen as aliovalent dopant because of the small difference in ionic radius of  $\text{Ti}^{4+}$  and  $\text{Nb}^{5+}$  [4]. Therefore series of titanium doped yttrium niobates were synthesized and thoroughly investigated.

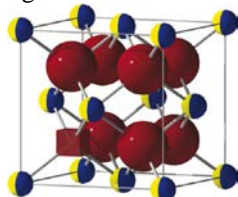


Fig. 1 Defect fluorite structure. Smaller hemispheres – yttrium/niobium, bigger spheres – oxygen. Cube – oxygen vacancy.

## EXPERIMENTAL

The samples were prepared by solid state reaction method.  $\text{Y}_2\text{O}_3$  (Alfa Aesar 99,99 %),  $\text{Nb}_2\text{O}_5$  (Alfa Aesar 99,9985 %) and  $\text{TiO}_2$  (Prolabo, min. 99 %) were mixed in an agate mortar and uniaxially pressed to pellets under pressure of 520 MPa. As prepared pellets were annealed at 1350 °C then reground, repelletized and annealed in two steps at 1150 °C for 24 h and at 1450 °C for 24 h. In studied compounds titanium concentration varied from 0 to 0.15 in molar ratio

In order to obtain structural properties, an X-Ray diffraction experiment was performed on X'Pert Phillips Diffractometer with  $\text{Cu K}\alpha_1$  radiation and  $\lambda = 1.540598 \text{ \AA}$ . The microstructure of the compositions was studied with Fei Quanta Feg-250 Scanning Electron Microscope. Electrochemical Impedance Spectroscopy measurements were performed on Solartron 1260 Impedance Analyzer with a frequency range from 1 Hz to 1 MHz at the temperature range from 350 °C to 750 °C with 50 °C step. Samples were examined in both wet and dry oxidizing and reducing conditions. ZView software was used for analysis of the impedance [5].

## RESULTS AND DISCUSSION

The X-Ray diffraction showed that the obtained compounds contain only defect fluorite phase and no impurities were detected. The SEM images of samples showed dense granular structure on the surface with polyhedral pores. The highest values of total conductivity was obtained in humid atmosphere at 750 °C for the sample with 15% concentration of Ti. In humid conditions total conductivities were higher than in dry in the whole temperature range. The activation energies of conductivity was between 0.55 eV and 1.65 eV. Fig.2 shows the contribution of grains and grain boundaries into the total conductivity. As can be seen grain boundaries have significantly lower conductivity than the grains.

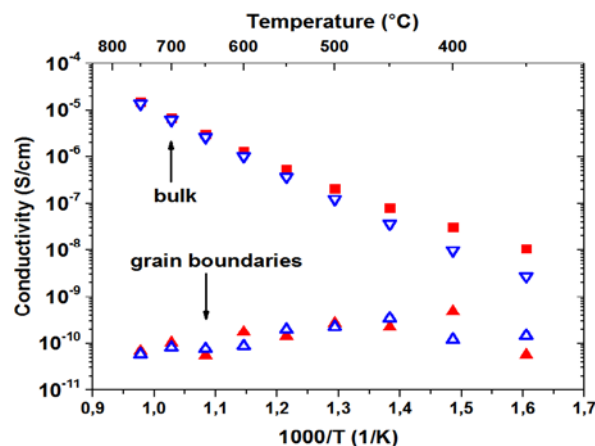


Fig. 2 Grains and grain boundaries contribution to total conductivity (open symbols – dry air, closed – wet air)

## CONCLUSIONS

Acceptor doped yttrium niobate is a good candidate as ionic conductor for potential applications in fuel cells as well as other electrochemical devices. Its electrical and structural properties and chemical stability was shown in this study.

## REFERENCES

1. A. Chesnaud, M. Braidia, S. Estradé, F. Peiró, A. Tarancón, A. Morata, G. Dezanneau, *J. of the European Ceramic Society* 35 (2015) 3051–3061
2. L. Cai, J.C. Nino, *J. of the European Ceramic Society* 27 (2007), 3971–3976
3. J.H. Lee, M. Yashima, M. Kakihana, M. Yoshimura, *J. Am. Ceram. Soc.* 81 (1998) 894–900
4. A. Mielewczyk-Gryń, A. Navrotsky, *American Mineralogist*, 100 (2015) 1578–1583
5. <http://www.scribner.com/software/general-electrochemistry/68-general-electrochemistr/376-zview-for-windows>

# Synthesis and physicochemical properties of layered oxides from $\text{La}_{2-x}(\text{Sr,Ba})_x\text{MO}_{4\pm\delta}$ (M: Cu, Ni) group

A. Niemczyk, K. Świerczek

AGH University of Science and Technology, Faculty of Energy and Fuels,  
al. A. Mickiewicza 30, 30-059 Krakow, Poland  
e-mail: niemczyk@agh.edu.pl

Keywords: MIEC, transport properties, layered oxides

## INTRODUCTION

Among the most promising materials, which are considered for manufacturing of ceramic membranes, electrodes in high-temperature fuel cells or steam electrolyzers, are oxides with  $\text{K}_2\text{NiF}_4$ -derived crystal structure. Among this group, lanthanum cuprates ( $\text{La}_2\text{CuO}_{4\pm\delta}$ ) and nickelates ( $\text{La}_2\text{NiO}_{4\pm\delta}$ ) have attracted attention, due to their relatively high electronic and ionic conductivity and limited thermal expansion [1].

It is interesting that ionic transport in  $\text{K}_2\text{NiF}_4$ -type oxides can be realized by two different mechanisms. First one, occurring through oxygen vacancies, is in fact similar to the one occurring in  $\text{ABO}_{3-\delta}$  perovskite-type oxides. The second mechanism proceeds by excessive oxygens incorporated in  $\text{A}_2\text{O}_2$  layer. Such interstitial defects may diffuse at higher temperatures relatively easily, and such the two-dimensional ionic conduction is characterized by a low value of the activation energy. This may allow to reduce working temperature of various high-temperature electrochemical devices, e.g. solid oxide fuel cells (SOFC) [2].

Due to a different ionic radius of  $\text{Ba}^{2+}$  and  $\text{Sr}^{2+}$ , their substitution at the La-site may lead to a different lattice distortions, changes of the oxygen stoichiometry, and corresponding modification of the transport properties. In this paper, the considered substitution is studied in terms of possible improvement of the mixed ionic electronic (MIEC) conductivity, as well as thermal and chemical stability for two groups of oxides based on  $\text{La}_2\text{CuO}_{4\pm\delta}$  and  $\text{La}_2\text{NiO}_{4\pm\delta}$ .

## EXPERIMENTAL

$\text{La}_{2-x}(\text{Sr,Ba})_x\text{MO}_{4\pm\delta}$  oxides (where M: Cu, Ni) were synthesized by two methods: standard solid state reaction and combined EDTA-citric acid sol-gel method. Structural studies were carried out at the room temperature and at high temperatures using X-ray diffraction method with Rietveld refinement, which allowed to elaborate on the crystal structure evolution at higher temperatures. Particle size of the synthesized powders was measured by light scattering (DLS) technique. Thermogravimetric measurements performed in synthetic air and in reducing atmosphere allowed to establish absolute value and dependence of  $\delta$  on temperature. Transport properties were measured on dense sinters of the materials by AC and four-probe DC methods, and revealed very high electronic component of conductivity, with a significant presence of the ionic conduction.

## RESULTS AND DISCUSSION

Both synthesis methods allowed to obtain single phase  $\text{La}_{1.6}\text{Ba}_{0.4}\text{MO}_{4\pm\delta}$  and  $\text{La}_{1.5}\text{Sr}_{0.5}\text{MO}_{4\pm\delta}$  (M: Cu, Ni), as well as  $\text{La}_{1.5}\text{Sr}_{0.3}\text{Ba}_{0.2}\text{CuO}_{4-\delta}$  oxide, with concurrent substitution of  $\text{Ba}^{2+}$  and  $\text{Sr}^{2+}$  in  $\text{La}_{1.5}\text{Sr}_{0.3}\text{Ba}_{0.2}\text{NiO}_{4\pm\delta}$  being the most difficult. All of the obtained materials are stable at high temperatures up to 900 °C in air and inert atmospheres, as it was confirmed by HT-XRD and TG measurements. As can be seen in Fig. 1, above 400 °C, a decrease of mass is observed for all Cu-containing samples, which can be related to the increasing number of the oxygen vacancies. Contrary to this, Ni-containing oxides behave differently. All investigated compounds exhibit total electrical conductivity on the order of  $100 \text{ S cm}^{-1}$ , with ionic component being strongly related to the oxygen content at a particular temperature.

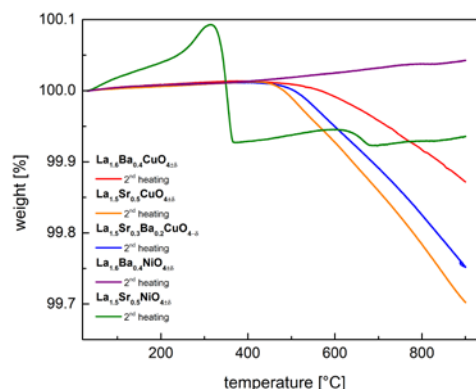


Fig. 1. Weight dependence on temperature for studied  $\text{La}_{2-x}(\text{Sr,Ba})_x\text{MO}_{4\pm\delta}$  oxides.

## CONCLUSIONS

Crystal structure and selected physicochemical properties of layered oxides from  $\text{La}_{2-x}(\text{Sr,Ba})_x\text{MO}_{4\pm\delta}$  group were investigated, showing strong influence of dopants for both series of materials. Considering crystal structure, stability and high, MIEC-type conductivity, the obtained compounds seem interesting for application as electrode materials for SOFCs, as well as ceramic membranes.

## ACKNOWLEDGMENT

This work is supported by National Science Centre Poland (NCN) on the basis of the decision number UMO-2015/19/B/ST8/00871.

## REFERENCES

1. A. Tarancon, M. Burriel, J. Santiso, S.J. Skinner, J.A. Kilner, *J Mater Chem* **20** (2010) 3799
2. J. Rodriguez-Carvajal, M.T. Fernandez-Diaz, J.L. Martinez, *J Phys Condens Matter* **3** (1991) 3215

# Influence of oxygen content on transport properties of $\text{LnBaCo}_2\text{O}_{5+\delta}$ and $\text{LnBaCo}_{1.5}\text{Mn}_{0.5}\text{O}_{5+\delta}$ oxides

*A. Olszewska, K. Świerczek*

AGH University of Science and Technology, Faculty of Energy and Fuels,  
al. A. Mickiewicza 30, 30-059 Krakow, Poland  
e-mail: olszewska@agh.edu.pl

Keywords: electrochemical oxidation, conductivity

## INTRODUCTION

Electrochemical oxidation is a relatively simple method, which allows to obtain oxides with controlled oxygen stoichiometry, as well as to achieve fully oxidized compounds without a need to apply a high oxygen pressure during synthesis or annealing. This process seems to be very useful, considering that for transition metal perovskites the oxygen stoichiometry has a strong influence on crystal structure and transport properties, as well as on magnetic and other physical and chemical characteristics. Especially, the method allows for a more precise studies on correlation between oxygen stoichiometry and mixed electronic and ionic conductivity in perovskites [1, 2].

In this work a detailed studies on relationship between crystal structure, oxygen content and transport properties were conducted for  $\text{LnBaCo}_2\text{O}_{5+\delta}$  and  $\text{LnBaCo}_{1.5}\text{Mn}_{0.5}\text{O}_{5+\delta}$  (Ln: La, Pr, Nd, Gd, Sm and Y) perovskite-type oxides. This is of importance from a point of view of possible application as cathodes in Solid Oxide Fuel Cells, as well as from basic science reasons, due to previously reported excellent total electrical conductivity of several fully oxidized  $\text{LnBaCo}_2\text{O}_6$  [2].

## EXPERIMENTAL

Selected  $\text{LnBaCo}_2\text{O}_{5+\delta}$  and  $\text{LnBaCo}_{1.5}\text{Mn}_{0.5}\text{O}_{5+\delta}$  oxides were synthesised with sol-gel method combined with annealing at high temperatures (respectively, 1100 °C and 1200 °C) in air/Ar atmospheres. Structural studies were carried out at room and high temperatures by using X-ray diffraction with Rietveld refinement, which allowed to study phase composition, crystal structure and structural stability at high temperatures. Thermogravimetric measurements performed during heating up to 500 °C in reducing atmosphere (5 vol.%  $\text{H}_2$  in Ar), as well as during studies in air up to 900 °C, together with analytical titration method, allowed to establish the absolute value of the oxygen content in the as-prepared oxides and its change with temperature. Electrochemical oxidation was carried out in KOH solution, with voltage set on a basis of an initial voltamperometry scan. The process allowed to obtain oxides with different oxygen content. For comparison, samples were also annealed in atmospheres with different  $p\text{O}_2$ . Studies of the transport properties, conducted by 4-probe technique enabled to prove influence of  $\delta$  and Ln cation on the mixed conductivity for both studied series of oxides.

## RESULTS AND DISCUSSION

$\text{LnBaCo}_2\text{O}_{5+\delta}$  and  $\text{LnBaCo}_{1.5}\text{Mn}_{0.5}\text{O}_{5+\delta}$  oxides were obtained as single phase, with no significant amount of

secondary phases visible. XRD data for the as synthesized samples could be refined with  $Pm-3m$  (Ln: La)  $P4/mmm$  (Ln: Pr and Y) or  $Pmmm$  (Ln: Nd, Sm and Gd) space groups, which correspond to, respectively, cubic, tetragonal and orthorhombic structure. Thermogravimetric measurements allowed to determine oxygen content in the as prepared materials. It was found that for  $\text{LnBaCo}_2\text{O}_{5+\delta}$  series the values decrease with a decreasing size of Ln cation, while for  $\text{LnBaCo}_{1.5}\text{Mn}_{0.5}\text{O}_{5+\delta}$  oxides there is no clearly visible dependency. Moreover, measurements carried out for all materials up to 900 °C in air atmosphere show reversibly decreasing value of  $\delta$  at elevated temperatures. Conductivity measurements were performed for samples differing in oxygen content and in the A- and B-site composition. The pristine  $\text{PrBaCo}_2\text{O}_{5+\delta}$  oxide with  $\delta = 0.76$  was found to exhibit total conductivity on the order of  $0.1\text{--}1\text{ S cm}^{-1}$  in 30–800 °C temperature range. Improvement of the transport properties was obtained by an increase of oxygen content, and for example, such material with  $\delta = 0.88$  possesses conductivity higher by about two orders of magnitude. Moreover, contrary to only Co-containing oxides, which show metallic-like conductivity, introduction of manganese at the B-site changes mechanism of the electron transfer in the materials to the activated type.

## CONCLUSIONS

All  $\text{LnBaCo}_2\text{O}_{5+\delta}$  and  $\text{LnBaCo}_{1.5}\text{Mn}_{0.5}\text{O}_{5+\delta}$  oxides were prepared as single phase with sol-gel method. Thermogravimetric measurement allowed to determine oxygen content of as-prepared samples, which depend on chemical composition in both A- and B- sublattice, as well as to evaluate its reversible changes with temperature increase. Conductivity measurements proved strong impact of oxygen content on transport properties of studied materials and change of the character of conductivity from metallic to activated as a result of partial substitution of cobalt by manganese in B-site.

## ACKNOWLEDGMENT

This work is supported by Ministry of Science and Higher Education under grant 0128/DIA/2016/45.

## REFERENCES

1. M. Karppinen, M. Matvejeff, K. Salomäki, H. Yamauchi, J. Mater. Chem., 12 (2002) 1761–1764
2. J.H. Kim, L. Moggi, F. Prado, A. Caneiro, J.A. Alonso, A. Manthiram, J. Electrochem. Soc. 156 (2009) B1376–B1382

# The Synthesis And Properties Of $\text{LaBaCo}_2\text{O}_{6-\delta}$ ceramics

*I. Lewandowska, S. Wachowski, M. Gazda, A. Mielewczyk-Gryn*

Gdańsk University of Technology – Faculty of Applied Physics and Mathematics,

Department of Solid State Physics, Narutowicza 11/12, 80-233 Gdańsk, Poland

e-mail: alegryn@pg.gda.pl

Keywords: cobaltites, oxygen nonstoichiometry, rare-earths

## INTRODUCTION

The magnetic and transport properties of cobaltites with the perovskite structure have been an object of multiple studies for more than a decade [1–3]. Within this group, lanthanum barium cobaltite seems to be one of the most interesting exhibiting order-disorder phenomena between  $\text{La}^{3+}$  and  $\text{Ba}^{2+}$  cations, which affects the transport properties of this system [4]. Such ordering can be induced by the presence of a specific nonstoichiometry in the oxygen sublattice [5]. Our research is focused on the synthesis of the material with specific oxygen nonstoichiometry and therefore specific crystal structure and ordering (see Fig. 1), and to determine their electrical properties in relation to these parameters.

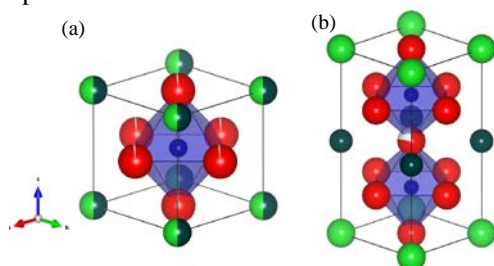


**Figure 1** Disordered cubic (a) and ordered tetragonal (b) perovskite structure of lanthanum barium cobaltite (figure produced by Vesta software [6] on the basis of the crystallographic data published in [7]).

## EXPERIMENTAL

Samples will be synthesized by a solid synthesis route starting from lanthanum oxide, barium carbonate and cobalt oxide. In order to vary the oxygen nonstoichiometry in the synthesized material, the sintering will be done in different atmospheres (air, argon, and hydrogen). The structure of the powders was confirmed to be a single-phase perovskite by X-ray powder diffraction (Phillips X'Pert Pro). The microstructure was analyzed by FEI Quanta FEG 250 Scanning Electron Microscope. Electrical properties of the sintered pellets have been determined by the means of impedance spectroscopy (Novocontrol FRA).

## PRELIMINARY RESULTS

The preliminary studies have shown that in the case of standard solid state synthesis in air at  $1350^\circ\text{C}$  for 12h the achieved phase can be indexed by ordered  $\text{LaBaCo}_2\text{O}_6$  cubic structure. The example of recorded X-ray diffractogram is depicted in Fig. 2

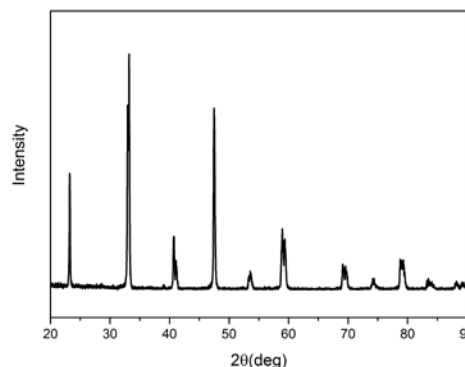


**Figure 2** X-ray diffraction pattern of lanthanum barium cobaltite sample synthesized at  $1200^\circ\text{C}$  in air for 12h.

The further studies include the different level of the ordering of the samples and investigation of this ordering on the electrical properties of the system.

## REFERENCES

1. J. Maria, S. Nazir, S. M. Alay-e-Abbas, and A. Shaukat, *J. Magn. Magn. Mater.* 368, 230 (2014).
2. T. Nakajima, M. Ichihara, and Y. Ueda, *J. Phys. Soc. Japan* 74, 1572 (2005).
3. A. K. Kundu, E.-L. Rautama, P. Boullay, V. Caignaert, V. Pralong, and B. Raveau, *Phys. Rev. B* 76, 184432 (2007).
4. E.-L. Rautama, P. Boullay, A. K. Kundu, V. Caignaert, V. Pralong, M. Karppinen, and B. Raveau, *Chem. Mater.* 20, 2742 (2008).
5. K. Conder, A. Podlesnyak, E. Pomjakushina, and M. Stingaciu, 111, (2007).
6. K. Momma and F. Izumi, *J. Appl. Crystallogr.* 44, 1272 (2011).
7. D. Garcés, C. F. Setevich, A. Caneiro, G. J. Cuello, and L. Moggi, in *J. Appl. Crystallogr.* (International Union of Crystallography, 2014), pp. 325–334.

# Li<sub>4</sub>Ti<sub>5</sub>O<sub>12</sub> doped with nickel, tungsten and chlorine – anode material for Li-ion batteries

D. Olszewska, J. Niewiedzial

Faculty of Energy and Fuels

AGH University of Science and Technology, al. A. Mickiewicza 30

30-059 Cracow, Poland

e-mail: dolszew@agh.edu.pl

Keywords: Li-ion batteries, anode, Li<sub>4</sub>Ti<sub>5</sub>O<sub>12</sub>

## INTRODUCTION

The lithium-ion batteries have been considered to be the promising energy storage technology not only for most of the electronic devices but also for the electric vehicles due to their high energy density, high work potential and good cycle life.

The spinel Li<sub>4</sub>Ti<sub>5</sub>O<sub>12</sub> (LTO) is one of the most attractive anode materials. It is considered to be a zero-strain material, because during lithium intercalation and deintercalation the lattice parameter does not change almost at all. What is more, its safety and good cycling performance makes it one the most important material for the batteries applied in electric vehicles. However, Li<sub>4</sub>Ti<sub>5</sub>O<sub>12</sub> still exhibits a poor rate capability due to its lower electronic and ionic conductivity [1-3].

Main goal of the research was: check if doping of LTO with Ni, W and Cl into three different lattices (Li, Ti and O respectively) is possible and if this will improve the conductivity of LTO.

## EXPERIMENTAL

Three materials with the stoichiometric composition Li<sub>4-x</sub>Ni<sub>x</sub>Ti<sub>5-y</sub>W<sub>y</sub>O<sub>12-z</sub>Cl<sub>z</sub> were obtained using solid-state reaction using lithium carbonate Li<sub>2</sub>CO<sub>3</sub>, titanium oxide TiO<sub>2</sub>, nickel oxide NiO, tungsten oxide WO<sub>3</sub> and lithium chloride LiCl.

The materials were characterized in terms of phase composition, crystal structure as well as conductivity. Phase composition and crystal structure parameters were determined using X-ray Panalytical Empyrean XRD diffractometer in the range of 10-110° with CuKα radiation. The results were analyzed using Rietveld refinement which was then implemented in the GSAS computer software. Measurement of conductivity of the materials was done by impedance spectroscopy.

## RESULTS

Examples of results are presented in the figure below. Fig. 1 presents conductivities of Li<sub>4-x</sub>Ni<sub>x</sub>Ti<sub>5-y</sub>W<sub>y</sub>O<sub>12-z</sub>Cl<sub>z</sub> materials.

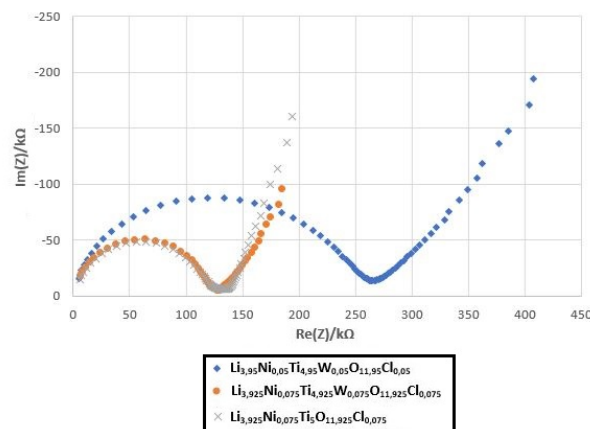


Fig. 1 Conductivities of Li<sub>4-x</sub>Ni<sub>x</sub>Ti<sub>5-y</sub>W<sub>y</sub>O<sub>12-z</sub>Cl<sub>z</sub> materials.

## CONCLUSIONS

To summarize:

- Two materials doped with Ni, W and Cl into 3 lattices of Li, Ti and O respectively were obtained.
- The addition of Ni, W and Cl could increase the conductivity of LTO up to 7 orders of magnitude.
- Li<sub>3.925</sub>Ni<sub>0.075</sub>Ti<sub>4.925</sub>W<sub>0.075</sub>O<sub>11.925</sub>Cl<sub>0.075</sub> is a promising material from the point of view of application in Li-ion cells.

## ACKNOWLEDGMENT

The financial support of D. Olszewska - the AGH project No.11.11.210.911

## REFERENCES

1. D. Linden, T.B. Reddy (Ed.), *Handbook of Batteries* (3rd Edition), McGraw-Hill 2002
2. Y.-J. Gu, Z. Guo, H.-Q. Liu, *Electrochim. Acta* **123** (2014) 576
3. Q. Zhang, H. Lu, H. Zhong, X. Yan, C. Ouyang, L. Zhang, *J. Mater. Chem. A*, 2015, 3, 13706



# Li<sub>4</sub>Ti<sub>5</sub>O<sub>12</sub> doped with nickel, copper and carbon - anode for Li-ion batteries

D. Olszewska, J. Niewiedzial

Faculty of Energy and Fuels  
AGH University of Science and Technology, al. A. Mickiewicza 30  
30-059 Cracow, Poland  
e-mail: dolszew@agh.edu.pl

Keywords: Li-ion batteries, anode, Li<sub>4</sub>Ti<sub>5</sub>O<sub>12</sub>

## INTRODUCTION

The lithium-ion batteries have been considered as the best power sources for most of the electronic devices and the electric vehicles due to their advantages of high energy density, high work potential, good cycle life, and environmental friendliness.

The spinel Li<sub>4</sub>Ti<sub>5</sub>O<sub>12</sub> is the most attractive material to use as a anode material alternatives because of its advantages. The charge–discharge voltage plateau (1.6V) and its zero-strain feature during the charge/discharge process, safety and good cycling performance are the most important. However Li<sub>4</sub>Ti<sub>5</sub>O<sub>12</sub> material possesses so many advantages, it still exhibits a poor rate capability due to its lower electronic and ionic conductivity [1-3].

Main goals of the research were: Check if doping with Cu and Ni will improve the conductivity and capacity of LTO and the study the influence of sucrose on structure and properties of LTO.

## EXPERIMENTAL

Li<sub>3.85</sub>Cu<sub>0.15</sub>Ti<sub>5</sub>O<sub>12</sub> material was obtained using solid state method. As the substrates lithium carbonate Li<sub>2</sub>CO<sub>3</sub>, titanium oxide TiO<sub>2</sub> and copper oxide CuO were used. Carbon additions to LTO: Carbon black – usually added to already prepared LTO material with polyvinylidene difluoride in an 80:10:10 (w<sub>LTO</sub>/w<sub>carbon black</sub>/w<sub>PVDF</sub>) ratio to increase the conductivity of an anode material. It is the most popular carbon addition to LTO.

Prepared material was characterized in terms of phase composition, crystal structure, grain size and surface morphology, as well as ionic and electronic conductivity. Phase composition and crystal structure parameters were determined using X-ray Panalytical Empyrean XRD diffractometer in the range of 10-110° with CuKα radiation. Obtained results were analyzed using Rietveld refinement implemented in GSAS computer software. Measurement of conductivity of produced materials by impedance spectroscopy. Electrochemical measurements of the samples (cycling, cyclic voltammetry).

## RESULTS

Examples of results presented in the drawings below. Fig. 1 presents conductivities of Li<sub>3.8</sub>Cu<sub>x</sub>Ni<sub>0.2-x</sub>Ti<sub>5</sub>O<sub>12</sub>/C materials.

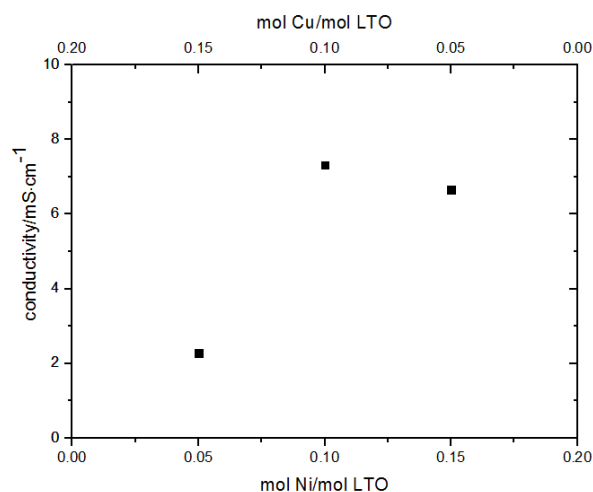


Fig. 1 Conductivities of Li<sub>3.8</sub>Cu<sub>x</sub>Ni<sub>0.2-x</sub>Ti<sub>5</sub>O<sub>12</sub>/C materials.

## CONCLUSIONS

To summarize:

- Addition of sucrose influences considerably the calcination process, so that the three-phase material is obtained;
- Adding sucrose to LTO enhances significantly the conductivity of LTO;
- Simplified process of material and battery preparation;
- Composites of LTO and sucrose are characterized by increased polarization;
- Samples composed with sucrose exhibit poor specific capacities at higher current rates;
- Lowering the content of sucrose is advisable;
- Li<sub>3.8</sub>Cu<sub>0.05</sub>Ni<sub>0.15</sub>Ti<sub>5</sub>O<sub>12</sub>/C is a promising material from the point of view of application in Li-ion cells.

## ACKNOWLEDGMENT

The financial support of D. Olszewska - the AGH project No.11.11.210.911

## REFERENCES

1. D. Linden, T.B. Reddy (Ed.), *Handbook of Batteries* (3rd Edition), McGraw-Hill 2002
2. Y.-J. Gu, Z. Guo, H.-Q. Liu, *Electrochim. Acta* **123** (2014) 576
3. L. Cheng, X. Li, H. Liu, H. Xiong, P. Zhang, Y. Xia, *J. Electrochem. Soc.* **154** (7) (2007) A692.



# Structural evolution of the $\text{Na}_x\text{Fe}_{0.33}\text{Ni}_{0.33}\text{Ti}_{0.33}\text{O}_2$ cathodes

*Anna Milewska, Wojciech Zajac, Janina Molenda*

AGH University of Science and Technology, Faculty of Energy and Fuels,  
al. A. Mickiewicza 30, 30-059 Krakow, Poland  
e-mail: molenda@agh.edu.pl

Keywords: Na-ion batteries, cathode materials, intercalation process, transport properties

## INTRODUCTION

All indicates that in future Na-ion batteries will be massively used as grid storage for renewable sources. However, for now, there is still a need to develop a cathodic material that would be better than cathode materials developed for Na-ion batteries so far.  $\text{NaFe}_{0.33}\text{Ni}_{0.33}\text{Ti}_{0.33}\text{O}_2$  is one of the cathode materials which raises a lot of interest due to the high working voltage, monotonic charge/discharge curve and possible high capacitance. In this paper we present the results of analysis of structural changes during charge and discharge of the  $\text{Na}/\text{Na}^+/\text{Na}_x\text{Fe}_{0.33}\text{Ni}_{0.33}\text{Ti}_{0.33}\text{O}_2$  cell using the insitu XRD technique, of EIS measurements of electrical conductivity of pristine  $\text{Na}_1\text{Fe}_{0.33}\text{Ni}_{0.33}\text{Ti}_{0.33}\text{O}_2$  cathode material and of the electrochemical tests.

## EXPERIMENTAL

$\text{NaFe}_{0.33}\text{Ni}_{0.33}\text{Ti}_{0.33}\text{O}_2$  oxide was obtained using the high temperature solid state method from the following reagents:  $\text{Na}_2\text{CO}_3$ ,  $\text{NiO}$ ,  $\text{Fe}_2\text{O}_3$  and  $\text{TiO}_2$ . The reactants were annealed four times at 850 °C for 12 h in air, with an intermediate grinding in a mortar. Crystal structure of the synthesized material was examined by X-ray diffraction method (XRD) in 10–110° range using Cu  $K_\alpha$  radiation. Studies were conducted on Panalytical Empyrean diffractometer equipped with PIXcel3D detector. The X-ray patterns were analysed by Rietveld method using GSAS/EXPGUI set of software [1,2]. In order to measure total conductivity of the pristine samples, electrochemical impedance spectroscopy method (EIS) was applied, with excitation voltage of 100 mV over 300 kHz to 0.01 Hz frequency range using Solartron 1252 frequency response analyzer. Electrochemical tests were carried out for cells consisting of sodium metal anode, 1M  $\text{NaPF}_6$  in propylene carbonate (PC) electrolyte and composite cathode. In-situ XRD measurements were conducted in the 20–70 degree on Panalytical Empyrean diffractometer. A custom-made gas-tight cell for these studies was made from Teflon and stainless steel containers, joint by screws and sealed by gaskets. A Beryllium window, was used as an X-ray transparent medium and a current collector at the same time [3]. The electrochemical tests during insitu XRD measurements were performed using an Autolab PGSTAT302N potentiostat/galvanostat. The charge/discharge rate was set to C/ 20.

## RESULTS AND DISCUSSION

The main phase in pristine  $\text{NaFe}_{0.33}\text{Ni}_{0.33}\text{Ti}_{0.33}\text{O}_2$  is hexagonal O3-type layered structure with  $R\bar{3}m$  space group. Also, a small amount of an additional hexagonal P3-type ( $R\bar{3}m$ ) layered structure and NiO were detected. During deintercalation the fraction of

the P3 phase increases at the expense of O3 phase, additionally monoclinic P'3-type ( $C2/m$ ) phase appears when lithium concentration is low (Fig. 1).

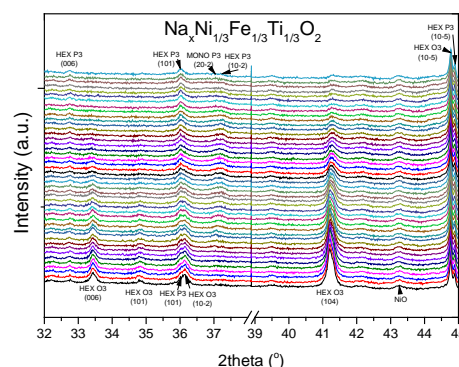


Fig. 1. Evolution of XRD patterns of  $\text{Na}_x\text{Fe}_{0.33}\text{Ni}_{0.33}\text{Ti}_{0.33}\text{O}_2$  compound during charging between 2-4.2V.

The electrical conductivity is thermally activated. The activation energy is equal 0.35 eV. Extrapolated value of electrical conductivity at room temperature is low and is of the order  $10^{-8}$  (S/cm). Electrochemical tests indicated that when the cutoff voltage increases the polarization of the cell increases and the capacity decreases, what is related with more intense cation mixing [4]. The best results were obtained when the cell was cycled between 2 and 3.8 V.

## CONCLUSIONS

At this stage, the investigated material does not meet the criteria assumed for cathode materials for Na-ion cells. Further modification of this compound should go towards the stabilization of the O3 phase.

## ACKNOWLEDGMENT

The project was funded by the National Science Centre Poland (NCN) under the “OPUS 12” programme on the basis of the decision number UMO-2016/23/B/ST8/00199 and Polish Ministry of Science and Higher Education, under project AGH No. 11.11.210.911. Work was realized by using the infrastructure of the Laboratory of Conversion and Energy Storage Materials in the Centre of Energy AGH.

## REFERENCES

1. A.C. Larson, R.B. Von Dreele, Los Alamos Natl. Lab. Rep. - LAUR 86-748, 2004,
2. B.H. Toby, J. Appl. Crystallogr., 34 (2001) 210.
3. A. Kulka, K. Świerczek, K. Walczak, A. Braun, J. Molenda, Solid State Ionics 288 (2016) 184.
4. G. Singh, F. Aguesse, L. Otaegui, E. Goikolea, E. Gonzalo, J. Segalini, T. Rojo, J. Power Sources 273 (2015) 333.

# Structural, electrical and electrochemical properties of the $\text{LiNi}_{0.9-y}\text{Co}_y\text{Mn}_{0.1}\text{O}_2$ cathodes for Li-ion batteries – electronic structure studies

*Anna Milewska, Wojciech Zajac, Janusz Tobola\*, Janina Molenda*

AGH University of Science and Technology, Faculty of Energy and Fuels,  
al. A. Mickiewicza 30, 30-059 Krakow, Poland

\*AGH University of Science and Technology, Faculty of Physics and Applied Computer Science,  
al. A. Mickiewicza 30, 30-059 Krakow, Poland  
e-mail: molenda@agh.edu.pl

Keywords: Li-ion batteries, cathode materials, intercalation process, transport properties, electronic structure

## INTRODUCTION

Chemical composition of cathode materials determines its electronic structure, which manifests itself through specific structural, transport and electrochemical properties. In this work we disclose the correlation between electronic structure of the mixed  $\text{Li}_x\text{Ni}_{0.55}\text{Co}_{0.35}\text{Mn}_{0.1}\text{O}_2$  layered oxides and experimentally measured structural, transport (electrical conductivity and thermoelectric power) and electrochemical properties.

## EXPERIMENTAL

$\text{LiNi}_{0.9-y}\text{Co}_y\text{Mn}_{0.1}\text{O}_2$  ( $y=0.2, 0.25, 0.3, 0.35, 0.5, 0.6$ ) oxides were synthesized by a soft chemistry EDTA-based method. Crystal structure of the considered materials was characterized using an X-ray diffraction (XRD) method on a PANalytical Empyrean diffractometer with  $\text{Cu K}\alpha$  radiation. Unit cell parameters of the materials were determined by the Rietveld refinement method with the GSAS/EXPGUI set of software [1, 2]. To examine the transport properties of deintercalated samples, lithium cells consisting of metallic lithium anode/1 M  $\text{LiPF}_6$  in EC+DEC/sintered samples of pure cathode material were constructed in an argon-filled glove-box ((MBraun, UNILAB) under argon atmosphere with controlled oxygen and water vapour pressure ( $<0.1$  ppm)). Deintercalation process of the cathode materials in the cells were performed under a constant current density of  $50 \mu\text{A}\cdot\text{cm}^{-2}$  until the intended  $x_{\text{Li}}$  value was obtained. Then the cell was kept under OCV (open circuit voltage) conditions to relax it to the steady-state potential. Electrical conductivity was measured using four-electrode alternating-current method (at a frequency of 33 Hz). Thermoelectric power was measured dynamically, by measuring the potential difference and temperature difference ( $\Delta T$  up to  $2^\circ$ ) at the ends of the sample. The measurements in the temperature range of 200–350K were carried out under vacuum ( $10^{-2}$  mbar). Charge–discharge tests were performed with metallic lithium anode/1 M  $\text{LiPF}_6$  in EC+DEC electrolyte/composite cathode cells.

In this work, electronic structure calculations for the  $\text{Li}_x\text{Ni}_{0.9-y}\text{Co}_y\text{Mn}_{0.1}\text{O}_2$  systems were performed using the KKR-CPA method.

## RESULTS AND DISCUSSION

All synthesized compounds have a layered structure and all peaks can be indexed on the basis of the  $\alpha\text{-NaFeO}_2$  structure with trigonal  $R\bar{3}m$  symmetry. The reversible capacity increases with increasing nickel content in the cathode material. Investigations

performed for the started materials show the electrical conductivity is thermally activated. The activation energy is of the order of 0.18–0.30 eV. The sign of the thermoelectric power is positive, indicating that electron holes are predominant charge carriers, however, the character of the temperature dependence of  $\alpha$  confirms that the transport occurs in more than one band. After deintercalation the electrical conductivity is getting worse and maintains its activated character. The thermoelectric power changes its sign from positive to negative. The charge and discharge curves are smooth.

## CONCLUSIONS

The results presented in the previous work show that stoichiometric  $\text{Li}_1\text{CoO}_2$  oxide is a semiconductor, but extraction of the lithium ions leads to the metallic properties of the system [3, 4]. Performed experimental investigations of the series of the  $\text{Li}_x\text{Ni}_{0.9-y}\text{Co}_y\text{Mn}_{0.1}\text{O}_2$  cathode material show that this system is more complex. And so for example  $\text{Li}_x\text{Ni}_{0.65}\text{Co}_{0.25}\text{Mn}_{0.1}\text{O}_2$  and  $\text{Li}_x\text{Ni}_{0.55}\text{Co}_{0.35}\text{Mn}_{0.1}\text{O}_2$  retain activated character of the electrical conductivity in the whole range of their chemical stability. This behaviour can be explained by electron configuration of transition metals and occurrence of the defect bands inside the energy gap due to oxygen nonstoichiometry.  $\text{Li}_x\text{Ni}_{0.65}\text{Co}_{0.25}\text{Mn}_{0.1}\text{O}_2$  and  $\text{Li}_x\text{Ni}_{0.55}\text{Co}_{0.35}\text{Mn}_{0.1}\text{O}_2$  maintains semiconducting properties due to low density of states around the Fermi level irrespective of lithium nonstoichiometry.

## ACKNOWLEDGMENT

The project was funded by the National Science Centre Poland (NCN) under the “OPUS 10” programme on the basis of the decision number UMO-2015/19/B/ST8/00856 and Polish Ministry of Science and Higher Education, under project AGH No. 11.11.210.911. Work was realized by using the infrastructure of the Laboratory of Conversion and Energy Storage Materials in the Centre of Energy AGH.

## REFERENCES

1. A.C. Larson, R.B. Von Dreele, Los Alamos Natl. Lab. Rep. - LAUR 86-748, 2004.
2. B.H. Toby, J. Appl. Crystallogr., 34 (2001) 210.
3. A. Milewska, K. Świerczek, J. Tobola, F. Boudoire, Y. Hu, D.K. Bora, B.S. Mun, A. Braun, J. Molenda, Solid State Ionics, 263 (2014) 110.
4. J. Molenda, D. Baster, A. Milewska, K. Świerczek, D. K. Bora, A. Braun, J. Tobola, Solid State Ionics, 271 (2015) 15.

# High-voltage $\text{Na}_{0.67}\text{Ni}_{0.33}\text{Mn}_{0.67-y}\text{Ti}_y\text{O}_{2-\delta}$ ( $0 \leq y \leq 0.33$ ) cathodes for Na-ion batteries

*Anna Milewska, Wojciech Zajac, Konrad Świerczek, Janusz Tobola\*, Janina Molenda*

AGH University of Science and Technology, Faculty of Energy and Fuels,

al. A. Mickiewicza 30, 30-059 Krakow, Poland

\*AGH University of Science and Technology, Faculty of Physics and Applied Computer Science,

al. A. Mickiewicza 30, 30-059 Krakow, Poland

e-mail: molenda@agh.edu.pl

Keywords: Na-ion batteries, cathode materials, intercalation process, transport properties

## INTRODUCTION

Na-ion batteries attract much attention within the research community as they can provide grid storage for renewable sources.  $\text{Na}_{2/3}\text{Ni}_{1/3}\text{Mn}_{2/3}\text{O}_2$  with P2-type structure is considered as one of the most promising cathode material for Na-ion batteries, which utilises  $\text{Ni}^{4+}/\text{Ni}^{2+}$  redox process. The main disadvantage of this material is step-like character of the charge/discharge curves, which can be modified into monotonic one by partial substitution of manganese for titanium [1]. In this paper we presents the results of investigations of the influence of titanium substitution on structural, electrical and electrochemical properties of  $\text{Na}_{0.67}\text{Ni}_{0.33}\text{Mn}_{0.67-y}\text{Ti}_y\text{O}_{2-\delta}$  ( $0 \leq x \leq 0.33$ ) cathode material.

## EXPERIMENTAL

$\text{Na}_{0.67}\text{Ni}_{0.33}\text{Mn}_{0.67-y}\text{Ti}_y\text{O}_{2-\delta}$  ( $0 \leq y \leq 0.33$ ) oxides were obtained using the high temperature solid state method from the following reagents:  $\text{Na}_2\text{CO}_3$ ,  $\text{NiO}$ ,  $\text{MnCO}_3$  and  $\text{TiO}_2$ . The reactants were annealed three times at 900 °C for 12 h in air, with an intermediate grinding in a mortar. Crystal structure of the synthesized material was examined by X-ray diffraction method (XRD) in 10-110° range using  $\text{Cu K}_\alpha$  radiation. Studies were conducted on Panalytical Empyrean diffractometer equipped with PIXcel3D detector. The X-ray patterns were analysed by Rietveld method using GSAS/EXPGUI set of software [2, 3].

In order to measure total conductivity of the pristine samples, electrochemical impedance spectroscopy method (EIS) was applied, with excitation voltage of 100 mV over 300 kHz to 0.01 Hz frequency range using Solartron 1252 frequency response analyzer. DC Asymmetric Polarisation (AP) method was also used to establish the electronic component of the electrical conductivity using Solartron 1287 potentiostat. Electrochemical tests were carried out for cells consisting of sodium metal anode, 1M  $\text{NaPF}_6$  in propylene carbonate (PC) electrolyte and composite cathode.

## RESULTS AND DISCUSSION

All the samples possess hexagonal P2-type layered structure and  $P6_3/mmc$  space group. Also, a small amount of an additional  $\text{NiO}$  phase was detected. Lattice parameter  $a$  was found to linearly increase with growing concentration of Ti, as expected due to a larger size of  $\text{Ti}^{4+}$  ions (0.605 Å), compared to  $\text{Mn}^{4+}$  ions (0.53 Å). Practically there is no variations of parameter  $c$ . Since electrochemical performance of

electrode materials in Li-ion batteries are affected by efficiency of both ionic and electronic transport, in order to assess and compare these two components of electrical conductivity in  $\text{P2-Na}_{0.67}\text{Ni}_{0.33}\text{Mn}_{0.67-y}\text{Ti}_y\text{O}_{2-\delta}$  ( $0 \leq y \leq 0.33$ ) samples, parallel impedance spectroscopy and DC polarization measurements were carried out. For the considered compound the ionic conductivity is three orders of magnitude higher than the electronic one. Titanium substitution improves the ionic and electronic conductivity. Partial substitution of manganese with titanium in  $\text{Na}_{0.67}\text{Ni}_{0.33}\text{Mn}_{0.67-y}\text{Ti}_y\text{O}_{2-\delta}$  ( $y > 0.1$ ) stabilize P2 structure in the whole sodium concentration range and modify character of the discharge curve into monotonous one. On the other hand Ti doping raises the voltage at which Ni redox couple is active. The best capacity retention is observed for  $\text{Na}/\text{Na}^+/\text{Na}_{0.67}\text{Ni}_{0.33}\text{Mn}_{0.47}\text{Ti}_{0.2}\text{O}_{2-\delta}$  cell.

## CONCLUSIONS

Titanium favourably influences the transport properties and structural stability of the investigated compound. Obtained for different cells charge and discharge curves indicate for modification of the electronic structure by titanium substitution, what confirm DFT ab initio numerical calculations of the electronic structure of undoped and Ti-doped  $\text{Na}_{0.67}\text{Ni}_{0.33}\text{Mn}_{0.67-y}\text{Ti}_y\text{O}_2$  cathode material.

## ACKNOWLEDGMENT

The project was funded by the National Science Centre Poland (NCN) under the “OPUS 10” programme on the basis of the decision number UMO-2015/19/B/ST8/00856, under the “OPUS 12” programme on the basis of the decision number UMO-2016/23/B/ST8/00199 and Polish Ministry of Science and Higher Education, under project AGH No. 11.11.210.911. Work was realized by using the infrastructure of the Laboratory of Conversion and Energy Storage Materials in the Centre of Energy AGH.

## REFERENCES

1. H. Yoshida, N. Yabuuchi, K. Kubota, I. Ikeuchi, A. Garsuch, Chem. Commun., 50 (2014) 3677.
2. A.C. Larson, R.B. Von Dreele, Los Alamos Natl. Lab. Rep. - LAUR 86-748, 2004.
3. B.H. Toby, J. Appl. Crystallogr., 34 (2001) 210.

# High-temperature synthesis and electrochemical properties of MoS<sub>2</sub> – anode material for Na-ion batteries

*A. Kulka\*, A. Plewa, K. Walczak, J. Molenda*

AGH University of Science and Technology,

Faculty of Energy and Fuels,

Al. Mickiewicza 30, 30-059 Kraków, Poland

e-mail: akulka@agh.edu.pl

Keywords: Na-ion batteries, MoS<sub>2</sub>, anode materials

## INTRODUCTION

In order to resolve problems with lithium supply risk, intensive search for alternative solution for Li-ion batteries technology is carried out. From this perspective, Na-ion batteries appear to be future technology of choice, since they are much cheaper, environmentally friendly and operate on the similar principles as Li-ion analogues. Both, Li-ion and Na-ion batteries exploit the ability of transition metal compounds MaX<sub>b</sub> (M - transition metal, X- O, S) with a layered or skeleton structure to reversibly incorporate one or more moles of lithium (or sodium) per mole of MaX<sub>b</sub> at room temperature. The key issue in developing the high density Na-ion cell technology lies in designing functional electrode materials fulfilling demanding electrochemical criteria. In the light of the above the fabrication of the high capacity anode materials with high working stability is in the particular importance. One of the especially interesting potential anode materials for Na-ion batteries is MoS<sub>2</sub>[1]. In this work we present high-temperature synthesis procedure of the MoS<sub>2</sub> anode as well as electrochemical investigation of the electrode performance of the material.

## EXPERIMENTAL

The MoS<sub>2</sub> was synthesised using high-temperature method using gas-tight Swagelok-type containers at temperatures 600-700°C. The crystal structure was examined using XRD technique, defect stoichiometry was calculated by means of the TG measurements. In order to verify electrochemical properties, cycling voltammetry and charge/discharge test were performed in Na/Na<sup>+</sup>/MoS<sub>2</sub> cells.

## RESULTS AND DISCUSSION

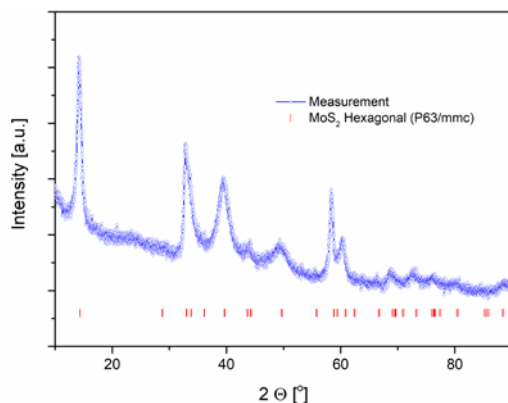


Fig.1. XRD data of the synthesized MoS<sub>2</sub>.

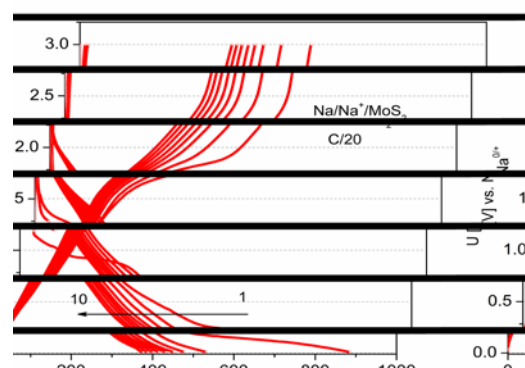


Fig.2. Voltage characteristics as a function of anode capacity for Na/Na<sup>+</sup>/MoS<sub>2</sub> cells.

The XRD analysis (Fig.1) revealed that synthesised materials are single-phased with MoS<sub>2</sub> possessing P6<sub>3</sub>/mm hexagonal structure. The obtained anode materials working in the Na/Na<sup>+</sup>/MoS<sub>2</sub> exhibit sloped voltage characteristics in the 1.5-0.05 V range. The discharge capacity for the first cycle reaches 900 mAh/g and during subsequent cycles decreases to 450 mAh/g (Fig.2). Cycling voltammetry and ex-situ XRD measurements revealed conversion-type reaction mechanism in the investigated MoS<sub>2</sub> anode upon Na insertion.

## CONCLUSIONS

High-temperature synthesis method using gas-tight Swagelok-type containers of the MoS<sub>2</sub> anode materials is presented. The synthesised materials delivers stable capacity on the order of 450 mAh/g.

## ACKNOWLEDGMENT

This work is supported by National Science Center, Poland under grant number 2016/21/D/ST5/01658.

## REFERENCES

- [1] X.L. Hu, W. Zhang, X.X. Liu, Y.N. Mei, Y. Huang, Nanostructured Mo-based electrode materials for electrochemical energy storage, Chem. Soc. Rev. 44 (2015) 2376–2404. doi:10.1039/c4cs00350k.

# Electrochemical properties of NASICON- $\text{Na}_3\text{V}_2(\text{PO}_4)_3$ and alluaudite- $\text{Na}_2\text{Fe}_3(\text{PO}_4)_3$

*K. Walczak and J. Molenda\**

AGH University of Science and Technology,  
Faculty of Energy and Fuels,  
Al. A. Mickiewicza 30, 31-059 Cracow, Poland  
e-mail: molenda@agh.edu.pl

Keywords: *Sodium-ion Batteries*, intercalation, NASICON,  $\text{Na}_3\text{M}_2(\text{PO}_4)_3$

## INTRODUCTION

Nowadays, *Sodium-Ion Batteries* draw attention in terms of low cost of sodium and the possibility of being partial substitute for *Lithium-Ion* technology, especially in large-scale energy storage systems. The polyanionic  $\text{Na}_3\text{M}_2(\text{PO}_4)_3$  [1] and  $\text{Na}_2\text{M}_3(\text{PO}_4)_3$  [2-3] (M=transition metal) cathode material groups are one of the most attractive due to their thermal and chemical stability, low cost and environment friendly elements as well as thermal and chemical stability ensuring safety of usage. Here we provided the study of the structural and electrochemical properties of  $\text{Na}_3\text{M}_2(\text{PO}_4)_3$  and  $\text{Na}_2\text{M}_3(\text{PO}_4)_3$  (M=V, Fe).

$\text{Na}_3\text{V}_2(\text{PO}_4)_3$  crystallizes in the NASICON structure ( $R\bar{3}c$  space group) and possesses high theoretical capacity ( $\sim 176$  mAh/g). In comparison,  $\text{Na}_2\text{Fe}_3(\text{PO}_4)_3$  crystallizes in the *alluaudite* structure ( $C2/m$  space group) and exhibits lower theoretical capacity about of 107 mAh/g. From the *Sodium-ion* technology perspective, both of them are intriguing due to structural stability.

The aims of presented studies were the synthesis, structure analysis and electrochemical tests of the  $\text{Na}_3\text{V}_2(\text{PO}_4)_3$  and  $\text{Na}_2\text{Fe}_3(\text{PO}_4)_3$  as a positive materials for *Na-ion Batteries*.

## EXPERIMENTAL

$\text{Na}_3\text{V}_2(\text{PO}_4)_3$  and  $\text{Na}_2\text{Fe}_3(\text{PO}_4)_3$  samples were obtained *via* solid-state reaction in the reduction atmosphere of 5% $\text{H}_2$ -95%Ar. The X-Ray Diffraction measurements with Rietveld analysis were carried out for each obtained sample. The crystallites size was calculated with Scherrer equation based on XRD data. The  $\text{Na}_3\text{V}_2(\text{PO}_4)_3$  and  $\text{Na}_x\text{Fe}_3(\text{PO}_4)_3$  samples were mixed with carbon precursors to produce cathode layers. The  $\text{Na}/\text{Na}^+/\text{Na}_3\text{V}_2(\text{PO}_4)_3$  and  $\text{Na}/\text{Na}^+/\text{Na}_2\text{Fe}_3(\text{PO}_4)_3$  cells were constructed and the electrochemical tests, including cyclic charge/discharge processes and cyclic voltammetry, were performed.

## RESULTS AND DISCUSSION

X-Ray diffraction data analysis of all the prepared samples confirmed that the materials were single-phased.

For  $\text{Na}_x\text{Fe}_3(\text{PO}_4)_3$  two compositions were obtained:  $x = 1.5$  and  $x = 2.0$ . Fig. 1. presents the subtle differences between diffractograms of the  $\text{Na}_x\text{Fe}_3(\text{PO}_4)_3$  samples. The cyclic charge/discharge processes exhibited discharge capacity of about 70% of the theoretical capacity for both of the samples.

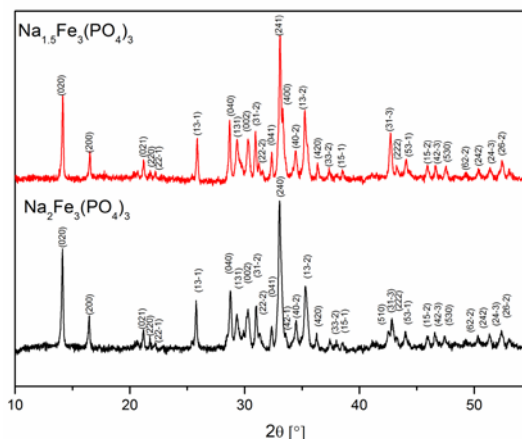


Fig. 1. X-Ray patterns of alluaudite  $\text{Na}_x\text{Fe}_3(\text{PO}_4)_3$ . The XRD measurement was carried out for  $2\theta$  range of  $10 - 110^\circ$ .

$\text{Na}_3\text{V}_2(\text{PO}_4)_3$  possesses two potential plateaux at about 3.4V and 1.6V. The cyclic deintercalation/intercalation processes showed discharge capacity at the level of about 100 mAh/g. It was also found that the transition metal sublattice modification (such as substitution with very small amount of iron) may affect the electrochemical properties.

## CONCLUSIONS

The obtained results showed that the *alluaudite* and NASICON phosphates exhibit very stable structure, which is able to reversible intercalation/deintercalation processes. Moreover, the possibility of substitution in transition metal sublattice creates the chance to improve the electrochemical properties

## ACKNOWLEDGMENT

This work was supported by the Polish Ministry of Science and Higher Education (MNiSW) on the basis of the decision number 0020/DIA/2016/45.

Work was realized by using the infrastructure of the Laboratory of Conversion and Energy Storage Materials in the Centre of Energy AGH.

## REFERENCES

1. K. Saravanan, C.W. Mason, A. Rudola, K.H. Wong, P. Balaya, *Adv. Energy Mater.*, **3** (2013) 444-450
2. K. Trad, D. Carlier, L. Croguennec, A. Wattiaux, M.B. Amara, C. Delmas, *Chem. Mater.*, **22** (2010) 5554-5562
3. W. Huang, B. Li, M. Saleem, X. Wu, Z. Wu, *Chem. Eur. J.* DOI: 10.1002/chem.201403062



# Cathode material based on $\text{Na}_x\text{Fe}_{1-y}\text{Mn}_y\text{O}_2$ for Na-ion batteries

K. Redel, K. Walczak and J. Molenda\*

AGH University of Science and Technology,  
Faculty of Energy and Fuels,  
Al. A. Mickiewicza 30,  
31-059 Cracow, Poland  
e-mail: molenda@agh.edu.pl

Keywords: sodium ion batteries, Na-ion cell,  $\text{Na}_x\text{Fe}_{1-y}\text{Mn}_y\text{O}_2$ , layered oxides, intercalation

## INTRODUCTION

Despite limitations related to the physicochemical properties of sodium, Na-ion technologies are gaining more and more interest and are an alternative to commercially available Lithium-ion cells. Particular attention is paid to the cathode materials with high mixed ionic – electronic conductivity, possessing a structure with space for larger sodium ions.

In recent years one of the most promising cathode materials for sodium ion batteries is layered oxide  $\text{Na}_x\text{Fe}_{1-y}\text{Mn}_y\text{O}_2$  [1] because of simple structure, high theoretical capacity ( $\sim 260$  mAh/g) and the gravimetric energy density ( $\sim 520$  mWh/g), what giving similar values to some cathode materials for lithium cells (e.g.  $\text{LiFePO}_4$ ). Moreover, this cathode material does not show voltage drop in the discharge curve and due to the addition of manganese,  $\text{Na}_x\text{Fe}_{1-y}\text{Mn}_y\text{O}_2$  exhibits relatively good stability. However, there is some disadvantage. The problem is low reversible discharge capacity [2].

Herein, we report the synthesis of layered oxide  $\text{Na}_x\text{Fe}_{1-y}\text{Mn}_y\text{O}_2$ , their structural characterization through X-Ray Diffraction (XRD) and their electrochemical behavior in Na-ion cells.

## EXPERIMENTAL

$\text{Na}_x\text{Fe}_{1-y}\text{Mn}_y\text{O}_2$  cathode materials were obtained via high-temperature solid-state synthesis. In order to analyze the structural properties the investigated materials have been subjected to X-ray diffraction XRD. Transport properties were determined on the basis of measurements of Electrochemical Impedance Spectroscopy. By means of battery charge/discharge cycle tests and measurements of diffusion coefficient of sodium analyzed electrochemical properties. The  $\text{Na}/\text{Na}^+/\text{Na}_x\text{Fe}_{1-y}\text{Mn}_y\text{O}_2$  cell was working in the range of 1,5 – 4,5 V.

## RESULTS AND DISCUSSION

The one-, two- or three-step solid-state synthesis in oxide atmosphere allowed to obtain single-phased materials from the  $\text{P2-Na}_{0,67}\text{Fe}_{1-y}\text{Mn}_y\text{O}_2$  group, which was confirmed with X-Ray measurements. The deeper analysis allowed to specify the border elemental composition for substitution of manganese:  $0,4 \leq y \leq 0,8$ . The electrochemical impedance spectroscopy measurement showed that conductivity of all the obtained oxides is thermally activated with activation energy of about 0,2 – 0,4 eV.

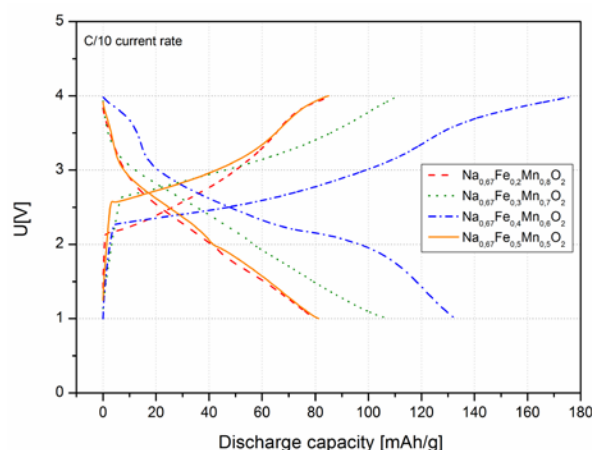


Fig. 1. Charge/discharge curves under  $I_{C/10}$  of  $\text{Na}/\text{Na}^+/\text{Na}_{0,67}\text{Fe}_{1-y}\text{Mn}_y\text{O}_2$  cells

All the  $\text{P2-Na}_{0,67}\text{Fe}_{1-y}\text{Mn}_y\text{O}_2$  samples were tested under different current load (with a scope of  $C/10$  to  $C/2$ ) and exhibit good cyclable reversibility (Fig. 1).

## CONCLUSIONS

The amount of the synthesis steps is the factor which affects the  $\text{P2}:\text{O3}$  structures ratio.

It was also proved that the structural, transport and electrochemical properties of  $\text{P2-Na}_{0,67}\text{Fe}_{1-y}\text{Mn}_y\text{O}_2$  group are strongly correlated with the chemical composition in transition metal sublattice.

## ACKNOWLEDGMENT

The project was funded by the National Science Centre Poland (NCN) on the basis of the decision number UMO-2016/23/B/ST8/00199. Work was realized by using the infrastructure of the Laboratory of Conversion and Energy Storage Materials in the Centre of Energy AGH.

## REFERENCES

1. N. Yabuuchi, R. Hara, M. Kajiyama, K. Kubota, T. Ishigaki, A. Hoshikawa, S. Komaba, *Advanced Energy Materials*, DOI: 10.1002/aenm.201301453
2. N. Yabuuchi, S. Komaba, *Sci. Technol. Adv. Mater.*, **15** (2014) 043501

# Li<sub>2</sub>MnO<sub>3</sub>-stabilized LiMO<sub>2</sub> (M = Mn, Co, Ni) composites as positive electrode materials for lithium-ion batteries

*K. Redel, A. Kulka and J. Molenda\**

AGH University of Science and Technology,  
Faculty of Energy and Fuels,  
Al. Mickiewicza 30, 30-059 Krakow, Poland  
\*e-mail: molenda@agh.edu.pl

Keywords: hybrid cathode materials, lithium-ion batteries, Li<sub>2</sub>MnO<sub>3</sub>, stabilized LiMO<sub>2</sub>

## INTRODUCTION

Among recently investigated cathode materials for Li-ion batteries, the new generation of hybrid composites containing manganese seem to be the most promising due to non-toxicity and relatively high resources of Mn causing the cost of producing electrode materials to be low [1]. Among the compounds containing Mn, high hope lies in layered oxide LiMnO<sub>2</sub> because of high potential (~3 V vs. Li<sup>0/+</sup>) and high theoretical capacity (285 mAh/g) [2]. However, the problem is structural instability of LiMnO<sub>2</sub> during the intercalation/deintercalation process. Near lithium content 0.67 mol/mol there is irreversible transformation to spinel LiMn<sub>2</sub>O<sub>4</sub> structure that leads to loss of reversible capacity of the cell.

To reduce the capacity loss and stabilize LiMnO<sub>2</sub> structure, simultaneous substitution of Mn by another transition metal (Ni, Co) and fabrication of the hybrid cathode with the layered Li<sub>2</sub>MnO<sub>3</sub> is proposed. This results in significantly increased theoretical capacity (~400 mAh/g) and high operating voltage of ~4 V. Despite these advantages in the new generation of hybrid cathodes, there is still decrease of an irreversible capacity during the first charge cycle (~50 mAh/g) [2,3].

In this work we fabricate Li<sub>2</sub>MnO<sub>3</sub>-stabilized LiMO<sub>2</sub> (M = Mn, Co, Ni) composites and analyze the structural and electrochemical properties.

## EXPERIMENTAL

Li<sub>2</sub>MnO<sub>3</sub> precursor and Li<sub>2</sub>MnO<sub>3</sub>-Stabilized LiMO<sub>2</sub> (M = Mn, Co, Ni) composites were synthesized via high temperature solid state reaction. The phase composition, crystal structure and average crystallite size of the synthesized materials were examined by XRD technique. Diffraction patterns were analyzed and fitted by Rietveld method. The morphology of the obtained materials was investigated by means of Scanning Electron Microscope (SEM) technique. With intention to analyze the electrochemical properties, the Li/Li<sup>+</sup>/(hybrid cathode) charge/discharge tests were used. By performing GITT experiments we also measured the lithium chemical diffusion coefficient in investigated hybrid cathodes.

## RESULTS AND DISCUSSION

Analysis of the collected XRD pattern that is given in Fig. 1. revealed existence of the diffraction peaks characteristic for Li<sub>2</sub>MnO<sub>3</sub> C2/m monoclinic structure, LiMO<sub>2</sub> (M = Mn, Co, Ni) C2/m monoclinic structure and existence of superstructure described as faults in

the stacking of the ordered cationic layers along the c monoclinic axis.

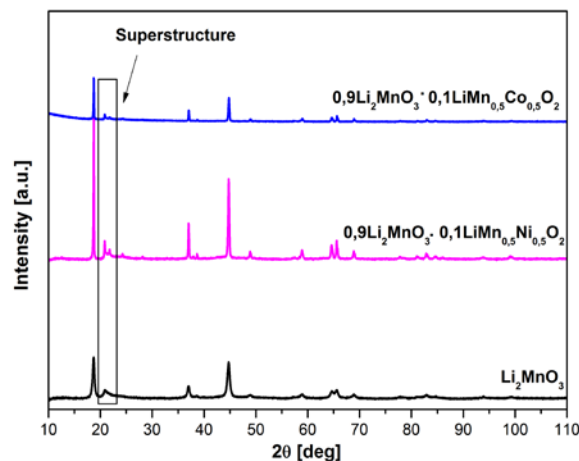


Fig. 1. XRD patterns of Li<sub>2</sub>MnO<sub>3</sub> and hybrid cathode materials based on 0.9Li<sub>2</sub>MnO<sub>3</sub>·0.1LiMn<sub>0.5</sub>Ni<sub>0.5</sub>O<sub>2</sub> and 0.9Li<sub>2</sub>MnO<sub>3</sub>·0.1LiMn<sub>0.5</sub>Co<sub>0.5</sub>O<sub>2</sub>

Average crystallite size of Li<sub>2</sub>MnO<sub>3</sub> in cathode material increases with the growth of Ni content whereas the average crystallite size of LiMn<sub>1-y</sub>Ni<sub>y</sub>O<sub>2</sub> in cathode material decreases with the growth of Ni content.

The lithium cells were cycled between 4.8 and 2.0 V at C/20. In each material there is observed irreversible loss of capacity during the first charging cycle.

## CONCLUSIONS

Simultaneously substitution of Mn by Ni or Co and fabrication the Li<sub>2</sub>MnO<sub>3</sub> – Stabilized LiMO<sub>2</sub> (M = Mn, Co, Ni) composites stabilize LiMnO<sub>2</sub> structure and increase theoretical capacity. However, there is still loss of capacity during first cycle.

## ACKNOWLEDGMENT

This work is supported by the Polish Ministry of Science and Higher Education (MNiSW) basis of the decision number 0197/DIA/2016/45. Work was realized by using the infrastructure of the Laboratory of Conversion and Energy Storage Materials in the Centre of Energy AGH.

## REFERENCES

1. C. S. Johnson, N. Li, C. Lefief, M. M. Thackeray, Electrochemistry Communications 9 (2007) 787
2. J. Li, S. Jeong, R. Kloepsch, M. Winter, S. Passerini, Journal of Power Sources 239 (2013) 490
3. J.T. Son, H.J. Jeon, J.B. Lim, Advanced Powder Technology 24 (2013) 270-274

# $\text{Na}_x(\text{Li}_y\text{Ti}_{1-y})\text{O}_2$ layered oxides as negative electrode for Na-ion batteries

*D. Baster, L. Kondracki, A. Plewa and J. Molenda*

AGH University of Science and Technology, Faculty of Energy and Fuels,  
al. A. Mickiewicza 30, 30-059 Krakow, Poland  
e-mail: molenda@agh.edu.pl

Keywords: Na-ion batteries, anode material, layered oxides,  $\text{Na}_x(\text{Li}_y\text{Ti}_{1-y})\text{O}_2$

## INTRODUCTION

Energy conversion and storage is one of the great challenges of the last decades. Hence, efficient, safe, low-cost, and environmentally friendly storage systems are required to response modern society's needs. One of possibilities is chemical energy storage in rechargeable Li-ion batteries, which offer the highest gravimetric and volumetric energy density among currently used electrochemical power sources [1]. However, sodium-ion batteries were proposed as a low cost alternative to Li-ion batteries due to high price and limited resources of lithium [2]. Na-ion batteries have attracted much attention because of their many advantages, such as high abundance of sodium in the Earth's crust, its low cost and suitable redox potential (only 0.3 V above that of lithium) [2].

Therefore, further development of rechargeable batteries is focused on the discovery of new, high-performance and low-cost electrode materials. Anode materials for sodium-ion batteries should possess high capacity and low chemical potential versus sodium, high reversibility of the intercalation/deintercalation reaction, environment-friendliness, low price of substrates, and especially mechanical stability during multiple insertion/deinsertion of sodium ions, which is an important limitation and challenge [2]. As experienced in anodes materials for Li-ion batteries, the volumetric expansion problem is difficult to solve because it stems from the intrinsic properties of the materials, which are related to structural changes during sodium intercalation.

$\text{P2-Na}_{0.66}[\text{Li}_{0.22}\text{Ti}_{0.78}]\text{O}_2$  layered oxide was proposed as the negative electrode, which exhibits only ~0.77% volume change during sodium insertion/extraction [3]. The electrode material also exhibits an average storage voltage of 0.75 V, a practical usable capacity equal to 100 mAh/g with high cyclability [3].

## EXPERIMENTAL

$\text{Na}_x(\text{Li}_y\text{Ti}_{1-y})\text{O}_2$  was synthesized by a solid-state high-temperature reaction from  $\text{Li}_2\text{CO}_3$  (Sigma-Aldrich, ≥99.0%),  $\text{Na}_2\text{CO}_3$  (Sigma-Aldrich, 99.99%),  $\text{TiO}_2$  (Sigma-Aldrich, 99.99%). Crystal structure of the considered material was investigated in using X-ray diffraction (XRD) method on Panalytical Empyrean diffractometer with  $\text{Cu K}\alpha$  radiation. For low temperature studies Oxford Instruments cryostat was used, while for high temperature measurements Anton Paar HTK1200N oven-chamber was mounted. Structural parameters of the considered material were determined by Rietveld refinement method with GSAS/EXPGUI set of software.

## RESULTS AND DISCUSSION

XRD measurements at room temperature show the presence of a single phase with  $P6_3/mmc$  symmetry for  $\text{Na}_{0.66}[\text{Li}_{0.22}\text{Ti}_{0.78}]\text{O}_2$ . This work presents a high-temperature method of synthesis of materials series with chemical formula  $\text{Na}_x(\text{Li}_y\text{Ti}_{1-y})\text{O}_2$ . Fig. 1 presents low temperature XRD studies of  $\text{Na}_{0.66}[\text{Li}_{0.22}\text{Ti}_{0.78}]\text{O}_2$ . Selected, single phase materials were applied as electrode material in  $\text{Na}/\text{Na}^+/\text{Na}_x[\text{Li}_{0.22}\text{Ti}_{0.78}]\text{O}_2$ -type cells. Specific capacity, reversibility and stability during charge-discharge cycles were evaluated to characterize electrochemical properties of the cells.

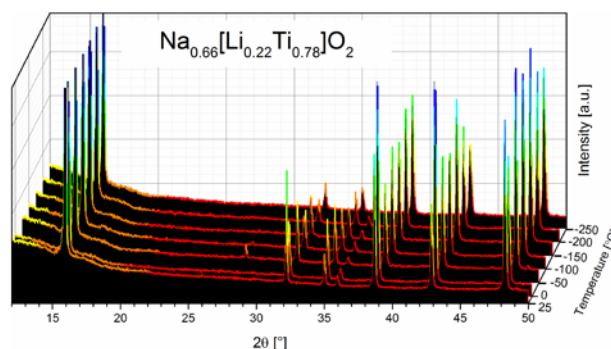


Fig. 1 XRD data for  $\text{Na}_{0.66}[\text{Li}_{0.22}\text{Ti}_{0.78}]\text{O}_2$ .

## ACKNOWLEDGMENT

The project was funded by the National Science Centre Poland (NCN) on the basis of the decision number UMO-2016/23/B/ST8/00199. Work was realized by using the infrastructure of the Laboratory of Conversion and Energy Storage Materials in the Centre of Energy AGH.

## REFERENCES

- [1] K. Ozawa, Lithium Ion Rechargeable Batteries: Materials, Technology, and New Applications, first ed., Wiley-VCH Verlag GmbH & Co. KGaA, Weinheim, 2009.
- [2] S.-W. Kim, D.-H. Seo, X. Ma, G. Ceder and K. Kang, Adv. Energy Mater. 2 (2012) 710
- [3] Y. Wang *et al.* Nat. Commun. 4 (2013) 2858

# An alluaudite $\text{Na}_2\text{Fe}_2(\text{SO}_4)_3$ as earth abundant cathode material for Na-ion batteries

*A. Plewa, D. Baster, A. Kulka and J. Molenda*

Faculty of Energy and Fuels  
AGH University of Science and Technology  
al. A. Mickiewicza 30, 30-059 Krakow, Poland  
molenda@agh.edu.pl

Keywords: Na-ion batteries, cathode material, polyanion compounds,  $\text{Na}_2\text{Fe}_2(\text{SO}_4)_3$

## INTRODUCTION

Fast development of portable electronics and renewable energy sources causes increased demand for energy storage technologies. Li-ion batteries are the most promising among energy storage systems due to many advantages. However, the limited resources of lithium and their locations in politically unstable areas involve great interest in dispensable Na-ion batteries [1,2]. Currently, the major challenge in advancing Na-ion batteries technology lies in finding suitable cathode material based on abundant, low-cost, safety and environmental benign elements such as iron and sulphur.

There are two major classes of cathode materials for Na-ion batteries: layered compounds and polyanion compounds. In the polyanion compounds, there are combined tetrahedral units  $(\text{XO}_4)^{n-}$  with  $\text{MO}_6$  polyhedra. Because of the strong covalent bonding in tetrahedral units  $(\text{XO}_4)^{n-}$ , polyanion materials have high thermal stability, which makes them more appropriate for large-scale energy storage applications [3]. One of the most promising candidates from this group is  $\text{Na}_2\text{Fe}_2(\text{SO}_4)_3$ . It contains low-cost and abundant elements: sodium, iron, sulphur and oxygen.  $\text{Na}_2\text{Fe}_2(\text{SO}_4)_3$  cathode exhibits the high  $\text{Fe}^{2+}/\text{Fe}^{3+}$  redox potential at 3.8 V (vs.  $\text{Na}/\text{Na}^+$ ) with specific capacity more than 100 mAh/g [4]. The theoretical energy density of alluaudite  $\text{Na}_2\text{Fe}_2(\text{SO}_4)_3$  is particularly high ( $>540 \text{ Whkg}^{-1}$  vs.  $\text{Na}/\text{Na}^+$ ) and enough to make Na-ion batteries competitive with Li-ion batteries.

## EXPERIMENTAL

This work presents a low-temperature solid-state synthesis of  $\text{Na}_2\text{Fe}_2(\text{SO}_4)_3$ , little-known material with a new structure with the first alluaudite-type sulphate framework. Crystal structure of the obtained powders was characterised using X-ray diffraction (XRD) method with Panalytical X'Pert Pro diffractometer. Crystal structure parameters were determined using the Rietveld method with GSAS/EXPGUI software package. The synthesised materials were applied as cathodes in  $\text{Na}/\text{Na}^+/\text{Na}_{2-x}\text{Fe}_2(\text{SO}_4)_3$  cells. The used electrolyte was a 1M solution of  $\text{NaPF}_6$  in EC: DEC. Specific capacity, reversibility and stability during charge-discharge cycles were evaluated in order to characterise electrochemical properties of the cells.

## RESULTS AND DISCUSSION

The main drawback of  $\text{Na}_2\text{Fe}_2(\text{SO}_4)_3$  is difficulties with obtaining single phase material. This compound decompose above  $400^\circ\text{C}$ . Increase of temperature above this limit leads to the emission of sulphur oxides

$\text{SO}_x$ . In addition, inherent dissolution of  $\text{SO}_4^{2-}$  in water makes it unstable in aqueous media. It rules out conventional high-temperature solid-state and aqueous solution-based synthesis methods. Thus, we used the low-temperature solid-state method to obtain  $\text{Na}_2\text{Fe}_2(\text{SO}_4)_3$  target compound.

The optimum conditions for the synthesis of the considered material are: a temperature of  $360^\circ\text{C}$  and atmosphere 5%  $\text{H}_2$  in Ar. At lower temperatures, not all substrates were reacted. In turn, the calcination process at temperatures exceeding  $390^\circ\text{C}$  resulted in thermal decomposition of the material and precipitation of iron sulphide.

The electrochemical tests carried out confirm good application characteristics of the material - high operating voltage (3-4 V) and specific capacities of about 70-80 mAh/g. The charging and discharging curves of the tested cells have stable potential plateaux around voltage 3.5 V and the capacity of the cells remains constant even with very high number of cycles and high current.

## CONCLUSIONS

Searching for novel low-cost cathode materials for rechargeable Na-ion batteries, we have synthesised a Fe-based  $\text{Na}_2\text{Fe}_2(\text{SO}_4)_3$ . High operating voltage (3-4 V) with stable voltage plateau and high specific capacities about 70-80 mAh/g make it promising for commercial application.

## ACKNOWLEDGMENT

This work is supported by the National Science Centre Poland (NCN) of the basis of the decisions number 2016/21/D/ST5/01658 and Polish Ministry of Science and Higher Education, under project AGH No. 15.11.210.398

## REFERENCES

- [1] V. Palomares, P. Serras et al. *Energy and Environmental Science*, 5 (2012) 5884
- [2] D. Baster, J. Molenda, *Biuletyn Polskiego Stowarzyszenia Wodoru i Ogniw Paliwowych* 8 (2014) 31
- [3] P. Barpanda, G. Oyama, S. Nishimura, S. Chung, A. Yamada, *Nat. Commun.* 5 (2014) 4358
- [4] G. Oyama, S. Nishimura, Y. Suzuki, M. Okubo and A. Yamada, *ChemElectroChem*, 7 (2015) 1019

# Preparation and properties of Ni-MH hydride cells based on $\text{La}_2\text{Ni}_9\text{Co}$ hydrogen storage alloys doped with Al or Sn

*H. Drulis, A. Hackemer, K. Giza\*, L. Adamczyk\*, M. Dymek\* and H. Bala\**

Institute of Low Temperatures and Structural Research PAS, Okólna 2, Wrocław, Poland  
\*Częstochowa University of Technology, Department of Chemistry, al. Armii Krajowej 19,  
Częstochowa, Poland  
e-mail: h.drulis@int.pan.wroc.pl

Keywords: hydrides, metal hydride batteries

## INTRODUCTION

The aim of the work was to fabricate and examine the standard button cell samples, in which the negative electrodes were the  $\text{La}_2\text{Ni}_9\text{Co}$  storage alloys doped with Al or Sn. The room temperature  $p$ - $c$  isotherms indicate the beneficial effect of Sn and Al addition which causes decrease of  $\text{H}_2$  equilibrium pressure and does not limit atomic hydrogen solubility in the initial  $\text{La}_2\text{Ni}_9\text{Co}$  alloy. The results obtained in some of our latest papers [1-2] indicate that amphoteric substitutes like Zn, Al, Bi, Sn etc. may also activate the charge/discharge processes in strong alkaline environment. In present study we evaluate the discharge current capacity, self-discharge after 7 days of storage and cyclic life of the standard button cell which contains these electrodes.

## EXPERIMENTAL

Two materials were designated  $\text{La}_2\text{Ni}_9\text{CoAl}_{0.2}$  and  $\text{La}_2\text{Ni}_9\text{CoSn}_{0.2}$  as negative electrode in the HB 156/064 type button cells. For each material the three cells were made and tested in parallel. The presented results are based on the average values of the cell series in which the alloy material is used. The tested materials have been obtained by arc-melting of chemical grade purity precursor,  $\text{La}_2\text{Ni}_9\text{Co}$  (American Elements, US) with corresponding addition of Sn or Al under high purity Ar-atmosphere. The composite pellets have been prepared by mixing of each materials (20-50  $\mu\text{m}$  powder fractions) with C-graphite and PVDF binder and isostatic pressing (50 bar force). The obtained tablets were then closed in baskets made of nickel mesh which constituting the current collector. As a positive electrode the material called NICOL G extra heavy were selected. The positive and negative electrodes after the formation were placed in separate containers and poured with KOH electrolyte. As a separator a non-woven absorbent Viledon FS2119 was used. The operation of soaking the electrodes and the separator with electrolyte was conducted max 24 hours before mounting the battery. After centrifugation of the excess electrolyte the button cells HB 156/066 (labelled according to EN 61951-2: 2011) type have been mounted.

The electrochemical capacity study was conducted using a galvanostatic method. In the course of the measurement the change in the voltage at time  $E = f(t)$  was measured. Model cells were subjected to cyclic electrochemical charging with a constant current of 8.5 mA by 12h. After an hour rest the continuous discharge process with a constant current of  $i = 17$  mA to the final voltage  $U = 1\text{V}$  were performed. The

10 charge/discharge cycles were carried out. The studies were made at  $20 \pm 5^\circ\text{C}$  using the VMP-3 BioLogic multi-channel potentiostat VMP-3.

## RESULTS AND DISCUSSION

The investigations have shown that the highest values of the current capacity determined during the 10 charge/discharge cycles were reached by the cells in which the  $\text{La}_2\text{Ni}_9\text{CoSn}_{0.2}$  alloy was used. Actual capacity of these cells was about 82 mAh and remained at this level from 1 to 10 cycles. The cells made with Al alloy reached a capacity value of 73-73 mAh. During the self-discharge test, the best result was also recorded for the cells in which the  $\text{La}_2\text{Ni}_9\text{CoSn}_{0.2}$  alloy was used. A decrease in average capacity of about 15% was observed while the capacity of  $\text{La}_2\text{Ni}_9\text{CoAl}_{0.2}$  cells was less than of over 30% of the initial capacity after 7 days of storage. The cyclic durability during 50 cycles were carried out in accordance with the requirements of EN 61951-2: 2011. The best stability have shown the  $\text{La}_2\text{Ni}_9\text{CoSn}_{0.2}$  cells. These cells after cyclic processes still kept of 91% of the initial value while the capacity of the cells produced with  $\text{La}_2\text{Ni}_9\text{CoAl}_{0.2}$  was about 83%. The capacity of all tested cells drastically dropped after the next 50 cycles. The most likely the cell destruction was caused by the drying of the electrolyte with time.

## CONCLUSIONS

The advantageous effect of Sn addition into  $\text{La}_2\text{Ni}_9\text{Co}$  alloy manifests itself primarily in improvement of electrochemical capacity which can be a consequence of equilibrium hydrogen pressure decrease for Sn-containing alloy. Also presumably Sn forms  $\text{SnH}_4$ -type intermediates that confine the lattice expansion/contraction and thus, reduce mechanical deterioration of the material. The encouraging effect of Sn on corrosion inhibition of  $\text{LaNi}_5$ -based materials deserves for further, systematic investigations.

## REFERENCES

1. M. Dymek, H. Bala, A. Hackemer, H. Drulis, *Solid State Ionics* 271(2015)116
2. M. Dymek, H. Bala, H. Drulis, A. Hackemer *Solid State Phenomena* 227(2015)263



# Characterization of LiVBO<sub>3</sub>F glass and nanomaterials

Jędrzej Doliński, Przemysław P. Michalski, Jan L. Nowiński, Jerzy E. Garbarczyk

Faculty of Physics

Warsaw University of Technology, ul. Koszykowa 75

00-662 Warszawa, Poland

e-mail: michalski@if.pw.edu.pl

Keywords: lithium borate glass, tavorite, nanocrystallization, cathode materials for Li-ion batteries

## INTRODUCTION

The lithium vanadium fluorophosphate (tavorite, LiVPO<sub>4</sub>F) is one of potential high-energy cathode materials for Li-ion batteries. With the voltage vs. Li<sup>+</sup>/Li<sup>0</sup> reaching 4.2 V, it could meet the demands of electric cars and mobile devices industry. The material also shows an excellent stability upon cycling, due to stable V–F bonds. On the other hand, it exhibits moderate gravimetric capacity (up to 156 mAh/g) [1]. An attempt to improve the capacity may be done by replacing heavy phosphate group with any other lighter anionic group. In this work, the phosphate group was substituted with a borate group, creating a compound of nominal composition LiVBO<sub>3</sub>F. In order to obtain a highly-conductive nanomaterial, a method of thermal nanocrystallization of precursor glass was applied. Previously, this method has proved to be useful in case of other systems, eg. LiFePO<sub>4</sub> with addition of V<sub>2</sub>O<sub>5</sub> [2].

## EXPERIMENTAL

Appropriate amounts of precursors: LiF (Aldrich, pa.), V<sub>2</sub>O<sub>5</sub> (Aldrich, pa.) and H<sub>3</sub>BO<sub>3</sub> (Polish Chemicals, pa.) were mixed in a mortar, melted at 1200 °C for 20 min in non-oxidizing atmosphere and rapidly quenched. The amorphousness of the as-prepared sample was confirmed with X-ray diffractometry (XRD Phillips X'Pert Pro) and thermal events occurring in the sample were observed with differential thermal analysis (DTA, TA Q600). Temperature-dependent X-ray measurements were performed in nitrogen flow. Electrical conductivity was measured upon heating and subsequent cooling with impedance spectroscopy (IS, Solatron 1260) within wide frequency range 10 mHz – 10 MHz. The amplitude of oscillating voltage was equal to 0.1 V.

## RESULTS AND DISCUSSION

XRD confirmed that the as-prepared sample was amorphous. DTA trace was also typical for glassy materials, consisting of a glass transition step followed by a few crystallization peaks. The conductivity of the initial glass was as low as 10<sup>–9</sup> S/cm with an activation energy of 0.63 eV. After annealing at temperatures in the range where the crystallization phenomenon occurs, the significant improvement in conductivity was achieved. The best results were obtained for heating up to 350 °C, where the conductivity increased to 7.1·10<sup>–5</sup> S/cm and activation energy decreased to 0.25 eV (Fig. 1). The nanocrystallization seems to improve electronic conductivity mostly. This statement is supported by impedance spectra presented in Fig. 2.

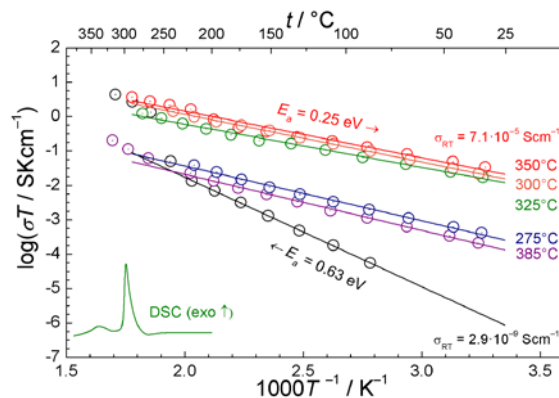


Fig. 1. Electrical conductivity of LiVBO<sub>3</sub>F upon heating to various temperatures and cooling down to RT. DSC curve is shown for comparison.

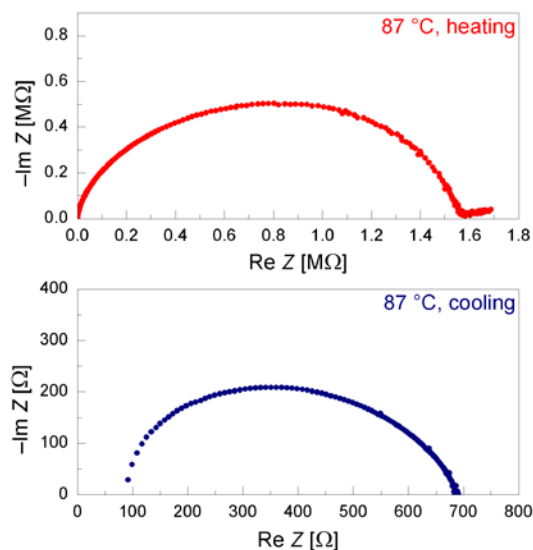


Fig. 2. Impedance spectra before and after nanocrystallization (during heating and cooling ramp, respectively) measured at 87 °C.

## CONCLUSIONS

A novel glass-ceramics composite of nominal composition LiVBO<sub>3</sub>F with highly enhanced conductivity was obtained. Electrochemical tests are planned in the near future.

## REFERENCES

1. M.V. Reddy, G.V. Subba Rao, B.V.R. Chowdari, *J. Power Sources* 195 (2010) 5768–5774.
2. T.K. Pietrzak, M. Wasiucionek, I. Gorzkowska *et al.*, *Solid State Ionics* 251 (2013) 40–46.

# Thermal and electrical properties of mixed sodium-lithium salts containing $\text{N}(\text{CF}_3\text{SO}_2)_2^-$ anion

*J. Kotwiński<sup>1</sup>, M. Marzantowicz<sup>1</sup>, M. Leszczyńska-Redek<sup>1</sup>, A. Gągor<sup>2</sup>, I. Abrahams<sup>3</sup>, F. Krok<sup>1</sup>*

- 1) Faculty of Physics, Warsaw University of Technology, Koszykowa 75, 00-662 Warszawa, Poland
- 2) Institute of Low Temperature and Structure Research, Okólna 2, 50-422 Wrocław, Poland
- 3) Centre for Materials Research, Department of Chemistry, Queen Mary, University of London, Mile End Road, London E1 4NS, United Kingdom of Physics  
e-mail: marzan@mech.pw.edu.pl

Keywords: lithium imide salt, sodium imide salt, mixed sodium-lithium salts

## INTRODUCTION

Lithium bis(trifluoromethane)sulfonimide salt, (LiTFSI) and sodium bis(trifluoromethane)sulfonimide salt (NaTFSI) are one of the most popular choices as sources of  $\text{Li}^+$  and  $\text{Na}^+$  ions in electrolytes for rechargeable batteries. The expanded TFSI<sup>-</sup> anion causes delocalization of negative charge within the molecule which enhances dissociation and suppresses anion mobility. Moreover, due to the flexibility of S-N-S bond, the TFSI<sup>-</sup> anion can act as plasticizing agent. Such an elastic bond allows to obtain different conformations, namely cis, trans or gauche. If salt based on TFSI<sup>-</sup> anion is used as additive to polymer it would introduce a structural disorder to the system preventing the matrix from crystallization. Such an effect improves the conductivity of electrolyte. Our studies on crystal structure of LiTFSI and NaTFSI proved that their crystal systems differ strongly, then mixing the salts can favor generating defects in the structure and enhance total conductivity. The proper molar ratio can also create eutectic mixture with much lower melting point than lithium and sodium salts themselves. This can be a strong advantage in development of “polymer-in-salt” electrolytes because of possible suppression of crystallization of salts.

## EXPERIMENTAL

Lithium bis(trifluoromethylsulfonyl)imide salt (Aldrich) and sodium bis(trifluoromethylsulfonyl)imide salt (Solvionic) were mixed in selected molar ratios of 1:2, 1:1, 1.8:1, 2:1 and 2.2:1 (LiTFSI:NaTFSI) in the presence of acetonitrile. Samples were left for several weeks in the vacuum chamber in order to evaporate the solvent. Mixed salts were then heated on the hot plate for ca 24 h to remove remains of the solvent and milled in agate mortar to obtain fine powder. To study thermal behaviour of samples and find eutectic mixture composition, differential scanning calorimetry measurements were carried out in the range of -120 °C to 230 °C with a heating rate of 5 °C/min. Electrical properties of mixed salts were investigated using impedance spectroscopy. Platinum electrodes were placed inside quartz test tube filled up with mixtures of salts and after that the binary system was melted to provide good electrical contact between the electrodes. The data were collecting within 10 mHz - 10 MHz frequency range and using 100 mV signal amplitude. Temperatures varied from 30 °C to 280 °C.

## RESULTS AND DISCUSSION

Differential scanning calorimetry measurements showed that eutectic phase can be obtained, with the composition close to 2:1 (LiTFSI:NaTFSI) molar ratio. This value has been determined by measuring enthalpy of fusion of the eutectic melting peak. This peak has been observed in the DSC curves at around 186 °C. The endothermic peak at ca 150 °C comes from LiTFSI structural transition and is present for all prepared samples, regardless the molar ratio. Events observed above 190 °C for non-eutectic compositions are related to melting of LiTFSI or NaTFSI salts.

## CONCLUSIONS

The eutectic point of LiTFSI-NaTFSI binary system was identified at 186 °C. Further measurements, including impedance spectroscopy, will verify whether the eutectic phase has higher conductivity than pristine salts and whether the mixed alkali effect occurs in such a mixtures. X-ray diffraction measurements should allow to determine, whether the eutectic mixtures adapt symmetry of one of the pristine salts, or crystallize in a different structure.

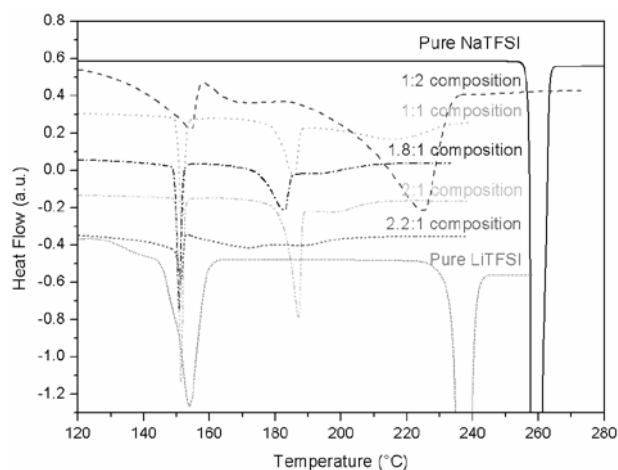


Fig. 1. DSC thermograms for various LiTFSI-NaTFSI compositions.

# Studies of structural and electrochemical properties of electrode nanocomposites with self-assembled conductive carbon layers

J. Świder<sup>1</sup>, M. Lis<sup>1</sup>, M. Gajewska<sup>2</sup>, M. Świętosławski<sup>1</sup>, M. Molenda<sup>1\*</sup>

<sup>1</sup>Faculty of Chemistry

Jagiellonian University, Ingardena 3  
30-060 Krakow, Poland

<sup>2</sup> AGH University of Science and Technology

Academic Centre for Materials and Nanotechnology, Mickiewicza 30  
30-059 Krakow, Poland

e-mail: molendam@chemia.uj.edu.pl

Keywords: nanocomposites, carbon conductive layers, CCL, LiFePO<sub>4</sub>, Li<sub>2</sub>MnSiO<sub>4</sub>, Li-ion batteries.

## INTRODUCTION

Nowadays, the majority of research and development efforts is aimed towards electrode materials due to their impact on energy density, safety and life cycle of Li-ion batteries for high performance energy storage systems. The polyanion-type cathode materials are promising compounds for the sake of the high theoretical capacity, low costs of the starting materials, the environmental friendliness and the high chemical and thermal stability<sup>1,2</sup>. The key drawback for the commercial application is its low electrical conductivity. The procedures used to increase electrical conductivity of polyanion-type cathode materials are: optimization the process of synthesis<sup>3</sup>, particle-size reduction<sup>4,5</sup>, addition of metal or conductive carbon powder<sup>5,6</sup> or carbothermal formation on the surface of conductive carbon layers (CCL)<sup>7,8</sup>. Procedure of active material modification with carbon was confirmed to be an effective method for the enhancement of electrochemical property of two described in this work cathode materials: lithium iron phosphate (LiFePO<sub>4</sub>, LFP) and dilithium manganese orthosilicate (Li<sub>2</sub>MnSiO<sub>4</sub>, LMS).

## EXPERIMENTAL

The technological process of preparation conductive carbon layer<sup>9</sup> on powdered supports consists of two main stages. First stage includes preparation of carbon precursor during free radical polymerization of hydrophilic polymer in water solution. The nanocoating precursor is the mixture of hydrophilic polymers with pyromellitic acid. The second stage covers the following processes: impregnation of active material in suspension by water solution of nanocoating precursor, water removal and composite precursor drying. Then the CCL nanocomposite is formed during carbonization of carbon precursor under controlled conditions.

## RESULTS AND DISCUSSION

The phase identification of the synthesized products was carried out by X-ray diffraction (XRD). The carbon content in the CCL/LiFePO<sub>4</sub> and CCL/Li<sub>2</sub>MnSiO<sub>4</sub> nanocomposites was estimated by thermogravimetric (TGA) method. Particle morphology and the internal structure of the samples were observed by transmission electronic microscopy (TEM) and the specific surface area was measured by using Branauer–Emmet–Tailor (BET) method. The

electrical properties of CCL coated nanocomposite powders were measured using 4-probe AC method within temperature range of -10 to 40 °C. The electrochemical performance was carried out in galvanostatic mode with stable charge-discharge current and performed in Li/Li<sup>+</sup>/(CCL/LFP) and Li/Li<sup>+</sup>/(CCL/LMS) type cells. As an electrolyte was used solution of 1M lithium hexafluorophosphate (LiPF<sub>6</sub>) dissolved in mixture of EC:DMC = 1:1.

## CONCLUSIONS

The process of CCL formation as a deposition of polymer precursor enables to control the morphology and electrical properties of formed carbon layers CCL. In presented studies nanocomposites confirm the physicochemical properties of CCL layers such as: increased electrical conductivity of the nanocomposites, provided easy diffusion paths of lithium ions through the carbon layer resulting from the unique mesoporous structure of CCL and increased chemical stability of active material surface towards electrolyte.

## ACKNOWLEDGMENT

This work is supported by National Science Centre, Poland under research grant no. 2014/13/B/ST5/04531.

## REFERENCES

1. A.K. Padhi *et al*, *J. Electrochem. Soc.* **144** (1997) 1188–1194
2. Z. Gong, Y. Yang, *Energy and Environ. Sci.* **4** (2011) 3223–3242
3. D. Jugovic, D. Uskokovic, *J. Power Sources* **190** (2009) 538–544
4. C. Delacourt *et al.*, *Electrochem. Solid-State Lett.* **9** **1** (2006) A352
5. S.L. Bewlay *et al.*, *Materials Letters* **58** (2004) 1788–1791
6. N. Zhou *et al.*, *Int. J. Electrochem. Sci.* **7** (2012) 12633 – 12645
7. M. Molenda *et al*, *Solid State Ionics* **251** (2013) 47–50
8. M. Molenda, *Funct. Mat. Lett.* **4** (2011) 129–134
9. M. Molenda, R. Dziembaj, A. Kochanowski, E. Bortel, M. Drozdek, Z. Piwowarska Pat. PL 216549 B1 (2014); Pat. US 8,846,135 B2 (2014); Pat. JP 5476383 B2 (2014); Pat. KR 10-2011-7004142 (2015), Pat. EP 2326745 A2 (2017)

# Electrochemical stability of modified spinel materials in wide potential range

K. Chudzik, M. Bakierska, M. Świętosławski\* and M. Molenda

Faculty of Chemistry

Jagiellonian University, ul. Ingardena 3 Str., 30-060 Kraków, Poland

e-mail: m.swietoslowski@uj.edu.pl

Keywords: li-ion battery, cathode material, manganese-oxide spinel

## INTRODUCTION

Due to rapid increase of power and energy storage systems demand, the search for improvement of battery materials is inevitable. Their applications, including currently most demanding and fast-growing automotive market, requires improved properties in terms of electrochemistry and stability. Other important factors that have to be considered are environmental impact and lowest possible cost of a material. One of various compounds that meets these demands is manganese oxide spinel  $\text{LiMn}_2\text{O}_4$  (LMO) due to its low cost, high abundance and good electrochemical properties – high operating voltage and acceptable capacity. All mentioned properties makes this material perfect for automotive purposes, nevertheless it is not totally free of some drawbacks due to its structural instability. Poor capacity retention of LMO in elevated temperatures (which are unavoidable in electric and hybrid-electric vehicle systems) is caused by structural instability caused by Jahn-Teller distortion effect and dissolution of manganese ions into the electrolyte solution[1]. Moreover, stoichiometric LMO at 2,96 V potential undergoes a phase transition leading to great lattice parameters change, that are too severe to maintain structural integrity of material [2]. Mentioned flaws can be overcome by doping lithium, manganese or oxygen sublattices by elements like potassium (increasing structural stability and  $\text{Li}^+$  diffusion coefficient) [3], nickel (increasing structural stability and energy density by shifting voltage of cell to higher potentials due to high-potential Ni redox couples) [4] or sulfur (increasing structural stability) [5].

## EXPERIMENTAL

R2032 coin-cells were assembled in argon atmosphere glovebox using aluminium foil as current collector, Celgard and Whatman separators and metallic lithium as an anode. As an electrolyte 1M solution of  $\text{LiPF}_6$  in EC/DEC 50:50 v/v have been used. The experimental methods used in cells testing includes galvanostatic charge/discharge tests (CELL TEST) and cyclic voltammetry (CV) in 1,5 - 4,5 V potential range, electrical impedance spectroscopy (EIS) and galvanostatic intermittent titration technique (GITT).

## RESULTS AND DISCUSSION

Performance of doped LMO materials in the wide potential range 1,5 - 4,5 V was studied on the basis of electrochemical tests. Composition of most stable and effective materials were determined. Diffusion coefficients of lithium ions for tested materials were determined.

## CONCLUSIONS

It has been observed that electrochemical stability of materials in wide potential range highly depends on combination and amount of used dopants. Various additives have also significant influence of diffusion coefficients of lithium ions, which is tightly connected with material performance in particular working conditions, especially for high-power applications.

## ACKNOWLEDGMENT

This work is supported by National Centre for Research and Development, Poland under research grant No. LIDER/463/L-6/14/NCBR/2015.

## REFERENCES

1. R. Gummow, A. De Kock, M. Thackeray, *Solid State Ionics* **69.1**(1994) 59-67
2. M. Thackeray, *Journal of the American Ceramic Society*, **82.12**(1999) 3347-3354
3. L. Xiong, Y. Xu, X. Xiao, J. Wang, Y. Li, *Electronic Materials Letters*, **11.1**(2015) 138-142
4. S. Patoux, L. Sannier, H. Lignier, Y. Reynier, C. Bourbon, S. Jouanneau, S. Martinet, *Electrochimica Acta* **53.12**(2008)4137-4145
5. M. Molenda, M. Bakierska, D. Majda, M. Świętosławski, R. Dziembaj, *Solid State Ionics*, **272**(2015)127-132

# Li<sup>+</sup> conducting solid composite electrolytes formed in the LiTi<sub>2</sub>(PO<sub>4</sub>)<sub>3</sub>–LiF system

*K. Kwatek, J.L. Nowiński*

Warsaw University of Technology, Faculty of Physics  
00-662 Warsaw, Poland  
e-mail: kwatek@if.pw.edu.pl

Keywords: solid electrolyte, composite, total ionic conductivity enhancement, lithium fluoride

## INTRODUCTION

Commonly used liquid electrolytes in lithium-ion batteries impede, in fact, process of further development of the technology due to their low chemical stability, high flammability and limited width of electrochemical window. There is believe that substitution of the liquid electrolytes in batteries by solid ones could remove most of those problems. Technical requirements of LIB technology appoint solid lithium ion conductors showing at room temperature conductivity higher than  $10^{-4}$  S·cm<sup>-1</sup> as the recommendable electrolytes. Lithium titanium phosphate (LTP) of NASICON-type structure meets most of the requirements. Ceramic or polycrystalline LTP demonstrate high grain ion conductivity but they suffer from very high grain boundary resistance, resulting in low total conductivity of these materials. Aono et. al [1] shown that insertion of some foreign phase into the base matrix of LTP could enhance total conductivity of LTP. In our previous work [2] we demonstrated that significant enhancement of the total ion conductivity was achieved for LTP–LiI composites.

## EXPERIMENTAL

The polycrystalline LiTi<sub>2</sub>(PO<sub>4</sub>)<sub>3</sub> was obtained by the means of solid-state reaction method. Starting reagents as Li<sub>2</sub>CO<sub>3</sub> (Sigma Aldrich), NH<sub>4</sub>H<sub>2</sub>PO<sub>4</sub> (POCH), TiO<sub>2</sub> (Sigma Aldrich) were weighted in stoichiometric amounts, then mixed with a mortar and pestle. The ground mixture was synthesized at 900°C for 10h to obtain the final compound. The second step of preparation the presented composites contain addition of LiF. Ball-milling technique was employed to form LTP–LiF composite materials. The as-prepared LTP powder was mixed with LiF in different molar ratio of the second component varying from 10 to 40 %. Both powders, immersed in ethanol, were ball-milled with rotation speed of 400 rpm for 1 h employing planetary ball-mill Pulverisette 7. Then, the obtained powders were uniaxially pressed to form pellets and subsequently sintered at 700°C, 800°C and 900°C for two hours. The composites were characterized by X-ray diffractometry (XRD), thermogravimetry (TGA), scanning electron microscopy (SEM) and density methods. Electric properties in the 30–100°C temperature range were investigated by means of impedance spectroscopy (IS) method. For electric measurements, both bases of the as-form pellets were, at first, polished and then covered with graphite as electrodes.

## RESULTS AND DISCUSSION

XRD investigation show good agreement of positions and relative intensities of the reflexes of polycrystalline LTP with those of the composite materials. However, sintering process cause also formation of a new phase identified as LiTiPO<sub>5</sub>. The contents of the newly formed phase after sintering increases with the concentration of the additive material. Thermal studies reveal that mass loss of ca. 2% is mainly related to the adsorbed moisture. Studies on the microstructure by means of scanning electron microscopy and density methods indicate densification of sintered composite material. Within each composition, it could be observed that sintering temperature is the most influential factor for densification. The most dense material could be obtained after sintering at 800°C. The impedance investigations showed that introduction of LiF to the base LTP matrix followed by sintering causes a significant enhancement of total ionic conductivity. However, when contents of the LiF additive in the composite was too high (20 %), then instead of enhancement, the decrease was observed. The maximum conductivity was obtained for the samples with 0.1 mol of LiF addition.

## CONCLUSIONS

The work presents the first report showing that electric conductivity of the LiTi<sub>2</sub>(PO<sub>4</sub>)<sub>3</sub> lithium ion conductor one can significantly increase by introducing LiF additive into the parent matrix and then sintering the composite at 700–900°C.

## REFERENCES

- [1] H. Aono, E. Sugimoto, Y. Sadaoka, N. Imanaka, G. Adachi, Solid State Ionics 47 (1991), 257–264
- [2] K. Kwatek, J.L. Nowiński, Solid State Ionics 302 (2017), 35–39



# Lithium-ion conducting ceramic composites based on $\text{LiTi}_2(\text{PO}_4)_3$ and $\text{Li}_{2.9}\text{B}_{0.9}\text{S}_{0.1}\text{O}_{3.1}$ glass

*K. Kwatek, J.L. Nowiński*

Warsaw University of Technology, Faculty of Physics  
00-662 Warsaw, Poland  
e-mail: kwatek@if.pw.edu.pl

Keywords: solid electrolyte, composite, total ionic conductivity enhancement, glass

## INTRODUCTION

Lithium ion batteries (LIBs) containing liquid electrolytes suffer from severe deficiencies i.e. high flammability and limited width of electrochemical window. Substitution of the liquid electrolyte by solid one could remove the mentioned problems. Additionally, it is believed that solid electrolyte will provide better thermal and chemical stability. Application of solid conductors as an electrolyte require total ionic conductivity at room temperature to be higher than  $10^{-4} \text{ S}\cdot\text{cm}^{-1}$ . Lithium titanium phosphate (LTP) of NASICON-type structure satisfies the most of technical criteria required by the LIBs technology. Ceramic or polycrystalline LTP demonstrate high grain ion conductivity, but their very high grain boundary resistance result in low total ionic conductivity. Aono *et. al* [1] shown that insertion of some foreign crystalline phase into the base matrix of LTP could enhance total conductivity of the material. Our work demonstrates that addition of amorphous  $\text{Li}_{2.9}\text{B}_{0.9}\text{S}_{0.1}\text{O}_{3.1}$  (LBSO) to the LTP also caused the significant enhancement of the total ion conductivity.

## EXPERIMENTAL

The  $\text{LiTi}_2(\text{PO}_4)_3$  material was synthesized by conventional solid-state reaction method. Stoichiometric amounts of  $\text{Li}_2\text{CO}_3$  (Sigma Aldrich),  $\text{NH}_4\text{H}_2\text{PO}_4$  (POCh),  $\text{TiO}_2$  (Sigma Aldrich) reagents were weighted, mixed with a mortar and pestle. The ground mixture was annealed at  $900^\circ\text{C}$  for 10h to synthesis the final compound. In the case of preparation of  $\text{Li}_{2.9}\text{B}_{0.9}\text{S}_{0.1}\text{O}_{3.1}$  glass, stoichiometric amounts of  $\text{Li}_2\text{CO}_3$  (Sigma Aldrich),  $\text{Li}_2\text{SO}_4$  (Sigma Aldrich) and  $\text{H}_3\text{BO}_3$  (POCh) were weighted, mixed with a mortar and pestle. Then, the formed mixture was placed in an alumina crucible and annealed at  $1100^\circ\text{C}$  for 15 min. to obtain the molten glass. The process of vitrification was completed by quenching the melt between two stainless steel plates. The studied ceramic composites were prepared by a two-step route. First, the precursor composite materials were prepared from crystalline LTP and ground LBSO glass by means of ball-milling. Then, the obtained powders were uniaxially pressed to form pellets and subsequently sintered at  $700^\circ\text{C}$ ,  $800^\circ\text{C}$  and  $900^\circ\text{C}$  for two hours. The family of the composites with different molar ratio of  $\text{Li}_{2.9}\text{B}_{0.9}\text{S}_{0.1}\text{O}_{3.1}$  to LTP varying from 0.1 to 0.3 was obtained. The final ceramic composites were characterized X-ray diffractometry (XRD), thermogravimetry (TGA), scanning electron microscopy (SEM) and density methods. Electric properties in the  $30\text{--}100^\circ\text{C}$  temperature range were

investigated by means of impedance spectroscopy (IS) method. For electric measurements, both bases of the as-form pellets were, at first, polished and then covered with graphite as electrodes.

## RESULTS AND DISCUSSION

The XRD investigation revealed that the sintering of the LTP-LBSO mixed powders at the temperatures above  $700^\circ\text{C}$  resulted in formation of the additional, new crystalline phase identified as  $\text{LiTiPO}_5$ . Thermal investigations by means of thermogravimetry method show ca. 2% mass loss for every presented composites associated with the moisture adsorbed on the surface of the grains. Studies on the microstructure of the presented composites reveal densification of the materials during heat treatment process. Values of total ionic conductivity at room temperature for the most of LTP-LBSO ceramic composites were ca.  $10^{-4} \text{ S}\cdot\text{cm}^{-1}$ . The study revealed that although the sintering itself had a significant impact on enhancement of total ion conductivity, the magnitude of this enhancement always was the same regardless sintering temperature within the range of  $700\text{--}900^\circ\text{C}$ .

## CONCLUSIONS

The  $\text{LiTi}_2(\text{PO}_4)_3$  based ceramic composites containing 0.1–0.3 mol% of  $\text{Li}_{2.9}\text{B}_{0.9}\text{S}_{0.1}\text{O}_{3.1}$  were prepared in a form of pellets. The composites demonstrated very high total ionic conductivity at room temperature, ca. four orders of magnitude higher compared to the LTP. Such enhancement could be related to the densification process providing better connection of the neighboring grains and in result of the reduction of grain boundary resistance.

## REFERENCES

- [1] H. Aono, E. Sugimoto, Y. Sadaoka, N. Imanaka, G. Adachi, *Solid State Ionics* 47 (1991), 257–264

# Electrochemical performance of LiVPO<sub>4</sub>F prepared by microwave radiation heating

Wioleta Ślubowska\*, Konrad Kwatek, Jan L. Nowiński

Warsaw University of Technology, Faculty of Physics, 00-662 Warsaw

e-mail: slubowska@if.pw.edu.pl

Keywords: Li-ion batteries (LIB), cathode, lithium vanadium fluorophosphate, microwave reduction;

## INTRODUCTION

Lithium vanadium fluorophosphate LiVPO<sub>4</sub>F is considered as an attractive cathode material for lithium-ion batteries because of a high theoretical capacity of 156mAh/g [1], an improved voltage profile and a higher discharge voltage of 4.2V vs Li<sup>+</sup>/Li<sup>0</sup> in comparison to the commonly used LiCoO<sub>2</sub>. Additionally, LiVPO<sub>4</sub>F exhibits the excellent lattice stability upon repeated Li<sup>+</sup> extraction/insertion reactions due to the presence of stable V–F bonds in the crystalline structure.

A number of experimental methods have been developed in order to obtain LiVPO<sub>4</sub>F, e.g. two-step solid state reaction [2] or sol-gel method [3]. As these methods have their drawbacks: complexity, time, energy consumption, in this study we propose a novel preparation route, the carbothermal reduction (CTR) stimulated by microwave radiation heating.

## EXPERIMENTAL

The LiVPO<sub>4</sub>F was synthesized using a two-step method. First, VPO<sub>4</sub> precursor was prepared from: V<sub>2</sub>O<sub>5</sub> (≥99.6%, Sigma-Aldrich), NH<sub>4</sub>H<sub>2</sub>PO<sub>4</sub> (≥99.9%, POCH) and one of the two reducing agents – citric acid (C<sub>6</sub>H<sub>8</sub>O<sub>7</sub>·H<sub>2</sub>O, ≥99%, POCH) or oxalic acid (C<sub>2</sub>H<sub>2</sub>O<sub>4</sub>·2H<sub>2</sub>O, ≥99%, WARCHEM). Stoichiometric amounts of reagents were ground with a mortar and pestle and pressed into pellets. The obtained pellets were placed in alumina crucibles and covered with the graphite powder. The synthesis was carried out for 8min in a microwave oven operating at the nominal power of 800W. Next, the synthesis procedure was repeated for the pelletized stoichiometric mixture of LiF (≥99%, Sigma-Aldrich) and VPO<sub>4</sub> in order to obtain the final product.

The VPO<sub>4</sub> and LiVPO<sub>4</sub>F powders were examined by means of scanning electron microscopy (morphology) using Raith e-LINE Plus setup and by means of X-ray diffraction (phase analysis, grain size) using Philips X'Pert Pro diffractometer.

Cathodes for LIBs were prepared by mixing 80 wt% LiVPO<sub>4</sub>F powder, 10 wt% polyvinylidene fluoride (PVDF), and 10 wt% TIMCAL Carbon SuperP in 1-methyl-2-pyrrolidone. The slurry was spread onto Al foil and dried. The electrolyte consisted of LiPF<sub>6</sub> in ethylene carbonate (EC) and diethyl carbonate (DEC). Swagelok type cells were assembled in a glove box using Li foil as the counter electrode. The cells were cycled using a battery tester Arbin BT-2043.

## RESULTS AND DISCUSSION

X-ray diffraction data for the VPO<sub>4</sub> precursor were comparable with those reported elsewhere for the material made by conventional solid-state synthesis

methods [4]. The XRD studies of LiVPO<sub>4</sub>F product confirmed the formation of triclinic structure (space group P-1). Low-intensity lines due to an impurity phase Li<sub>3</sub>V<sub>2</sub>(PO<sub>4</sub>)<sub>3</sub> and residual carbon were also observed.

Charge-discharge cycling of LiVPO<sub>4</sub>F (Fig.1) in the voltage range between 3.0V and 4.4V at a current rate of 7.75mA g<sup>-1</sup> (C/20) after 5 cycles showed a charge capacity of 128mAh g<sup>-1</sup> and a discharge capacity of 84 mAh g<sup>-1</sup>. For a current rate of 15.5mA g<sup>-1</sup> (C/10) after 10 cycles charge capacity achieved the value of 90mAh g<sup>-1</sup> whereas the discharge capacity was of 70mA g<sup>-1</sup>.

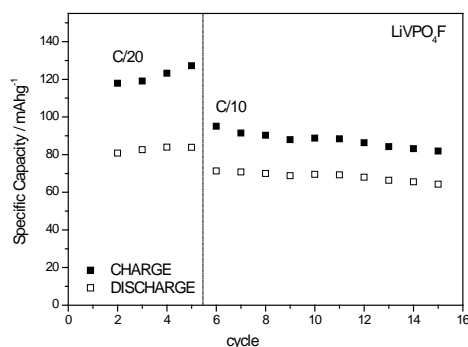


Fig. 1 Capacity vs. cycle number plot for LiVPO<sub>4</sub>F obtained by microwave radiation heating.

Differential capacity vs. voltage profiles (analogous to cyclic voltammetry) exhibited peaks at 4.30V and 4.39V for Li extraction, and 4.12V and 3.95V for Li insertion which were assigned to the V<sup>3+/4+</sup> redox couple.

## CONCLUSIONS

In the present study we show that the LiVPO<sub>4</sub>F cathode material can be obtained by the simplified two-step microwave radiation heating method. Although the method needs to be further optimized in order to obtain the product with improved electrochemical performance, it was proved that it can be considered as a simpler, faster and cheaper alternative for other preparation routes.

## REFERENCES

1. M.V. Reddy, G.V. Subba Rao, B.V.R. Chowdari, J. Power Sources 195 (2010) 5768–5774,
2. J. Barker, M.Y. Saidi, J.L. Swoyer, J. Electrochem. Soc. 150 (2003) A1394–A1398,
3. Y. Li, Z. Zhou, X.P. Gao, J. Yan, J. Power Sources 160 (2006) 633–637,
4. E.J. Baran, J. Mater. Sci. 33 (1998) 2479.

# Bio-derived and hierarchically arranged carbons for high-performance lithium-ion batteries and supercapacitors

*M. Bakierska<sup>1,\*</sup>, J. Świder<sup>1</sup>, M. Gajewska<sup>2</sup> and M. Molenda<sup>1,\*\*</sup>*

<sup>1</sup> Jagiellonian University, Faculty of Chemistry, Ingardena 3, 30-060 Krakow, Poland

<sup>2</sup> AGH University of Science and Technology, Academic Centre for Materials and Nanotechnology, Mickiewicza 30, 30-059 Krakow, Poland

\*e-mail: bakierska@chemia.uj.edu.pl; \*\*e-mail: molendam@chemia.uj.edu.pl

Keywords: Li-ion battery, supercapacitor, carbon electrode, starch, electrochemical performance

## INTRODUCTION

Carbon is the most versatile material and due to its highly diverse forms as well as properties plays remarkable role in various applications [1]. In the past decades, carbon materials have attracted huge attention in the field of energy storage because of their outstanding physicochemical properties, such as high conductivity, excellent chemical stability, controllable porosity and high specific surface area [2,3]. The aforementioned advantages cause that carbon is still considered as the dominant electrode material for commercial lithium-ion batteries (LIBs) and supercapacitors (SCs) [4]. Unfortunately, the reserves of commonly used natural graphite and petroleum coke-derived active carbons are limited and nonrenewable [3], thus naturally-derived compounds which will serve as sustainable sources for preparing carbon materials must be explored [5].

Starch, next to the cellulose, chitin and lignin, is one of the most abundant, renewable natural polymers, occurring with a large variation depending on the origin, which exhibit huge potential to derive advanced carbons with desired properties for LIBs and SCs. Low cost and environmental benignity of starch make it even more preferred precursor for the synthesis of sustainable carbon [6].

Herein, we describe hierarchically arranged, nanostructured carbon materials derived from starch and theirs application in two different energy storage systems (LIBs and SCs).

## EXPERIMENTAL

To obtain carbon materials, different types of starch (potato, maize, rice and wheat) were taken as the starting materials. Briefly, starches were dispersed in distilled water with appropriate dilution ratio. Suspensions of starches were placed in a water bath, stirred and heated up to the gelatinization temperature. After 30 min from gelatinization of starch suspension, the obtained product was removed from the water bath. Then, the samples were poured over with ethanol or acetone solution and left for a while in order to replace water trapped inside the pores. After the solvent exchange, the obtained gels were subjected to pyrolysis at a temperature of 700, 800 and 900°C under argon atmosphere (99.999%) for 6 hours.

The chemical composition, structure, porosity and microstructure of the carbons produced in the present work were determined using elemental analysis (EA), X-ray powder diffraction (XRD), nitrogen adsorption-desorption method (N<sub>2</sub>-BET) and scanning electron

microscopy (SEM), respectively. The electrochemical characterization of lithium batteries and supercapacitor cells based on the fabricated carbon electrodes was carried out using the most common techniques in electrochemical study, namely the electrochemical impedance spectroscopy (EIS), cyclic voltammetry (CV) and galvanostatic charge discharge tests (GCDT).

## RESULTS AND DISCUSSION

All the raw materials were successfully processed by gelatinization process that allowed preparation of carbon materials which exhibit hierarchically arranged structure, high specific surface area and highly developed microporosity. The synthesized carbons, when used as electrode materials in LIBs and SCs, exhibited great electrochemical performance.

## CONCLUSIONS

All things considered, the carbon materials obtained from renewable plant polysaccharides represent very attractive materials for electrochemical applications, especially for high-performance LIBs and SCs.

## ACKNOWLEDGMENT

This work is financially supported by National Science Centre – Poland, under research grant no. 2015/19/B/ST8/01077.

## REFERENCES

1. B. Campbell, R. Ionescu, Z. Favors, C.S. Ozkan, M. Ozkan, *Scientific Reports* **5**(2015)1.
2. X. He, H. Yu, L. Fan, M. Yu, M. Zheng, *Materials Letters* **195**(2017)31.
3. Z. Gao, Y. Zhang, N. Song, X. Li, *Materials Research Letters* **5**(2017)69.
4. A.K. Mondal, K. Kretschmer, Y. Zhao, H. Liu, H. Fan, G. Wang, *Microporous and Mesoporous Materials* **246**(2017)72.
5. X. Hao, J. Wang, B. Ding, Y. Wang, Z. Chang, H. Dou, X. Zhang, *Journal of Power Sources* **352**(2017)34.
6. M. Bakierska, M. Molenda, D. Majda, R. Dziembaj, *Procedia Engineering* **98**(2014)14.

# Performance of Li-ion batteries based on modified $\text{LiMn}_2\text{O}_4$ spinel cathode materials and commercial carbon anodes

*M. Bakierska, M. Świętosłowski\* and M. Molenda*

Jagiellonian University, Faculty of Chemistry, Ingardena 3, 30-060 Krakow, Poland

\*e-mail: m.swietoslawski@uj.edu.pl

Keywords: Li-ion battery, cathode material,  $\text{LiMn}_2\text{O}_4$ , carbon anode, electrochemistry

## INTRODUCTION

Among different kinds of cathode materials for lithium-ion batteries (LIBs), lithium manganese oxide spinel ( $\text{LiMn}_2\text{O}_4$ , LMO) is regarded as one of the most promising candidate for large-scale and high-energy applications [1]. The attractiveness of the LMO spinel is associated with good rate capability, high operating voltage, high specific capacity, excellent safety characteristics, low cost owing to a high natural abundance of manganese and significantly lower toxicity compared to other transition metal oxides [2,3]. Unfortunately, due to the solubility of  $\text{Mn}^{3+}$  ions in the liquid electrolyte and unstable crystalline structure of the stoichiometric LMO spinel near room temperature, a severe drop in the capacitance and a deterioration of the cell life occur [4,5]. To overcome the aforementioned obstacles, many efforts have been made so far and through the most widely adopted method is cation and anion doping [6-8]. Our previous studies on spinel materials revealed that modification of the LMO composition with potassium, nickel or sulphur leads to the suppression of the unfavorable phase transition and restrains the capacity loss during subsequent charge and discharge cycles, while performing the cycling tests in relation to lithium electrode.

This work is intended to examine the electrochemical characteristics of LIBs based on modified LMO spinel cathodes and different types of commercial carbon anodes.

## EXPERIMENTAL

Nanosized stoichiometric ( $\text{LiMn}_2\text{O}_4$  – LMO) and substituted spinels ( $\text{Li}_{1-x}\text{K}_x\text{Mn}_2\text{O}_4$  – LKMO,  $\text{LiMn}_{2-y}\text{Ni}_y\text{O}_4$  – LMNO oraz  $\text{LiMn}_2\text{O}_{4-z}\text{S}_z$  – LMOS) were synthesized via a sol-gel method [8]. The syntheses were carried out with an argon flow to prevent oxidation of the  $\text{Mn}^{2+}$  ions. Condensation of the formed soles was performed at 90 °C for 3-4 days, and then obtained xerogels were calcined in air at 300 °C and subsequently at 650 °C. In order to examine the electrochemical performance of the modified spinels vs. commercial carbons, electrochemical impedance spectroscopy (EIS), cyclic voltammetry (CV) and galvanostatic charge/discharge tests (GCDT) were employed using R2032 coin-type cells, assembled in an argon-filled glove box. The cathodes were prepared by mixing 80 wt.% of active material (LMO-based system), 10 wt.% of carbon black (CB) additive and 10 wt.% of polyvinylidene fluoride (PVDF) binder in N-methyl-2-pyrrolidone (NMP). As anodes CMS graphite (95.7% of active material) coated on copper

foil with SBR binder was used. The anodes were purchased from MTI Corporation. An electrolyte was 1M solution of  $\text{LiPF}_6$  in EC:DEC (1:1 v/v).

## RESULTS AND DISCUSSION

The LIBs with LMO-based cathode materials and commercial carbon anodes were successfully tested (at room and elevated temperature) in order to investigate the electrochemical performance of the modified spinels with regard to the commercial CMS graphite.

## CONCLUSIONS

The LMO-based electrodes revealed good electrochemical characteristics relating to the commercial carbonaceous anode materials. The performed studies suggest that the modified spinels obtained by the sol-gel method can undoubtedly be applied in commercial cells. Furthermore, the introduction of these materials into the industrial production will not require any modifications in the commonly used anodes or any other part of Li-ion system.

## ACKNOWLEDGMENT

This work is financially supported by National Centre for Research and Development – Poland, under research grant no. LIDER/463/L-6/14/NCBR/2015.

## REFERENCES

1. L. Duan, X. Zhang, K. Yue, Y. Wu, J. Zhuang, W. Lu, *Nanoscale Research Letters* **12**(2017)1.
2. R. Wang, X. Li, Z. Wang, H. Guo, *Journal of Solid State Electrochemistry* **20**(2016)19.
3. Y. Shilina, B. Ziv, A. Meir, A. Banerjee, S. Ruthstein, S. Luski, D. Aurbach, I.C. Halalay, *Analytical Chemistry* **88**(2016)4440.
4. L. Yang, M. Takahashi, B. Wang, *Electrochimica Acta* **51**(2006)3228.
5. Y. Shin, A. Manthiram, *Journal of Electrochemical Society* **151**(2004)A204.
6. C. Vogler, A. Butz, H. Dittrich, G. Arnold, M. Wohlfahrt-Mehrens, *Journal of Power Sources* **84**(1999)243.
7. L. Xiong, Y. Xu, X. Xiao, J. Wang, Y. Li, *Electronic Materials Letters* **11**(2015)138.
8. M. Molenda, M. Bakierska, D. Majda, M. Świętosłowski, R. Dziembaj, *Solid State Ionics* **272**(2015)127.

# Studies of structural changes induced by lithium extraction from $\text{LiMn}_2\text{O}_{3.99}\text{S}_{0.01}$

M. Lis, M. Świętosławski\* and M. Molenda

Faculty of Chemistry,  
Jagiellonian University, Ingardena 3,  
30-060 Krakow, Poland

\*e-mail: m.swietoslowski@uj.edu.pl

Keywords: delithiation, structural changes,  $\text{LiMn}_2\text{O}_{3.99}\text{S}_{0.01}$ , cathode material, Li- ion batteries

## INTRODUCTION

The rapid development of industry and technology is one of the reasons for the continuously growing worldwide energy demand. Moreover the last decades have seen that there is a need for dynamic progress in the field of energy storage systems. Because of these even the most popular Li-ion technology, which is nowadays prevailing portable energy source, is constantly being optimized by using new, better materials [1].

$\text{LiMn}_2\text{O}_4$  (LMO) is one of the alternative cathode material due to its specific capacity, high operating voltage, low cost and environmentally friendliness. However, stoichiometric spinel is unstable in Li-ion cell. Near room temperature, it is observed a reversible adverse phase transition which is related to Jahn-Teller distortion of high-spin  $\text{Mn}^{3+}$  ions. Furthermore,  $\text{LiMn}_2\text{O}_4$  has limited stability towards organic solvents in liquid electrolytes [2]. One of the possibility to handle these problems is partial substitution of the cationic or the anionic sublattice [3]. In this work, in order to improve structural properties of LMO, sulphur substitution in the oxygen sublattice of lithium manganese oxide spinel was implemented ( $\text{LiMn}_2\text{O}_{3.99}\text{S}_{0.01}$ , LMOS) [4].

It is commonly known that the working principle of Li-ion batteries is based on intercalation/deintercalation processes. These processes greatly influence the structure of the electrode materials and are very important to understand the behaviour of cathode during charge/discharge cycles. That is why the main aim of this research is to investigate the structural properties of delithated  $\text{LiMn}_2\text{O}_{3.99}\text{S}_{0.01}$ .

## EXPERIMENTAL

The spinel materials  $\text{LiMn}_2\text{O}_4$  and  $\text{LiMn}_2\text{O}_{3.99}\text{S}_{0.01}$  were prepared by sol-gel synthesis followed by thermal treatment [5]. Afterwards the lithium extraction from the LMOS was performed by chemical and electrochemical procedures. The results were compared to those obtained for the chemical delithiation of stoichiometric spinel (LMO) under identical experimental conditions.

The chemical delithiation was investigated with various oxidizing agents. The phase purity of the initial materials and the structural changes of the obtained products were verified by X-ray powder diffraction (XRD). Their composition was determined by inductively coupled plasma-optical emission spectrometers (ICP-OES). The particle size and

morphology were analysed by the transmission and scanning electron microscope (TEM/SEM).

The electrochemical lithium extraction was characterized by using *in-situ* X-ray powder diffraction (*in situ*-XRD) to monitor the phase transformation during cycling. The cathode electrode was prepared by mixing 80 wt% of active material with 10 wt% of conductive agent- carbon black and 10 wt% of polyvinylidene fluoride used as binder, in N-methyl-2-pyrrolidone solvent. Further, the Li-ion cell consisted of metallic lithium electrode, as counting and reference electrode, and a 1M commercial solution of  $\text{LiPF}_6$  in a mixed solvents of ethylene carbonate and dimethyl carbonate EC/DEC (50:50 v/v), as electrolyte. Tests were conducted within 3.0- 4.5 V potential range at C/10 rates at room temperature.

## RESULTS, DISCUSSION AND CONCLUSIONS

The pure, crystalline, nanosized  $\text{LiMn}_2\text{O}_4$  as well as  $\text{LiMn}_2\text{O}_{3.99}\text{S}_{0.01}$  materials were obtained. Then the lithium extraction from  $\text{LiMn}_2\text{O}_{3.99}\text{S}_{0.01}$  spinel was successfully performed by chemical and electrochemical methods and the results were compared to delithated  $\text{Li}_{1-x}\text{Mn}_2\text{O}_4$  products. The amount of lithium, that can be extracted, increased with rising the oxidation potential of oxidizing agents. It was found that the difficulties of chemical delithiation occurred in the appropriate choice of oxidizing agent which is strongly dependent on the nature of the pristine material.

The conducted experiments allowed to investigate the structural changes of materials during delithiation process and their nature.

## ACKNOWLEDGMENT

This work is supported by the National Centre for Research and Development (NCBiR), Poland under research Grant No. LIDER/463/L-6/14/NCBR/2015.

## REFERENCES

1. J. M. Tarascon, M. Armand, *Nature* **414**(2001)359
2. J. S. Chen, L. F. Wang, B. J. Fang, S. Y. Lee, R. Z. Guo, *Journal of Power Sources* **157**(2006)515
3. W. Wen, B. Ju, X. Wang, C. Wu, H. Shu, X. Yang, *Electrochimica Acta* **147**(2014)271
4. M. Molenda, R. Dziembaj, E. Podstawka, W. Łasocha, L. M. Proniewicz, *Journal of Physics and Chemistry of Solids* **67**(2006)1347
5. M. Molenda, M. Bakierska, D. Majda, M. Świętosławski, R. Dziembaj, *Solid State Ionics* **272**(2015)127

# Studies of temperature effect on electrochemical performance of CCL/LiFePO<sub>4</sub> nanocomposites with commercial anode

R. Knura, J. Świder, M. Molenda\*

Faculty of Chemistry  
Jagiellonian University, ul. Ingardena 3  
30-060 Krakow, Poland  
e-mail: molendam@chemia.uj.edu.pl

Keywords: conductive carbon layer (CCL), graphite, LiFePO<sub>4</sub>, nanocomposite, Li-ion batteries.

## INTRODUCTION

Since the solution of its poor electronic conductivity and low ionic diffusion coefficient issues, lithium iron phosphate (LiFePO<sub>4</sub>) has become a desired cathode material for lithium ion batteries. This is due to its advantages over other cathode materials, in particular its low cost and abundance of components, nontoxicity and reasonable energy density (above 500 Wh/kg) along with high thermal and chemical stability<sup>1,2,3</sup>. Main applications of lithium-ion batteries based on LiFePO<sub>4</sub> are the power supply of numerous types of electrical devices, such as power tools, hybrid electric vehicles (HEVs) as well as electric vehicles (EVs), and providing capacity for grid energy storage<sup>2,3,4</sup>. While stationary and steady exploitation allow optimal working conditions, maximizing the battery efficiency and high power, outdoor usage of devices may change the overall battery efficiency due to, e.g. harsh work conditions or elevated resting temperatures<sup>5</sup>. Such circumstances may occur, for example, while using power tools, driving or parking electric vehicles in hot weather conditions without proper cooling. The aim of this work is to study the temperature effect on electrochemical performance of cells consisting of commercially available materials in relation to solution based on active material coated by conductive carbon layers (CCL)<sup>6</sup>.

## EXPERIMENTAL

In order to compare proposed CCL/LiFePO<sub>4</sub> nanocomposite with commercially available electrode materials, as cathodes were used aluminum foil coated by LiFePO<sub>4</sub> (MTI Corporation), cathode prepared from LiFePO<sub>4</sub> powder (Pulead Technology Industry Co., Ltd) As an anode copper foil coated by MCMB (mesocarbon microbeads) graphite powder (MTI Corporation) was used. The solution of 1M lithium hexafluorophosphate (LiPF<sub>6</sub>) dissolved in EC/DEC=50/50 (v/v) was used as an electrolyte. Electrochemical tests were performed on R2032 coin cells. Performed cell analysis includes cyclic voltammetry (CV), cell charge/discharge tests at various temperatures and currents along with cell potential vs. capacity measurements in order to determine actual capacity, coulombic efficiency and charge/discharge potential curves of cells at different working conditions.

## RESULTS AND DISCUSSION

Results obtained from charge/discharge tests performed on cells assembled from commercially

available anode and CCL/LiFePO<sub>4</sub> nanocomposite show useful range of potential plateau, cyclability, as well as sufficient capacity and coulombic efficiency for power applications. Temperatures elevated to some extent do not cause any significant deterioration of cell performance, nor any hazardous cell behavior was observed (e.g. rapid cell performance deterioration due to short-circuiting) because of thermal and chemical stability of materials. This partially confirms possibility of commercial usage of CCL/LiFePO<sub>4</sub> as cathode material with graphite anode for some applications that require high level of safety, average level of energy density and resistance to harsh work conditions.

## CONCLUSIONS

Obtained cell characteristics can be useful in comparing information regarding cell performance of novel types of CCL/LiFePO<sub>4</sub> nanocomposite with already existing and commercially available materials. Results, concerning reversible capacities at various temperatures and currents, are sufficient for some aforementioned applications, nevertheless further studies are necessary to obtain more efficient, safer and affordable materials based on lithium iron phosphate that will allow to work with reversible capacities as close to its theoretical value (170 mAh/g)<sup>1,2,3</sup>. Such solution would have a tremendous impact on various industries, including automotive and energetic industries, as well as on environment protection.

## ACKNOWLEDGMENT

This work is supported by National Science Centre, Poland under research grant no. 2014/13/B/ST5/04531.

## REFERENCES

1. S. Franger *et al.*, *J. Power Source*. **119-121** (2003) 252
2. C.M. Julien *et al.* *Inorganics* **2** (2014) 132
3. D. Andre *et al.* *J. Mater. Chem. A* **3** (2015) 6709
4. B. Dunn *et al.* *Science* **334** (2011) 928
5. A. Eddahech *et al.* *Energy* **84** (2015) 542
6. M. Molenda, R. Dziembaj, A. Kochanowski, E. Bortel, M. Drozdek, Z. Piwowarska Pat. PL 216549 B1 (2014); Pat. US 8,846,135 B2 (2014); Pat. JP 5476383 B2 (2014); Pat. KR 10-2011-7004142 (2015), Pat. EP 2326745 A2 (2017)



# Determination of physicochemical and electrochemical parameters of silicon-based electrode as an anode in lithium-ion battery

**B. Hamankiewicz<sup>1</sup>, M. Ratyński<sup>1</sup>, Z. Rogulski<sup>1,2</sup> and A. Czerwiński<sup>1,3</sup>**

<sup>1</sup>Faculty of Chemistry, University of Warsaw, ul. Pasteura 1, 02-093 Warsaw, Poland

<sup>2</sup>Biological and Chemical Research Centre, University of Warsaw, ul. Żwirki i Wigury 101, 02-093 Warsaw, Poland

<sup>3</sup>Industrial Chemistry Research Institute, ul. Rydygiera 8, 01-793 Warsaw, Poland

e-mail: bhamankiewicz@chem.uw.edu.pl

Keywords: lithium-ion battery, silicone anode, electrochemistry

## INTRODUCTION

Nowadays the used carbonaceous materials in state-of-the-art lithium-ion batteries are able to store up to one lithium ion per 6 carbon atoms in the case of fully crystalline graphite. That results in a rather low specific capacity of 372 Ah/kg. The application of metals or metalloids, which are able to store lithium under formation of an intermetallic phase, represents a very promising alternative. Especially silicon is able to store up to 4.4 lithium ions per silicon atom, which results in a specific capacity of 4199 Ah/kg. The main challenges associated with silicon anodes are structural degradation and instability of the solid electrolyte interphase (SEI) caused by the large volume change (~300 %) during cycling, the occurrence of side reactions with the electrolyte and the low volumetric capacity when the material size is reduced to a nanometric-scale. Up to now, many strategies to overcome these problems have been applied [1], although most of them are not compatible with industrial practices and therefore not easily and cost effective integrated in production lines.

In our studies we present a physicochemical and electrochemical properties of silicon-based electrode prepared in large scale production line by Varta Microbattery GMBH. Determined parameters will be than used for construction of an electrochemical model to investigate the voltage response of the cell, which subsequently will facilitate the prediction of capacity-power loss and life-time.

## EXPERIMENTAL

Examined silicon-based electrodes have been prepared and received from Varta Microbattery GMBH. Structural and morphological properties of the samples have been examined by several techniques: TEM, SEM, BET, XPS and SIMS. A wide range of electrochemical techniques (cyclic voltammetry, potentiometry, galvanostatic and potentiostatic intermittent titration technique, impedance spectroscopy, galvanostatic charge-discharge tests) have been employed in order to examine the main electrochemical processes during oxidation and reduction of silicon-based electrodes and to determine thermodynamic and kinetic parameters of lithium intercalation.

## RESULTS AND DISCUSSION

The results show that prepared electrodes consist of mainly graphite (ca. 66% wt.) and 3M silicon alloy (ca. 25% wt.) as an active materials, 7% wt. of binder and 2% wt. of conductive additive. Average active

layer thickness and mass density (38  $\mu\text{m}$ , 5,5  $\text{mg}/\text{cm}^2$  respectively) was in acceptable range for high specific energy electrodes. The specific capacity of the electrodes determined from galvanostatic charge-discharge tests was ca. 470 mAh/g at 0,2 C current rate (110 mA/g). For initial cycles capacity fade has been observed and subsequent capacity increase in further cycles. This behaviour is probably caused by initial blocking of  $\text{Li}^+$  ion diffusion patch in active layer (cycles 1-4) and poor ion conductivity of  $\text{SiO}_2$  layer on the surface of silicon grains. After 4 cycles of expanding and shrinking of the material the silica layer is damaged, thus allowing for easier ion penetration inside silicon grains.

In subsequent cycles a linear drop of capacity has been observed with capacity fade of 2,6 mAh/cycle. Coulombic efficiency, which is defined as charging and discharging specific capacity ratio, very quickly reach value above 99% at cycle 4<sup>th</sup> and maximum value of 99.8% after 20 cycles. This indicates that no new SEI layer is formed during cycling, with is surprisingly in conflict with the observation of electrode degradation (capacity fade).

From the initial scans of CV measurements it can be concluded that there are 3 main oxidation peaks – two correspond to lithium deintercalation from graphite (0,2 and 0,3 V vs.  $\text{Li}/\text{Li}^+$ ) and one from silicon alloy (0,5 V). Deconvolution of these peaks by Breit-Wigner-Fano asymmetric line fitting allow to determine the lithium diffusion coefficient both in graphite and silicon material in one experiment. The results indicate that lithium mobility is higher in silicon matrix.

## CONCLUSIONS

Due to a complex nature of composite electrode determination of its electrochemical properties is non-trivial task. Based on careful analysis of cell voltage response it is possible to distinguish between lithium intercalation in graphite and silicon matrix host.

## ACKNOWLEDGMENT



This project has received funding from the European Union's Horizon 2020 research and innovation programme under grant agreement No 685716.

## REFERENCES

1. H. Wu, G. Yu, L. Pan, N. Liu, M.T. McDowell, Z. Bao, Y. Cui., *Nature Communications* **4**:1943 (2013)

# Structural, morphological and electrochemical properties of $\text{Li}_2\text{MnSiO}_4$ composites

*M. Krajewski<sup>1,\*</sup>, M. Boczar<sup>1</sup>, B. Hamankiewicz<sup>1</sup> and A. Czerwinski<sup>1,2</sup>*

<sup>1</sup>Faculty of Chemistry, University of Warsaw, Pasteura 1, 02-093 Warsaw, Poland

<sup>2</sup>Industrial Chemistry Research Institute, Rydygiera 8, 01-793 Warsaw, Poland

\*e-mail: mkrajewski@chem.uw.edu.pl

Keywords: lithium-manganese orthosilicate, doping, surface modification, lithium-ion battery

## INTRODUCTION

Research in lithium-ion battery field is constantly growing since the first commercialization of graphite-lithium-cobalt oxide system by SONY in early 90's [1]. A lot of attention were put into developing a new cathode materials with high stability and high capacities. Recently, a new type of cathode materials are emerging, as potential high-capacity compounds capable of insertion/extraction of more than one lithium ion per formula unit [2]. One of them is lithium-manganese orthosilicate ( $\text{Li}_2\text{MnSiO}_4$ , LMS), showing a high theoretical specific capacity of ca.  $333 \text{ mAh}\cdot\text{g}^{-1}$  due to involvement of both  $\text{Mn}^{4+}/\text{Mn}^{3+}$  and  $\text{Mn}^{3+}/\text{Mn}^{2+}$  redox couples in electrochemical processes [2]. However, up to date there were no significant reports about obtaining a electrochemically stable LMS compounds which could reversibly exchange more than one lithium ion per formula unit in room temperature. The reasons behind poor electrochemical performance of  $\text{Li}_2\text{MnSiO}_4$  powders are its low conductivity (ca.  $10^{-16} \text{ S}\cdot\text{cm}^{-1}$ ) and structural instability [2, 3].

In this work, we propose doping lithium-manganese orthosilicate with  $\text{Al}^{3+}$  ions at  $\text{Si}^{4+}$  sites, which introduces extra charge carries and  $\text{Li}^+$  ions into the LMS structure, enhancing its conductivity and, due to extra lithium ions present in the system, possibility of involving more than one  $\text{Li}^+$  ion in electrochemical reactions. Moreover,  $\text{Li}_2\text{MnSiO}_4$  powders were also modified by silver nanoparticles, which would further improve LMS conductivity and its electrochemically active surface area [4].

## EXPERIMENTAL

$\text{Li}_{2-x}\text{MnSi}_{1-x}\text{Al}_x\text{O}_4$  powders were synthesized by a modified sol-gel method, with  $\text{CH}_3\text{COOLi}$ ,  $(\text{CH}_3\text{COO})_2\text{Mn}$  and tetraethyl orthosilicate (TEOS) as Li, Mn and Si sources, respectively. Different substrates for Al substitution were used, namely  $\text{Al}_2\text{O}_3$ ,  $(\text{CH}_3\text{COO})_2\text{AlOH}$  and  $\text{Al}(\text{NO}_3)_3$ .

The Ag-modified samples were prepared by a low temperature technique [5] with  $\text{AgNO}_3$  as an Ag source. The prepared powders were subject to structural and morphological analysis by XRD, SEM, TEM and  $\text{N}_2$  adsorption/desorption techniques. Electrochemical measurements were carried out in three-electrode Swagelok® systems, with Li metal as counter and reference electrodes and LMS:Vulcan XC72R:PVdF (8:1:1 wt.) as working electrode. LMS electrodes were analysed by CP, CV and EIS electrochemical methods.

## RESULTS AND DISCUSSION

$\text{N}_2$  adsorption/desorption analysis showed, that after Al substitution ( $x=0.1$ ), while using  $\text{Al}_2\text{O}_3$  as aluminum source, BET surface area was reduced from  $40.19 \pm$

$0.05$  to  $13.49 \pm 0.05 \text{ m}^2\cdot\text{g}^{-1}$  for pristine and Al-doped LMS, respectively. Moreover, average grain size calculated from  $\text{N}_2$  adsorption/desorption experiment increased from 37 to 111 nm for pristine and Al-doped LMS, respectively. This effect can be related to insolubility of  $\text{Al}_2\text{O}_3$  in the reaction media, which can lead to insufficient doping of  $\text{Li}_2\text{MnSiO}_4$  structure. In the case of Ag-modified samples BET surface area and average grain size remained unchanged after the surface modification process. Galvanostatic charge/discharge experiments revealed, that after Al-doping process (with  $\text{Al}_2\text{O}_3$ ), the specific capacity of LMS material decreased, from  $94.0 \pm 2.0$  to  $39.9 \pm 1.4 \text{ mAh}\cdot\text{g}^{-1}$  during 1<sup>st</sup> discharge for pristine and Al-doped LMS, respectively. It can be related to insufficient doping of LMS matrix, which resulted in a presence of non-electrochemically active mass in prepared powders. In the case of Ag-modified  $\text{Li}_2\text{MnSiO}_4$ , the specific capacity of LMS powder increased, from  $101.4 \pm 0.2$  to  $120.8 \pm 6.5 \text{ mAh}\cdot\text{g}^{-1}$  during 1<sup>st</sup> discharge for pristine and Ag-modified LMS, respectively. Increased capacity is a result of enhanced conductivity and electrochemically active surface area of lithium-manganese orthosilicate.

## CONCLUSIONS

Surface modification of  $\text{Li}_2\text{MnSiO}_4$  with highly conductive media can be an efficient way of improving its electrochemical properties. However, further studies must be employed to find a stable and cheap surface modification to fully enhance LMS material in lithium-ion batteries. Al-doping of lithium-manganese orthosilicate is still under development, with a high chances of succeeding in improving the electrochemical performance of  $\text{Li}_2\text{MnSiO}_4$  powders.

## ACKNOWLEDGMENT

This work is supported by Polish National Centre of Science under grant UMO-2014/15/B/ST5/02118.

## REFERENCES

1. T. Nagura, K. Tazawa, *Progress in Batteries and Solar Cells* **9** (1990) 209-217.
2. R. Dominko, *Journal of Power Sources* **184** (2008) 462-468
3. R. Dominko, M. Bele, A. Kokalj, M. Gaberscek, J. Jamnik, *Journal of Power Sources* **174** (2007) 457-461.
4. M. Krajewski, B. Hamankiewicz, A. Czerwinski, *Electrochimica Acta* **219** (2016) 277-283.
5. M. Krajewski, M. Michalska, B. Hamankiewicz, D. Ziolkowska, K.P. Korona, J.B. Jasinski, M. Kaminska, L. Lipinska, A. Czerwinski, *Journal of Power Sources* **245** (2014) 764-771.

# Na<sub>0.4</sub>MnO<sub>2</sub>/C composites as cathode materials for Na-ion batteries

*M. Przybylczak, K. Wasiński,\* P. Pótrolniczak and M. Walkowiak*

Institute of Non-Ferrous Metals, Division in Poznań  
Central Laboratory of Batteries and Cells, ul. Forteczna 12  
61-362 Poznań, Poland

e-mail: krzysztof.wasinski@claio.poznan.pl

Keywords: Na-ion batteries, cathode, half-cell, composites

## INTRODUCTION

Recently, the sodium-ion (Na-ion) systems are introduced as an alternative to lithium-ion batteries developed in early 90'. The sodium-ion primary batteries (NIBs) are promising and inexpensive new class of insertion based energy storage systems. Now these new designed chemical power sources offer longer life-times and higher energy densities. NIB technology is safe and has potential application in grid energy storage.

As an important component of Na-ion battery, a variety of anode materials have been proposed such as: hard carbons [1] and group 14 or 15 metal alloys [2]. Transition metal mixed oxides have been described several times as cathode active material for NIBs [3]. This materials with general formula Na<sub>x</sub>MeO<sub>2</sub> offer low cost and simple preparation synthesis methods [4,5]. Now the continuous improvement in relationship between structure and electrochemical performance, kinetic aspects and working potentials are still required. In this work we decided to improve cathode maximum current densities by using sodium-manganese composites with some carbon materials.

## EXPERIMENTAL

The Na-ion cathode active material (sodium-manganese mixed oxide - Na<sub>0.4</sub>MnO<sub>2</sub>) was synthesized using Mn<sub>2</sub>O<sub>3</sub> and Na<sub>2</sub>CO<sub>3</sub> in one-step solid state reaction. This process was performed at 800°C in air atmosphere. The Na<sub>0.4</sub>MnO<sub>2</sub> was mixed with one carbon material (C): multi-walled carbon nanotubes (MWCNTs) or reduced graphene oxide (rGO) or acetylene black (AB). Then this mixtures were ball milled. After milling the obtained composites were dried at 105°C in vacuum dryer. The crystallographic phase of Na<sub>0.4</sub>MnO<sub>2</sub>/C composite was characterized by powder X-ray diffraction Analysis was performed by using X'Pert PANalytical diffractometer in the 2θ range of 5° - 100°. The composition and arrangement of the particles were characterized by scanning and transmission electron microscopy using Zeiss EVO 40 (SEM) and JOEL JEM 1200 EX (TEM) instruments. The Na to Mn stoichiometric ratio of the composites were determined by inductively coupled plasma optical emission spectroscopy (ICP-OES) using Agilent 7000 apparatus. Finally, the carbon concentration in samples was checked by elemental analysis.

The electrochemical characterization was conducted in two-electrode electrochemical Swagelok®-type cells. Electrochemically active material Na<sub>0.4</sub>MnO<sub>2</sub>/C (90 wt %) and poly(vinylidene fluoride-co-

hexafluoropropylene) (10 wt %) were mixed with NMP in agate mortar. The resultant slurry was spread uniformly on aluminium foils, followed by drying at 60°C for 4h and at 105°C under vacuum for 20 h. The coated aluminium foils were used as the working electrodes in half-cells mounted in argon-filled glove box (MBraun, Germany, O<sub>2</sub> <0.5ppm, H<sub>2</sub>O <0.5ppm). The counter sodium electrodes were prepared by pressing sodium on copper foils as the current collector. The Celgard® 2400 as separators, and 1 M NaClO<sub>4</sub> in propylene carbonate (PC) solution as electrolyte were used. The cells were tested at various current densities and scan rates using a VMP-3 (Biologic, France) multichannel test instrument with voltage window of 2.0 – 4.0 V (vs. Na/Na<sup>+</sup>) at room temperature.

## RESULTS AND DISCUSSION

The ball milling method provides to obtain Na<sub>0.4</sub>MnO<sub>2</sub>/AB, Na<sub>0.4</sub>MnO<sub>2</sub>/MWCNT and Na<sub>0.4</sub>MnO<sub>2</sub>/rGO composites. All physicochemical characterization results clearly confirm that predicted phases were obtained. The preliminary electrochemical measurements of composites showed that in terms of capacities this materials are promising for NIBs systems.

## CONCLUSIONS

This work presents comparison of data concerning prolonged charge/discharge experiments in half-cells at wide range of current densities. We hope that our work will help to achieve higher densities sodium-ion primary batteries.

## ACKNOWLEDGMENT

This work is supported by Ministry of Science and Higher Education - statutory activity, decision number: 3787/E-138/S/2017.

## REFERENCES

1. S.Komaba, W.Murata, T. Ishikawa, N.Yabuuchi, T. Ozeki, T.Nakayama, A.Ogata, K.Gotoh, K.Fujiwara, Advanced Functional Materials21(2011)3859
2. M.H.Han, E.Gonzalo, G.Singh, T.Rojo, Energy and Environmental Science 8(2015)81-102
3. Xiang, X., Zhang, K., Chen, J. Advanced Materials27(2015)5343
4. R.J.Clément, P.G.Bruce, C.P.Grey, Journal of the Electrochemical Society 162(2015)2589
5. P.Barpanda, Chemistry of Materials28(2016)1006

# Influence of vacancy defects and alloying on electronic properties of $\text{Li}_x\text{Co}_{1-y-z}\text{Ni}_y\text{Mn}_z\text{O}_2$ from band structure calculations

*M. Rybski, S. Kaprzyk, J. Molenda\*, J. Tobola*

Faculty of Physics and Applied Computer Science,  
\*Department of Hydrogen Energy, Faculty of Energy and Fuels  
AGH University of Science and Technology, Mickiewicza 30, 30-059 Krakow, Poland  
e-mail: rybski@fis.agh.edu.pl

Keywords: Li-ion batteries, electronic band structure, KKR-CPA

## INTRODUCTION

Lithium-ion battery materials are still considered to be the most promising energy converter, due to excellent electrochemical parameters. Their industrial applications, especially for power electronic devices are extremely high and important. Moreover, outstanding commercial success of Li-ion cathode materials based on lithium cobaltate ( $\text{LiCoO}_2$ ) caused that they became materials for personal use. That, together with the technological transformation of daily life demand constantly better and better material parameters such as high energy density, long life-cycle, light-weight, safety.

In recent years, in order to have a deeper insight into electrochemical properties of Li-ion and other battery cathode materials, theoretical investigations using quantum electrodynamics based methods, including electronic structure calculations, have been undertaken in systematic way. Quite recently, the step-like vs. continuous-like character of the discharge curve have been interpreted in terms of close correlations between electronic structure and electrochemical properties in selected Na- and Li-ion cathode materials, respectively. Moreover, the particular impact of electronic structure features on the discharge curve in the series of alloys as  $\text{A}_x\text{MO}_2$  ( $\text{A}=\text{Li}, \text{Na}, \text{M}=\text{Mn}, \text{Co}, \text{Ni}$ ) have been recently notified based on detailed experimental and theoretical investigations [1, 2]. In this work, the results of electronic structure computations together with the analysis of crystal stability based on the total energy analysis are presented for a novel variant of the well-known Li-ion cathode material  $\text{Li}_x\text{Co}_{1-y-z}\text{Ni}_y\text{Mn}_z\text{O}_2$ .

## THEORETICAL DETAILS AND DISCUSSION

Electronic structure calculations of  $\text{Li}_x\text{Co}_{1-y-z}\text{Ni}_y\text{Mn}_z\text{O}_2$  were performed for different Li ( $0 \leq x \leq 1$ ) and Co-Ni-Mn concentrations, starting with the well-known  $\text{Li}_x\text{CoO}_2$  material with the use of the first principles technique allowing to account for chemical disorder. To obtain such results, the Korringa-Kohn-Rostoker (KKR) combined with the coherent potential approximation (CPA) [3,4] was employed, which allows to consider fully disordered model and to keep the symmetry of the unit cell unchanged for all alloy compositions. Chemical disorder such as Li vacancy defects and Co/Ni/Mn alloying was accounted for the KKR-CPA calculations, which resulted in evolution of total-, site-decomposed and  $l$ -decomposed density of states in the whole range of Li contents and alloy compositions. It was found that electronic structure of

$\text{Li}_x\text{Co}_{1-y-z}\text{Ni}_y\text{Mn}_z\text{O}_2$  exhibits semiconducting-like, half-metallic-like or metallic-like properties depending on Li content as well as relative concentrations of transition metal elements (Co, Ni and Mn).

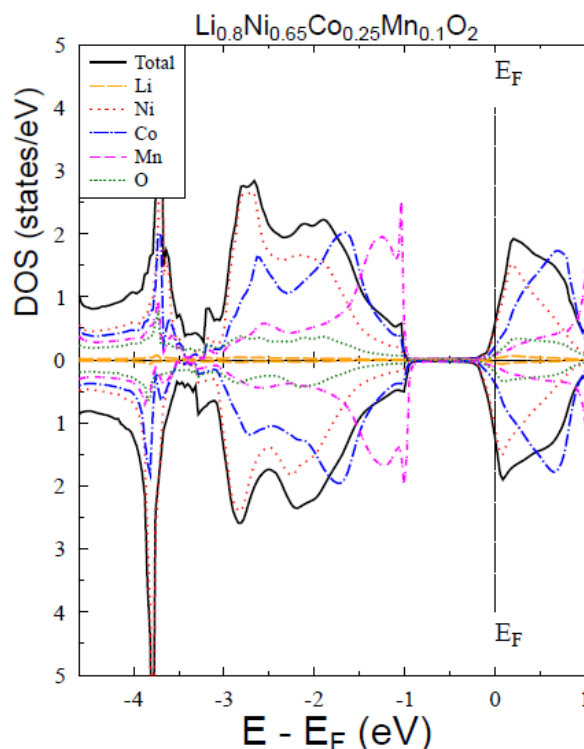


Fig 1: KKR-CPA total and site-decomposed density of states in  $\text{Li}_{0.8}\text{Ni}_{0.65}\text{Co}_{0.25}\text{Mn}_{0.1}\text{O}_2$ .

Moreover, the magnetic moments are found for selected compositions as resulted from spin-polarised KKR-CPA computations, which affect the overall DOS shape near EF. Finally, the correlations between electronic structure of  $\text{Li}_x\text{Co}_{1-y-z}\text{Ni}_y\text{Mn}_z\text{O}_2$  and its electrochemical properties are discussed. at wide range of current densities. We hope that our work will help to achieve higher densities sodium-ion primary batteries.

## REFERENCES

- [1] J. Molenda, D. Baster, M. Molenda, K. Świerczek, J. Tobola, *Phys. Chem. Chem. Phys.*, 16 (2014) 14845.
- [2] A. Milewska K. Świerczek, J. Tobola, F. Boudoire, Y.Hu, D.K. Bora, B.S. Mun, A. Braun, J. Molenda, *Sol. St. Ionics*, 263 (2014) 110.
- [3] A. Bansil, S. Kaprzyk, P. E. Mijnaerends, J. Tobola, *Condens. Matter Mater. Phys.*, 1999, 60, 13396.
- [4] T. Stopa, S. Kaprzyk, J. Tobola, *Phys. Condens. Matter*, 2004, 16, 4921.

# Composites based on silicon oxycarbide and carbon nanoparticles as anode materials for lithium-ion cells

*M. Wilamowska-Zawłocka\*, M. Kujawa, A. Dettlaff, E. Klugmann-Radziemska*

Gdansk University of Technology, Faculty of Chemistry,

Narutowicza 11/12, 80-233 Gdańsk, Poland

\*e-mail: monika.wilamowska@pg.gda.pl

Keywords: Lithium-Ion Batteries, Silicon Oxycarbide, Composites, Anodes

## INTRODUCTION

Polymer-derived ceramics have been widely studied as anode materials for lithium-ion batteries [1-6]. Silicon oxycarbides (SiOCs) containing high amount of free carbon within their structure display high reversible capacities of 500 – 650 mAh g<sup>-1</sup> [1-3]. Carbon phase may be incorporated in ceramic matrix by organic functional groups attached to preceramic polymer and/or as an additional carbon source (e.g. natural organic polymer, graphite, hard carbons, carbon nanotubes, graphene, divinylbenzene etc.) [5,6].

In this work we use graphene oxide (GOx) and carbon nanotubes (CNTs) as additional carbon sources for preparation of carbon-rich SiOC composite materials.

## EXPERIMENTAL

Preceramic polymers were obtained by sol-gel synthesis using various alkoxy-silanes (e.g. vinyl triethoxysilane VTEOS) and aqueous solution of GOx or CNTs. Prepared polysiloxanes/GOx and polysiloxanes/CNTs gels were pyrolyzed in controlled argon atmosphere at 1000°C giving carbon-rich ceramic composites. Chemical composition and structure of obtained materials were investigated by several techniques (elemental analysis, XRD, Raman spectroscopy, solid state <sup>29</sup>Si MAS NMR). Prepared composites were electrochemically tested as anode materials for Li-ion batteries.

## RESULTS AND DISCUSSION

Incorporation of carbon material during sol-gel synthesis leads to homogenous distribution of free carbon phase in final ceramic product. Graphene oxide is reduced during pyrolysis creating well conducting paths inside ceramic matrix. Elemental analysis confirm an increased fraction of free carbon in the composite samples compared to samples obtained from pure polysiloxanes. Raman spectroscopy measurements reveal that the additional carbon sources in the form of GOx and CNTs influence the structure of free carbon phase in the investigated silicon oxycarbide samples.

Electrochemical studies show high capacity values of carbon-rich composite samples. An example of delithiation capacity as a function of cycle number of investigated SiOC electrodes together with the first lithiation-delithiation curves is shown in Fig. 1.

The electrodes were charged and discharged with the same current density of 186 mAh g<sup>-1</sup>. The shape of first lithiation/delithiation curves is almost identical for both samples. However, the composite sample prepared with graphene oxide (VTEOS/GOx) exhibit

much better stability than the sample prepared from pure polysiloxane (VTEOS).

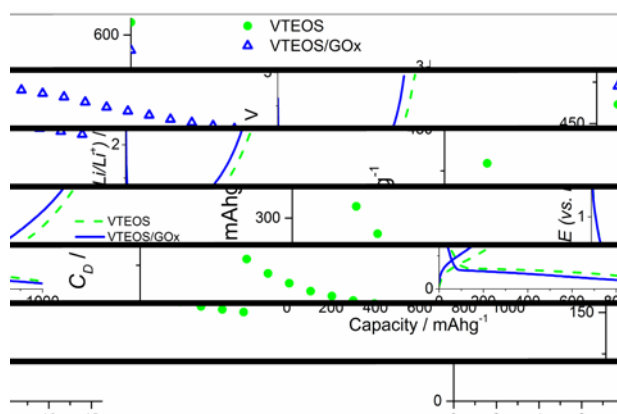


Fig. 1. Delithiation capacity of SiOC samples as a function of cycle number. Inset: first lithiation/delithiation cycle of SiOC electrodes.

## CONCLUSIONS

Sol-gel synthesis is a good method for homogenous incorporation of additional carbon material within polysiloxanes and hence final ceramic product. Carbon-rich silicon oxycarbide composites exhibit improved electrochemical properties compared to SiOC prepared without additional carbon material.

## ACKNOWLEDGMENT

This work is supported by Foundation for Polish Science under grant HOMING PLUS/2012-6/16.

## REFERENCES

1. M. Wilamowska-Zawłocka, P. Puczkarski, Z. Grabowska, J. Kaspar, M. Graczyk-Zajac, R. Riedel, G. D. Soraru, RSC Advances, 6 (2016) 104597-104607.
2. J. Kaspar, M. Graczyk-Zajac, S. Choudhury, R. Riedel, Electrochim. Acta, 216 (2016) 196–202.
3. M. Graczyk-Zajac, L. Reinold, J. Kaspar, P. Sasikumar, G.-D. Soraru, R. Riedel, Nanomaterials. 5 (2015) 233–245.
4. H. Fukui, K. Eguchi, H. Ohsuka, T. Hino, K. Kanamura, J. Power Sources. 243 (2013) 152–158.
5. R. Bhandavat, G. Singh, J. Phys. Chem. C, 117 (2013) 11899–11905.
6. M. Wilamowska, M. Graczyk-Zajac, R. Riedel, J. Power Sources. 244 (2013) 80–86.

# Novel silane-based electrolyte for high energy lithium-sulfur batteries

*P. Pólrolniczak, M. Walkowiak, K. Wasiński*

Institute of Non-Ferrous Metals, Division in Poznań,  
Central Laboratory of Batteries and Cells,  
Forteczna 12 St., 61-362 Poznań, Poland  
e-mail: paulina.polrolniczak@claio.poznan.pl

Keywords: lithium-sulfur batteries, electrolyte, silane, chemical power sources

## INTRODUCTION

It is widely recognized that conventional lithium-based battery technologies have almost reached their technological limits in terms of energy density, therefore there is an urgent need to go beyond the existing solutions, in order to achieve the desired performance targets, that is at least 400 Wh/kg for as far as energy density is concerned [1].

Among various types of prospective rechargeable systems, lithium-sulfur batteries are widely regarded as one of the most promising [2]. Unlike conventional Li-ion systems, Li-S batteries utilize metallic lithium which is characterized by a very high electronegativity and the lowest density among all metals, leading to the highest theoretical specific capacity of 3861 mAh g<sup>-1</sup>. Sulfur, one of the most abundant elements in the earth crust, exhibits a theoretical capacity of 1673 mAh g<sup>-1</sup>, which is an order of magnitude higher than those of the transition-metal oxide cathodes. Thus, Li-S batteries can potentially reach unparalleled gravimetric and volumetric energy densities of 2500 Wh kg<sup>-1</sup> and 2800 Wh L<sup>-1</sup>. Moreover, sulfur is considered to be safer for the user and environment as compared to battery chemistries utilizing highly toxic and expensive heavy metals [3].

Nevertheless, there are still several major issues facing rechargeable Li-S batteries that impede their practical application, which include: low charging efficiency, poor cyclic stability and high self-discharge rate. Disadvantages of Li-S batteries result from a number of reasons. Sulfur has a poor electrical conductivity, and therefore composing the cathode a large amount of conductive additive has to be added, which reduces the amount of sulfur itself and reduces the energy density of the cell. The second major problem is the solubility of lithium polysulfides formed during the electrode reaction in organic electrolytes and their migration towards the anode, wherein further reaction of lithium leads to the formation of insoluble and non-conducting Li<sub>2</sub>S and Li<sub>2</sub>S<sub>2</sub>. These polysulfides are accumulated at the anode causing the corrosion and polarization, and thus reduce the amount of the cathode active material. At the same time the reduction of sulfur and the formation of polysulfides in the lithium electrode is a key reaction in the cell, Li-S [4].

## EXPERIMENTAL

The positive electrodes for the electrochemical tests were prepared by casting the slurry consisting of 70 wt.% elemental sulfur (SigmaAldrich), 20 wt.% carbon black (Timcal) and 10 wt.% binder (sodium carboxymethyl cellulose - SigmaAldrich) onto the aluminium current collector. The cathodes were

assembled in an argon-filled glovebox (MBraun LABstar) in Swagelok-type cells with metallic lithium as the anode and Celgard 2400 as the separator. The electrolyte was a solution of lithium trifluoromethanesulfonate (0.5 M, SigmaAldrich) and of LiNO<sub>3</sub> (0.5 M, Fluka) in a silane-based electrolyte. The cells were galvanostatically charged/discharged at a current density of 0.005, 0.05, 0.1, 0.5 and 1 C between 1.7 and 2.7 V vs. Li/Li<sup>+</sup>. Cyclic voltammetry experiments were carried out at the scan rate of 0.05 mV s<sup>-1</sup> also between 1.7 and 2.7 V. All electrochemical measurements were carried out using multi-channel VMP3 potentiostat/galvanostat (Bio-Logic).

## RESULTS

In our study novel electrolyte based on silanes have been prepared and tested in lithium-sulfur batteries. The motivation of this work was to improve cyclic stability of cells by increasing electrolyte conductivity and reducing sulfur and lithium polysulfides dissolution and redox shuttle mechanism.

Preliminary electrochemical tests of novel electrolyte LiS system show excellent cyclic stability and satisfactory specific capacity of lithium-sulfur battery. This new electrolyte composition is attractive alternative for commonly used in lithium-sulfur batteries ether-based electrolytes.

## ACKNOWLEDGMENT

This work is supported within statutory activity of the Institute of Non-Ferrous Metals Division in Poznań, Central Laboratory of Batteries and Cells no. 3787/E-138/S/2017.

## REFERENCES

1. L. Chen, L.L. Shaw, J. Power Sources 2014, 267, 770.
2. A. Manthiram, Y. Fu, S.-H. Chung, Ch. Zu, Y.S. Su, Chem. Rev. 2014, 114, 11751.
3. S.S. Zhang, J. Power Sources 2013, 231, 153.
4. Z. Yang, J. Zhang, M.C.W. Kintner-Meyer, X. Lu, D. Choi, J.P. Lemmon, J. Liu, Chem. Rev. 2011, 111, 3577.



# A-site composition as a factor tailoring disorder in $\text{La}_{2/3-x}\text{Li}_{3x}\text{TiO}_3$ solid electrolyte

W. Zajac, T. Polczyk, M. Pytel, P. Beer, A. Turek

Faculty of Energy and Fuels  
AGH University of Science and Technology, Al. Mickiewicza 30  
30-059 Kraków, Poland  
e-mail: wojciech.zajac@agh.edu.pl

Keywords: Li-ion conductors, solid-state-batteries, LLTO, perovskites

## INTRODUCTION

Lithium Solid State Batteries are among the extensively investigated paths crossing the limitations of conventional Li-ion batteries in terms of energy density and safety [1]. A key element of any solid state battery is the solid electrolyte, which has to be chemically and electrochemically stable, possess high Li-ion conductivity and low contact resistance at the electrolyte-electrode interfaces [2]. Among safe and chemically stable solid electrolytes,  $\text{La}_{2/3-x}\text{Li}_{3x}\text{TiO}_3$  oxide (LLTO) exhibits one of the highest ionic conductivities, values above 0.1 mS/cm at room temperature were reported [3]. LLTO belongs to a family of P4/mmm tetragonal A-site layer-ordered double perovskites with alternating La-rich and Li-rich layers, restricting mobility of lithium ions to 2-dimensional a-b planes (Fig. 1a). However, among intriguing features of LLTO is its inherent ability to accept large amount of disorder in the sequence of layers, known as stacking faults (Fig. 1b). The aim of this work was to determine factors affecting density of stacking faults and their connection with mobility of lithium ions in the crystal lattice.

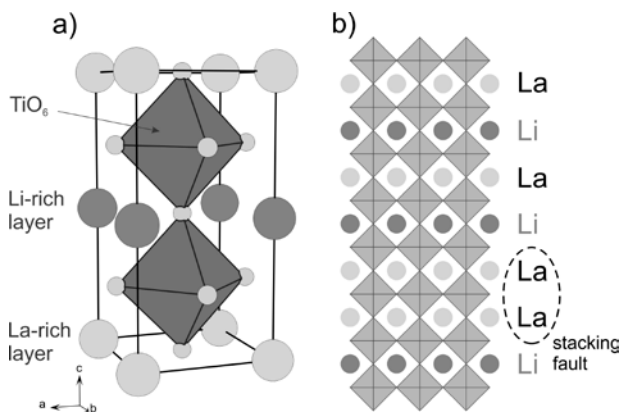


Fig. 1. a) Unit cell of P4/mmm  $\text{La}_{2/3-x}\text{Li}_{3x}\text{TiO}_3$  double perovskite, b) stacking fault scheme.

## EXPERIMENTAL

A series of A-site doped or substituted  $\text{La}_{2/3-x}\text{Li}_{3x}\text{TiO}_3$  oxides was synthesized using high-temperature solid state method. Samples with substitution of  $\text{Ca}^{2+}$ ,  $\text{Sr}^{2+}$ ,  $\text{Ba}^{2+}$ ,  $\text{Pr}^{3+}$  and  $\text{Nd}^{3+}$  in the  $\text{La}^{3+}$  sublattice were prepared. Crystal structure of the obtained samples was analysed using X-ray diffraction technique at room temperature, and as a function of temperature, up to 1100°C, to analyse high temperature order-disorder transition. Rietveld analysis of the diffraction data and modelling of density of stacking-faults were performed

in GSAS-EXPGUI pack of software. Ionic conductivity of the samples was measured from room temperature to 200°C using impedance spectroscopy technique.

## RESULTS AND DISCUSSION

At room temperature slowly cooled materials exhibited P4/mmm tetragonal structure with well-defined layered ordering, as depicted in Fig. 1a. All samples underwent order-disorder transition at heating above 900°C, which resulted in disordered  $\text{Pm}\bar{3}\text{m}$  cubic perovskite structure. Several cooling rates were examined and it was found that disordered-structure samples could be quenched down to room temperature if sufficiently fast cooling was applied, with critical cooling rate determined to be above 70°C/min. Quenching was found to have pronounced impact on the ionic conductivity of the samples leading to considerable improvement of the conductivity. However, high cooling rate can introduce mechanical stress and could result in cracking of brittle ceramic samples. Therefore another path for stabilization was proposed. It turned out that alkaline earth elements substituted for La can play a role of effective stabilizing factors, and that Sr is the most suitable among them. Substitution of other lanthanides at the place of  $\text{La}^{3+}$  ions led to increased ordering and decreased ionic conductivity. The effect of these substitutions on high temperature order-disorder transition is reported and discussed.

## CONCLUSIONS

Careful selection of the A-site composition as well as heat-treatment procedure can affect significantly functional properties of  $\text{La}_{2/3-x}\text{Li}_{3x}\text{TiO}_3$  solid electrolytes. Deeper understanding of relations governing ordering of A-site stacking may help to obtain improved functional properties of the materials.

## ACKNOWLEDGMENT

This work was funded by the National Science Centre Poland under grant no. 2012/05/D/ST5/00472.

## REFERENCES

- [1] E.C. Evarts, *Nature*. **526** (2015) S93–S95.
- [2] W.D. Richards, L.J. Miara, Y. Wang, J.C. Kim, G. Ceder, *Chem. Mater.* **28** (2015) 266–273.
- [3] W.J. Kwon, H. Kim, K.-N. Jung, W. Cho, S.H. Kim, J.-W. Lee, et al., *J. Mater. Chem. A* **5** (2017) 6257–6262.

# Surface engineered $\text{La}_{2/3-x}\text{Li}_{3x}\text{TiO}_3$ perovskite for lithium solid-state batteries

<sup>a</sup>T. Polczyk, <sup>a</sup>W. Zajac, <sup>a</sup>D. Przyczyna, <sup>a</sup>A. Bombala, <sup>b</sup>M. Ziabka, <sup>a</sup>K. Świerczek

<sup>a</sup>Faculty of Energy and Fuels

<sup>b</sup>Faculty of Materials Science and Ceramics

AGH University of Science and Technology, al. Mickiewicza 30

30-059 Kraków, Poland

e-mail: topol@agh.edu.pl

Keywords: solid-state-batteries, perovskites, LLTO, surface engineering

## INTRODUCTION

The instability of renewable energy sources and the increased use of electric cars are among the key reasons for the development of new, more efficient energy storage methods. In recent years, due to the high density of energy, Li-ion batteries have become one of the primary sources of energy for portable electronic devices. However, this technology slowly reaches its fundamental limits. Increasingly, new solutions are proposed that go beyond existing Li-ion technology [1]. Among them is a battery composed only of materials in the solid state, so called *solid-state battery* (SSB). Replacing a liquid electrolyte with a thin layer of solid electrolyte can potentially increase the density of energy because of application of high voltage electrodes and at the same time increased safety due to higher stability of solid electrolytes as compared with flammable and reactive liquid electrolytes [2]. Lithium lanthanum titanate,  $\text{Li}_{3x}\text{La}_{2/3-x}\text{TiO}_3$  (LLTO), is a promising candidate for lithium conducting solid electrolyte due to high ionic conductivity and ability of forming dense sinters. One of the fundamental issues of using solid electrolytes is a high charge transfer resistance between the electrodes and the electrolyte. In this work an idea of asymmetrically porous LLTO electrolyte is explored and directed towards mitigation of the contact resistance. Electrolytes obtained by this approach have thin, dense anode side, and open pores cathode side. High-voltage  $\text{LiNi}_{0.5}\text{Mn}_{1.5}\text{O}_4$  spinel was applied as a cathode and metallic lithium as an anode in hybrid setup (with additional glass fibre separator soaked with non-aqueous liquid electrolyte. The results of preliminary works on SSB batteries formation and electrochemical characterization are presented.

## EXPERIMENTAL

The  $\text{Li}_{0.33}\text{La}_{0.56}\text{TiO}_3$  electrolyte was obtained by high temperature solid state reaction method in two steps: calcination at 1000°C for 12 h and reactive sintering at 1150°C for 12 h. Phase composition and crystal structure were examined using X-ray diffraction technique on polycrystalline powder. Ionic conductivity was measured using impedance spectroscopy technique as a function of temperature. Asymmetrically porous LLTO pellet was fabricated by a 2-step pressing: first, small amount of LLTO fine powder was uniaxially pressed under 75 MPa, next, the second layer was co-pressed under 150 MPa from a mixture of LLTO powder and starch form rice, as a pore-former. Prepared samples were sintered at

1200°C for 12h in Ar atmosphere, and on cooling stage the atmosphere was changed from Ar to synthetic air to burn up the starch. Microstructure of the resulting electrolyte was determined by the Scanning Electron Microscopy imaging.

The  $\text{LiNi}_{0.5}\text{Mn}_{1.5}\text{O}_4$  spinel cathode was obtained by sol-gel method from proper nitrates, and synthesized at 800°C for 8h. The cathode-electrolyte interface was formed by cathode slurry impregnation of porous side of the electrolyte. The quality of the connection was determined by EIS spectroscopy technique. Applicability of the formed solid-state batteries was examined using galvanostatic charge/discharge technique.

## RESULTS AND DISCUSSION

The obtained  $\text{Li}_{0.33}\text{La}_{0.56}\text{TiO}_3$  electrolytes were found to possess a single-phase P4/mmm double perovskite crystal structure. Bulk ionic conductivity was  $7.54 \cdot 10^{-4}$  S/cm at room temperature, and grain boundary contribution was  $5.45 \cdot 10^{-6}$  S/cm in the same conditions, which is similar to data reported in the literature [3]. In order to minimise cathode-electrolyte charge transfer resistance, starch-to-LLTO ratio was optimized. The highest starch-to-LLTO ratio allowing for obtaining a mechanically stable structure was found to be 1:1 by volume. SEM images show that the porous-to-dense electrolyte layer thickness ratio was ca. 4:1 and the dense layer had thickness of below 200 µm. Carried out electrochemical measurements proved improvement in electrochemical performance of surface engineered  $\text{La}_{2/3-x}\text{Li}_{3x}\text{TiO}_3$  electrolyte in lithium solid state hybrid battery.

## CONCLUSIONS

The proposed approach allows for fabrication of a solid state battery with low thickness of the electrolyte and improved electrochemical performance. Presented results help understanding the mass and charge transfer between cathode and electrolyte in lithium solid state batteries.

## REFERENCES

1. A. Luntz, The Journal of Physical Chemistry Letters 6 (2015) 300-301
2. J. Janek, W.G. Zeier, Nature Energy, 1 (2016) 16141
3. Y. Ren, K. Chen, R. Chen, T. Liu, Y. Zhang, C.W. Nan, Journal of American Ceramic Society 98 (2015) 3603-3623

# Composite anion conducting polymers for electrochemical energy technologies

M.L. Di Vona, E. Sgreccia, R. Narducci

University of Rome Tor Vergata, Dip. Industrial Engineering, 00133 Rome, Italy  
International Associated Laboratory (L.I.A.), Ionomer Materials for Energy (Aix Marseille University, CNRS,  
University of Rome Tor Vergata) France/Italy  
e-mail: divona@uniroma2.it

Keywords: functionalized  $\text{TiO}_2$ , layered double hydroxides

## INTRODUCTION

Composite polymer electrolytes offer various advantages, such as stable hydration and excellent mechanical and electrical properties. The realization of a homogeneous filler dispersion is paramount to produce high-performance composites. Recently we have studied organic-inorganic hybrid anionic exchange membranes (AEM) based on polysulfone (PSU) with quaternary ammonium groups and two classes of inorganic fillers:  $\text{TiO}_2$  with two model cases of functionalization, as typical hydrophilic or hydrophobic surface modifiers, and layered double hydroxides (LDH). The hydrophilic/hydrophobic  $\text{TiO}_2$  functionalization can optimize the microstructure of the nano-phase separated channels, while the use of LDH can limit the loss of conductivity due to the presence of the second phase and favor the dispersion in the polymer due to the affinity with AEM.

## EXPERIMENTAL

PSU-TMA and PSU-DABCO were dissolved in DMSO, and the resulting solution was mixed with a weighed amount of filler in DMSO. Two types of functionalized  $\text{TiO}_2$  were used: for the hydrophilic treatment 10% tri(hydroxymethyl) propane (TMP) was added to the powders; the hydrophobic treatment was obtained with 10% 2-ethyl-2-(hydroxymethyl)-1,3-propanediol (PMHS). Nanometric  $\text{MgAl-LDH}$  in chloride form was synthesized as reported in literature.

## RESULTS AND DISCUSSION

*Functionalized  $\text{TiO}_2$  composites.*

Thermal analysis (TGA and DSC) showed the loss of quaternary ammonium groups at 300 °C and the backbone decomposition above 400 °C starting from the quaternary carbon. The decompositions were confirmed by temperature-dependent FTIR spectroscopy. The thermomechanical study (DMA) showed a secondary relaxation, probably due to DABCO side groups motions, around 130 °C followed by the glass transition around 250 °C and by a partial crystallization of the polymer, which is also observed by DSC. AFM observations showed a more homogeneous dispersion of hydrophobic  $\text{TiO}_2$  nanoparticles whereas agglomeration is evident for hydrophilic surface treatment. The ionic conductivity is higher for PMHS- $\text{TiO}_2$ , probably related to the more homogeneous filler distribution with lower agglomeration.

## *LDH composites.*

Composites were prepared from polysulfone and dispersed nanoparticles of LDH with composition  $\text{Mg}_{0.62}\text{Al}_{0.38}(\text{OH})_2(\text{Cl})_{0.38} \cdot 0.6\text{H}_2\text{O}$  as inorganic filler. The composite membranes have a distinctly lower water uptake and swelling and they can be hydrated at 60 °C without dissolution. Their mechanical properties in fully humidified conditions are clearly enhanced with especially a nearly 3-fold increase of the Young modulus. In spite of their strongly reduced hydration, the conductivity of the composite membranes is comparable with that of the pristine ionomers. The membranes can be treated in alkaline conditions at 60°C without losing their properties.

## CONCLUSIONS

Composite AEM with functionalized  $\text{TiO}_2$  show enhanced mechanical properties and lower water uptake. Some crystallization is observed, probably because the oxide nanoparticles can facilitate the nucleation. Samples with TMP show some agglomeration, whereas PMHS nanoparticles are better distributed in the membrane. The ionic conductivity of composites is higher with hydrophobic than with hydrophilic  $\text{TiO}_2$ . The LDH inorganic nanoparticles were added to improve the mechanical stability of the membranes and the presence of mobile hydroxide ions in LDH was expected to mitigate the loss of hydroxide ion conductivity due to the presence of the second phase. The mechanical properties are considerably improved in the composites, especially a threefold increase of Young modulus is observed. Consequently, the water uptake and swelling are reduced and the stability against attack in alkaline conditions is considerably improved.

## REFERENCES

1. P Knauth, L Pasquini, ML Di Vona Solid State Ionics 300, 97-105, 2017
2. R Narducci, L Pasquini, JF Chailan, P Knauth, ML Di Vona ChemPlusChem 81, 550-556, 2016
3. R Narducci, JF Chailan, A Fahs, L Pasquini, ML Di Vona, P Knauth Journal of Polymer Science Part B: Polymer Physics 54, 1180-1187, 2016
4. Di Vona ML, Pasquini L, Narducci R, Pelzer K, Donnadio A, Casciola M, Knauth P. Journal of Power Sources 243, 488-493, 2013

# Effect of the geometry of the titania nanotubes on the photoactivity of organic-inorganic junction

*M. Szkoda, A. Lisowska-Oleksiak and K. Siuzdak \**

Faculty of Chemistry, Gdansk University of Technology, Narutowicza 11/12, 80-233, Gdansk, Poland

\*The Szewalski Institute of Fluid Flow Machinery, Fiszer 14, 80-231 Gdansk, Poland

e-mail: mariusz-szkoda@wp.pl

Keywords: titania nanotubes, photoelectrochemical activity, electrochemical polymerization

## INTRODUCTION

In recent decades, titanium dioxide has been extensively investigated as a promising photoelectrode material, which was widely used for photocatalytic waters splitting, solar cells, sensors and photocathodic protection [1]. A number of techniques have been used to prepare titania nanotubes (NTs) configurations, such as hydrothermal treatment of  $\text{TiO}_2$  in NaOH solution, anodization of titanium sheets, template methods, and electrospinning [2]. The most common procedure are based on the electrochemical anodic oxidation [3]. Many authors have focused their studies on the preparation conditions and determined the influence of many synthesis parameters. Among them, the applied voltage, current density and the anodization time are recognized as the most important [4]. Other variables are related to the electrolyte composition employed such as the water content or fluoride ions concentration [5]. Since listed parameters significantly affect the  $\text{TiO}_2$ NT dimensions, the physico-chemical properties and the photo-response the obtained NTs as well as composite materials exploiting  $\text{TiO}_2$ NT are under morphology control. Herein, the discussion undertaken on the relation between  $\text{TiO}_2$  geometry and properties of the organic-inorganic heterojunction wherein as an inorganic part  $\text{TiO}_2$ NT are used. The titania nanotubes were fabricated *via* anodization of titanium foil in various types of electrolytes based on ethylene glycol-water solutions containing fluoride ions. The organic element of the junction was formed by poly(3,4-ethylenedioxythiophene) doped with poly(styrenesulphonate) (PEDOT:PSS).

## EXPERIMENTAL

The  $\text{TiO}_2$ NTs were produced *via* a two-step electrochemical oxidation of a Ti plate in etching electrolytes of different composition. After calcination, the electrochemical hydrogenation process was performed in a three-electrode configuration, using the crystallized, anatase nanotubes as a working electrode, Ag/AgCl as a reference and platinum mesh as counter electrode. This treatment lead to the material activation that facilitate further polymer deposition. Electrochemical polymerization was carried out to prepare H- $\text{TiO}_2$ NTs/pEDOT:PSS. According to [6], the electrochemical deposition was performed in an aqueous solution containing NaPSS and EDOT, by potentiostatic polymerization at +1.6 V vs. Ag/AgCl/0.1 M KCl. Its crystal structure was revealed by Raman spectroscopy. Morphology details were examined using the Schottky field emission scanning electron microscope. The absorbance ability both of  $\text{TiO}_2$ NTs and heterojunction was verified using UV-Vis reflectance spectroscopy. The series of composite

materials were illuminated with a 150 W Xenon lamp equipped with an AM1.5 filter.

## RESULTS AND DISCUSSION

Depending on the water content in the electrolyte batch, both the layer thickness and titania diameter could be controlled, as shown in Fig. 1.

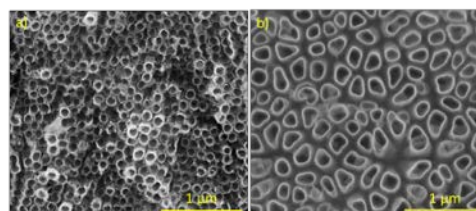


Fig. 1. SEM image of  $\text{TiO}_2$ NT surfaces obtained in an electrolyte with a) 5% and b) 30% water content.

As a result, the titania layers with different active surface area that is available for polymer deposition are formed. Additionally, in the case of higher water content, between  $\text{TiO}_2$ NT additional free space arises. Thus, not only the value of active surface area but also the surface character, i.e. tube interior or outer tube sphere affect the contact between n and p element of the junction.

## CONCLUSIONS

We have demonstrated that the photoelectrochemical efficiency of organic-inorganic heterojunction based on hydrogenated  $\text{TiO}_2$  nanotube array can be tuned by the adjusted architecture of titania. The geometry of  $\text{TiO}_2$ NT controlled by the water content in anodizing bath allowed for change in active surface area and in type of surface, namely interior and outer NTs sphere ready for the polymer coverage. The increase in the contact area between organic and inorganic element leads to a significant enhancement of photoelectroactivity of formed p-n junction.

## ACKNOWLEDGMENT

The financial support of the Polish National Science Centre: grant n°. 2012/07/D/ST5/02269 is gratefully acknowledged and the research was supported by the Foundation for Polish Science (FNP).

## REFERENCES

1. N. Liu, X. Chen, J. Zhang, J.W. Schwan, *Catalysis Today*, **225**(2014)34
2. M.D. García Rodríguez, B. Sánchez, J.M. Coronado, *Nanoscale*, **3** (2011)2233
3. M. Szkoda, K. Siuzdak, A. Lisowska-Oleksiak, *J Solid State Electrochem*, **20** (2016)563
4. H.E. Prakasam, K. Shankar, M. Paulose, O.K. Varghese, C.A. Grimes, *Phys. Chem. C*, **111**(2007)7235
5. P. Roy, S. Berger, P. Schmuki, *Angew. Chem. Int. Ed*, **50**(2011)2904
6. K. Siuzdak, M. Szkoda, A. Lisowska-Oleksiak, J. Karczewski J. Ryl, *RSC Adv*. **6**(2016)33101

# Integrated energy storage systems from solar panels for households

P. Kielczykowska, M. Olszewski, D. Olszewska

Faculty of Energy and Fuels  
AGH University of Science and Technology, ul. Reymonta 30  
30-059 Cracow, Poland  
e-mail: dolszew@agh.edu.pl

Keywords: Li-ion batteries, solar panel, storage

## INTRODUCTION

Environment care has many aspects. This paper attempts to pay attention to the possibility of innovative energy solutions usage in households in Poland, which greatly contribute to the environment degradation. Attention was paid to the most harmed by low emission area in Poland and there were proposed solutions already very popular in the Western Europe.

The usage of photovoltaics/energy bank systems for obtaining and storing energy can be an additional limiting factor for pollution, while investment costs, as in the case of gas-fired furnaces exchange, could be co-financed by local government.

## SOLAR ENERGY CONVERSION USAGE

Three types of conversion can be distinguished: photochemical, photovoltaic, photothermic. These processes allow the conversion of solar energy into heat or electricity. Photovoltaic conversion allows conversion of solar radiation into electrical energy with the use of semiconductors or so-called solar cells. The photovoltaic cell consists of a silicon semiconducting plate, inside which there is an electrical field in the form of a p-n (positive - negative). The advantages of photovoltaic cell are primarily the direct electricity production without any additional conversion and the possibility to produce power in cloudy days using diffused light. In addition, harmful gases are not produced during electricity generation.

Tesla is a global leader in the electric vehicle industry. The same manufacturer has decided to change the power management in the home and change the way it is used. Their offer includes the Powerwall 1 (2015) and Powerwall 2 (2016) batteries, which encourage the storage of the energy produced by solar panels mounted on the roofs and around home.

In order to answer the question of whether to use an innovative solution photovoltaics/energy bank in single-family houses worthwhile in Poland, the costs of connecting a new single-family house to the power grid and photovoltaics system with a modern lithium battery connection, for example Tesla, were calculated. Such a solution could help to reduce the low emission (pollution from the coal burning in households). Holders of such a system could use the solar energy, while the excess could be resale to distributors or use it in months requiring increased power consumption, for example usage of electric heating in winter.

Based on the available data, a comparison of energy savings over a 10 years period has been made for a single-family house connected to a power grid with a

home where photovoltaics system and lithium battery Powerwall 1 and Powerwall 2 were installed. It is higher than an average electricity consumption in Poland, which is about 4500kWh per year. For electricity consumption in a single-family household one should add the cost of connection to the power grid. The charge depends on the region in which the house is located. The connection of photovoltaic installation is related to the investment costs that will be discussed below for a single family house with a power consumption of 5,450.5 kWh. In practice, the installation of this power requires the installation of 21 NSP D6P\_B3a photovoltaic panels at an angle 30 degrees and its surface of 34.16 m<sup>2</sup>. In case of such installation the costs are balanced. Assuming: the installation cost is PLN 27,403, annual energy consumption at level of 5,450 kWh, the PV energy yield for the 25 year warranty period is 127,034 MWh, the annual power reduction 0.8%, the electricity price increase of 7%.

## CONCLUSIONS

The above calculations show that after about 9 years, with a lower level of sunshine, the costs of installing a plant based on renewable energy sources will return and after that time only the profit from storage and electricity generation can be noted.

## ACKNOWLEDGMENT

The financial support of D. Olszewska - the AGH project No.11.11.210.911 and P. Kielczykowska and M. Olszewski - "Grant of Rector 2017" - Students Scientific Association at the AGH - Coal&Clay.

# Evidence of the metal-insulator transition in $M_xV_2O_5-P_2O_5$ glasses and nanomaterials ( $M = Li, Na, Mg$ )

Wiktoria K. Zajkowska, Tomasz K. Pietrzak, Marek Wasiucione, Jerzy E. Garbarczyk

Faculty of Physics

Warsaw University of Technology, ul. Koszykowa 75

00-662 Warszawa, Poland

e-mail: topie@if.pw.edu.pl

Keywords: MIT transition, nanocrystallization, cathode materials for batteries

## INTRODUCTION

Crystalline  $V_2O_5$  has a layered structure, which enables reversible intercalation and deintercalation of cations of lithium and some other metals. For that reason this compound had been investigated already many years ago as a prospective cathode material for lithium batteries. Recently, an interest in  $V_2O_5$  has revived, because of possible applications of Na and Mg batteries with  $V_2O_5$ -based cathodes [1]. Unfortunately for applications,  $V_2O_5$  – like many other cathode materials – has low electrical conductivity. Main ways to overcome this problem consist in preparation of composites of the active cathode materials with carbon. We have proposed another method to increase the conductivity – a thermal nanocrystallization of glassy analogs of interesting cathode materials such as  $V_2O_5-P_2O_5$  and V-doped  $LiFePO_4$  [2, 3].

In this research, special attention has been paid to an observation of the metal-insulator transition (MIT) in lithium/sodium/magnesium-vanadate-phosphate glasses and nanomaterials, containing vanadium in several oxidation states. An important vanadium oxide  $V_2O_4$  (with  $V^{4+}$ ) is a semiconductor at room temperature. However, at  $67^\circ\text{C}$  its monoclinic structure changes into tetragonal, leading to a modification of its band structure and to a transition from a semiconductor („insulator”) to a “metal” [4]. The phenomenon can be observed and identified by thermal analysis (DTA or DSC) (presence of an endothermic peak), X-ray diffractometry (XRD) (changes in diffraction patterns) and electrical measurements (a substantial reversible electronic conductivity increase).

## EXPERIMENTAL

Vitreous  $90M_xV_2O_5 \cdot 10P_2O_5$  ( $M = Li, Na, Mg$ ) samples were prepared by melt-quenching technique from appropriate amounts of starting chemicals ( $NH_4H_2PO_4$ ,  $V_2O_5$  and  $Li_2CO_3$  or  $Na_2CO_3$  or  $MgO$ ) in reducing atmosphere. XRD measurements were carried out to check their amorphousness and crystallization processes during heating. Glass transition and crystallization temperatures were determined from DSC measurements. Electrical conductivity was measured as a function of temperature.

## RESULTS AND DISCUSSION

DSC traces of as-received samples were typical for glassy materials. E.g. for the Mg-based material they consisted in a glass transition followed by two crystallization peaks. In addition, an endothermic peak was observed at low temperature centered at  $67^\circ\text{C}$  (onset at  $60^\circ\text{C}$ ). The temperature dependence of the

conductivity (Fig. 1) above  $75^\circ\text{C}$  is typical for nanocrystallized materials. The final conductivity at room temperature is one order of magnitude higher than the conductivity of the initial glass. In addition, there is a stepwise reversible change in electrical conductivity around  $60^\circ\text{C}$  (visible in heating and cooling runs — Fig. 1). Such a transition, which coincides well with an endothermic peak in DSC trace of the sample, can be ascribed to MIT in  $VO_2$ , which occurs at exactly the same temperature [4]. This attribution is supported by the fact that  $VO_2$  phase was detected and identified in the XRD patterns of the materials under study.

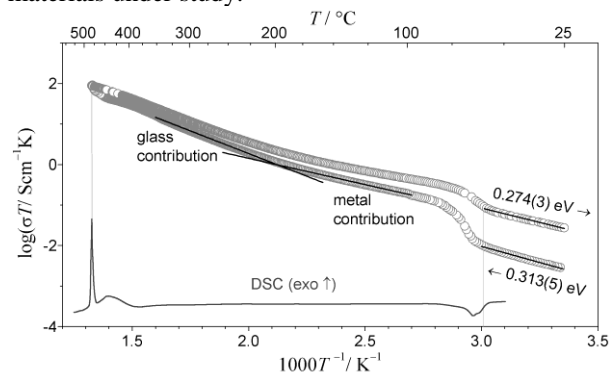


Fig. 1. Electrical conductivity of  $90MgV_2O_5 \cdot 10P_2O_5$  glass upon heating to  $480^\circ\text{C}$  and cooling down to RT. Vertical lines show the same processes observed by two methods.

## CONCLUSIONS

In this research, we have shown the difference between reversible conductivity changes in glasses and nanomaterials containing vanadium oxides due to metal-insulator transition and irreversible conductivity increase due to formation of highly-conductive nanocrystallites.

## REFERENCES

1. G.S. Gautam, P. Canepa, A. Abdellahi, A. Urban, R. Malik, G. Ceder, *Chemistry of Materials* **27** (2015) 3733–3742.
2. T.K. Pietrzak, M. Wasiucione, P.P. Michalski, A. Kaleta, J.E. Garbarczyk, *Materials Science and Engineering B* **213** (2016) 140–147.
3. T.K. Pietrzak, J.E. Garbarczyk, I. Gorzkowska, M. Wasiucione, J.L. Nowinski, S. Gierlotka, P. Jozwiak, *Journal of Power Sources* **194** (2009) 73–80.
4. M.M. Qazilbash, M. Brehm, Byung-Gyu Chae, P.-C. Ho, G.O. Andreev, Bong-Jun Kim, Sun Jin Yun, A.V. Balatsky, M.B. Maple, F. Keilmann, Hyun-Tak Kim, D.N. Basov, *Science* **318** (2007) 1750–1753.



# Synthesis and characterization of nanocrystallized $\text{Li}(\text{Fe}_{1-x}\text{Mn}_x)_{0.88}\text{V}_{0.08}\text{PO}_4$ cathode materials ( $x = 0.25, 0.5, 0.75$ )

Justyna E. Frąckiewicz, Tomasz K. Pietrzak, Marek Wasiucione, Jerzy E. Garbarczyk

Faculty of Physics

Warsaw University of Technology, ul. Koszykowa 75

00-662 Warszawa, Poland

e-mail: topie@if.pw.edu.pl

Keywords: triphylite, nanocrystallization, cathode materials for Li-ion batteries

## INTRODUCTION

Since the pioneering publication by J.B. Goodenough et al. [1], phospho-olivines  $\text{LiMPO}_4$  ( $M = \text{Fe}, \text{Mn}, \text{Co}, \text{Ni}$ ) had been studied for their application as cathodes for Li-ion cells. From the whole family of isostructural compounds, only cathodes prepared from  $\text{LiFePO}_4$  had been introduced into mass production.  $\text{LiMnPO}_4$  has higher potential versus metallic lithium compared to  $\text{LiFePO}_4$ , but synthesis of  $\text{LiMnPO}_4$  compounds which can work in batteries with high loads is more difficult [2]. One of the successful synthetic routes consists in preparation of intentionally non-stoichiometric compositions [3]. Other possible way is to synthesize  $\text{LiMn}_{1-x}\text{Fe}_x\text{PO}_4$  phospho-olivines [4, 5]. In recent years, our group has proposed and investigated an alternative route to the conductivity enhancement, namely a thermal nanocrystallization of glassy analogs of the important crystalline cathode materials, such as:  $\text{V}_2\text{O}_5$ ,  $\text{LiFePO}_4$  and  $\text{Li}_3\text{V}_2(\text{PO}_4)_3$  [6, 7]. The advantages of this approach include the absence of carbon additives, simplicity and straightforwardness of synthesis, which consists of two stages only: (i) glass preparation by melt-quenching and (ii) thermal treatment of the glass to induce its nanocrystallization. Our experience with that method has shown that one can, by the appropriate heat-treatment, achieve a gigantic (even by a factor  $10^9$ ) and irreversible conductivity enhancement.

## EXPERIMENTAL

In this research, we aimed to replace some of iron ions in  $\text{LiFe}_{0.88}\text{V}_{0.08}\text{PO}_4$  glass with manganese in order to obtain highly conductive nanomaterials. Appropriate amounts of precursors:  $\text{Li}_2\text{CO}_3$ ,  $\text{FeC}_2\text{O}_4 \cdot 2\text{H}_2\text{O}$ ,  $\text{Mn}(\text{CH}_3\text{COO})_2 \cdot 4\text{H}_2\text{O}$ ,  $(\text{NH}_4)_2\text{H}_2\text{PO}_4$  and  $\text{V}_2\text{O}_5$  were mixed in a mortar, melted at  $1300^\circ\text{C}$  in reducing atmosphere and rapidly quenched. Their amorphousness was confirmed with X-ray diffractometry (XRD) and thermal events occurring in the samples were observed with differential thermal analysis (DTA). Electrical conductivity was measured upon heating and subsequent cooling ramps with impedance spectroscopy within wide frequency range 10 mHz – 10 MHz.

## RESULTS AND DISCUSSION

DTA curves of as-received samples were typical for glassy materials. A glass transition and two crystallization peaks were observed. Preliminary electrical results (Fig. 1) showed that initial conductivity ( $1.2 \cdot 10^{-13} \text{ S/cm}$ ) can be increased of at least 10 orders of magnitude to ca  $10^{-3} \text{ S/cm}$ . XRD

patterns acquired upon heating to  $580^\circ\text{C}$  indicated three crystalline phases: triphylite  $\text{LiFePO}_4$ , lithiophilite  $\text{LiMnPO}_4$  and lithium iron phosphate  $\text{Li}_3\text{Fe}_2(\text{PO}_4)_3$ . All of the three structures are electrochemically active and therefore are suitable to be used as cathodes in Li-ion batteries.

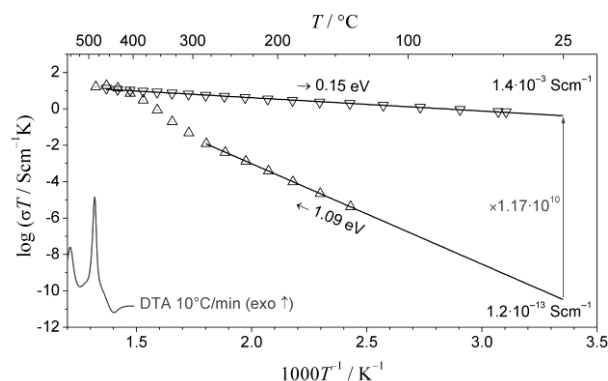


Fig. 1. Electrical conductivity upon heating to  $480^\circ\text{C}$  and cooling down to  $25^\circ\text{C}$  for  $\text{LiFe}_{0.44}\text{Mn}_{0.44}\text{V}_{0.08}\text{PO}_4$  sample.

## CONCLUSIONS

This research has shown that thermal nanocrystallization of glassy analogs of  $\text{LiFe}_{1-x}\text{Mn}_x\text{PO}_4$  resulted in highly conducting materials that may be used as a cathode in Li-ion battery. The addition of vanadium was to improve its glass forming properties and to provide favorable conditions for electron hopping in the nanomaterials.

## REFERENCES

1. A.K. Padhi, K.S. Nanjundaswamy, J.B. Goodenough, *Journal of the Electrochemical Society* **144** (1997) 1188–1194.
2. J.O. Herrera, H. Camacho-Montes, L.E. Fuentes, L. Ivarez-Contreras, *Journal of Materials Science and Chemical Engineering* **3** (2015) 54–64.
3. B. Kang, G. Ceder, *Journal of The Electrochemical Society* **157** (2010) A808–A811.
4. L. Damen, F. De Giorgio, S. Monaco, F. Veronesi, M. Mastragostino, *Journal of Power Sources* **218** (2012) 250–253.
5. J. Molenda, W. Ojczyk, J. Marzec, *Journal of Power Sources* **174** (2007) 689–694.
6. J.E. Garbarczyk, T.K. Pietrzak, M. Wasiucione, A. Kaleta, A. Dorau, J.L. Nowinski, *Solid State Ionics* **272** (2015) 53–59.
7. T.K. Pietrzak, M. Wasiucione, P.P. Michalski, A. Kaleta, J.E. Garbarczyk, *Materials Science and Engineering B* **213** (2016) 140–147.

# Structural and electrical properties of Cr and Y doped SrTiO<sub>3</sub> porous materials

*L. Łańcucki, E. Drożdż, A. Łącz*

AGH University of Science and Technology, Faculty of Materials Science and Ceramics,  
al. A. Mickiewicza 30, 30-059 Kraków, Poland  
e-mail: lancucki@agh.edu.pl

Keywords: Cr and Y doped SrTiO<sub>3</sub>, anode materials for SOFC

## INTRODUCTION

Strontium titanate (SrTiO<sub>3</sub>), in which A and B sites are occupied by divalent Sr<sup>2+</sup> and tetravalent Ti<sup>4+</sup>, is a well-known cubic perovskite structure. Among the possible alternative materials for SOFC technology, doped strontium titanate ceramics have attracted increasing interest during the last few years. Although the robustness of SrTiO<sub>3</sub> ceramics makes them suitable as anode backbones, they have significant disadvantages: the lack of catalytic activity for the oxidation of anode fuels, and the limited ionic conductivity. The former can be compensated by introduction with acceptor like chromium while for the latter it can be enhanced by yttrium addition. Doping the B site of SrTiO<sub>3</sub> with Cr<sup>3+</sup> can create perovskite type ceramics with improved conductivity in oxidising atmospheres and excellent chemical, redox, thermal and mechanical stabilities. Additionally doping A site with yttrium improves conductivity of obtained samples in hydrogen atmosphere. The resulting Y and Cr doped SrTiO<sub>3</sub> (SYTCO) materials find potential application as electrodes in solid-oxide fuel cells, solid-oxide electrolysis cells, and high-temperature steam electrolysis.

## EXPERIMENTAL

Ti(O-iPr)<sub>4</sub>—titanium(IV) isopropoxide was mixed with proper amount of citric acid (this method gives a total ions concentration to citric acid equal to 1:2 molar ratio) in anhydrous ethanol, afterward the solution of strontium nitrate yttrium nitrate and chromium nitrate were added and the solution was dried to form gel. The resultant mixtures were calcinated at 900 °C. Powders obtained in such way were formed into pellets and sintered at 1200 °C. Such methodology allowed to obtain a series of samples of the general formula Sr<sub>0.96</sub>Y<sub>0.04</sub>Ti<sub>1-x</sub>Cr<sub>x</sub>O<sub>3</sub> where x =0, 2, 4, 8 mol.%.

Phase composition and unit cell parameters were determined based on XRD measurements carried out on Philips X'Pert Pro diffractometer. The morphology study was performed using scanning electron microscopy (SEM) (Nova NanoSEM 200 FEI and Oxford Instruments).

The electrical properties of obtained samples were examined by DC method for temperature range 300-800°C and in air and H<sub>2</sub>/Ar atmosphere.

## RESULTS AND DISCUSSION

The XRD analysis revealed that both yttrium and chromium have been incorporated into SrTiO<sub>3</sub> taustonite structure as presented in Fig 1.

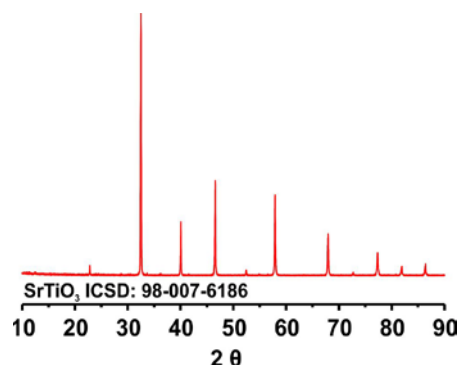


Figure 1. The Sr<sub>0.96</sub>Y<sub>0.04</sub>Ti<sub>0.92</sub>Cr<sub>0.08</sub>O<sub>3</sub> X-ray diffraction pattern after sintering.

Moreover, the decrease of unit cell parameter for Y and Cr doped samples was observed as presented in Table 1. This phenomenon can be explained on behalf of differences between the ionic radii of Ti(IV) - 74.5pm and Cr(III) - 69pm.

Table 1. The values of cell parameter Y and Cr doped SrTiO<sub>3</sub> samples.

Sample	Cell parameter [Å]
SrTiO <sub>3</sub>	3.9064
Sr <sub>0.96</sub> Y <sub>0.04</sub> TiO <sub>3</sub>	3.9034
Sr <sub>0.96</sub> Y <sub>0.04</sub> Ti <sub>0.98</sub> Cr <sub>0.02</sub> O <sub>3</sub>	3.9027
Sr <sub>0.96</sub> Y <sub>0.04</sub> Ti <sub>0.96</sub> Cr <sub>0.04</sub> O <sub>3</sub>	3.9017
Sr <sub>0.96</sub> Y <sub>0.04</sub> Ti <sub>0.92</sub> Cr <sub>0.08</sub> O <sub>3</sub>	3.9005

## CONCLUSIONS

A series of single-phase porous strontium titanate materials doped by different amounts of chromium and 4mol.% yttrium were obtained by the sol-gel method. The comparison of cell parameters indicate incorporation of Y and Cr into the strontium and titanium sublattice, respectively. The results of the electrical tests show the opposite effect of the introduced dopant on the conductivity of the samples in the oxidizing and reducing atmosphere.

## ACKNOWLEDGMENT

This work is supported by the National Science Centre of the Republic of Poland under Grant No 2014/14/E/ST5/00763

## **Polish Hydrogen and Fuel Cell Association**

Polish Hydrogen and Fuel Cell Association was founded in 2004 as a non-profit organization to promote hydrogen as a sustainable energy carrier as well as modern technologies for energy conversion and storage. The Association is a rapidly growing organization, which gathered many scientists (to date 197 members, including 44 professors and 12 supporting members).

Members of the Association are employees of universities and research institutes, as well as directors of state-owned enterprises. Supporting members include universities and research institutes. Association collaborates closely with Polish Technological Platform of Hydrogen and Fuel Cells organizing meetings, schools and preparing national "hydrogen" research program. The Association is a member of EHA (European Hydrogen Association) and PATH (Partnership for Advancing the Transition to Hydrogen). Comparing the size and structure of the membership, the Polish Association is one of the largest in Europe, and has significant intellectual potential.

### **Mission**

- development of collaboration among universities, research institutes and industry,
- support of high-risk projects focused on basic studies of new materials for energy conversion and storage,
- stimulation of educational activities promoting modern technologies for energy conversion and storage.

### **Activity**

- Annual Bulletin,
- Every 2 years Association is organizing Forum dedicated to fuel cells, hydrogen production and storage, Li-ion and Na-ion batteries, supercapacitors, thermoelectrics, solar conversion,
- Every 2 years, interchangeably with Forum, Association is organizing Summer Schools on energy conversion and storage,
- Lectures at Technical Open University of AGH University of Science and Technology,

## NOTES

## NOTES

## NOTES



## NOTES

## NOTES

## Barcelona SmartMoto Challenge 2017

Students's Scientific Society *Hydrogenium*, which works at Department of Hydrogen Energy AGH, took part in E-Moto AGH project. E-Moto AGH team debuted at the SmartMoto Challenge, on 6 - 9 July in Barcelona. AGH students proved to be the best in three competitions:

- autocross - crossing the track by two drivers
- slalom on the asphalt
- mechanical solutions of the motorcycle and braking system.

The team was also considered to be the best new team in the competition. Overall, the Team took 4<sup>th</sup> place in the general results. Judges especially appreciated the mechanical part. Students announce that another motorcycle will be built for the next start of the year. Over 20 students from 3 students' scientific societies were involved in the project: *Mechanics* – construction, propulsion and business plan, *Telephoners* – wireless communication, and *Hydrogenium* – battery package and charging system.



Congratulations!

<https://www.facebook.com/emoto.agh/>

<http://www.hydrogenium.agh.edu.pl/>

## Authorities of the Association

### PRESIDENT

**Prof. dr hab. inż. Janina Molenda**

Faculty of Energy and Fuels

AGH University of Science and Technology

al. Mickiewicza 30, 30-059 Kraków



### VICE-PRESIDENT

**Dr hab. Andrzej Budziak, prof. IFJ PAN**

Institute of Nuclear Physics PAN

ul. Radzikowskiego 152, 31-342 Kraków



### VICE-PRESIDENT

**Dr hab. inż. Piotr Jasiński, prof. PG**

Faculty of Electronics, Telecommunications and Informatics

Gdańsk University of Technology

Gabriela Narutowicza 11/12, 80-233 Gdańsk



### VICE-PRESIDENT

**Dr inż. Jakub Kupecki**

Thermal Processes Department

Institute of Power Engineering - Research Institute

ul. Augustówka 36, 02-981 Warszawa



### TREASURER

**dr inż. Dominika Baster**

Faculty of Energy and Fuels

AGH University of Science and Technology

Al. Mickiewicza 30, 30-059 Kraków



### SECRETARY

**dr inż. Anna Milewska**

Faculty of Energy and Fuels

AGH University of Science and Technology

Al. Mickiewicza 30, 30-059 Kraków



### AUDITING COMMITTEE

Prof. dr hab. Leszek Czepirski

Prof. dr hab. Paweł Nowak

Prof. dr hab. inż. Janusz Tobała

Dr hab. Antoni Paja, prof. AGH

Dr inż. Mariusz Krauz